

20880

NATIONAL LIBRARY
OTTAWA



BIBLIOTHÈQUE NATIONALE
OTTAWA

NAME OF AUTHOR..... MARTIN COWIE.....

TITLE OF THESIS..... STRUCTURAL DETERMINATIONS
of SOME TRANSITION METAL HYDRIDO,
AND TRIS (BENZENE-1,2-DITHIOLATO) COMPLEXES

UNIVERSITY..... UNIVERSITY of ALBERTA.....

DEGREE FOR WHICH THESIS WAS PRESENTED..... PHD.....

YEAR THIS DEGREE GRANTED..... 1974.....

Permission is hereby granted to THE NATIONAL LIBRARY
OF CANADA to microfilm this thesis and to lend or sell copies
of the film.

The author reserves other publication rights, and
neither the thesis nor extensive extracts from it may be
printed or otherwise reproduced without the author's
written permission.

(Signed)..... *Martin Cowie*.....

PERMANENT ADDRESS:
896 UPPER OTTAWA ST.
HAMILTON
ONTARIO, CANADA

DATED..... Dec 20..... 1973

THE UNIVERSITY OF ALBERTA

STRUCTURAL DETERMINATIONS OF SOME TRANSITION
METAL HYDRIDO, AND *TRIS* (BENZENE-1,2-DITHIOLATO)
COMPLEXES

by

© MARTIN COWIE

A THESIS

SUBMITTED TO THE FACULTY OF GRADUATE STUDIES
AND RESEARCH IN PARTIAL FULFILMENT OF THE
REQUIREMENTS FOR THE DEGREE OF DOCTOR OF PHILOSOPHY

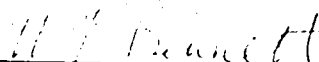
DEPARTMENT OF CHEMISTRY

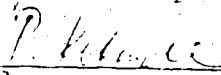
EDMONTON, ALBERTA

SPRING, 1974

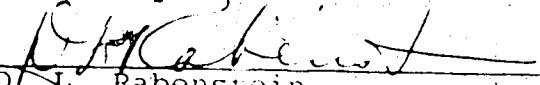
THE UNIVERSITY OF ALBERTA
FACULTY OF GRADUATE STUDIES AND RESEARCH

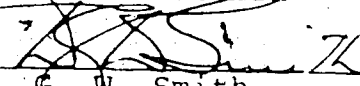
The undersigned certify that they have read, and recommend to the Faculty of Graduate Studies and Research, for acceptance, a thesis entitled STRUCTURAL DETERMINATIONS OF SOME TRANSITION METAL HYDRIDO AND TRIS (BENZENE-1,2-DITHIOLATO) COMPLEXES submitted by MARTIN COWIE in partial fulfilment of the requirements for the degree of Doctor of Philosophy in Chemistry.

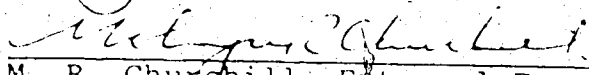

M. J. Bennett, Supervisor


P. Kebarle


G. Kotowycz


D. L. Rabenstein


D. G. W. Smith


M. R. Churchill, External Examiner

DATE:

Dec 17/73

TO MY PARENTS

ABSTRACT

The crystal and molecular structures of $\text{Re}_2(\text{CO})_6\text{H}_4[\text{Si}(\text{C}_2\text{H}_5)_2]_2$ and $\text{Re}_2(\text{CO})_7\text{H}_2[\text{Si}(\text{C}_2\text{H}_5)_2]_2$ have been determined. The central Re_2Si_2 clusters are similar in both molecules and form a rhombus with a Re-Re bond across the shorter diagonal. The Re-Si bond lengths in both compounds are all similar, and are therefore consistent with the hydrogen ligands being terminally bound to the rhenium atoms rather than bridging the rhenium-silicon bonds. The mode of bonding of the hydride ligands is discussed in relation to other similar systems.

The crystal and molecular structures of three η^3 (benzene-1,2-dithiolato) complexes, $(\text{Mo}(\text{S}_2\text{C}_6\text{H}_4)_3)_2$, $[\text{As}(\text{C}_6\text{H}_5)_4][\text{Nb}(\text{S}_2\text{C}_6\text{H}_4)_3]$ and $[(\text{CH}_3)_4\text{N}]_2[\text{Zr}(\text{S}_2\text{C}_6\text{H}_4)_3]$ have been determined in an attempt to explain the stability of the trigonal prism with respect to the octahedron. In the molybdenum and niobium complexes the metals are surrounded by six sulfur atoms in trigonal prismatic coordination. The zirconium complex, however, has a coordination which is best described as a distorted octahedron. The increase in S-C distances, observed through this series, indicates an increasing tendency of the ligands towards the reduced $\text{S}_2\text{C}_6\text{H}_4^{2-}$ formulation. This ten-

dency is discussed in relation to a molecular orbital scheme for trigonal prismatic dithiolenes (by Gray *et. al.*) and is correlated to the destabilization of the prism which is observed progressing through this series.

A disorder in $\text{Re}_2(\text{CO})_8[\text{Si}(\text{C}_6\text{H}_5)_2]_2$, involving a small translation of the complete molecule along the crystallographic b axis, was investigated in order to ascertain the effect on molecular geometry and thermal parameters.

PREFACE

This thesis presents the results of two independent problems. The first section deals with a structural study of a particular class of transition metal hydrides. The second section is concerned with the structures of transition metal complexes of ligands coordinated through sulfur atoms. The same technique, namely single crystal X-ray diffraction, was used for both problems. The theoretical and experimental details of X-ray diffraction are described in several standard reference texts.^{1,2,3,4}

ACKNOWLEDGEMENT

The author wishes to express his gratitude and sincere appreciation to:

Professor M. J. Bennett for his expert guidance and friendly assistance during the course of this research.

Professor W. A. G. Graham and Mr. J. K. Hoyano for supplying the rhenium hydrido complexes.

Professor J. Takats and Mr. J. L. Martin for supplying the *tris* (1,2-dithiolato) complexes.

The group, past and present, for their friendship and assistance.

Mrs. Lu Ziola for her expert preparation of this manuscript.

The National Research Council for its generous financial support.

The University of Alberta for affording me the experience as a teaching assistant.

Gail for her constant encouragement and companionship.

TABLE OF CONTENTS

CHAPTER	PAGE
I.	TRANSITION METAL HYDRIDE INTRODUCTION 1
II.	THE CRYSTAL AND MOLECULAR STRUCTURE OF DIHYDRIDO TRICARBONYL RHENIUM BIS (μ -DIETHYLSILICON) DIHYDRIDO TRICAR- BONYL RHENIUM, $[\text{Re}_2(\text{CO})_6\text{H}_4[\text{Si}(\text{C}_2\text{H}_5)_2]_2]$. EXPERIMENTAL 16 STRUCTURE SOLUTION AND REFINEMENT 20 RESULTS 30 DESCRIPTION OF STRUCTURE 39
III.	THE CRYSTAL AND MOLECULAR STRUCTURE OF DIHYDRIDO TRICARBONYL RHENIUM BIS (μ -DIETHYLSILICON) TETRACARBONYL RHENIUM, $[\text{Re}_2(\text{CO})_7\text{H}_2[\text{Si}(\text{C}_2\text{H}_5)_2]_2]$. EXPERIMENTAL 41 STRUCTURE SOLUTION AND REFINEMENT 45 RESULTS 47 DESCRIPTION OF STRUCTURE 59
IV.	MODE OF BONDING OF THE HYDRIDE LIGANDS IN $\text{Re}_2(\text{CO})_6\text{H}_4[\text{Si}(\text{C}_2\text{H}_5)_2]_2$ AND $\text{Re}_2(\text{CO})_7\text{H}_2[\text{Si}(\text{C}_2\text{H}_5)_2]_2$ 63

CHAPTER		PAGE
V.	DITHIOLENE INTRODUCTION	73
	THE CRYSTAL AND MOLECULAR STRUCTURE OF <i>TRIS</i> (BENZENE-1,2-DITHIOLATO) MOLYBDENUM, $[\text{Mo}(\text{S}_2\text{C}_6\text{H}_4)_3]$.	
	EXPERIMENTAL	82
	STRUCTURE SOLUTION AND REFINEMENT	85
	RESULTS	91
	DESCRIPTION OF STRUCTURE	105
VII.	THE CRYSTAL AND MOLECULAR STRUCTURE OF TETRAPHENYLARSONIUM <i>TRIS</i> (BENZENE- 1,2-DITHIOLATO) NIOBIUM, $([\text{C}_6\text{H}_5)_4\text{As}][\text{Nb}(\text{S}_2\text{C}_6\text{H}_4)_3]$.	
	EXPERIMENTAL	115
	STRUCTURE SOLUTION AND REFINEMENT	119
	RESULTS	121
	DESCRIPTION OF STRUCTURE	148
VIII.	THE CRYSTAL AND MOLECULAR STRUCTURE OF <i>BIS</i> (TETRAMETHYLAMMONIUM) <i>TRIS</i> (BENZENE-1,2-DITHIOLATO) ZIRCONIUM, $([\text{CH}_3)_4\text{N}]_2[\text{Zr}(\text{S}_2\text{C}_6\text{H}_4)_3]$.	
	EXPERIMENTAL	157
	STRUCTURE SOLUTION AND REFINEMENT	161

CHAPTER	PAGE
RESULTS	164
DESCRIPTION OF STRUCTURE	181
IX. TRIGONAL PRISMATIC vs. OCTAHEDRAL COORDINATION IN TRIS (1,2-DITHIOLATO) COMPLEXES	192
REFERENCES	210
APPENDIX 1: MOLECULAR DISORDER IN TETRACARBONYL RHENIUM BIS (μ -DIPHENYLSILICON) RHENIUM TETRACARBONYL, $[\text{Re}_2(\text{CO})_8[\text{Si}(\text{C}_5\text{H}_5)_2]_2]$	223
APPENDIX 2: PROGRAMMES USED IN CRYSTAL STRUCTURE SOLUTION, REFINEMENT AND ANALYSIS	235

LIST OF TABLES

	PAGE
<u>CHAPTER II:</u>	
Table 1: Derivation of Re-Re, Re-Si, and Si-Si Vectors for Space Group $P\bar{1}$	22
Table 2: Assignment of Most Intense Patterson Vectors	23
Table 3: Observed and Calculated Electron Densities for Varying $\sin \theta/\lambda$ Cut-Offs	27
Table 4: Observed and Calculated Structure Factor Amplitudes	31
Table 5: Atomic Positional Parameters	34
Table 6: Thermal Parameters	35
Table 7: Intramolecular Distances and Angles	36
<u>CHAPTER III:</u>	
Table 8: Patterson Vectors for $\text{Re}_2(\text{CO})_7\text{H}_2[\text{Si}(\text{C}_2\text{H}_5)_2]_2$	44
Table 9: Refinement Outline	45
Table 10: Observed and Calculated Structure Factor Amplitudes	49
Table 11: Fractional Coordinates	52
Table 12: Thermal Parameters	53
Table 13: Intramolecular Distances	55
Table 14: Intramolecular Angles	56
Table 15: Least Squares Plane Calculations for $\text{Re}_2(\text{CO})_7\text{H}_2(\text{SiEt}_2)_2$	57

CHAPTER IV:

Table 16: Relevant Bond Lengths in Some Transition Metal Silicon-Bridged Complexes 68

Table 17: Relevant Angles in Some Transition Metal Silicon-Bridged Complexes 68

CHAPTER V:

Table 18: Electronic Spectra for Molybdenum, Niobium, and Zirconium Benzene Dithiols 81

CHAPTER VI:

Table 19: Harker Vectors for Mo(bdt)₃ 86

Table 20: Refinement Outline 88

Table 21: Observed and Calculated Structure Factor Amplitudes 93

Table 22: Atom Coordinates and Isotropic Temperature Factors 96

Table 23: Anisotropic Temperature Factors 97

Table 24: Intramolecular Contacts 98

Table 25: Intramolecular Angles 99

Table 26: Intermolecular Contacts 100

Table 27: Least Squares Plane Calculations 101

Table 28: Dihedral Angles between Selected Planes 103

CHAPTER VII:

Table 29: Major Patterson Peaks and their Assignment 118

Table 30: Refinement Outline 119

Table 31: Observed and Calculated Structure Factor Amplitudes 123

	PAGE
Table 32: Atom Coordinates and Isotropic Temperature Factors	131
Table 33: Anisotropic Thermal Parameters	137
Table 34: Intra-ionic Contacts	139
Table 35: Intra-ionic Angles	140
Table 36: Inter-ionic Contacts	142
Table 37: Least Squares Plane Calculations	145
Table 38: Dihedral Angles Between Selected Planes	147

CHAPTER VIII:

Table 39: Refinement Outline	162
Table 40: Observed and Calculated Structure Factor Amplitudes	166
Table 41: Atom Coordinates and Isotropic Temperature Factors	169
Table 42: Anisotropic Thermal Parameters	172
Table 43: Intra-Ionic Contacts	174
Table 44: Intra-Ionic Angles	175
Table 45: Inter-Ionic Contacts	176
Table 46: Least Squares Plane Calculations	177
Table 47: Dihedral Angles Between Selected Planes	178
Table 48: Selected Distances for <i>Tris</i> (1,2-Dithiolene) Complexes	188
Table 49: Selected Angles for <i>Tris</i> (1,2-Dithiolene) Complexes	189

APPENDIX 1:

	PAGE
Table 50: Anisotropic Thermal Parameters for Ordered Model	226
Table 51: Positional Parameters and Isotropic B's for Ordered Model	226
Table 52: Selected Bond Lengths and Angles	227
Table 53: Anisotropic Thermal Parameters for Disordered Model	231
Table 54: Positional Parameters and Isotropic B's for Disordered Model	232

LIST OF FIGURES

<u>CHAPTER I:</u>	PAGE
Fig. 1: Central Frameworks of the Silicon-Bridged Transition Metal Series	12
<u>CHAPTER II:</u>	
Fig. 2: Electron Density Difference Map through the Re_2Si_2 Plane [$(\sin \theta/\lambda)_{\text{max}} = 0.35$]	28
Fig. 3: A Perspective View of $\text{Re}_2(\text{CO})_6\text{H}_4[\text{Si}(\text{C}_2\text{H}_5)_2]_2$	37
Fig. 4: Packing Diagram for $\text{Re}_2(\text{CO})_6\text{H}_4[\text{Si}(\text{C}_2\text{H}_5)_2]_2$, Projected on the bc Plane	38
<u>CHAPTER III:</u>	
Fig. 5: A Perspective View of $\text{Re}_2(\text{CO})_7\text{H}_2[\text{Si}(\text{C}_2\text{H}_5)_2]_2$	58
<u>CHAPTER IV:</u>	
Fig. 6: Possible Bonding Schemes for the Hydrogen Ligand in $\text{W}_2(\text{CO})_8\text{H}_2[\text{Si}(\text{C}_2\text{H}_5)_2]_2$	64
Fig. 7: A Comparison of the Geometries of (A) $\text{Re}_2(\text{CO})_7\text{H}_2[\text{Si}(\text{C}_2\text{H}_5)_2]_2$, (B) $\text{Re}_2(\text{CO})_8[\text{Si}(\text{C}_6\text{H}_5)_2]_2$, and (C) $\text{Re}_2(\text{CO})_6\text{H}_4[\text{Si}(\text{C}_2\text{H}_5)_2]_2$	65
Fig. 8: Hydrogen Ligand Environments in the Silicon-Bridged Transition Metal Hydrides	67
<u>CHAPTER VI:</u>	
Fig. 9: A Perspective View of $\text{Mo}(\text{S}_2\text{C}_6\text{H}_4)_3$	104
Fig. 10: Dimensions Within the Dithiolene Ligands	107

	PAGE
Fig. 11: Dithiolato and Dithioketonic Limiting Formulations for the "bdt" Ligand	107
Fig. 12: View of $\text{Mo}(\text{S}_2\text{C}_6\text{H}_4)_3$ down the Crystallographic c Axis.	110
Fig. 13: Packing Diagram for $\text{Mo}(\text{S}_2\text{C}_6\text{H}_4)_3$, Projected on the ab Plane	113
 <u>CHAPTER VII:</u>	
Fig. 14: A Perspective View of the $\text{Nb}(\text{S}_2\text{C}_6\text{H}_4)_3$ Anion	149
Fig. 15: Dimensions Within the Dithiolene Ligands	152
Fig. 16: A Perspective View of $[\text{As}(\text{C}_6\text{H}_5)_4][\text{Nb}(\text{S}_2\text{C}_6\text{H}_4)_3]$, Viewed down the Crystallographic b Axis	155
 <u>CHAPTER VIII:</u>	
Fig. 17: A Perspective View of the $\text{Zr}(\text{S}_2\text{C}_6\text{H}_4)_3^{2-}$ Dianion, Viewed down the Approximate Molecular 3-Fold Axis	179
Fig. 18: A Perspective View of $[\text{N}(\text{CH}_3)_4]_2[\text{Zr}(\text{S}_2\text{C}_6\text{H}_4)_3]$	180
Fig. 19: <i>Trans</i> S-M-S Angles in the Trigonal Prism and the Octahedron	182
Fig. 20: Trigonal Twist Angle Projected Perpendicular to the Molecular 3-Fold Axis	183
Fig. 21: Dimensions within the Dithiolene Ligands	187
 <u>CHAPTER IX:</u>	
Fig. 22: Molecular Orbital Energy Levels of Interest for Trigonal Prismatic Dithiolenes, by G. N. Schrauzer and V. P. Mayweg	193

	PAGE
Fig. 23: Molecular Orbital Energy Levels of Interest for Trigonal Prismatic Dithiolenes, by H. B. Gray <i>et. al.</i>	195
Fig. 24: Representations of the Molecular Orbitals and Energy Levels for $S_2C_2H_2$ and $S_2C_2H_2^{2-}$	198
Fig. 25: Representations of the Molecular Orbitals and Energy Levels for $S_2C_6H_4$ and $S_2C_6H_4^{2-}$	199
Fig. 26: Predicted Bond Lengths and π Bond Orders for $S_2C_6H_4$ and $S_2C_6H_4^{2-}$	200
Fig. 27: S-C Bond Lengths vs. π Bond Order for Ethylene and Benzene Dithiol Ligands	204

APPENDIX 1:

Fig. 28: A Perspective View of $Re_2(CO)_8[Si(C_6H_5)_2]_2$	224
Fig. 29: Mode of Disorder in $Re_2(CO)_8[Si(C_6H_5)_2]_2$	229

CHAPTER I: TRANSITION METAL HYDRIDE

INTRODUCTION

The discovery of the first transition metal hydride complexes,^{5,6} $\text{FeH}_2(\text{CO})_4$ and $\text{CoH}(\text{CO})_4$, in the 1930's marked the beginning of approximately twenty years of controversy concerning the structures of hydride complexes and the mode of bonding of the hydrogen atoms in these complexes.

The first electron diffraction study⁷ on gaseous $\text{CoH}(\text{CO})_4$ and $\text{FeH}_2(\text{CO})_4$ led to the conclusion that the metals were surrounded tetrahedrally by the carbonyl groups. The hydrogen atoms were assumed to be bound to the oxygen atoms of the carbonyl groups. Hieber later suggested⁸ that the hydrogens were actually bonded to the metals, but were buried in the electron density of the metal and thus had no stereochemical influence.

The infrared spectrum of $\text{CoH}(\text{CO})_4$ was initially interpreted⁹ as being consistent with the hydrogen atom being primarily bonded to the carbon p_π orbitals at approximately 2.0 \AA from the cobalt atom. In this model the hydrogen was believed to be bridging three carbonyl groups. However the findings of Cotton and Wilkinson,¹⁰ based on nuclear magnetic

resonance and acid dissociation constants for $\text{CoH}(\text{CO})_4$ and $\text{FeH}_2(\text{CO})_4$, agreed with Hieber,⁸ suggesting that the hydrogens were close to and primarily bonded to the metal atoms. Subsequent L.C.A.O. calculations¹¹ on $\text{CoH}(\text{CO})_4$ yielded the greatest total overlap integral of Co-H and C-H for a Co-H distance of 1.2 Å. This distance was again consistent with the hydrogen being buried in the Co orbitals, since a covalent distance of 1.593 Å had been obtained¹² in CoH.

Since $\text{HMn}(\text{CO})_5$ had physical properties¹³ similar to $\text{Fe}(\text{CO})_5$, its infrared spectrum was interpreted assuming it, like $\text{Fe}(\text{CO})_5$, had trigonal bipyramidal coordination,^{14,15} with the hydrogen buried in the manganese orbitals and exerting no stereochemical influence. In addition the identification¹⁶ of the Co-H stretching frequency at 1934 cm^{-1} added further proof that the hydrogen was bound to the metal. The large shifts to high field of the proton resonance that were observed in transition metal hydrides were also initially interpreted as evidence for "buried" hydrogens. However subsequent studies^{17,18} showed that these shifts were due to more subtle electronic effects and could be explained assuming normal metal-hydrogen covalent distances.

In addition it was shown¹⁹ that the neglect of quadrupole effects which resulted^{20,21} in short M-H distances, was not justified.

Thus until 1959 the experimental evidence was interpreted as indicating that the hydrogen atom exerted no stereochemical influence and was buried in the transition metal orbitals.

Discovery of the true coordination in the metal hydride complexes had to await the availability of good quality X-ray and neutron diffraction data and also the discovery of stable crystals of these hydrides [$\text{CoH}(\text{CO})_4$ and $\text{FeH}_2(\text{CO})_4$ were unstable gases]. In X-ray diffraction studies, since the X-rays are scattered by electrons, hydrogen atoms contribute little to the total scattering. Therefore location of the hydrogen atom requires extremely high quality data, and the difficulty of direct observation of hydrogen atoms increases with increasing atomic number of the atoms present. However, even when the hydrogen atom is not located, its approximate position can be deduced from the coordination of the other ligands. In neutron diffraction the scattering of thermal neutrons is by the nucleus and varies²² approximately as $A^{1/3}$ (where A is the atomic mass number). Thus the scattering amplitudes

of all atoms are of the same order of magnitude, allowing the hydrogen atoms to be located with a precision comparable to that of heavier atoms.

The X-ray structural determinations^{23,24} of $\text{PtHBr}[\text{P}(\text{C}_2\text{H}_5)_3]_2$ and $\text{OsHBr}(\text{CO})[\text{P}(\text{C}_6\text{H}_5)_3]_3$ and later²⁵ of $\alpha\text{-HMn}(\text{CO})_5$ failed to locate the hydrogen atoms but showed the empty coordination sites where the hydrogens were probably located. In the X-ray crystallographic study²⁶ of $\text{RhH}(\text{CO})[\text{P}(\text{C}_6\text{H}_5)_3]_3$, however, the hydrogen atom *was* located, at 1.72(15) Å from the rhodium atom, a distance consistent with the sum of the rhodium and hydrogen covalent radii.²⁷ (The reliability of this hydrogen identification has recently been challenged.²⁸ However the original paper²⁶ clearly outlined the conditions that would favour the direct observation of hydrogen atoms in heavy atom structures and provided the impetus for crystallographers to attempt hydrogen atom location.)

Neutron diffraction experiments^{29,30} on K_2ReH_9 and also $\beta\text{-HMn}(\text{CO})_5$ proved unequivocally that the hydrogens acted as typical ligands and were not buried in the metal orbitals. The Re-H distances average 1.68(1) Å and the Mn-H distance is 1.601(16) Å in these compounds.

It was a fortunate sequence of events that the molecular structure³¹ of $\text{RhH}[\text{P}(\text{C}_6\text{H}_5)_3]_4$ was not determined prior to those mentioned above. Otherwise the hypothesis that the hydrogen was buried in the metal orbitals might have had a longer lifetime. In this compound the phosphorus atoms form, within experimental error, a regular tetrahedron about the Rh atom. Although it seems that the hydrogen is exerting no stereochemical influence, its influence is just minimized by the bulky $\text{P}(\text{C}_6\text{H}_5)_3$ groups. Comparing for example the volume^{32,33,34} of a $\text{P}(\text{C}_6\text{H}_5)_3$ group at $\sim 370 \text{ \AA}^3$ to that of CO ($\sim 45 \text{ \AA}^3$)³⁵ and H ($\sim 7 \text{ \AA}^3$)³⁶ it becomes obvious that this distortion is reasonable.

Of the many subsequent transition metal hydride complexes to be studied^{35,37,38} some of the most interesting involved bridging hydrogens, where the hydrogen ligands were simultaneously bonded to two atoms. Two main categories of bridging hydrogens exist, the most common being between two transition metals, and the second involving bridging between a transition metal and a non-transition metal. In the former category two types have been observed, involving either a bent or a linear M-H-M bond.

A linear M-H-M bond^{39,40} was deduced in the

structure of $\text{Cr}_2\text{H}(\text{CO})_{10}^-$. Although the hydrogen atom position was not located, stereochemical and bonding arguments suggest that it is collinear with the two chromium atoms and equidistant from each. [It is to be noted, however, that the X-ray data cannot differentiate between two possibilities: either the hydrogen is bonded symmetrically to both chromium atoms (single-minimum potential well), or it is preferentially bonded to one chromium atom (double-minimum potential well) and is "tunnelling" between the two sites.] The observed Cr...Cr distance of 3.41(1) Å is considerably longer than the Cr-Cr bond length³⁹ of 2.97(1) Å in $\text{Cr}_2(\text{CO})_{10}^{2-}$ and yields a Cr-H distance of 1.70 Å which is in good agreement with the other known metal-hydrogen distances. The hydrogen ligand then occupies the sixth coordination site of each $\text{Cr}(\text{CO})_5$ fragment giving the anion D_{4h} symmetry. The insertion of the hydrogen ligand causing the two $\text{Cr}(\text{CO})_5$ moieties to be further apart also results in the carbonyl groups being eclipsed, compared with the staggered carbonyls in $\text{Cr}_2(\text{CO})_{10}^{2-}$. More recently a linear Re-H-Cr bond has also been inferred⁴¹ in $(\text{OC})_5\text{ReHCr}(\text{CO})_5$. Although the hydrogen was not located it was considered to be collinear with the Re and Cr atoms, since again the two metal-

pentacarbonyl groups are eclipsed and since the least squares planes containing the equatorial CO groups are within 2.5° of being parallel. The Re-Cr distance is $3.435(1) \text{ \AA}$, which is again consistent with hydrogen insertion between the two metals.

Bent M-H-M bonds have been deduced in several complexes. In $\text{Re}_3\text{H}(\text{CO})_{12}^{2-}$ and $\text{Re}_3\text{H}_2(\text{CO})_{12}^-$ the triangular species^{42,43} contain an isosceles triangle of rhenium atoms with Re-Re distances of 3.04 \AA and 3.17 \AA , with the longer distances presumably being bridged by the hydrogen ligands. These bent hydrogen bridges were confirmed recently⁴⁴ in the analogous $\text{H}_3\text{Mn}_3(\text{CO})_{12}$ complex, in which the hydrogen atoms were located. The manganese atoms form an equilateral triangle with the hydrogen ligands symmetrically bridging the triangle edges. The average Mn-Mn distance is 3.111 \AA compared with 2.923 \AA in $\text{Mn}_2(\text{CO})_{10}$ ⁴⁵ and thus again shows the lengthening of the bridged metal-metal bond, a feature which has been used as evidence for hydrogen bridging in the rhenium clusters.^{42,43} The average Mn-H distance is 1.72 \AA .

In $\text{Re}_2\text{MnH}(\text{CO})_{14}$ ^{46,47} and $\text{Re}_3\text{H}(\text{CO})_{14}$ ⁴⁸ the hydrogen ligands are located between the rhenium atoms in a position which is almost collinear with

these atoms. However the estimated Re-H-Re angles, calculated assuming octahedral coordinations, are 164° in $\text{Re}_2\text{MnH}(\text{CO})_{14}$ and 159° in $\text{Re}_3\text{H}(\text{CO})_{14}$.

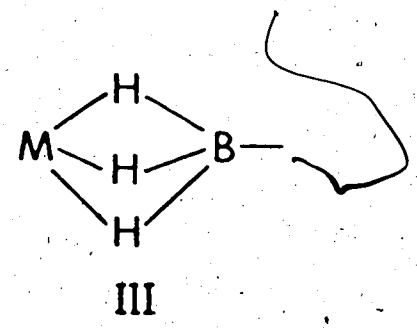
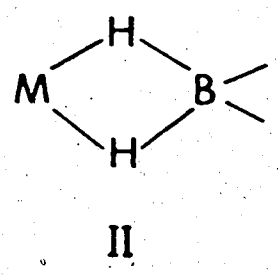
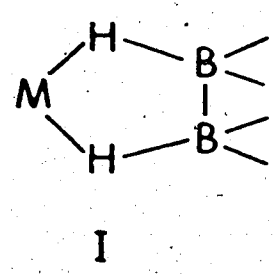
The structure⁴⁹ of $\text{Mo}_2\text{H}(\text{CO})_4(\pi\text{-C}_5\text{H}_5)_2[\text{P}(\text{CH}_3)_2]$ consists of two $(\pi\text{-C}_5\text{H}_5)\text{Mo}(\text{CO})_2$ fragments joined at the Mo atoms by a symmetrically bridged $\text{P}(\text{CH}_3)_2$ group and presumably by a hydrogen atom. The structure⁵⁰ of $\text{Mn}_2\text{H}(\text{CO})_8[\text{P}(\text{C}_6\text{H}_5)_2]$ closely resembles that of $\text{Mo}_2\text{H}(\text{CO})_4(\pi\text{-C}_5\text{H}_5)_2[\text{P}(\text{CH}_3)_2]$ with two carbonyl groups on each metal replacing a $(\pi\text{-C}_5\text{H}_5)$ group.

However, in the manganese compound the hydrogen atom was located, in the position equivalent to that postulated in the molybdenum complex, with a Mn-H distance of $1.86(6)$ Å and a Mn-H-Mn angle of $104(5)^\circ$.

Hydrogen bridging three metal atoms has been postulated in $\text{Ru}_6\text{H}_2(\text{CO})_{18}$ ⁵¹ and $\text{Rh}_3\text{H}(\pi\text{-C}_5\text{H}_5)_4$ ^{52,53}. The ruthenium structure consists of an octahedron of Ru atoms each bound to three terminal carbonyl groups. The hydrogen ligands appear to occupy two opposite faces of the octahedron. In $\text{Rh}_3\text{H}(\pi\text{-C}_5\text{H}_5)_4$ the equilateral triangle of Rh atoms has one cyclopentadienyl ring bonded to each Rh with the fourth ring parallel to the rhodium triangle. The hydrogen ligand is then postulated as being equidistant from each Rh on the opposite side of the triangle from

the fourth C₅H₅ group.

Hydrogen bridging between a transition metal and a non-transition metal has been observed in boron complexes with the hydrogen bridging the boron and the transition metal. Three basic types exist:



Structures of type I were observed in Mn₃H(BH₃)₂(CO)₁₀,⁵⁴ Cu(B₃H₈)[P(C₆H₅)₃]₂⁵⁵ and Cr(B₃H₈)(CO)₄⁻.^{56,57,58}

In the manganese compound all hydrogen atoms of the BH₃ group are coordinated to a Mn atom and in addition a bent Mn-H-Mn bond exists between the two Mn(CO)₃ moieties. In Cu(B₃H₈)[P(C₆H₅)₃]₂ the coordination of the copper atom is a distorted tetrahedron with two of the coordination sites occupied by bridging hydrogens. The P-Cu-P and H-Cu-H angles of 120° and 103° respectively, reflect this distortion. Cr(B₃H₈)(CO)₄⁻ has an octahedrally hybridized chromium atom with two sites again being occupied by bridging hydrogens.

Coordination of type I is exhibited^{59,60} by $\text{Cu}(\text{BH}_4)[\text{P}(\text{C}_6\text{H}_5)_3]_2$. The copper geometry again is distorted tetrahedral with two hydrogen atoms of the borohydride group bridging the copper and boron atoms. The short Cu-B distance of 2.184(9) Å and long Cu-H distance of 2.02(5) Å suggests delocalized bonding between the copper atom and the borohydride group in which direct Cu-B overlap might be significant.

In $\text{Zr}(\text{BH}_4)_4$ ⁶¹ the molecule is crystallographically required to possess T_d symmetry. The zirconium atom is tetrahedrally surrounded by the four boron atoms, and one terminal hydrogen atom is located on each C_3 axis. So it appears that M-H-B bonding of type III is present with the Zr atom surrounded by twelve H atoms.

The reactions of disubstituted silanes with dirhenium decacarbonyl and with both tungsten and molybdenum hexacarbonyls produced an interesting series of silicon-bridged, metal-metal bonded species which were also postulated as containing hydrogen-bridged metal-silicon bonds.^{62,63} Since this was only the second class of compounds in which hydrogen was postulated as bridging a transition metal-non-transition metal bond, a systematic study of the representative molecules from this series was therefore

undertaken to elucidate the major structural characteristics of the systems.

Viewing only the central cluster and ignoring the carbonyl groups, the molecules fall into five major classes:

- I. no hydrogen ligands,⁶⁴ e.g. $\text{Re}_2(\text{CO})_8[\text{Si}(\text{C}_6\text{H}_5)_2]_2$,
- II. two hydrogens, each on different transition metals but adjacent to the same silicon atom^{62,65}
e.g. $\text{Re}_2(\text{CO})_8\text{H}_2\text{Si}(\text{C}_6\text{H}_5)_2$,
- III. two hydrogens, each on different transition metals and adjacent to two different silicon atoms,⁶⁶ e.g. $\text{W}_2(\text{CO})_8\text{H}_2[\text{Si}(\text{C}_2\text{H}_5)_2]_2$,
- IV. two hydrogens, both on the same transition metal but adjacent to different silicons; e.g.
 $\text{Re}_2(\text{CO})_7\text{H}_2[\text{Si}(\text{C}_2\text{H}_5)_2]_2$, and
- V. four hydrogens, two attached to each transition metal, each silicon having two adjacent hydrogens,
e.g. $\text{Re}_2(\text{CO})_6\text{H}_4[\text{Si}(\text{C}_2\text{H}_5)_2]_2$.

The structural fragments are shown in Fig. 1 using valence bond description and normal terminal transition metal hydride formulation, with the exceptions of III(b) where bridging hydrogens are indicated and III(c) where the terminal hydrogens interact weakly with the silicon atoms. The main interest in this series centred around the central cluster of transition

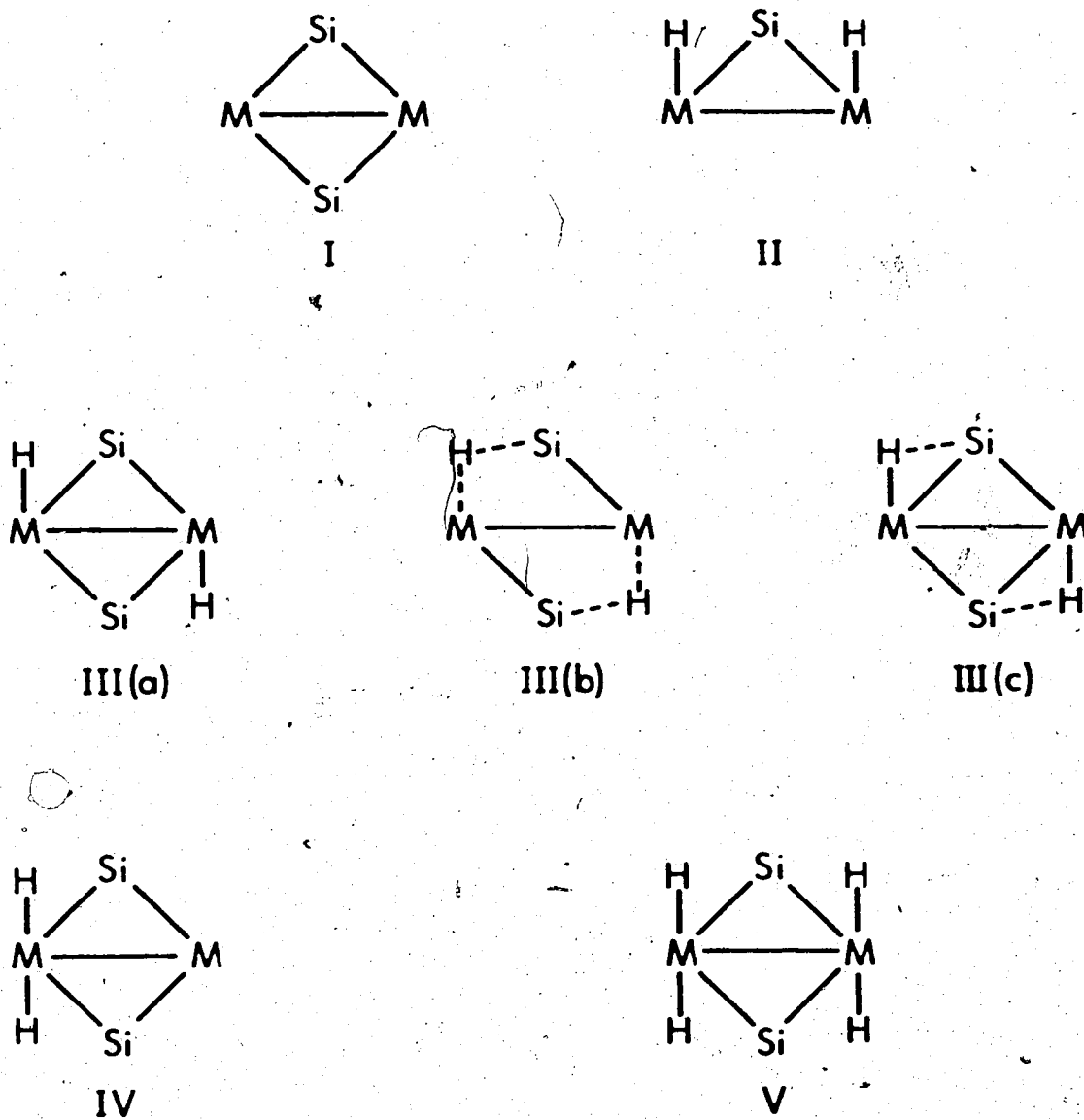


Fig. 1: CENTRAL FRAMEWORKS OF THE SILICON-BRIDGED
TRANSITION METAL SERIES.

metal and silicon atoms, especially when hydrogen ligands were present, to obtain information concerning the nature of the bonding of the hydrogen ligands.

It had been suggested on the basis of spectroscopic evidence that in these compounds the hydrogen ligands bridged the metal-silicon bonds rather than being bonded terminally to the metals.^{62,63} The basis of this argument was the spectroscopic studies by Kaesz and coworkers^{67,68} on the trimeric rhenium hydride $[\text{HRe}(\text{CO})_4]_3$ and its deuteride $[\text{DRe}(\text{CO})_4]_3$, in which the absence of a distinct metal-hydrogen stretching frequency in the infrared was interpreted as evidence that the hydrogens were bridging. Since the terminal metal-hydrogen stretch should be visible in the infrared, its silence was postulated as a characteristic feature of M-H-M bridges. This was extended to the series of transition metal silicon hydrides where the metal-hydrogen stretch was again absent in the infrared,⁶³ and consequently a Si-H-M bridge was postulated. In addition, in $\text{Re}_2(\text{CO})_8\text{H}_2\text{Si}(\text{CH}_3)_2$, the methyl resonance appeared as a 1:2:1 triplet at $\tau = 8.87$ with a coupling constant $J = 1.5 \text{ Hz}$.⁶³ The magnitude of this coupling constant also suggested that the high field protons, which are splitting the methyl resonance, were close to the dimethyl-silicon moiety since $J(\text{CH}_3\text{-Si-H}) = 4.2 \text{ Hz}$ for dimethyl-

silane alone.

The first member of this series to have its molecular structure solved by X-ray techniques was $\text{Re}_2(\text{CO})_8\text{H}_2\text{Si}(\text{C}_6\text{H}_5)_2$.^{62,65} Unfortunately, due to the dominance of the rhenium scattering, location of the hydrogen ligands was not possible. However, the coordination sites adjacent to the metal-silicon bonds were conspicuously vacant so the approximate locations of the hydrogens were apparent. Elder postulated⁶⁵ that the hydrogens were located in the Re_2 plane such that the Re-Re-H angle was 90° . Thus for a rhenium-hydrogen bond length²⁹ of 1.68 \AA , a silicon-hydrogen bond length of 1.59 \AA would result. This position he said would give the proper orientation for a three centre Si-H-Re bond.

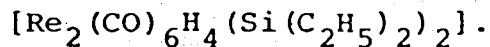
However, the subsequent structure determination of the non-hydridic species $\text{Re}_2(\text{CO})_8[\text{Si}(\text{C}_6\text{H}_5)_2]_2$ ⁶⁴ showed a remarkable similarity in Re-Si bond lengths [$2.542(3) \text{ \AA}$] with $\text{Re}_2(\text{CO})_8\text{H}_2\text{Si}(\text{C}_6\text{H}_5)_2$, [$2.544(9) \text{ \AA}$], which was not expected if a three centre two electron Si-H-Re bond is involved in the latter. An unambiguous comparison of the two structures was hindered, however, by the realization that a disorder problem was present in $\text{Re}_2(\text{CO})_8[\text{Si}(\text{C}_6\text{H}_5)_2]_2$ (see Appendix 1). Although it was not believed that this

would affect the bond lengths in the central Re_2Si_2 cluster, it did cast some doubt on accurate comparisons of the two compounds.

Further evidence favouring the three centre Si-H-M bond arose from the structural determination of $\text{W}_2(\text{CO})_8\text{H}_2[\text{Si}(\text{C}_2\text{H}_5)_2]_2$,⁶⁶ [type III(b) in Fig. 1] in which two differing tungsten-silicon bonds were found [2.586(5) Å and 2.703(4) Å]. This was interpreted as being due to hydrogen insertion in the tungsten-silicon bond, thus forming a three centre W-H-Si bond. Therefore the crystal and molecular structure determinations of members IV and V ($\text{Re}_2(\text{CO})_7\text{H}_2[\text{Si}(\text{C}_2\text{H}_5)_2]_2$ and $\text{Re}_2(\text{CO})_6\text{H}_4[\text{Si}(\text{C}_2\text{H}_5)_2]_2$) were undertaken to obtain further information concerning the bonding of the hydrogen ligand in this series. These structure determinations are described in Chapters II and III.

CHAPTER II: THE CRYSTAL AND MOLECULAR STRUCTURE OF
DIHYDRIDO ~~TRICARBONYL~~ RHENIUM *BIS*

(*p*-DIETHYLSILICON) DIHYDRIDO TRICARBONYL RHENIUM,



EXPERIMENTAL

The sample of $\text{Re}_2(\text{CO})_6\text{H}_4[\text{Si}(\text{C}_2\text{H}_5)_2]_2$ which was kindly supplied by Dr. Graham and Mr. Hoyano⁶³ was recrystallized from normal hexane, yielding colourless crystals with the shape of a general parallelepiped. Preliminary photography indicated only Laue symmetry $\bar{1}$ indicative of a triclinic space group. The systematic absences for the working cell, as determined by Weissenberg ($0k\ell$, $1k\ell$, $2k\ell$: CuK_α X-radiation), and Precession methods ($h0\ell$, $h1\ell$, $h2\ell$, $hk0$, $hk1$, $hk2$: MoK_α X-radiation), are hkl : $h + k = 2n + 1$, $h + \ell = 2n + 1$, $k + \ell = 2n + 1$, and are consistent with the non-standard space groups $F1$ and $F\bar{1}$. The non-standard cell was retained as the working cell for its convenience with respect to the crystal morphology and unit cell angles. Precise lattice parameters were obtained at 23°C from an analysis of the setting angles for 18 reflections which had been carefully centred on a Picker manual four circle diffractometer using CuK_α radiation of wavelength 1.54051 Å.

A Delaunay reduction was performed⁶⁹ and failed to show the presence of higher symmetry. The F centred cell parameters are : $a = 8.357(3) \text{ \AA}$, $b = 16.228(6) \text{ \AA}$, $c = 18.184(6) \text{ \AA}$, $\alpha = 118.98(2)^\circ$, $\beta = 92.62(3)^\circ$ and $\gamma = 95.44(3)^\circ$, and the reduced primitive cell parameters are: $a = 8.357(3) \text{ \AA}$, $b = 8.767(3) \text{ \AA}$, $c = 8.776(3) \text{ \AA}$, $\alpha = 109.07(3)^\circ$, $\beta = 97.76(3)^\circ$, and $\gamma = 112.88(3)^\circ$. The reduced primitive cell is related to the F centred cell by: $a_P = -a_F$, $b_P = 1/2(b_F + a_F)$, $c_P = -1/2(b_F + c_F)$. The observed density [2.23(2) g cm^{-3}] obtained by floatation in aqueous Clerici's solution (Thallos formate-malonate, $\rho_{\text{max}} = 4.3 \text{ g ml}^{-1}$), is in satisfactory agreement with that calculated on the basis of four molecules in the F centred cell (2.25 g cm^{-3}). For space group $F\bar{1}$ the imposed symmetry on the molecule is $\bar{1}$, while no restrictions are possible for space group $F1$. Since $\text{Re}_2(\text{CO})_6\text{H}_4[\text{Si}(\text{C}_2\text{H}_5)_2]_2$ can have $\bar{1}$ symmetry, $F\bar{1}$ was chosen and was later verified by successful refinement of the model. The General Equivalent Positions for the space group $F\bar{1}$ are : $\pm(x, y, z; 1/2 + x, 1/2 + y, z; 1/2 + x, y, 1/2 + z; x, 1/2 + y, 1/2 + z)$.

Intensity data were collected on the Picker manual diffractometer using CuK_α radiation monochromated by the (002) reflecting plane of an oriented graphite

crystal using a take-off angle of 2° . Two crystals were used during data collection and in each case they were aligned with their a^* axis coincident with the ϕ axis of the diffractometer. The crystal faces were identified and the perpendicular distances between parallel faces of the same form were measured as: crystal 1 - $\{1,0,0\}$, 0.095 mm; $\{0,1,0\}$, 0.065 mm; $\{0,\bar{1},1\}$, 0.084 mm; and crystal 2 - $\{1,0,0\}$, 0.077 mm; $\{0,0,1\}$, 0.065 mm; and $\{0,\bar{1},1\}$, 0.036 mm. Data were collected for reflections with 2θ values between 0° and 125° using the coupled $\omega/2\theta$ scanning technique with a 2θ scan speed of $2^\circ/\text{min}$ and scan width of three degrees (to allow for increase in mosaic spread as crystal decomposition occurred). Stationary background counts were measured at the limits of each scan for 20 seconds. Assuming approximate linearity of background, the intensity of the peak (I) is given by:

$$I = P - t(B_1 + B_2) \quad (1)$$

where P = peak count, $t = t_p/t_B$ or the ratio of peak scan time to the sum of the background times, and B_1 and B_2 are the background counts. Standard deviations of the intensities were computed from the relationship:

$$\sigma(I) = (P + t^2 B + P^2 I^2)^{1/2} \quad (2)$$

where $B = B_1 + B_2$. An ignorance factor (p) of 0.03 was used to account for machine errors and to prevent unreasonably high weighting being applied to reflections of high intensity.⁷⁰ The detector was a scintillation counter and was used in conjunction with a pulse height analyzer which was tuned to accept 95% of the CuK_α peak.

Eight well distributed standard reflections were monitored at approximately 10 hour intervals to investigate possible decomposition. The decomposition was found to be approximately linear with time and was essentially free of $\sin \theta/\lambda$ dependence. The total decomposition for the data collection was about 10%. The 1690 unique reflections collected were reduced to 1510 using the criterion that a peak is significantly above background when $I/\sigma(I) \geq 3.0$. The significant data were reduced to structure factor amplitudes by correction for Lorentz, polarization, decomposition, and absorption effects. Standard deviations in the structure factors, $\sigma(F)$, were obtained from the expression:⁷¹

$$\sigma(F) = \frac{1}{2} \sqrt{\frac{D}{ALp'}} \cdot \frac{\sigma(I)}{I^{1/2}} \quad (3)$$

where D , A , L , and p' are the decomposition, absorption,⁷² Lorentz, and polarization correction factors res-

pectively. The high linear absorption coefficient⁸⁶ for $\text{Re}_2(\text{CO})_6\text{H}_6[\text{Si}(\text{C}_2\text{H}_5)_2]_2$ using CuK_α X-radiation (226.07 cm^{-1}) gave rise to a wide range of transmission factors (0.138 to 0.382) which made an absorption correction imperative. The absorption correction was verified by observation of the variation in I_{h00} ($\chi = 90^\circ$) as ϕ was varied. The final corrected intensities of this ϕ scan data showed variation from the mean of less than 10% and thus were judged to be internally consistent.

STRUCTURE SOLUTION AND REFINEMENT

A Patterson map^{73,74} was computed between the limits $0 \leq u \leq 0.5$, $0 \leq v \leq 0.5$, and $0 \leq w \leq 0.5$. The Re-Re, Re-Si, and Si-Si vectors are derived for space group $\text{P}\bar{1}$ in Table 1. The vectors for space group $\text{F}\bar{1}$ are generated by adding $(0,0,0)$, $(1/2,1/2,0)$, $(1/2,0,1/2)$ and $(0,1/2,1/2)$ to those derived for $\text{P}\bar{1}$. In addition all vector multiplicities increase by a factor of 4. The origin peak is due to the sum of the vectors between every atom and itself, thus the magnitude of the origin vector is roughly given by: $(2 \times 75^2 + 2 \times 14^2 + 6 \times 8^2 + 14 \times 6^2 + 24 \times 1^2) = 12554$. In the Fourier

program used to calculate the vector map, however, the origin peak is normalized to 1000. Therefore taking account of the largest negative peak (~ -40), and assuming the temperature factors are comparable, one expects the Re-Re vectors to have approximate magnitude 466, the Re-Si vectors ~ 174 and the Si-Si vectors ~ 17 above background. Viewing the Patterson map (summarized in Table 2) it is obvious that the first two vectors correspond to Re-Re vectors. On inspection of the map the first vector is identified as associated with the $0, 1/2, 1/2$ origin therefore is attributed as $(2x_R, 1/2 + 2y_R, 1/2 + 2z_R)$. The coordinates of the rhenium atom are then calculated as $(0.120, -0.010, -0.061)$. The second peak then corresponds to the edge of the vector $(1/2, 1/2, 0) - (2x_R, 2y_R, 2z_R)$.

The next most intense peak, having a magnitude approximately comparable to that expected for a Re-Si vector, was situated at approximately 2.44 \AA from the origin (a distance which is similar to the Re-Si distance in $\text{Re}_2(\text{CO})_8\text{H}_2\text{Si}(\text{C}_6\text{H}_5)_2$ ^{62,65}). For this reason it was chosen as the $(x_R - x_S, y_R - y_S, z_R - z_S)$ vector and from this the silicon coordinates were calculated as $(-0.08, -0.13, +0.61)$. The next two vectors were then identified as $(1/2, 1/2, 0) - (x_R - x_S,$

TABLE 1: DERIVATION OF Re-Re, Re-Si, AND Si-Si VECTORS FOR SPACE GROUP $P\bar{1}$

	x_R, y_R, z_R ^a	$-x_R, -y_R, -z_R$	x_S, y_S, z_S	$-x_S, -y_S, -z_S$
x_R, y_R, z_R	$0, 0, 0$	$-2x_R, -2y_R, -2z_R$	$-(x_R - x_S),$ $-(y_R - y_S),$ $-(z_R - z_S)$	$-(x_R + x_S),$ $-(y_R + y_S),$ $-(z_R + z_S)$
$-x_R, -y_R, -z_R$	$2x_R, 2y_R, 2z_R$	$0, 0, 0$	$x_R + x_S,$ $y_R + y_S,$ $z_R + z_S$	$x_R - x_S,$ $y_R - y_S,$ $z_R - z_S$
x_S, y_S, z_S	$x_R - x_S,$ $y_R - y_S,$ $z_R - z_S$	$-(x_R + x_S),$ $-(y_R + y_S),$ $-(z_R + z_S)$	$0, 0, 0$	$-2x_S, -2y_S, -2z_S$
$-x_S, -y_S, -z_S$	$x_R + x_S,$ $y_R + y_S,$ $z_R + z_S$	$-(x_R - x_S),$ $-(y_R - y_S),$ $-(z_R - z_S)$	$2x_S, 2y_S, 2z_S$	$0, 0, 0$

^a (x_R, y_R, z_R) and (x_S, y_S, z_S) are the coordinates for the rhenium and silicon atoms respectively.

TABLE 2: ASSIGNMENT OF MOST INTENSE
PATTERSON VECTORS

u	v	w	RELATIVE PEAK HEIGHT	ASSIGNMENT
0.240	0.480	0.378	487	$(0, 1/2, 1/2) +$ $(2x_R, 2y_R, 2z_R)$
0.240	-0.500	0.126	370	$(1/2, 1/2, 0) -$ $(2x_R, 2y_R, 2z_R)^b$
0.200	0.120	0.0	131	$(x_R - x_S, y_R - y_S, z_R - z_S)$
0.280	0.380	0.0	123	$(1/2, 1/2, 0) -$ $(x_R - x_S, y_R - y_S, z_R - z_S)$
0.040	0.360	0.360	119	$(0, 1/2, 1/2) +$ $(x_R + x_S, y_R + y_S, z_R + z_S)$
0.240	0.040	0.396	98	Re-C and Re-O vector build-up.
0.480	0.460	0.234	91	
0.0	0.140	0.126	90	$-(x_R + x_S, y_R + y_S, z_R + z_S)^b$

^bshoulder of the peak.

$y_R - y_S, z_R - z_S$) and $(0, 1/2, 1/2) + (x_R + x_S, y_R + y_S, z_R + z_S)$. Image seeking around the Re-Re vectors then identified three of the next four vectors as being due to build-ups of Re-C and Re-O vectors from the molecules at $(1/2, 1/2, 0)$ and $(0, 1/2, 1/2)$. The peak observed at $(-0.00, 0.140, 0.126)$ was identified as the edge of the vector $-(x_R + x_S, y_R + y_S, z_R + z_S)$.

At this point it was obvious that the Re_2Si_2 core had an inversion centre or at least was very close to having one, otherwise a more complex vector pattern would have been expected corresponding to independent Re(1), Re(2), Si(1), and Si(2) positions.

A least squares refinement phased on the rhenium and silicon positions converged in two cycles yielding a discrepancy index, $R_1 = 0.132$, and a weighted residual, $R_2 = 0.186$. These "R factors" as calculated in the least squares program are defined as:

$$R_1 = \frac{\sum ||F_o| - |F_c||}{\sum |F_o|} \quad (4)$$

$$R_2 = \left\{ \frac{\sum w(|F_o| - |F_c|)^2}{\sum w|F_o|^2} \right\}^{1/2} \quad (5)$$

where $|F_o|$ and $|F_c|$ are the observed and calculated structure factor amplitudes respectively, and w the weighting factor is defined by $w = 1/\sigma^2(F)$.

Structure factors were calculated using the atomic scattering factors⁷⁵ for rhenium and silicon atoms to which the anomalous dispersion corrections,⁷⁶ both real and imaginary were applied⁷⁷ ($\Delta f'_{\text{Re}} = -5.58$, $\Delta f''_{\text{Re}} = 5.37$, $\Delta f'_{\text{Si}} = 0.23$, $\Delta f''_{\text{Si}} = 0.36$). The function which was minimized during the least squares refinement was $\sum w(|F_o| - |F_c|)^2$.

An electron density difference map, phased on the rhenium and silicon atom positions, yielded the location of all other non-hydrogen atoms. A least squares calculation performed on all non-hydrogen atoms converged in two cycles to $R_1 = 0.061$ and $R_2 = 0.074$. Decomposition and absorption corrections were applied to the data and one further cycle of refinement gave $R_1 = 0.055$ and $R_2 = 0.073$. Comparison of $|F_o|$ and $|F_c|$ showed no indication of extinction problems so no correction was applied. This was reasonable considering the width of the peaks ($\sim 2^\circ$) indicating high mosaicity of the crystals.

Refinement of the model with rhenium and silicon atoms having anisotropic temperature factors gave $R_1 = 0.039$ and $R_2 = 0.053$ after two cycles. An electron density difference map phased on this model showed features in the regions of the other atoms which suggested that they too be given anisotropic temperature

factors. This gave $R_1 = 0.034$ and $R_2 = 0.045$ after a further two cycles of refinement. The form of the temperature factors used was:

$$\exp [-(\beta_{11}h^2 + \beta_{22}k^2 + \beta_{33}l^2 + 2\beta_{12}hk + 2\beta_{13}hl + 2\beta_{23}kl)].$$

The validity of the anisotropic refinement was verified by a Hamilton's R test⁷⁹ at the 0.005 significance level.

An electron density difference map was calculated in an attempt to locate the hydrogen atoms in the structure, especially those attached to the rhenium atoms. It was encouraging that the highest peaks in the electron density difference map ($1.75 - 1.14 \text{ e } \text{\AA}^{-3}$) were located in the space between the rhenium and silicon atoms in the approximate position expected for a hydrogen bound to rhenium. For this reason the method of La Placa and Ibers³³ was used in an attempt to discern whether these peaks were hydrogen atoms or just artifacts arising from the improper treatment of the rhenium scattering or vibrations. Ibers reasoned that if the peak is not due to hydrogen scattering, then as the number of terms in the Fourier series is varied, the peak should disappear or shift markedly. A peak due to a hydrogen atom, however, should remain approximately in the same position and the peak height would be expected to vary in accordance

with the equation

$$\rho_H = \frac{1}{2\pi^2} \int_0^{s_0} (1 + a^2 s^2/4)^{-2} \exp(-Bs^2/16\pi^2) s^2 ds \quad (6)$$

where ρ_H is the electron density of the hydrogen atom, a is the Bohr radius = 0.5292 Å, $s = 4\pi\lambda^{-1} \sin \theta$, and B is the hydrogen temperature factor. Using a temperature factor of 3.6, electron density difference maps were calculated for $\sin \theta/\lambda$ cut-offs of 0.2, 0.25, 0.3, 0.35, 0.4, 0.58 (Complete Data). The results are summarized in Table 3.

TABLE 3: OBSERVED AND CALCULATED ELECTRON DENSITIES
FOR VARYING $\sin \theta/\lambda$ CUT-OFFS

SIN θ/λ LIMIT	NUMBER OF TERMS	$\rho_{CAL.}$ ($e\text{Å}^{-3}$)	$\rho_{OBS.}$ ($e\text{Å}^{-3}$)
0.20	74	0.16	0.49 - 0.42
0.25	143	0.25	0.78 - 0.6
0.30	243	0.33	1.07 - 0.87
0.35	371	0.41	1.25 - 0.97
0.40	556	0.47	1.44 - 1.02
0.58 (Complete Data)	1509	0.63	1.75 - 1.14

The electron density observed is in all cases much greater than that calculated by Ibers' formula. A representation of the electron density difference

factors. This gave $R_1 = 0.034$ and $R_2 = 0.045$ after a further two cycles of refinement. The form of the temperature factors used was:

$$\exp[-(\beta_{11}h^2 + \beta_{22}k^2 + \beta_{33}l^2 + 2\beta_{12}hk + 2\beta_{13}hl + 2\beta_{23}kl)].$$

The validity of the anisotropic refinement was verified by a Hamilton's R test⁷⁹ at the 0.005 significance level.

An electron density difference map was calculated in an attempt to locate the hydrogen atoms in the structure, especially those attached to the rhenium atoms. It was encouraging that the highest peaks in the electron density difference map ($1.75 - 1.14 \text{ e } \text{\AA}^{-3}$) were located in the space between the rhenium and silicon atoms in the approximate position expected for a hydrogen bound to rhenium. For this reason the method of La Placa and Ibers³³ was used in an attempt to discern whether these peaks were hydrogen atoms or just artifacts arising from the improper treatment of the rhenium scattering or vibrations. Ibers reasoned that if the peak is not due to hydrogen scattering, then as the number of terms in the Fourier series is varied, the peak should disappear or shift markedly. A peak due to a hydrogen atom, however, should remain approximately in the same position and the peak height would be expected to vary in accordance

with the equation

$$\rho_H = \frac{1}{2\pi^2} \int_0^{s_0} (1 + a^2 s^2/4)^{-2} \exp(-Bs^2/16\pi^2) s^2 ds \quad (6)$$

where ρ_H is the electron density of the hydrogen atom, a is the Bohr radius = 0.5292 Å, $s = 4\pi\lambda^{-1} \sin \theta$, and B is the hydrogen temperature factor. Using a temperature factor of 3.6, electron density difference maps were calculated for $\sin \theta/\lambda$ cut-offs of 0.2, 0.25, 0.3, 0.35, 0.4, 0.58 (Complete Data). The results are summarized in Table 3.

TABLE 3: OBSERVED AND CALCULATED ELECTRON DENSITIES
FOR VARYING $\sin \theta/\lambda$ CUT-OFFS

SIN θ/λ LIMIT	NUMBER OF TERMS	$\rho_{CAL.}$ ($e\text{\AA}^{-3}$)	$\rho_{OBS.}$ ($e\text{\AA}^{-3}$)
0.20	74	0.16	0.49 - 0.42
0.25	143	0.25	0.78 - 0.69
0.30	243	0.33	1.07 - 0.87
0.35	371	0.41	1.25 - 0.97
0.40	556	0.47	1.44 - 1.02
0.58 (Complete Data)	1509	0.63	1.75 - 1.14

The electron density observed is in all cases much greater than that calculated by Ibers' formula. A representation of the electron density difference

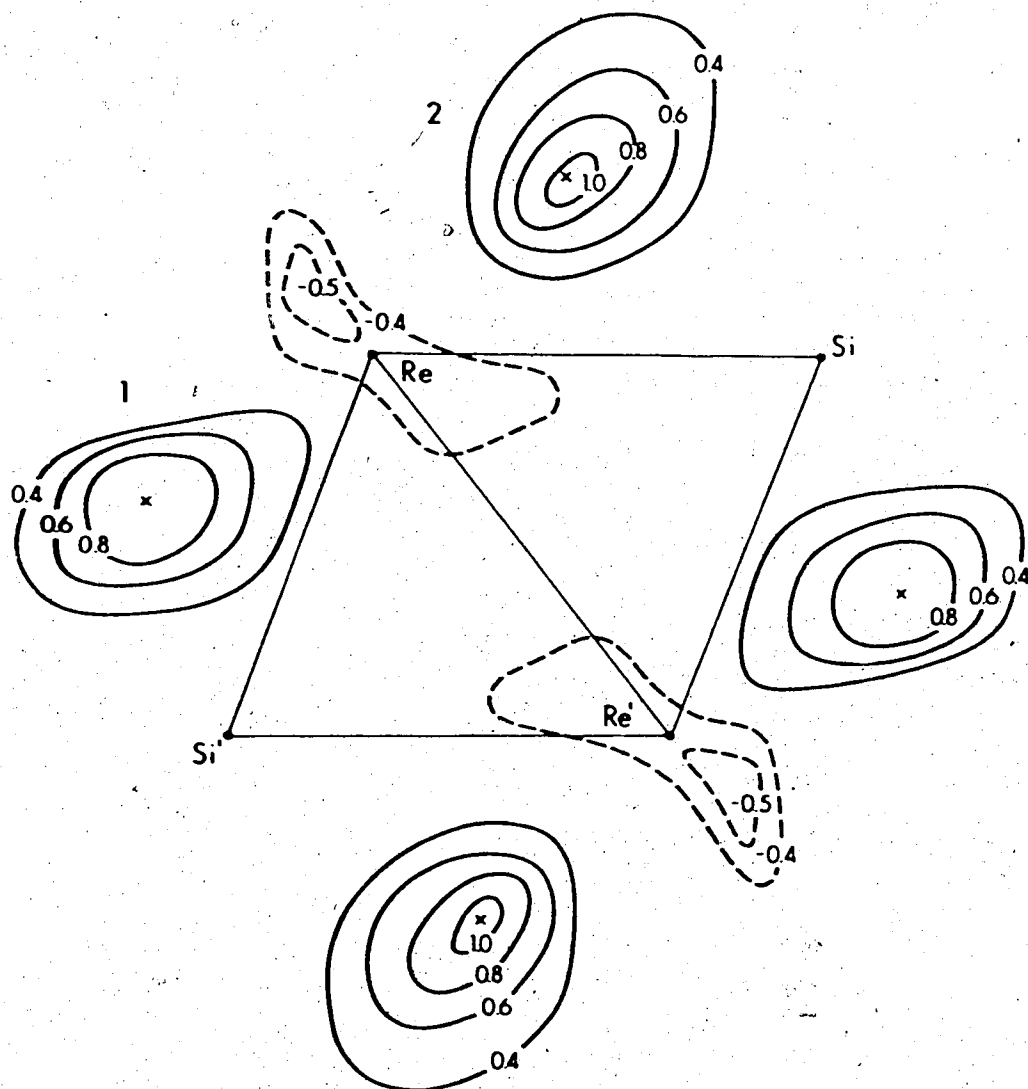


Fig. 2: ELECTRON DENSITY DIFFERENCE MAP THROUGH
 THE Re_2Si_2 PLANE [$(\text{SIN } \theta/\lambda)_{\text{MAX}} = 0.35$].

map calculated through the plane of the rhenium and silicon atoms for a $\sin \theta/\lambda$ limit of 0.35 is shown in Figure 2. The hydrogen, which could be situated anywhere within the $0.4e \text{ \AA}^{-3}$ contour on this diagram, therefore cannot be located with certainty. This implied that the peak height, although being contributed to by the hydrogen, could be receiving a strong contribution due to the inadequacy in description of the rhenium scattering. For this reason several least squares refinements and corresponding electron density difference maps were calculated making changes of $\pm 0.5 e$ to each of the real and imaginary parts of the anomalous dispersion corrections in turn. This produced no changes in the refinements or in the difference maps. It was therefore concluded that the peaks, although possibly containing contributions due to the hydrogen atoms, are due mainly to inadequacies of the model or systematic errors in the data. Among these are inadequate description of the scattering due to the rhenium atoms and residual absorption effects. In addition, doubt concerning the degree of contribution of the hydrogen ligands to these peaks existed because of the failure to locate the methylene hydrogen atoms of the ethyl groups.

The computer programmes used in solution and

refinement of structure and presentation of Data are listed and briefly described in Appendix 2.

RESULTS

The observed and calculated structure factor amplitudes, $|F_o|$ and $|F_c|$, are shown in Table 4. The final fractional coordinates of all atoms except hydrogens are shown in Table 5, their standard deviations being obtained from the inverse matrix of the final least squares analysis. The anisotropic U 's⁸⁰ and the equivalent isotropic B 's⁸¹ of all atoms are shown in Table 6. Relevant bond lengths and bond angles are shown in Table 7. The bond lengths and angles along with their standard deviations were obtained from ORFFE. A packing diagram for the face centred cell, viewed onto the $0kl$ plane is shown in Figure 4. The open bonds indicate molecules in the $0kl$ plane whereas solid bonds indicate molecules in the $1/2 kl$ plane.

TABLE 4: OBSERVED AND CALCULATED STRUCTURE

FACTOR AMPLITUDES (ELECTRONS X 10)

K	L	POBS	PCAL	K	L	POBS	PCAL	K	L	POBS	PCAL	K	L	POBS	PCAL
1	15	670	640	10	-8	1724	1780	-5	-5	1047	1004	7	1	4724	4657
5	11	1151	1111	10	-2	2559	2624	-5	-3	1870	1991	7	3	1579	1527
5	11	1194	1156	10	0	1572	1649	-5	1	1048	1220	7	5	788	777
7	11	1138	1054	10	2	274	318	-5	3	3108	3419	7	7	1838	1735
7	13	1085	1118	10	4	1658	1594	-5	5	3258	2929	7	9	1717	1672
9	7	1145	1135	10	6	658	698	-5	7	865	816	7	11	679	616
9	9	671	620	12	-16	1190	1253	-5	11	2774	2623	9	-15	2029	2061
9	11	1159	1195	12	-14	573	574	-5	13	1355	1364	9	-13	1395	1395
11	3	1715	1604	12	-12	1046	988	-5	15	526	506	9	-11	545	467
11	5	1639	1351	12	-10	2062	1939	-5	17	1540	1500	9	-9	2492	2872
13	1	542	490	12	-8	1597	1478	-5	19	1137	1133	9	-7	2953	2946
13	3	1100	998	12	-6	503	608	-3	-13	1818	1747	9	-5	677	651
13	5	850	840	12	-4	1105	1070	-3	-11	1690	1617	9	-3	583	631
15	-3	1374	1315	12	-2	1768	1750	-3	-7	2212	2242	9	-1	2349	2413
15	-1	368	365	12	0	1084	1038	-3	-5	4397	4512	9	1	2458	2750
15	1	360	365	12	2	874	794	-3	-3	3350	3653	9	3	665	639
17	-5	1291	1326	12	4	1110	1149	-3	-1	614	564	9	5	899	850
17	-3	1617	1015	14	-18	942	1030	-3	1	3449	3517	9	7	1289	1254
-12	18	947	994	14	-16	1216	1245	-3	3	5258	4857	9	9	934	942
-12	20	429	425	14	-14	418	359	-3	5	1253	1378	11	-17	874	928
-12	16	1881	1840	14	-12	1078	1055	-3	7	1074	1080	11	-15	1872	1877
-10	18	1677	1476	14	-10	1895	1750	-3	9	3026	2978	11	-13	1147	1137
-10	20	474	501	14	-8	1542	1443	-3	11	3174	3212	11	-11	1541	1503
-8	12	829	822	14	-6	452	395	-3	13	1085	1112	11	-9	2249	2117
-8	14	1676	1595	14	-4	1294	1218	-3	15	1161	1189	11	-7	1531	1368
-8	16	2740	2584	14	-2	1498	1719	-3	17	1800	1743	11	-5	1704	1483
-6	18	1364	1363	14	0	924	906	-3	19	992	1030	11	-3	1852	1795
-6	18	2705	2342	14	2	777	820	-3	19	1407	1382	11	1	1852	1795
-6	14	1782	1859	14	4	903	932	-3	13	2821	2649	11	3	815	798
-6	16	2131	2002	14	-2	1078	1118	-3	11	1657	1640	11	5	307	337
-6	18	942	909	14	-10	1842	1751	-3	9	902	812	13	-17	1137	1150
-6	6	1811	1646	14	-8	1070	1033	-3	7	3554	3521	13	-15	1851	1891
-6	8	3954	3857	14	-6	1157	1181	-3	5	5726	5777	13	-13	1174	1250
-4	10	2528	2467	14	-4	481	534	-3	3	3190	3193	13	-11	2105	2011
-4	12	267	260	14	0	481	534	-3	1	2204	2152	13	-9	2308	2227
-4	14	1393	1370	14	2	345	328	-3	1	4243	5578	13	-7	989	940
-4	16	2074	1959	14	-12	949	1017	-3	3	4097	4268	13	-5	527	509
-4	18	943	942	14	-10	975	995	-3	1	51026	958	13	-3	1479	1609
-2	4	1506	1656	14	-8	349	403	-3	1	72231	2342	13	-1	1455	1678
-2	6	1799	1736	14	-6	327	367	-3	1	9348	8121	13	1	439	457
-2	8	4109	4301	14	-4	755	611	-3	1	12428	2464	13	3	439	457
-2	10	2406	2473	14	-2	979	974	-3	1	151305	1380	13	5	640	690
-2	12	1580	1547	14	0	1397	1224	1	1	1444	1671	15	-17	1116	1152
-2	14	2048	1985	14	2	955	1040	1	1	585	533	15	-13	693	677
-2	16	924	925	14	4	298	339	1	1	1880	1728	15	-11	799	850
-2	18	4021	4355	14	6	1464	1394	1	1	2332	2212	15	-9	1404	1738
0	4	1623	1535	14	8	390	314	1	1	812	813	15	-7	1420	1392
0	6	2199	2485	14	10	848	797	1	1	1358	1350	15	-5	323	337
0	8	3853	4072	14	12	1284	1313	1	1	3448	3464	15	-3	844	813
0	10	2149	2204	14	14	1008	1025	1	1	5770	3426	15	-1	1331	1362
0	12	830	834	14	16	630	641	1	1	12894	2838	15	1	792	848
0	14	2345	2254	14	18	432	513	1	1	4243	4707	17	-15	934	940
0	16	1729	1710	14	20	1626	1542	1	1	32475	2477	17	-11	824	832
0	18	431	484	14	22	1680	1612	1	1	5527	4887	17	-9	1140	1132
2	-2	8554	8848	14	24	845	940	1	1	72206	2345	17	-7	801	788
2	0	5623	6229	14	26	904	884	1	1	2485	2754	17	-5	801	788
2	2	2028	2023	14	28	11849	1090	1	1	11355	1345	-18	6	1137	1139
2	4	871	925	14	30	1338	1332	1	1	151163	1124	-18	8	784	729
2	6	2706	2833	14	32	15291	274	1	1	17124	1148	-18	12	721	712
2	8	2526	2684	14	34	547	585	1	1	19464	544	-18	16	421	613
2	10	457	420	14	36	1073	1158	1	1	151651	1549	-18	20	708	704
2	12	1024	1039	14	38	1199	914	1	1	132477	2381	-18	24	1260	1204
2	14	1485	1441	14	40	144	604	1	1	111175	1200	-18	28	818	776
2	16	1083	1050	14	42	2494	2444	1	1	91185	1094	-18	32	663	735
2	18	671	394	14	44	5242	2539	1	1	72827	2480	-18	36	828	887
2	20	2760	2807	14	46	608	547	1	1	52791	2585	-18	40	478	557
4	0	5761	5654	14	48	9243	1258	1	1	32543	2408	-18	44	431	439
4	2	1924	1916	14	50	1247	2580	1	1	2042	2160	-18	48	1140	1085
4	4	1134	1218	14	52	1978	2028	1	1	1204	1412	-18	52	1042	1012
4	6	1945	2084	14	54	305	294	1	1	32231	2421	-14	4	1094	967
4	8	1945	1941	14	56	1031	1052	1	1	5297	380	-14	8	1871	1782
4	10	897	954	14	58	1381	1404	1	1	7470	958	-14	12	1343	1249
4	12	542	570	14	60	2419	2445	1	1	92482	2441	-14	16	873	930
4	14	1331	1220	14	62	2619	2645	1	1	111732	1722	-14	20	1222	1317
4	16	3827	3795	14	64	1980	1974	1	1	15443	941	-14	24	14	844
4	18	1939	2021	14	66	1823	1829	1	1	19449	422	-12	28	953	949
4	20	2594	2917	14	68	4092	4158	1	1	17542	514	-12	32	1424	1423
4	22	4553	4040	14	70	7498	2825	1	1	152113	1980	-12	36	1394	1354
4	24	1507	1449	14	72	494	450	1	1	132753	2585	-12	40	1775	1731
4	26	1250	1164	14	74	2493	2547	1	1	112491	1228	-12	44	2461	2754
4	28	2570	2517	14	76	3373	3374	1	1	91717	1660	-12	48	1368	1374
4	30	2121	2083	14	78	1815	1624	1	1	37559	3848	-12	52	618	639
4	32	1875	1818	14	80	520	520	1	1	52472	2495	-12	56	1553	1587
4	34	1270	1270	14	82	1474	1491	1	1	576	451	-12	60	1634	1621
4	36	3098	3040	14	84	1343	1362	1	1	12481	3171	-12	64	712	737
4	38	1903	1852	14	86	1594	1519	1	1	53771	5467	-12	68	611	648
4	40	1917	1923	14	88	2454	2439	1	1	32038	2834	-10	72	987	942
4	42	1349	1400	14	90	1982	1841	1	1	1982	1993	-10	76	354	344
4	44	3515	3449	14	92	2317	2453	1	1	92500	2447	-10	80	1719	1650
4	46	3149	2955	14	94	3470	3843	1	1	111093	1092	-10	84	2371	2380
4	48	2704	274	14	96	5125	1352	1	1	13318	244	-10	88	1107	1289
4	50	1773	1712	14	98	881	814	1	1	171083	1049	-10	92	21018	1045
4	52	2774	2679	14	100	9207	1905	1	1	152735	2455	-10	96	2749	2804
4	54	1540	1525	14	102	2790	2444	1	1	132304	2245	-10	100	62818	2784
4	56	634	588	14	104	1048	1081	1	1	92444	2458	-10	104	905	

Table 4 (continued)

K	L	POBS	PCAL	K	L	POBS	PCAL	K	L	POBS	PCAL	K	L	POBS	PCAL	K	L	POBS	PCAL
2	12	1817	1803	-15	7	1400	1301	-1	11	1354	1327	15	-11	1121	1117	-2	2	2191	2082
2	14	327	324	-15	9	1257	1216	-1	13	1742	1757	15	-7	813	577	-2	4	278	224
2	16	360	379	-15	11	864	805	-1	15	933	939	15	-5	844	846	-2	6	2128	2117
4	-18	1236	1249	-15	15	1251	1307	1	-17	1340	1304	15	-3	769	828	-2	8	3114	3125
4	-14	1880	1850	-15	17	1002	1070	1	-15	837	830	17	-11	990	943	-2	10	1149	1186
4	-12	3348	3204	-13	-5	477	520	1	-9	3451	3282	17	-9	101	250	-2	12	297	279
4	-10	1914	1815	-13	-3	600	517	1	-7	2127	2022	17	-9	101	250	-2	14	809	903
4	-8	367	275	-13	-1	1478	1502	1	-5	1034	1050	17	-9	101	250	-2	16	116	1168
4	-6	3781	3909	-13	1	1528	1555	1	-3	3406	3290	17	-9	101	250	0	-14	1351	1352
4	-4	4094	6304	-13	3	593	554	1	-1	2578	2597	16	8	833	711	0	-10	1310	1318
4	-2	2325	2633	-13	5	1057	1017	1	-1	1383	1458	16	10	1300	1261	0	-10	1302	1287
4	0	1190	1158	-13	7	2299	2140	1	1	3133	3914	16	12	810	881	0	-8	3160	3047
4	2	3408	3611	-13	9	1580	1526	1	3	3871	3593	16	14	1129	1139	0	-6	2497	2414
4	4	3472	3500	-13	11	1111	1134	1	5	2598	2593	16	16	1545	1561	0	-4	322	223
4	6	927	929	-13	13	1663	1642	1	7	267	314	16	18	843	775	0	-2	2906	2714
4	8	1383	1342	-13	15	968	990	1	9	1275	1248	16	20	652	328	0	0	3966	4023
4	10	2212	2229	-11	-7	939	982	1	11	1749	1771	16	22	1256	1178	0	2	2154	2144
4	12	1633	1650	-11	-5	316	301	1	13	1075	1098	16	24	655	674	0	4	2461	2446
4	14	294	312	-11	-3	999	982	1	15	1075	1098	16	26	607	667	0	6	2974	3018
6	-20	1484	1533	-11	-1	2133	2161	3	-19	1237	1286	16	28	607	667	0	8	1172	1155
6	-18	872	871	-11	1	1667	1610	3	-17	1778	1785	16	30	1046	1108	0	10	1255	1282
6	-16	451	472	-11	3	1646	1670	3	-15	753	731	16	32	975	1035	0	12	555	543
6	-14	2214	2080	-11	5	2582	2603	3	-13	975	963	16	34	649	662	0	14	1271	1282
6	-12	3141	3163	-11	7	1172	1417	3	-11	2888	2800	16	36	537	419	2	-18	844	918
6	-10	1377	1430	-11	9	323	326	3	-9	3613	3431	16	38	1327	1316	2	-16	1652	1692
6	-8	1410	1425	-11	11	1273	1260	3	-7	1282	1182	16	40	1467	1621	2	-14	1282	1285
6	-6	3701	3682	-11	13	1520	1575	3	-5	3080	2965	16	42	794	834	2	-10	2732	2454
6	-4	3485	3654	-11	15	1774	797	3	-3	4943	5057	16	44	577	604	2	-8	4643	4474
6	-2	1115	1202	-11	17	255	321	3	-1	2310	2758	16	46	1427	1424	2	-6	1742	1721
6	0	1736	1692	-9	-9	1109	1097	3	1	252	213	16	48	1142	1219	2	-4	1093	1090
6	2	3408	3384	-9	-7	996	1065	3	3	2755	2848	16	50	373	338	2	-2	2986	3104
6	4	2047	2026	-9	-5	1311	1322	3	5	3971	4053	16	52	704	683	2	0	3853	4116
6	6	1305	1278	-9	-3	1900	1942	3	7	1799	1817	16	54	1126	1127	2	2	1557	1459
6	8	1422	1411	-9	-1	1228	1275	3	9	411	338	16	56	757	784	2	4	1359	1369
6	10	891	926	-9	1	1757	1730	3	11	1722	1697	16	58	674	678	2	6	2948	2491
6	12	1205	1238	-9	3	2918	2997	3	13	1723	1761	16	60	1140	1156	2	8	2355	2384
6	14	470	470	-9	5	1173	1190	5	-19	1427	1440	16	62	767	745	2	10	375	391
6	16	444	482	-9	7	395	416	5	-17	1295	1292	16	64	486	453	2	12	1005	995
6	18	1982	2050	-9	9	948	902	5	-15	1262	1213	16	66	1495	1537	2	14	1208	1250
6	20	2406	2400	-9	11	1378	1364	5	-13	2820	2782	16	68	1822	1844	2	16	1044	1051
6	22	443	508	-9	13	761	742	5	-11	2074	2074	16	70	828	853	2	18	1628	1620
6	24	1391	1381	-9	15	386	347	5	-9	717	570	16	72	640	639	2	20	540	500
6	26	2467	2478	-9	17	707	604	5	-7	3055	3206	16	74	1494	1502	2	22	894	898
6	28	2230	2296	-7	-9	1485	1422	5	-5	3477	3740	16	76	1354	1385	2	24	2534	2442
6	30	554	507	-7	-7	1519	1479	5	-3	1493	1482	16	78	527	491	2	26	3111	3080
6	32	1762	1727	-7	-5	516	504	5	-1	423	397	16	80	785	798	2	28	1041	1100
6	34	2504	2440	-7	-3	1137	1141	5	1	2384	2360	16	82	1377	1445	2	30	1228	1225
6	36	1281	1235	-7	-1	3225	3396	5	3	2636	2587	16	84	1857	1847	2	32	2653	2634
6	38	888	871	-7	1	2336	2531	5	5	732	730	16	86	986	1011	2	34	2140	2167
6	40	1049	1100	-7	3	1937	1956	5	7	674	657	16	88	1737	1673	2	36	261	194
10	-20	1024	1112	-7	5	3509	3453	5	9	1207	1240	16	90	1257	1273	2	38	1191	1175
10	-18	639	668	-7	7	2187	2266	7	11	1280	1307	16	92	505	449	2	40	2077	2010
10	-16	472	458	-7	9	1592	1540	7	13	1215	1199	16	94	2212	2328	2	42	1395	1404
10	-14	1659	1643	-7	11	1764	1724	7	15	1405	1417	16	96	2463	2557	2	44	732	748
10	-12	1843	1881	-7	13	854	809	7	17	2052	2035	16	98	1125	1165	2	46	1044	1058
10	-10	854	915	-7	15	373	388	7	19	1238	1278	16	100	959	950	2	48	1444	1470
10	-8	744	694	-5	-11	1246	1257	7	21	2454	2401	16	102	2533	2522	2	50	544	605
10	-6	2081	2076	-5	-9	2407	2677	7	23	1454	1401	16	104	1994	1953	2	52	444	347
10	-4	1926	1916	-5	-7	1978	1977	7	25	1130	1231	16	106	1424	409	2	54	1884	1948
10	-2	623	642	-5	-5	410	431	7	27	1522	1485	16	108	1047	1030	2	56	2949	3082
10	0	1222	1207	-5	-3	2569	2770	7	29	1872	1846	16	110	1692	1658	2	58	1272	1233
10	2	2100	2069	-5	-1	3778	4085	7	31	745	774	16	112	1060	1075	2	60	1053	1051
10	4	1290	1270	-5	1	1944	2113	7	33	372	370	16	114	538	574	2	62	1956	2008
10	6	672	663	-5	3	583	624	7	35	1189	911	16	116	622	591	2	64	1802	1830
12	-18	607	582	-5	5	3604	3512	9	37	1284	1305	16	118	1920	1871	2	66	941	922
12	-16	737	730	-5	7	4430	4263	9	39	1059	1010	16	120	2324	2310	2	68	840	843
12	-14	1978	1967	-5	9	1107	1094	9	41	1124	1044	16	122	404	615	2	70	1457	1479
12	-12	2209	2144	-5	11	1532	1557	9	43	2328	2335	16	124	1829	1916	2	72	1234	1267
12	-10	473	523	-5	13	2049	2030	9	45	1643	1650	16	126	3178	3295	2	74	1818	1200
12	-8	1711	1644	-5	15	1591	1560	9	47	272	274	16	128	2393	2527	2	76	1547	1557
12	-6	2366	2297	-5	17	428	447	9	49	2677	2255	16	130	448	440	2	78	781	830
12	-4	1600	1540	-3	-15	704	738	9	51	1447	1541	16	132	2547	2540	2	80	2320	2312
12	0	1590	1607	-3	-13	1834	1744	9	53	267	101	16	134	3460	3594	2	82	2470	2425
12	2	2049	2102	-3	-11	3128	2994	9	55	1737	1708	16	136	1520	1474	2	84	811	852
12	4	845	878	-3	-9	1572	1612	9	57	1702	1659	16	138	357	305	2	86	1174	1230
12	6	1007	1043	-3	-7	1071	1117	9	59	559	508	16	140	1740	1742	2	88	2345	2457
14	-18	1828	1745	-3	-5	3384	3508	11	-19	1480	1541	16	142	741	741	2	90	1934	1940
14	-16	1069	1058	-3	-														

Table 4 (continued)

E	L	POBS	PCAL	E	L	POBS	PCAL	E	L	POBS	PCAL	E	L	POBS	PCAL	E	L	POBS	PCAL
94	-16	704	721	1	-13	2104	2277	-8	-8	332	328	10	-8	943	903	7	-1	1425	1425
94	-12	699	675	1	-11	720	670	-8	-6	687	697	10	-6	1108	1352	7	-1	430	428
94	-10	1189	1123	1	-7	1401	1329	-8	-4	1516	1524	10	-4	894	861	7	1	644	675
94	-8	818	817	1	-7	2832	2664	-8	-2	1637	1657	10	0	868	882	7	3	1091	1098
94	-4	901	950	1	-5	2452	2364	-8	0	1292	1307	10	-2	897	943	9	-13	986	1031
94	-2	1097	1132	1	-3	407	429	-8	4	1813	1815	12	-12	874	903	9	-11	1275	1259
94	-10	1108	1150	1	-1	2247	2264	-8	6	947	1011	12	-8	847	820	9	-9	399	481
94	-8	593	674	1	1	3447	3453	-8	10	1216	1210	12	-6	1275	1284	9	-5	940	967
				1	3	1793	1814	-8	12	1774	1678	12	-4	799	840	9	-3	1180	1170
				1	7	1939	1848	-8	14	-741	747					9	-1	440	446
-95	1	553	542	1	9	2118	2129	-6	-10	804	848	-13	3	298	282	11	-9	512	548
-95	3	1116	1078	1	11	839	804	-6	-6	691	739	-13	5	430	612	11	-7	340	324
-95	5	844	837	1	13	323	338	-6	-4	1440	1534	-13	7	2223	1186	11	-5	1072	1084
-95	7	355	329	3	-17	628	630	-6	-2	1366	1340	-13	9	793	785				
-95	9	852	803	3	-15	1610	1590	-6	-2	1242	1220	-11	-8	664	657	-10	3	495	754
-95	11	1218	1298	3	-13	1360	1357	-6	4	1704	1704	-11	-1	891	797	-10	2	740	743
-95	13	695	767	3	-9	1220	1204	-6	6	987	951	-11	-6	987	951	-10	6	675	579
-13	-3	777	793	3	-7	2294	2282	-6	10	1125	1092	-11	5	1075	1107	-10	8	816	888
-13	-1	418	147	3	-5	1575	1401	-6	12	1453	1430	-11	7	1513	1409	-10	8	816	888
-13	1	588	607	3	-3	447	430	-6	14	720	680	-11	9	668	724	-8	-2	364	395
-13	3	1092	1144	3	-1	2080	2158	-6	-12	1015	1014	-11	11	231	224	-8	0	949	888
-13	5	860	790	3	1	2281	2260	-6	-10	1082	1099	-9	-3	978	901	-8	2	921	903
-13	7	910	842	3	3	1080	1060	-6	-8	845	514	-9	-1	1270	1287	-8	6	703	734
-13	9	1230	1294	3	7	1480	1492	-6	-6	725	720	-6	1	638	685	-8	10	715	684
-13	11	724	731	3	9	1594	1577	-6	-4	2123	2134	-9	3	410	378	-6	-6	1029	1032
-13	13	932	943	3	11	454	450	-6	-2	1803	1874	-9	5	1280	1195	-6	-4	527	315
-11	-3	1110	1128	5	-9	450	487	-4	-2	1524	1545	-8	7	1289	1374	-6	-4	527	315
-11	-1	383	374	5	-15	1409	1332	-4	4	2470	2431	-9	9	508	541	-6	-2	605	634
-11	1	1029	990	5	-13	1444	1473	-4	6	1523	1472	-9	11	374	395	-6	0	1313	1344
-11	3	1644	1655	5	-11	520	551	-4	8	1021	1175	-9	13	743	797	-6	2	1102	1083
-11	5	1025	997	5	-9	1434	1344	-4	10	1024	1725	-7	-7	636	618	-6	6	1071	1073
-11	7	796	853	5	-7	2471	2490	-4	12	841	842	-7	-3	1087	1083	-6	8	1341	1404
-11	9	1174	1197	5	-5	1447	1440	-2	-14	545	410	-7	-1	1423	1475	-6	10	810	797
-11	11	1033	1045	5	-3	377	395	-2	-12	1541	1543	-7	1	730	679	-4	-6	1099	1017
-9	-9	291	298	5	-1	1385	1374	-2	-10	1391	1354	-7	5	1091	1045	-8	-2	1301	1315
-9	-7	449	624	5	1	2419	2544	-2	-8	1425	1413	-7	9	1341	1353	-8	0	1593	1584
-9	-5	1643	1632	5	3	1528	1484	-2	-6	2747	2624	-7	4	574	617	-8	2	730	712
-9	-3	1442	1453	5	7	1290	1265	-2	-4	1495	1744	-7	11	424	384	-6	4	328	349
-9	-1	1400	1412	5	9	1357	1365	-2	-2	2474	2541	-7	13	827	841	-6	6	1354	1331
-9	1	2393	2474	7	-17	771	794	-2	4	2924	2919	-5	-9	1242	1320	-4	8	1443	1425
-9	3	1449	1444	7	-15	1708	1747	-2	6	1075	1070	-5	-7	831	830	-4	10	874	844
-9	5	1642	1516	7	-13	1293	1307	-2	8	507	499	-5	-3	1288	1329	-2	-6	1285	1257
-9	7	1944	1949	7	-11	1784	1789	-2	10	1572	1574	-5	-1	2075	2052	-2	-6	625	590
-9	9	942	948	7	-9	2487	2434	-2	12	1569	1545	-5	1	1207	1207	-2	-2	1138	1097
-9	11	403	353	7	-7	1719	1734	-2	14	403	426	-5	3	435	444	-2	0	1424	1404
-9	13	941	995	7	-5	399	403	-2	16	1080	1130	-5	5	1077	1084	-2	2	627	644
-7	-17	725	784	7	-3	2232	2244	0	-12	1803	1747	-5	7	1524	1495	-2	4	445	471
-7	-15	1219	1239	7	-1	2213	2174	0	-10	453	411	-5	9	599	621	-2	6	1092	1093
-7	-13	2254	2252	7	3	946	872	0	-8	405	338	-5	11	609	583	-2	8	944	937
-7	-11	1748	1421	7	5	431	418	0	-6	1924	1741	-5	13	1132	1174	0	-10	813	811
-7	-9	748	848	7	7	1461	1473	0	-4	3099	2903	-3	-1	1118	1159	0	-8	1375	1312
-7	-7	2448	2514	7	-17	1031	1049	0	-2	1235	1154	-3	-9	1560	1534	0	-6	403	394
-7	-5	2813	2940	7	-15	1447	1544	0	0	1153	1171	-3	-7	439	427	0	-2	1417	1324
-7	-3	1155	1044	7	-13	830	841	0	2	2353	2294	-3	-5	740	748	0	0	1458	1434
-7	-1	743	784	7	-11	374	444	0	4	2145	2090	-3	-3	2148	2040	0	2	690	678
-7	1	1768	1744	7	-9	2049	2084	0	6	711	715	-3	-1	2244	2218	0	4	934	939
-7	3	1474	1444	7	-7	2412	2444	0	8	449	484	-3	1	449	484	0	6	1055	1080
-7	5	888	515	7	-5	789	738	0	10	1340	1344	-3	3	1251	1204	2	10	1085	1102
-7	7	934	913	7	-3	401	495	0	12	944	975	-3	5	1733	1700	2	-8	1549	1553
-7	9	1124	1140	7	-1	1707	1452	2	-14	1331	1114	-3	7	1261	1252	2	-6	751	737
-7	11	1124	1125	7	1	1454	1414	2	-12	1654	1618	-3	9	1110	1074	2	-4	457	501
-5	-13	1025	1125	9	3	454	414	2	-10	672	648	-3	11	409	478	2	-2	1570	1540
-5	-11	638	653	9	5	740	757	2	-8	943	955	-3	13	338	320	2	0	1624	1644
-5	-9	444	423	9	7	1072	1051	2	-6	1817	1773	-3	15	129	1308	2	2	643	634
-5	-7	1322	1381	11	-17	1072	1051	2	-4	2115	2081	-3	17	1049	1012	2	4	604	604
-5	-5	1902	1945	11	-15	1130	1123	2	-2	788	752	-3	19	2044	1904	2	6	1194	1214
-5	-3	893	913	11	-13	370	332	2	0	455	426	-3	21	1527	1472	2	8	441	445
-5	-1	737	770	11	-11	428	502	2	2	1949	1884	-3	23	1175	1153	2	10	1374	1352
-5	1	2155	2177	11	-9	1555	1551	2	4	1854	1830	-3	25	1522	1504	2	12	1421	1421
-5	3	2371	2395	11	-7	1577	1558	2	6	829	818	-3	27	820	782	2	14	420	444
-5	5	777	771	11	-5	409	382	2	8	454	427	-3	29	254	161	2	16	1556	1631
-5	7	754	774	11	-3	724	714	2	10	931	958	-3	31	447	444	2	18	1313	1322
-5	9	1579	1481	11	-1	1151	1144	2	12	1202	1207	-3	33	840	831	2	20	849	879
-5	11	1241	1224	11	1	854	834	4	-18	1202	1207	-3	35	1285	1255	2	22	1038	1122
-5	13	724	693	13	-15	941	984	4	-12	1472	1488	-3	37	1213	1213	2	24	821	879
-5	15	1440	1409	13	-13	482	502	4	-10	898	934	-3	39	1008	1444	2	26	729	735
-5	17	697	742	13	-11	338	281	4	-8	1543	1555	-3	41	1533	1516	2	28	1114	1174
-5	19	1407	1345	13	-9	1144	1145	4	-6	2431	2377	-3	43	1280	1264	2	30	740	797
-5	21	2449	2441	13	-7	1335	1329	4	-4	1132	1224	-3	45	1280	1264	2	32	813	844
-5	23	1494	1512	13	-5	514	500	4	-2	2045	1959	-3	47	1439	1405	2	34	545	555
-5	25	751	743																

TABLE 5: ATOMIC POSITIONAL PARAMETERS^a

ATOM	x	y	z
Re	0.11870 (5)	-0.01029 (3)	-0.06551 (2)
Si	-0.0875 (3)	-0.1386 (2)	-0.0709 (2)
C1	0.271 (1)	-0.0259 (7)	-0.1477 (7)
C2	-0.041 (1)	0.0202 (7)	-0.1282 (7)
C3	0.278 (1)	-0.0428 (8)	-0.0045 (7)
C4	-0.409 (2)	-0.240 (1)	-0.1392 (8)
C5	-0.261 (1)	-0.1901 (8)	-0.1570 (6)
C6	-0.006 (1)	-0.2389 (8)	-0.0638 (6)
C7	0.075 (2)	-0.3048 (9)	-0.1401 (8)
O1	0.364 (1)	-0.0351 (7)	-0.1945 (6)
O2	-0.129 (1)	0.0377 (7)	-0.1691 (6)
O3	0.377 (1)	-0.0623 (8)	0.0298 (6)

^aStandard deviations in parentheses refer to last digit quoted.

TABLE 6: THERMAL PARAMETERS (\AA^2)

Atom	U_{11}	U_{22}	U_{33}	U_{12}	U_{13}	U_{23}	B^a (\AA^2)
Re	0.0380(3)	0.0406(3)	0.0331(3)	0.0010(2)	0.0037(2)	0.0175(2)	2.98
Si	0.0471(14)	0.0394(13)	0.0379(13)	-0.0013(10)	0.0018(10)	0.0176(11)	3.37
C1	0.062(7)	0.048(6)	0.048(6)	-0.006(5)	-0.001(5)	0.021(5)	4.36
C2	0.064(7)	0.043(6)	0.054(6)	0.000(5)	0.013(5)	0.020(5)	4.39
C3	0.052(6)	0.058(6)	0.054(6)	0.004(5)	0.016(5)	0.026(5)	4.35
C4	0.060(8)	0.098(11)	0.068(8)	-0.028(7)	-0.004(6)	0.037(7)	6.38
C5	0.055(6)	0.060(6)	0.045(6)	-0.008(5)	-0.005(5)	0.020(5)	4.53
C6	0.076(8)	0.052(6)	0.046(6)	0.008(5)	0.013(5)	0.027(5)	4.49
C7	0.116(11)	(8)	0.068(8)	0.043(8)	0.028(7)	0.030(7)	6.50
O1	0.086(7)	0.103(8)	0.076(6)	0.004(5)	0.034(5)	0.036(6)	7.19
O2	0.082(6)	0.097(7)	0.063(5)	0.026(5)	-0.003(4)	0.049(5)	5.99
O3	0.054(5)	0.129(8)	0.095(7)	0.024(5)	0.006(4)	0.076(6)	6.53

^aEquivalent isotopic thermal parameter.

TABLE 7: INTRAMOLECULAR DISTANCES AND ANGLES

INTRAMOLECULAR DISTANCES ^a (Å)			
Re-Re' ^b	3.084(1)	Si-C6	1.88(1)
Re-Si	2.533(2)	Cl-O1	1.14(2)
Re-Si'	2.535(3)	C2-O2	1.17(1)
Re-Cl	1.94(1)	C3-O3	1.17(1)
Re-C2	1.96(1)	C4-C5	1.54(1)
Re-C3	1.97(1)	C6-C7	1.52(2)
Si-C4	1.885(8)		
INTRAMOLECULAR ANGLES ^a (DEGREES)			
Re-Re'-Cl ^b	178.5(3)	C3-Re-C2	179.1(5)
Re-Re'-C2	91.0(3)	C4-Si-C6	108.5(5)
Re-Re'-C3	89.3(3)	Re-Si-Re'	74.9(1)
Re-Re'-Si	52.6(1)	Re-Cl-O1	178.0(9)
Re-Re'-Si'	52.5(1)	Re-C2-O2	175.7(9)
Cl-Re-C3	89.4(4)	Re-C3-O3	177.5(9)
Cl-Re-C2	90.3(4)	Si-C4-C5	114.5(8)
Cl-Re-Si	126.6(3)	Si-C6-C7	115.0(10)
Cl-Re-Si'	128.3(3)		

^aStandard deviations in parentheses refer to last digit quoted.

^bPrimed atoms related by an inversion centre.

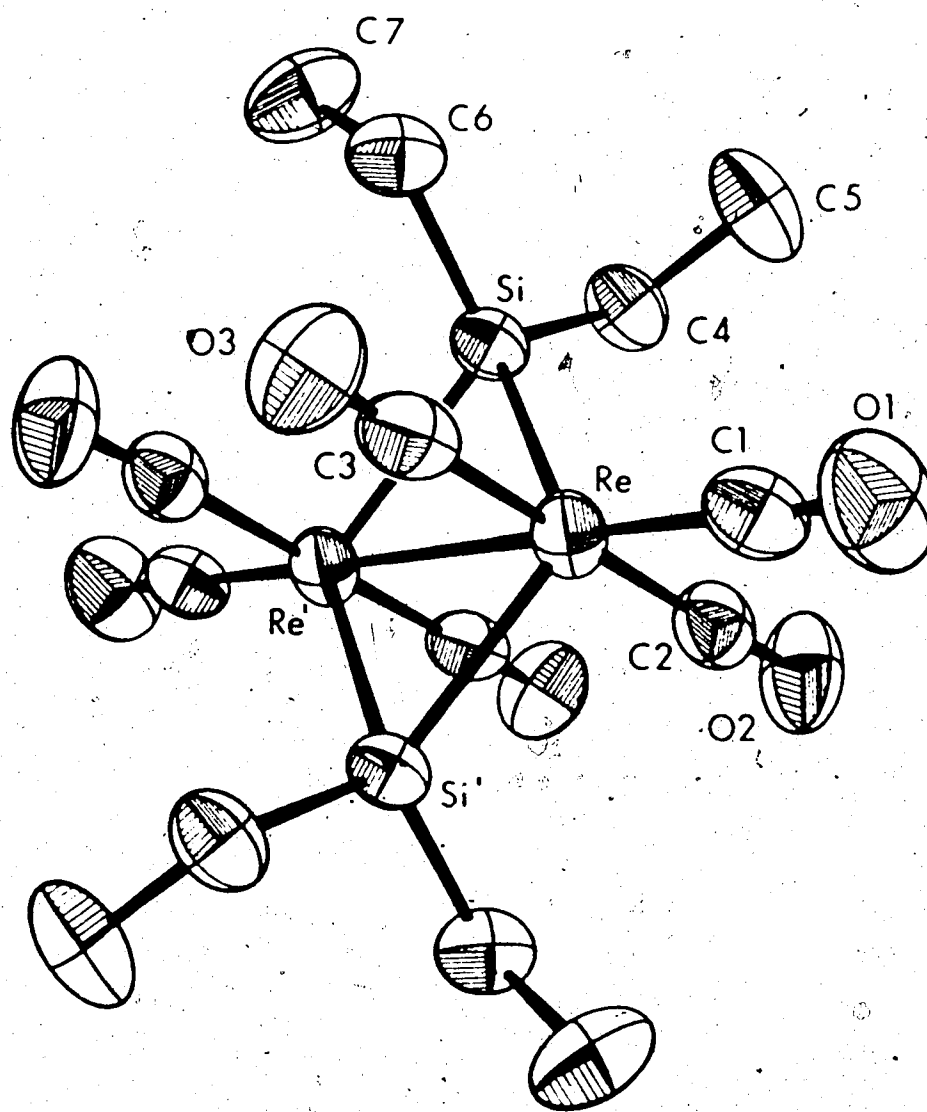


Fig. 3: A PERSPECTIVE VIEW OF $\text{Re}_2(\text{CO})_6\text{H}_4[\text{Si}(\text{C}_2\text{H}_5)_2]_2$.

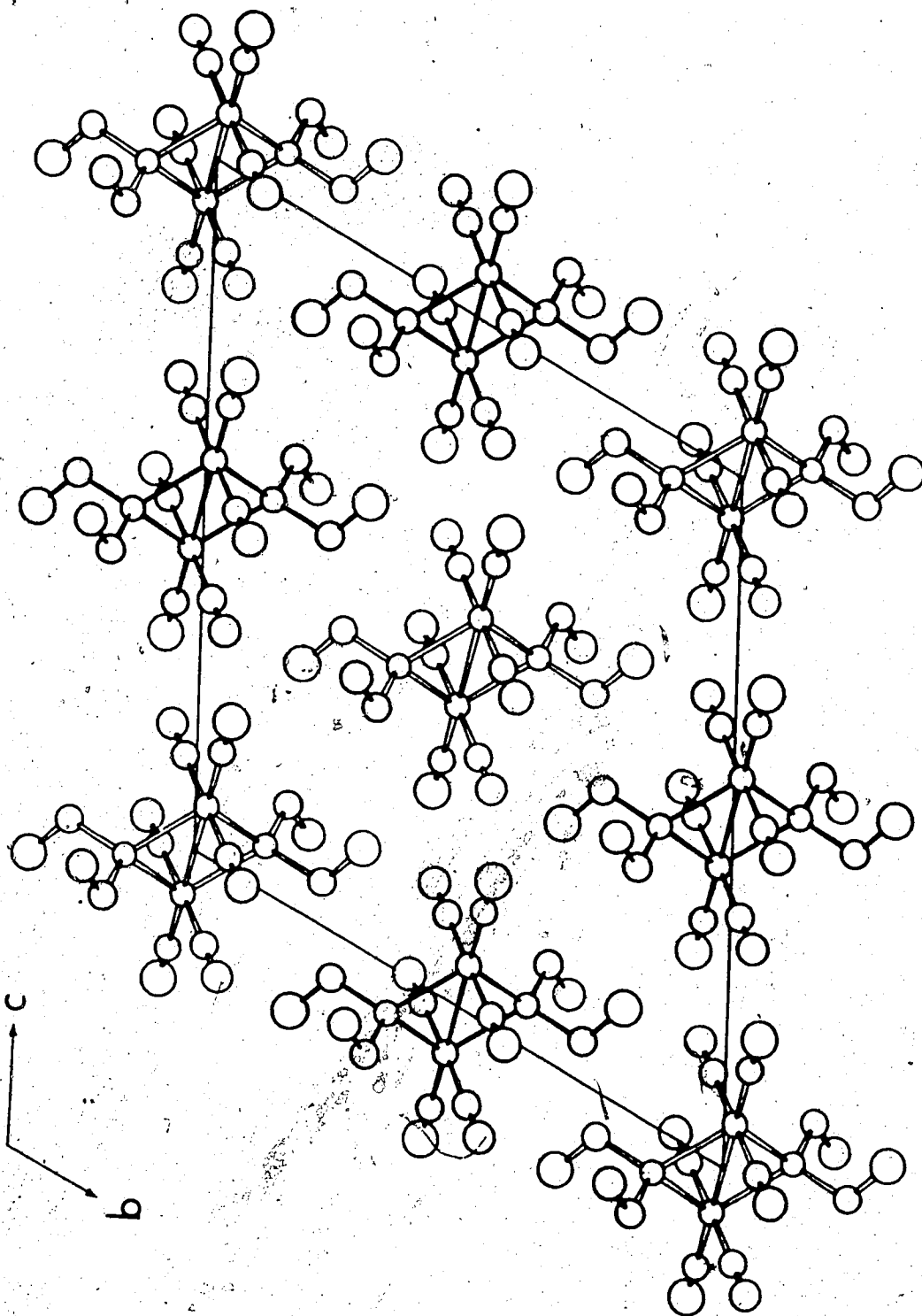


Fig. 4: PACKING DIAGRAM FOR $\text{Re}_2(\text{CO})_6\text{H}_4[\text{Si}(\text{C}_2\text{H}_5)_2]_2$,
PROJECTED ON bc PLANE.

DESCRIPTION OF STRUCTURE

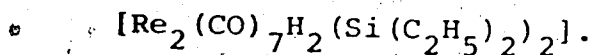
$\text{Re}_2(\text{CO})_6\text{H}_4[\text{Si}(\text{C}_2\text{H}_5)_2]_2$ has approximate C_{2h} molecular symmetry. Its molecular structure is shown in Figure 3. The molecule is composed of a central cluster of two rhenium and two silicon atoms in the shape of a rhombus, with like atoms at opposing corners, and a bond joining the two rheniums across the shorter diagonal. One carbonyl group on each rhenium lies approximately along the Re-Re axis, while the other four lie above and below the plane of the rhombus, two on each rhenium. The ethyl groups are bonded two to each silicon, one above and one below the rhombus plane, giving the silicon atoms a distorted tetrahedral environment.

The Re-Re distance is $3.084(1) \text{ \AA}$, compared with $3.121(2) \text{ \AA}$ in $\text{Re}_2(\text{CO})_8\text{H}_2\text{Si}(\text{C}_6\text{H}_5)_2$,^{62,65} $3.001(1) \text{ \AA}$ in $\text{Re}_2(\text{CO})_8[\text{Si}(\text{C}_6\text{H}_5)_2]_2$,⁶⁴ and 3.02 \AA in $\text{Re}_2(\text{CO})_{10}$,^{45,82,83} and thus is again consistent with a Re-Re single bond. This is further substantiated by the acute Re-Si-Re angle $[74.9(1)^\circ]$. The average Re-C (carbonyl) distance is 1.96 \AA and the average C-O distance is 1.16 \AA . These agree well with the carbonyl distances in other rhenium carbonyl derivatives.^{62,64,65} The Re-C and C-O bonds along the Re-Re bond are not significantly different from the two *trans* carbonyl

groups perpendicular to the Re_2Si_2 plane. In addition the average Si-C (ethyl) distance (1.88 Å) and C-C distance (1.53 Å) both agree with the sums of the Si-C (sp^3) and C(sp^3)-C(sp^3) covalent radii^{27,84} (1.91 Å and 1.54 Å respectively).

The Re-Si bond lengths (2.534 Å) are in close agreement with those found in $\text{Re}_2(\text{CO})_8\text{H}_2\text{Si}(\text{C}_6\text{H}_5)_2$ ^{62,65} and $\text{Re}_2(\text{CO})_8[\text{Si}(\text{C}_6\text{H}_5)_2]_2$ ⁶⁴ (2.544 Å and 2.542 Å respectively). This was not expected if bridging hydrogens were present in the two hydrides. Rather a difference in bridged and unbridged Re-Si bonds, analogous to that observed in $\text{W}_2(\text{CO})_8\text{H}_2[\text{Si}(\text{C}_2\text{H}_5)_2]_2$ ⁶⁶ was expected. A complete discussion of this phenomenon follows in Chapter IV, with emphasis on the existence of bridging hydrogens and their relation to the transition metal-silicon bonds.

CHAPTER III: THE CRYSTAL AND MOLECULAR
STRUCTURE OF DIHYDRIDO TRICARBONYL RHENIUM
BIS (μ -DIETHYLSILICON) TETRACARBONYL RHENIUM,



EXPERIMENTAL

The sample of $\text{Re}_2(\text{CO})_7\text{H}_2[\text{Si}(\text{C}_2\text{H}_5)_2]_2$, supplied by Dr. Graham and Mr. Hoyano,⁶³ was sublimed in a sealed tube to give crystals that were suitable for a single crystal diffraction study. The crystals produced were clear colourless plates. Preliminary photographs showed $\bar{1}$ Laué symmetry and no systematic absences, consistent with the triclinic space groups $P1$ and $P\bar{1}$. Precise lattice parameters were obtained at 22°C from the 2θ angles of 17 reflections centred on a Picker manual four circle diffractometer using $\text{CuK}_{\alpha 1}$ X-radiation ($\lambda = 1.54051 \text{ \AA}$). The parameters are: $a = 8.664(1) \text{ \AA}$, $b = 14.066(2) \text{ \AA}$, $c = 9.343(1) \text{ \AA}$, $\alpha = 96.57(2)^\circ$, $\beta = 93.86(1)^\circ$, $\gamma = 91.63(1)^\circ$. A Delaunay reduction⁶⁹ showed no higher symmetry. The experimental density [$2.21(2) \text{ g cm}^{-3}$] determined by floatation in aqueous Clerici's solution, is in acceptable agreement with that calculated (2.23 g cm^{-3}) assuming two molecules of molecular weight 742.9

a.m.u. in a unit cell of volume 1107 \AA^3 .

Intensity data were collected on the Picker manual diffractometer using CuK_α X-radiation monochromated using the (002) reflecting plane of an oriented graphite crystal and using a 2° take-off angle. The crystal was aligned with its a^* axis coincident with the ϕ axis of the diffractometer. The crystal faces were identified and the perpendicular distances between parallel faces of the same form measured as: $\{1,0,0\}$, 7.7×10^{-2} mm; $\{0,1,0\}$, 5.3×10^{-2} mm; $\{0,0,1\}$, 1.9×10^{-2} mm. A coupled $\omega/2\theta$ scan technique was used with a 2θ scan speed of $2^\circ/\text{min}$ to collect all reflections with $2\theta \leq 125^\circ$. Initially a peak scan of 90 secs. (3 deg.) and a stationary background count of 20 secs. at the limits of the scan were used, however as the crystal decomposed and the mosaic spread increased this was changed to 99 sec. peak scans and 19 sec. backgrounds.⁸⁵ A scintillation counter in conjunction with a pulse height analyser, tuned to accept 95% of the CuK_α peak, was used to detect the scattered X-rays. Nine well distributed standard reflections were monitored at approximately 10 hr. intervals to assess decomposition effects. The 2836 unique reflections collected were reduced to

2020 significant observations using the criterion that a peak was significantly above background for $I/\sigma(I) \geq 3.0$, where $\sigma(I)$ was computed as described in Chapter II. The data were then reduced to structure factor amplitudes by correction for Lorentz, polarization, decomposition, and absorption effects. The decomposition was approximately linear with time and no significant $\sin \theta/\lambda$ dependence was observed. Total decomposition for the data collection was about 13%. Standard deviations, $\sigma(F)$, in the structure factors were computed as described in the previous chapter using a "p factor" of 0.03.

The high linear absorption coefficient⁸⁶ of 216.78 cm^{-1} for $\text{CuK}\alpha$ X-radiation, and the platy habit of the crystals gave rise to a considerable range of transmission factors (0.14 - 0.47). The absorption correction was verified experimentally by investigation of the behavior of I_{h00} as a function of ϕ . The internal consistency of the corrected intensities showed maximum deviations of less than 10% from the mean and was considered acceptable.

TABLE 8: PATTERSON VECTORS^a FOR $\text{Re}_2(\text{CO})_7\text{H}_2[\text{Si}(\text{C}_2\text{H}_5)_2]_2$

u	v	w	Multiplicity	Relative Peak Height ^c	Assignment ^b
0.167	0.200	0.080	2	523	$(x_1-x_2), (y_1-y_2), (z_1-z_2)$
0.210	0.500	0.500	2	520	$(x_2+x_1), (y_2+y_1), (z_2+z_1)$
-0.384	0.300	0.403	1	288	$2x_1, 2y_1, 2z_1$
0.036	0.325	0.414	1	231	$2x_2, 2y_2, 2z_2$
0.090	-0.150	0.070	2	184	$-(x_1-x_4), -(y_1-y_4), -(z_1-z_4)$
0.254	0.050	0.145	2	169	$(x_1-x_3), (y_1-y_3), (z_1-z_3)$

^aCentrosymmetrically related vectors are not listed.

^b $(x_1, y_1, z_1), (x_2, y_2, z_2), (x_3, y_3, z_3)$, and (x_4, y_4, z_4) are the coordinates of the Re1, Re2, Si1 and Si2 atoms respectively.

^cExpected Peak Heights calculated as in Chapter II.

Re1-Re2, 444; 2Re, 222; Re-Si, 166.

STRUCTURE SOLUTION AND REFINEMENT

A Patterson^{73,74} map was computed between the limits $-0.5 \leq u \leq 0.5$, $-0.5 \leq v \leq 0.5$, and $0.0 \leq w \leq 0.5$. The rhenium-rhenium vectors were readily identified in the Patterson map and a consistent solution for the coordinates of the two independent rhenium atoms was found to be: Re₁, (0.185, 0.363, 0.287) and Re₂, (0.018, 0.163, 0.207). Image seeking around the origin and Re-Re vectors provided consistent solutions for the silicon atom coordinates as: Si₁, (-0.069, 0.313, 0.142), and Si₂, (0.275, 0.213, 0.357). The major vectors and their assignments are shown in Table 8.

A resumé of the refinement is shown in Table 9.

TABLE 9: REFINEMENT OUTLINE

MODEL	R ₁	R ₂
1) Rhenium and Silicon atoms isotropic	0.166	0.238
2) All non-hydrogen atoms isotropic	0.106	0.131
3) Decomposition and Absorption Corrections	0.061	0.078
4) Re and Si anisotropic temperature factors	0.047	0.064
5) All non-hydrogen atoms with anisotropic temperature factors	0.040	0.057

Structure factors were calculated using the atomic scattering factors⁷⁵ for the neutral atoms for rhenium, silicon, carbon, and oxygen. The real and imaginary parts of anomalous dispersion corrections⁷⁶ were applied to the rhenium and silicon scattering factors.⁷⁷ All non-hydrogen atoms were located from an electron density difference map phased on model 1. Refinement of the model with all temperature factors anisotropic was suggested by features on an electron density difference map phased on model 4, and was verified by a Hamilton's R Test⁷⁹ at the 0.005 significance level. Anisotropic temperature factors were of the form:

$$\exp [-(\beta_{11}h^2 + \beta_{22}k^2 + \beta_{33}l^2 + 2\beta_{12}hk + 2\beta_{13}hl + 2\beta_{23}kl)].$$

In an attempt to locate the hydrogen atoms an electron density difference map was calculated, phased on model 5. The highest features were of the approximate magnitude $1.1e^{-3}$ and were located in the vicinity of the rhenium atoms, but could not be interpreted as hydrogen atom peaks. Similarly no peaks were observed in the positions predicted for the methylene hydrogens of the ethyl groups. The inability to locate hydrogens in this structure is due to similar problems as encountered for $\text{Re}_2(\text{CO})_6\text{H}_4[\text{Si}(\text{C}_2\text{H}_5)_2]_2$.

The scattering is dominated too much by the heavy
r m atoms and hampers location of the hydrogens.
As it is probable that residual absorption effects
severely limit the data. This is especially true
in this structure due to the wide range of trans-
mission factors.

RESULTS

The observed and calculated structure factor
amplitudes, $|F_o|$ and $|F_c|$, are shown in Table 10.
Table 11 contains the final fractional coordinates of
all atoms except hydrogen, their standard deviations
being obtained from the inverse matrix of the final
least squares analysis. The anisotropic thermal
parameters⁸⁰ (U's) and equivalent isotropic B's⁸¹
of all atoms are shown in Table 12 and bond lengths
and angles are given in Tables 13 and 14 respectively.
The bond lengths and angles along with their standard
deviations were obtained from ORFFE. Fig. 5 shows a
three dimensional representation of the molecule.
Least squares plane calculations are shown for the
Re₂Si₂ plane (Table 15) showing the deviations of the
Re and Si atoms from the plane and also the distances
of the carbonyl groups, C202, C303 and C606, from

this plane. Also the plane through the four carbonyl groups perpendicular to the Re_2Si_2 plane is calculated and also selected atom distances from this plane.

TABLE 10: OBSERVED AND CALCULATED STRUCTURE FACTOR AMPLITUDES (ELECTRONS X 10)

Table with 16 columns: L, F OBS, F CAL, L, F OBS, F CAL. The table contains numerical data for observed and calculated structure factor amplitudes across various indices.

Table 10 (continued)

K	L	FOBS	FCAL	K	L	FOBS	FCAL	K	L	FOBS	FCAL	K	L	FOBS	FCAL	K	L	FOBS	FCAL
3	1	824	820	-6	2	645	684	5	1	879	892	-6	-6	300	315	5	2	708	758
3	2	100	106	-6	6	967	960	5	2	577	400	-4	-5	254	278	5	3	204	212
3	3	164	165	-6	6	676	662	5	3	965	900	-4	-4	639	614	5	4	651	470
3	4	158	158	-5	-7	422	426	5	4	885	880	-4	-3	689	848	6	-7	168	163
3	5	758	736	-5	-3	470	472	5	5	564	549	-4	-2	979	981	6	-5	519	521
3	6	172	170	-5	-1	1155	1154	6	-8	245	257	-4	-1	611	650	6	-4	270	277
3	7	603	633	-5	0	101	1179	6	-5	201	218	-4	-1	242	238	6	-1	725	765
4	0	372	572	-5	3	881	922	6	-7	365	412	-4	0	274	294	6	-1	755	762
4	1	854	893	-5	5	502	484	6	-2	780	839	-4	0	539	551	6	-2	312	310
4	2	290	293	-5	-8	618	613	6	-1	631	660	-3	-7	378	406	6	-1	725	765
4	3	1007	1042	-4	-2	1304	1342	6	0	820	791	-3	-4	308	310	7	-6	429	461
4	4	215	207	-4	-2	1304	1342	6	0	820	791	-3	-4	308	310	7	-6	429	461
4	5	893	952	-4	0	1644	1671	6	1	472	450	-3	-5	459	433	7	-5	220	208
4	6	394	368	-4	2	718	698	6	2	690	723	-3	-4	502	502	7	-4	275	307
4	7	661	678	-4	6	153	104	6	3	422	434	-3	-3	694	706	7	-2	550	580
4	8	274	262	-4	-7	827	820	6	4	405	407	-3	-2	606	571	7	4	275	307
4	9	998	978	-3	-5	504	524	7	-5	505	554	-3	-1	381	432	8	-5	483	555
4	0	333	310	-3	-3	1280	1281	7	-4	517	575	-3	1	173	108	8	-3	385	425
4	1	907	961	-3	-1	1334	1340	7	-3	633	632	-3	0	297	368	8	-3	385	425
4	2	172	171	-3	1	627	654	7	-2	599	639	-3	3	560	549	8	1	349	316
4	3	894	673	-3	3	104	151	7	-1	852	854	-3	4	574	546	8	1	349	316
4	4	224	236	-3	5	691	641	7	0	382	361	-3	5	563	535	9	0	539	544
4	5	743	785	-3	7	581	572	7	1	312	305	-3	6	607	593	9	1	182	154
4	6	243	249	-2	-5	504	520	7	2	200	200	-3	7	352	351	9	2	711	704
4	7	231	245	-2	-4	748	737	8	-7	174	181	-2	-4	438	413	10	-1	542	548
4	8	525	559	-2	-4	1038	994	8	-6	330	301	-2	-4	438	413	10	-1	542	548
4	9	164	165	-2	-3	188	174	8	-5	417	459	-2	-5	273	294	10	1	608	658
4	0	1212	1248	-2	-2	802	799	8	-6	470	735	-2	-4	374	305	11	-2	533	507
4	1	214	209	-2	0	367	396	8	-3	559	599	-2	-3	302	312	-10	0	171	164
4	2	995	1005	-2	4	442	442	8	-2	600	612	-2	0	224	252	-9	-2	816	811
4	3	552	572	-2	4	1231	1183	8	-1	331	343	-2	1	354	350	-9	-1	178	165
4	4	544	545	-2	5	163	80	8	0	175	225	-2	2	727	689	-9	0	158	144
4	5	506	492	-2	6	794	779	8	2	229	199	-2	3	770	726	-9	2	200	145
4	6	799	878	-1	-7	850	817	8	3	193	197	-2	4	960	854	-9	3	183	208
4	7	1023	1045	-1	-5	890	501	8	4	298	304	-2	5	688	658	-9	3	183	208
4	8	1247	1257	-1	-3	382	325	8	5	230	255	-2	6	381	394	-9	3	191	184
4	9	643	637	-1	-1	160	172	8	-6	222	232	-2	7	278	293	-9	0	1350	354
4	0	454	470	-1	1	403	390	9	-5	324	383	-1	-7	383	344	-8	2	278	254
4	1	177	165	-1	2	133	115	9	-4	305	354	-1	-6	221	219	-8	4	192	227
4	2	205	229	-1	3	1344	1324	9	-3	375	388	-1	-3	167	145	-8	4	192	227
4	3	862	1007	-1	4	171	170	9	1	394	392	-1	-2	284	290	-7	-2	210	234
4	4	1332	1300	-1	5	1118	1097	9	2	846	835	-1	-1	684	693	-7	-1	230	209
4	5	1094	1074	-1	6	163	145	9	1	519	524	-1	0	522	573	-7	0	495	501
4	6	473	492	-1	7	534	545	9	0	111	623	-1	1	819	801	-7	1	294	301
4	7	308	347	0	-8	603	549	10	-1	316	254	-1	2	794	782	-7	2	462	494
4	8	763	811	0	-4	395	338	10	0	383	391	-1	3	747	754	-7	4	513	553
4	9	1210	1227	0	-2	239	255	10	1	497	490	-1	4	902	864	-6	-5	189	220
4	0	895	964	0	-2	259	245	10	2	572	544	-1	5	447	450	-6	-3	420	443
4	1	392	336	0	-2	803	803	10	3	554	542	-1	6	292	301	-6	-2	259	278
4	2	553	603	0	-1	253	240	11	-2	208	211	0	-5	265	265	-6	-1	650	675
4	3	611	691	0	0	1133	1097	11	-3	302	274	0	-4	311	338	-6	0	258	257
4	4	792	817	0	1	221	201	11	-2	389	359	0	-3	694	652	-6	4	647	713
4	5	552	508	0	2	1164	1128	11	-1	454	447	0	-2	619	590	-6	2	200	284
4	6	158	38	0	3	344	344	11	0	394	392	0	-1	839	771	-6	3	457	455
4	7	471	475	0	4	953	939	11	1	444	449	0	0	659	638	-6	5	158	162
4	8	581	589	0	5	244	234	11	2	531	534	0	1	832	784	-6	5	197	181
4	9	478	507	0	6	438	424	12	-3	344	341	0	2	555	548	-6	5	508	554
4	0	380	364	0	-5	378	362	12	-2	358	341	0	3	587	589	-6	5	221	214
4	1	205	203	0	-4	250	261	12	-1	354	358	0	4	344	347	-6	5	718	774
4	2	750	754	0	-3	1270	1303	12	0	244	244	0	5	294	299	-6	6	499	515
4	3	684	697	0	-2	349	345	-11	-1	535	525	0	7	174	177	-6	2	275	267
4	4	174	175	1	-1	1009	1742	-11	-4	154	166	1	-6	165	165	0	-4	165	165
4	5	409	400	1	0	1164	440	-11	0	535	525	1	-6	165	165	0	-4	165	165
4	6	692	702	1	1	973	977	-11	1	534	529	1	-5	653	626	0	-3	495	399
4	7	622	638	1	2	325	301	-11	2	142	130	1	-4	708	649	0	-2	314	331
4	8	329	342	1	3	699	690	-10	-2	620	611	1	-3	334	397	0	-1	394	363
4	9	512	524	1	4	174	177	-10	-1	251	252	1	-2	491	457	0	0	324	294
4	0	616	594	1	5	234	231	-10	0	660	643	1	-1	418	401	0	-4	547	441
4	1	454	453	1	6	179	170	-10	1	208	211	1	0	590	630	0	-3	477	512
4	2	581	612	2	-4	280	273	-10	2	358	344	1	-2	289	285	0	-4	475	461
4	3	192	160	2	-5	187	183	-10	4	134	55	1	-3	219	218	0	-3	219	218
4	4	889	504	2	-6	1203	1194	-9	-3	458	465	2	-4	617	584	0	-2	382	419
4	5	138	108	2	-3	397	408	-9	-2	249	247	2	-7	417	384	-1	-2	493	648
-12	-2	173	168	2	-4	1133	1524	-9	-2	462	623	2	-5	624	602	-2	-5	217	202
-12	-2	253	252	2	-5	1242	892	-9	0	242	231	2	-6	651	617	-2	-1	474	468
-11	-1	304	297	2	2	309	304	-9	5	341	352	2	-2	934	911	-2	1	1073	1020
-11	0	212	225	2	4	359	327	-8	-5	194	141	2	-1	516	517	-2	2	150	157
-11	1	523	517	2	6	379	372	-8	-4	344	342	2	1	226	225	-2	5	504	501
-11	2	750	734	2	7	243	234	-8	-2	409	402	2	2	272	242	-1	-4	247	241
-11	3	482	485	3	-7	512	501	-8	0	181	142	2	3	481	454	-1	-2	753	712
-11	4	199	204	3	-5	690	703	-8	2	240	291	2	6	489	500	-1	0	897	957
-11	5	434	415	3	-4	427	407	-8	3	185	174	2	5	489	500	-1	0	897	957
-10	-1	209	224	3	-3	1054	1054	-8	4	479	458	2	4	275	250	-1	2	84	

TABLE 11: FRACTIONAL COORDINATES

Atom	x	y	z
Re1	0.02212(8)	0.16212(5)	0.20948(7)
Re2	0.19138(8)	0.35578(5)	0.29300(7)
Si1	0.2768(5)	0.1950(3)	0.3623(5)
Si2	-0.0608(5)	0.3230(3)	0.1359(5)
C1	0.143(2)	0.141(1)	0.040(2)
C2	-0.166(2)	0.123(1)	0.093(2)
C3	0.054(2)	0.037(1)	0.266(2)
C4	-0.092(2)	0.187(1)	0.381(2)
C5	0.309(2)	0.342(1)	0.117(2)
C6	0.303(2)	0.479(2)	0.351(2)
C7	0.078(2)	0.378(1)	0.470(2)
C8	0.460(2)	0.147(1)	0.284(2)
C9	0.273(2)	0.172(1)	0.560(2)
C10	0.479(2)	0.040(1)	0.287(2)
C11	0.426(2)	0.216(2)	0.650(2)
C12	-0.057(2)	0.342(1)	-0.061(2)
C13	-0.242(2)	0.369(1)	0.208(2)
C14	-0.198(2)	0.292(2)	-0.157(2)
C15	-0.288(2)	0.469(2)	0.169(2)
O1	0.212(2)	0.130(1)	-0.059(1)
O2	-0.281(2)	0.097(1)	0.027(1)
O3	0.081(2)	-0.041(1)	0.293(2)
O4	-0.164(2)	0.199(1)	0.482(1)
O5	0.378(1)	0.336(1)	0.019(1)
O6	0.362(2)	0.550(1)	0.393(2)
O7	0.015(2)	0.394(1)	0.574(1)

TABLE 12: THERMAL PARAMETERS (\AA^2)

Atom	U_{11}	U_{22}	U_{33}	U_{12}	U_{13}	U_{23}	$B(\text{\AA}^2)^a$
Re1	0.0497(5)	0.0456(5)	0.0432(5)	-0.0010(4)	-0.0004(3)	0.0031(4)	3.67
Re2	0.0448(5)	0.0436(5)	0.0483(4)	0.0010(4)	-0.0038(4)	0.0039(4)	3.63
Si1	0.0585(30)	0.0501(26)	0.0519(26)	0.0069(23)	-0.0042(21)	0.0098(21)	4.22
Si2	0.0512(28)	0.0553(27)	0.0483(25)	-0.0024(23)	-0.0051(21)	0.0101(21)	4.09
C1	0.070(13)	0.058(11)	0.071(14)	0.003(10)	0.014(11)	-0.013(11)	5.33
C2	0.076(13)	0.056(10)	0.040(10)	-0.017(9)	0.005(9)	-0.012(8)	4.68
C3	0.087(14)	0.053(11)	0.051(11)	-0.017(10)	-0.020(10)	0.008(9)	5.13
C4	0.055(12)	0.060(11)	0.059(13)	0.009(9)	0.006(10)	0.001(10)	4.58
C5	0.050(10)	0.054(10)	0.051(9)	-0.008(8)	-0.005(8)	0.014(8)	4.08
C6	0.038(10)	0.096(15)	0.067(12)	0.001(10)	-0.014(8)	0.001(11)	5.39
C7	0.074(12)	0.051(11)	0.052(10)	0.003(9)	-0.001(9)	0.006(8)	4.68
C8	0.057(12)	0.075(12)	0.082(14)	0.021(10)	0.012(10)	0.019(10)	5.50
C9	0.083(13)	0.077(12)	0.044(10)	-0.004(11)	-0.010(9)	0.015(9)	5.40

TABLE 12 CONTINUED

Atom	U ₁₁	U ₂₂	U ₃₃	U ₁₂	U ₁₃	U ₂₃	B(A ²) ^a
C10	0.091(15)	0.065(13)	0.111(15)	0.027(11)	0.011(12)	0.025(12)	6.88
C11	0.092(15)	0.111(17)	0.069(13)	-0.014(13)	-0.033(11)	0.019(12)	7.28
C12	0.091(14)	0.067(12)	0.049(10)	-0.012(11)	-0.003(9)	0.008(8)	5.50
C13	0.054(11)	0.065(12)	0.089(13)	0.011(9)	0.000(9)	0.008(10)	5.48
C14	0.095(15)	0.101(15)	0.057(11)	-0.026(13)	-0.023(10)	0.019(11)	6.75
C15	0.066(13)	0.060(12)	0.115(16)	0.021(10)	0.004(11)	-0.000(11)	6.38
O1	0.111(12)	0.099(11)	0.074(10)	-0.009(9)	0.033(9)	-0.012(8)	7.52
O2	0.084(10)	0.093(10)	0.074(9)	-0.015(9)	-0.009(8)	-0.011(8)	6.79
O3	0.124(13)	0.063(9)	0.120(11)	0.007(9)	-0.006(9)	0.021(8)	8.06
O4	0.089(11)	0.107(11)	0.060(9)	-0.013(9)	0.008(8)	0.011(8)	6.75
O5	0.070(9)	0.101(10)	0.078(9)	0.007(8)	0.021(7)	0.010(8)	6.48
O6	0.087(11)	0.069(9)	0.124(12)	-0.020(8)	-0.024(9)	-0.002(9)	7.61
O7	0.108(11)	0.085(10)	0.076(9)	0.012(9)	0.031(8)	-0.018(7)	7.15

^aEquivalent isotropic thermal parameter.

TABLE 13: INTRAMOLECULAR DISTANCES^a (Å)

Atoms	Distance	Atoms	Distance
Re1-Re2	3.052 (1)	Re2-Si1	2.539 (4)
Re1-Si1	2.547 (5)	Re2-Si2	2.549 (4)
Re1-Si2	2.548 (5)	Re1-C1	1.96 (2)
Re1-C2	1.93 (2)	Re1-C3	1.92 (2)
Re1-C4	1.94 (2)	Re2-C5	1.98 (2)
Re2-C6	1.97 (2)	Re2-C7	1.98 (2)
C1-O1	1.13 (2)	C2-O2	1.15 (2)
C3-O3	1.18 (2)	C4-O4	1.16 (2)
C5-O5	1.12 (2)	C6-O6	1.12 (2)
C7-O7	1.15 (2)	Si1-C8	1.90 (2)
Si1-C9	1.91 (2)	Si2-C12	1.89 (2)
Si2-C13	1.85 (2)	C9-C11	1.59 (2)
C8-C10	1.53 (2)	C12-C14	1.56 (2)
C13-C15	1.54 (2)		

^aStandard deviations in parentheses refer to last digit quoted.

TABLE 14: INTRAMOLECULAR ANGLES (DEGREES)

Atoms	Angle	Atoms	Angle
Si1-Re2-Rel	53.3(1)	Si1-Rel-Re2	53.0(1)
Si2-Re2-Rel	53.2(1)	Si2-Rel-Re2	53.2(1)
Re2-Si1-Rel	73.7(1)	Re2-Si2-Rel	73.5(1)
Si1-Rel-C3	80.4(5)	Si2-Rel-C2	79.8(5)
Re2-Rel-C1	89.7(5)	Re2-Rel-C4	88.2(5)
Rel-Re2-C5	92.4(5)	Rel-Re2-C6	178.6(5)
Rel-Re2-C7	91.1(5)	Rel-C1-O1	179(2)
Rel-C2-O2	178(2)	Rel-C3-O3	175(2)
Rel-C4-O4	178(2)	Re2-C5-O5	178(2)
Re2-C6-O6	175(2)	Re2-C7-O7	178(2)
C8-Si1-C9	110.4(8)	C12-Si2-C13	109.6(8)
C10-C8-Si1	115(1)	C11-C9-Si1	110(1)
C14-C12-Si2	114(1)	C15-C13-Si2	116(1)
Si1-Re2-C6	125.5(5)	Si2-Re2-C6	128.0(5)

TABLE 15: LEAST SQUARES PLANE CALCULATIONS ^aFOR $\text{Re}_2(\text{CO})_7\text{H}_2(\text{SiEt}_2)_2$

(A) ATOMS DEFINING PLANE: Re1, Re2, Si1, Si2

EQUATION OF PLANE:

$$-0.5693X + 0.0653Y + 0.8195Z - 1.6898 = 0.0$$

DISTANCES OF ATOMS FROM PLANE: Re1 0.0029

Re2 0.0031

Si1	-0.020	Si2	-0.020
C6	0.026	O6	0.127
C2	-0.017	O2	0.002
C3	0.179	O3	0.184
C5	-1.980		

(B) ATOMS DEFINING PLANE: Re1, Re2, C1, C4, C5, C7.

EQUATION OF PLANE:

$$0.6782X - 0.5229Y + 0.5163Z + 0.0354 = 0.0$$

DISTANCES OF ATOMS FROM PLANE:

Re1	0.0004	Re2	0.0004
C1	0.049	C4	-0.029
C5	-0.049	C7	0.016
O1	0.065	O4	-0.055
O5	-0.077	O7	0.038
C6	0.043	O6	0.089
Si1	-2.041		

^aX, Y, and Z are orthogonal coordinates (Å) with X along the a-axis, Y in the (a,b) plane, and Z along the c*-axis.

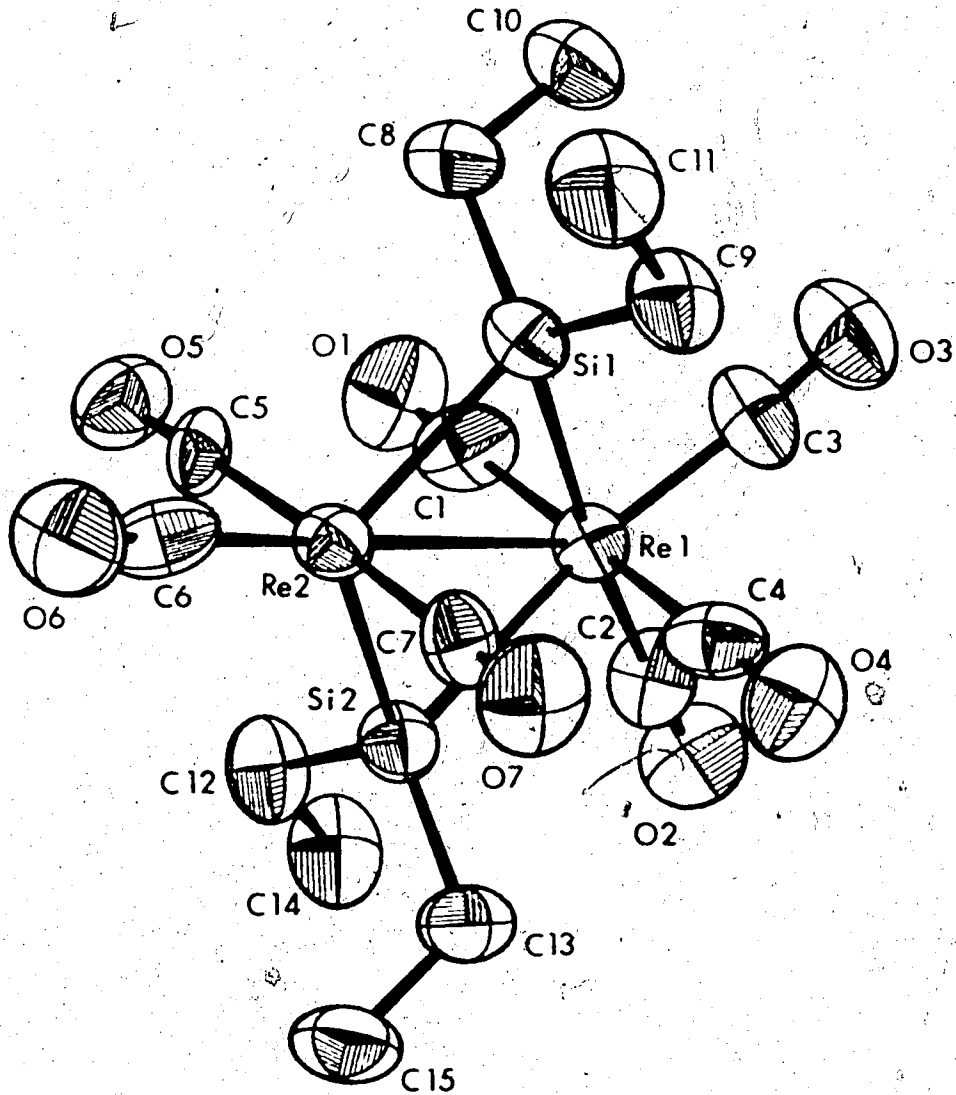


Fig. 5: A PERSPECTIVE VIEW OF $\text{Re}_2(\text{CO})_7\text{H}_2[\text{Si}(\text{C}_2\text{H}_5)_2]_2$.

DESCRIPTION OF STRUCTURE

$\text{Re}_2(\text{CO})_7\text{H}_2[\text{Si}(\text{C}_2\text{H}_5)_2]_2$ has approximate C_s symmetry. A perspective view of the molecule is shown in Fig. 5. The central cluster is similar to that of $\text{Re}_2(\text{CO})_6\text{H}_4[\text{Si}(\text{C}_2\text{H}_5)_2]_2$ shown in Chapter II. The two rhenium atoms and two silicon atoms are planar and located at the corners of a rhombus, with like atoms at opposing corners, and a rhenium-rhenium bond across the shorter diagonal. Two carbonyl groups (C303 and C202) on Re1 are also approximately in this plane and trans to the Re1-Si1 and Re1-Si2 bonds, while one carbonyl group (C606), also in this plane and bonded to Re2, lies along the Re-Re bond. The two remaining carbonyls on each rhenium are perpendicular to the Re_2Si_2 plane above and below the rhenium atoms.

The rhenium-carbon (carbonyl) and carbon-oxygen distances are regular and similar to those observed in $\text{Re}_2(\text{CO})_6\text{H}_4[\text{Si}(\text{C}_2\text{H}_5)_2]_2$ and other rhenium carbonyl compounds.^{64,65,82,83,87,88,89} The coordination around the silicon atoms is a distorted tetrahedron due to the small Re1-Si-Re2 angles. There are no unusual distances in the silicon-carbon (ethyl) or carbon-carbon (ethyl) bonds (compare Chapter II). The rhenium-rhenium distance [3.052(1) Å] is consistent with a rhenium-rhenium single bond, and this is further

substantiated by the acute Re1-Si1-Re2 and Re1-Si2-Re angles of $73.7(1)^\circ$ and $73.5(1)^\circ$. It is also interesting that there is a progression in Re-Re bond lengths through the series $\text{Re}_2(\text{CO})_8[\text{Si}(\text{C}_6\text{H}_5)_2]_2$,⁶⁴ $\text{Re}_2(\text{CO})_7\text{H}_2[\text{Si}(\text{C}_2\text{H}_5)_2]_2$, $\text{Re}_2(\text{CO})_6\text{H}_4[\text{Si}(\text{C}_2\text{H}_5)_2]_2$ and $\text{Re}_2(\text{CO})_8\text{H}_2\text{Si}(\text{C}_6\text{H}_5)_2$,⁶⁵ whereas the Re-Si bonds are approximately constant (Table 16).

The longer Re-Re bond in $\text{Re}_2(\text{CO})_8\text{H}_2\text{Si}(\text{C}_6\text{H}_5)_2$ reflects the fact that only one Si bridge is constraining the rhenium atoms together and also that the two extra eclipsed carbonyls are present causing added repulsion of the two $\text{Re}(\text{CO})_4$ moieties. It is believed however that the Re-Re bond length differences in the other three compounds indicate that there is significant π bonding present in the Re-Re bonds whereas the Re-Si bonds are primarily σ . Thus varying the number of π -withdrawing carbonyl groups in the molecules would be expected to affect the Re-Re bonds if π bonding is important, but have little effect on the Re-Si bonds if the π bonding contribution here is not great.

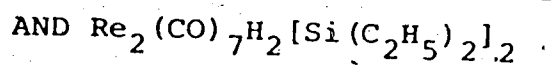
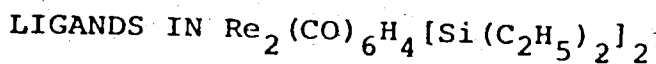
Using the covalent radii of Pauling²⁷ for Si (1.17 Å) and Re (1.283 Å) a single bonded Re-Si distance of 2.45 Å is predicted, which is less than the observed value of approximately 2.54 Å in these

compounds (Table 16). Although the radius used for rhenium may not be suitable, the larger observed Re-Si bond length does not weaken the argument that rhenium-silicon π bonding is of little significance in these compounds. A similar trend was observed⁹⁰ in $\text{Cl}(\pi\text{C}_5\text{H}_5)_2\text{ZrSi}(\text{C}_6\text{H}_5)_3$ where the observed Zr-Si distance [2.813(2) Å] exceeded the value calculated with Pauling radii (2.62 Å). Here Zr(IV) is formally d^0 so no back-donation into empty silicon d orbitals can occur. Thus it was postulated that only σ bonding was important. This contrasts with $\text{Co}(\text{SiCl}_3)(\text{CO})_4$ ⁹¹ and $\text{RhHCl}(\text{SiCl}_3)(\text{PPh}_3)_2$ ⁹² where the Co-Si [2.254(3) Å] and Rh-Si [2.303(4) Å] distances are both less than the values predicted using Pauling's covalent radii (2.33 Å and 2.42 Å respectively). It seems therefore that metal-silicon π bonding is present in these two compounds, whereas it is minimal in the zirconium and rhenium compounds. Any explanation of bond shortening as due to π bonding in these transition metal silyl compounds should be approached cautiously, however, since it is difficult to separate these effects from a σ -inductive effect. Thus the changes in metal-silicon distances in the series $(\pi\text{-C}_5\text{H}_5)(\text{CO})_2\text{HMnSi}(\text{C}_6\text{H}_5)_3$ ⁹³ [2.424(2) Å]; $(\pi\text{-C}_5\text{H}_5)(\text{CO})_2\text{HMnSiCl}_2(\text{C}_6\text{H}_5)$ ⁹⁴ [2.310(2) Å]; and also

the series $\text{Co}(\text{SiH}_3)(\text{CO})_4$,⁹⁵ [2.381(7) Å]; $\text{Co}(\text{SiCl}_3)(\text{CO})_4$,⁹¹ [2.254(3) Å]; and $\text{Co}(\text{SiF}_3)(\text{CO})_4$,⁹⁶ [2.226(5) Å]; can be attributed to shrinkage of the silicon orbitals by the more electronegative substituents, thereby shortening the metal-silicon bonds.

However uncertain the mode of bonding between the rhenium and silicon atoms, it is still possible to compare the distances within the series mentioned in Chapter II since all substituents are similar. Thus the most interesting feature of $\text{Re}_2(\text{CO})_7\text{H}_2[\text{Si}(\text{C}_2\text{H}_5)_2]_2$ is the similarity in the Re-Si bond lengths and their similarity to the other members of the series. The Re2-Si1 and Re2-Si2 bonds are adjacent to the hydrogen ligands whereas the Re1-Si1 and Re1-Si2 bonds are "hydrogen-free". As was explained in Chapter II, the similarity of these bonds in the two differing environments is not expected in view of the proposed hydrogen bridging.^{62,63} Again, complete discussion of this phenomenon is deferred until Chapter IV.

CHAPTER IV: MODE OF BONDING OF THE HYDRIDE



Although location of the hydrogen atoms in this series of hydrides was not possible due to high dominance of the rhenium and tungsten scattering and also large absorption effects, the investigation of the central framework, in particular the transition metal-silicon bond, has proved exceedingly valuable in obtaining information about the bonding exhibited by the hydrogens attached to the metals.⁶⁶ Three possibilities exist for the hydrogen bonding in these compounds as shown for $\text{W}_2(\text{CO})_8\text{H}_2[\text{Si}(\text{C}_2\text{H}_5)_2]_2$ in Fig. 6: (1) the hydrogen is terminally bonded to the transition metal with no interaction with the silicon, (2) the hydrogen bridges the transition metal-silicon bond thus forming a three centre two electron bond, and (3) the hydrogen is terminally bonded to the transition metal, but with weak attractive interaction with the silicon. A hydrogen bridge of type (2) was postulated⁶⁶ for $\text{W}_2(\text{CO})_8\text{H}_2[\text{Si}(\text{C}_2\text{H}_5)_2]_2$ in which the W-Si distances differed significantly (Table 16), with the hydrogen presumably bridging the longer distance. However,

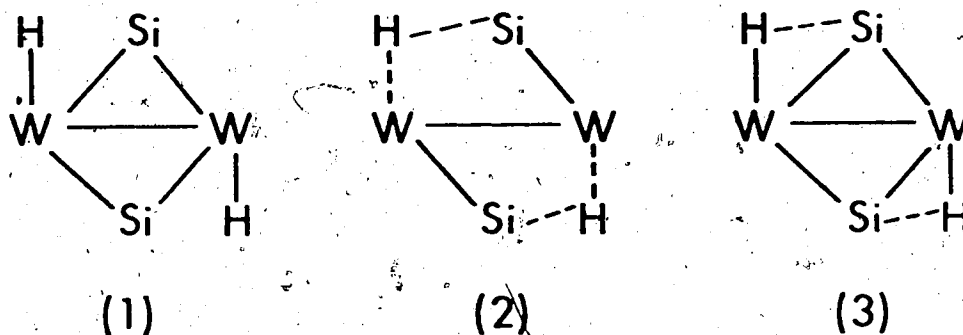


Fig. 6: Possible Bonding Schemes for the Hydrogen Ligand in $W_2(CO)_8H_2[Si(C_2H_5)_2]_2$.

in $Re_2(CO)_6H_4[Si(C_2H_5)_2]_2$ the Re-Si bond lengths are not consistent with a three centre Si-H-Re bond, but rather seem consistent with a terminally bound hydrogen ligand.

It was expected that if the hydrogen was involved in a three centre Si-H-Re bond, a significant lengthening of this Si-Re distance would be observed, analogous to $W_2(CO)_8H_2[Si(C_2H_5)_2]_2$. There is no significant difference in Re-Si bond lengths, however, between the two hydrides $Re_2(CO)_8H_2Si(C_6H_5)_2$ ⁶⁵ and $Re_2(CO)_6H_4[Si(C_2H_5)_2]_2$, and $Re_2(CO)_8[Si(C_6H_5)_2]_2$ ⁶⁴ which contains no hydrogen ligand. Moreover these Re-Si distances are similar to the shorter (unbridged) W-Si distance in $W_2(CO)_8H_2[Si(C_2H_5)_2]_2$, and therefore

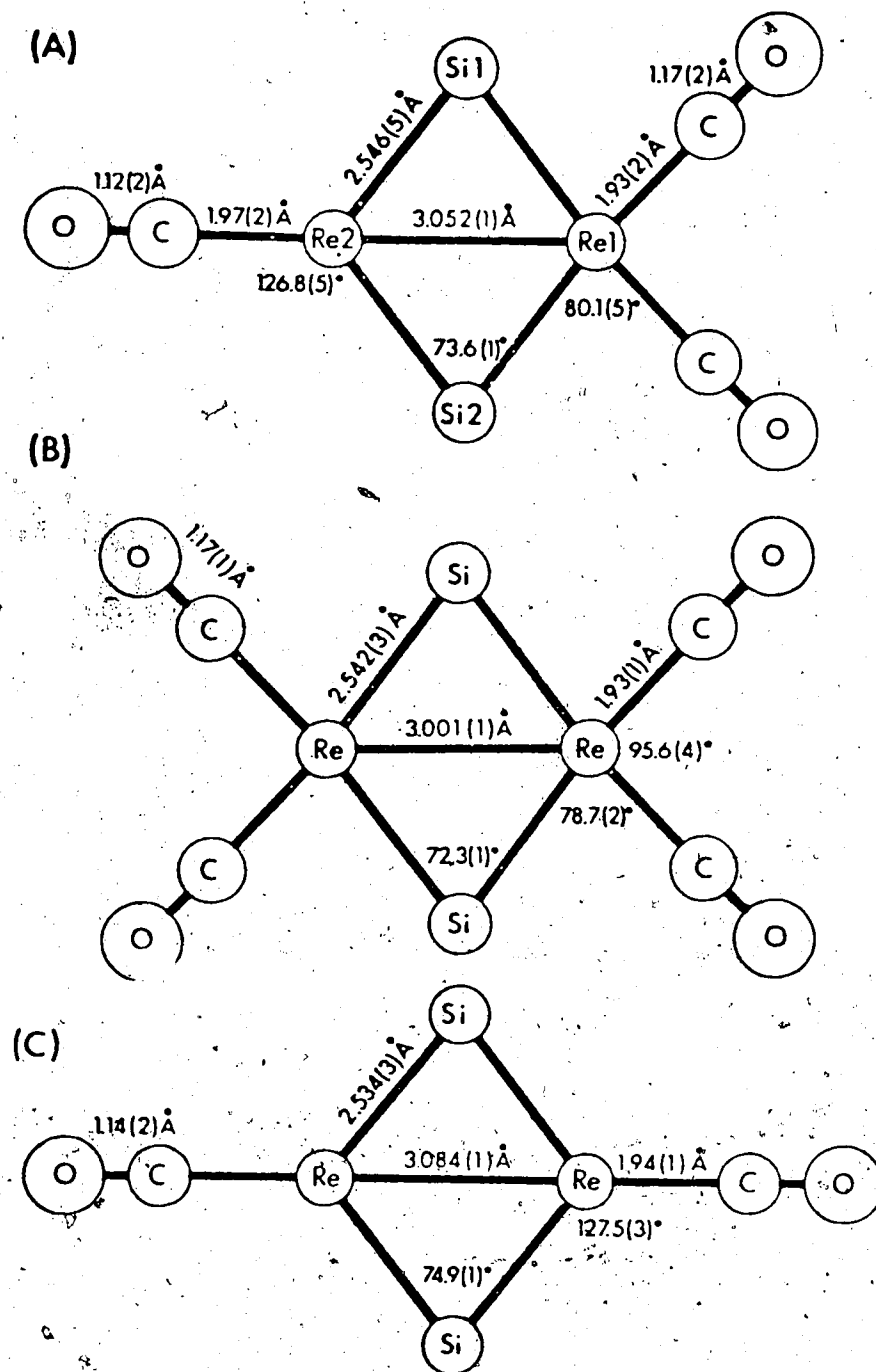


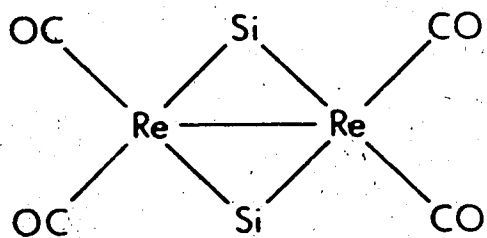
Fig. 7: A COMPARISON OF THE GEOMETRIES OF
 (A) $\text{Re}_2(\text{GO})_7\text{H}_2[\text{Si}(\text{C}_2\text{H}_5)_2]_2$, (B) $\text{Re}_2(\text{CO})_8[\text{Si}(\text{C}_6\text{H}_5)_2]_2$, AND
 (C) $\text{Re}_2(\text{CO})_6\text{H}_4[\text{Si}(\text{C}_2\text{H}_5)_2]_2$.

are more consistent with terminal hydrides.

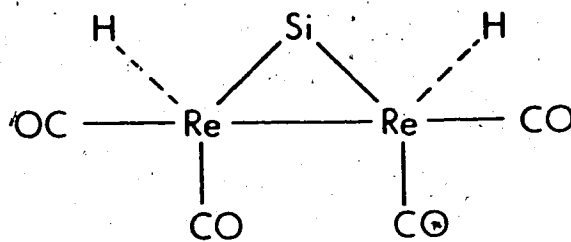
The ambiguity in comparison of the Re-Si bond lengths in the hydrides and $\text{Re}_2(\text{CO})_8[\text{Si}(\text{C}_6\text{H}_5)_2]_2$, in which the disorder problem existed (Appendix 1), was overcome with the structural determination of $\text{Re}_2(\text{CO})_7\text{H}_2[\text{Si}(\text{C}_2\text{H}_5)_2]_2$, which, like the tungsten complex, was an internal standard containing metal-silicon bonds both adjacent to hydrogen ligands and "hydrogen-free". The similarity of the Re-Si bonds in this structure was added proof that the hydrogen ligands were not bonded in a fashion analogous to $\text{W}_2(\text{CO})_8\text{H}_2[\text{Si}(\text{C}_2\text{H}_5)_2]_2$ and were therefore probably bound terminally to the rhenium atom. This reinforced the previous argument that the other rhenium hydrides in this series were also terminal.

Fig. 7 shows $\text{Re}_2(\text{CO})_8[\text{Si}(\text{C}_6\text{H}_5)_2]_2$, $\text{Re}_2(\text{CO})_7\text{H}_2[\text{Si}(\text{C}_2\text{H}_5)_2]_2$ and $\text{Re}_2(\text{CO})_6\text{H}_4[\text{Si}(\text{C}_2\text{H}_5)_2]_2$ viewed perpendicular to the Re_2Si_2 planes and including only those atoms lying approximately in this plane. Included are relevant bond lengths and angles for ready comparison of the three.

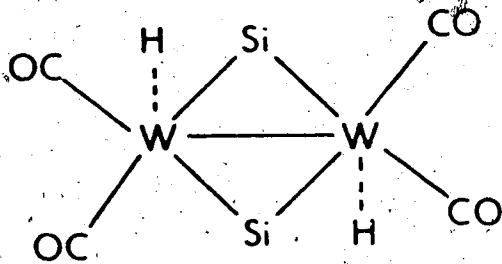
To explain why the hydrogen ligands seem to be terminally bound for the rhenium compounds, but bridging in the case of the tungsten compound, it is useful to consider the coordination about the metal atoms, as shown in Fig. 8. In each compound there are two mutually *trans* carbonyl groups on each metal which are not shown. These are perpendicular to the



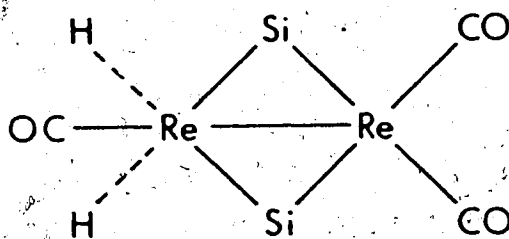
(A)



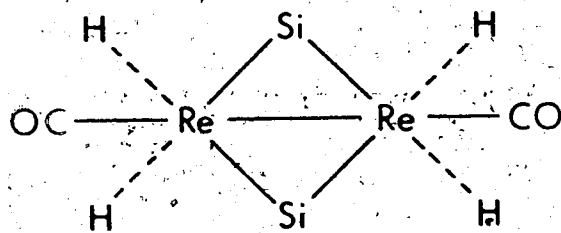
(B)



(C)



(D)



(E)

Fig. 8: HYDROGEN LIGAND ENVIRONMENTS IN THE SILICON BRIDGED TRANSITION METAL HYDRIDES.

TABLE 16: RELEVANT BOND LENGTHS (Å)
IN SOME TRANSITION METAL SILICON-BRIDGED COMPLEXES

COMPOUND	M-Si	M-M	REFERENCE
$W_2(CO)_8H_2[Si(C_2H_5)_2]_2$	2.586(5), 2.703(4)	3.183(1)	66
$Re_2(CO)_8H_2Si(C_6H_5)_2$	2.544(9)	3.121(2)	65
$Re_2(CO)_8[Si(C_6H_5)_2]_2$	2.542(3)	3.001(1)	64
$Re_2(CO)_6H_4[Si(C_2H_5)_2]_2$	2.533(2), 2.535(3)	3.084(1)	THIS WORK
$Re_2(CO)_7H_2[Si(C_2H_5)_2]_2$	2.547(5), 2.548(5), 2.539(4), 2.549(4)	3.052(1)	THIS WORK

TABLE 17: RELEVANT ANGLES (DEGREES) IN SOME
TRANSITION METAL SILICON-BRIDGED COMPLEXES

COMPOUND	Si-M-M	M-Si-M	Si-M-C
$W_2(CO)_8H_2[Si(C_2H_5)_2]_2$	53.02(10)	73.97(12)	109.1(5)
$Re_2(CO)_8H_2Si(C_6H_5)_2$	53.9(1)	72.3(1)	124.8(13)
$Re_2(CO)_8[Si(C_6H_5)_2]_2$	52.2(2)	75.7(3)	78.7(2)
$Re_2(CO)_6H_4[Si(C_2H_5)_2]_2$	52.6(1)	74.9(1)	127.5(3)
$Re_2(CO)_7H_2[Si(C_2H_5)_2]_2$	53.2(1)	73.6(1)	126.8(5)

plane of the central cluster and are a constant feature of all the structures. Hydrogen atoms, although not located experimentally, are positioned in what are thought to be their approximate locations.

Viewing the hydrogen ligand environments in the examples shown, it is obvious that in the tungsten hydride (C), the hydrogen is more crowded than in the rhenium hydrides. The Si-W-C (carbonyl) angle, which encloses the hydrogen ligand is $109.1(5)^\circ$ in the tungsten hydride, compared to the analogous angles of $124.8(13)^\circ$, $126.8(5)^\circ$, and $127.5(3)^\circ$ in the rhenium hydrides (B), (D), and (E) respectively. It has been shown^{93,94,97} that a normal non-bonded H-C (carbonyl) contact can be as low as 2.0 \AA . For a Re-H distance²⁹ of 1.68 \AA calculations show that in the rhenium hydrides, maintaining the minimum C-H contact, a H-Si contact of greater than 2.2 \AA arises. However the situation is much different for $\text{W}_2(\text{CO})_8\text{H}_2[\text{Si}(\text{C}_2\text{H}_5)_2]_2$. If no hydrogen bridging concept is utilized, then using the unbridged W-Si distance of 2.586 \AA , and maintaining the minimum C-H contact, a very short Si-H contact of 1.72 \AA occurs (this calculated assuming a W-H distance⁹⁸ of 1.70 \AA). Even using the larger W-Si distance, a short Si-H contact of 1.81 \AA arises. Therefore the hydrogen

ligands are constrained to be considerably closer to the silicon atoms in the tungsten compound. It is believed that the crowding of the hydrogen by the carbonyl group is then responsible for the appearance of the three centre W-H-Si bond, since it is possible that the three centre bond is favoured energetically over a terminal hydride involving the high repulsion energy which must be associated with the very short Si-H non-bonded contacts mentioned.

The non-bonded Si-H contact of 2.2 Å calculated for the rhenium hydrides is believed to be reasonable. In $(\pi\text{-C}_5\text{H}_5)(\text{CO})\text{HFe}(\text{SiF}_3)_2$ the hydrogen was not believed⁹⁹ bonded to either silicon atom and was located at 2.06(7) Å from both silicons. Although seemingly short, these non-bonded contacts can occur because in these systems the hydrogens approach the silicon atoms in electron density nodes, for example between the F-Si-F covalent bonds in $(\pi\text{-C}_5\text{H}_5)(\text{CO})\text{HFe}(\text{SiF}_3)_2$, or between the C-Si-C bonds in the rhenium hydrides discussed. The repulsion is minimized in these bonding nodes thus facilitating the approach of the hydrogen ligand to the silicon atom.

There seems therefore to be no inherent stability of the hydrogen-bridged metal-silicon bond. Rather, the three centre bond is the result of steric crowding

by an adjacent carbonyl group and only appears, as for $W_2(CO)_8H_2[Si(C_2H_5)_2]_2$, when the hydrogen ligand is restricted to be close to the silicon atom.

Although evidence obtained from the structural investigations of $Re_2(CO)_6H_4[Si(C_2H_5)_2]_2$ and $Re_2(CO)_7H_2[Si(C_2H_5)_2]_2$ combined with that obtained from ^{64,66} $W_2(CO)_8H_2[Si(C_2H_5)_2]_2$ and $Re(CO)_8[Si(C_2H_5)_2]_2$ exclude the possibility of a three centre Re-H-Si bond, it does not exclude the existence of weak attractive interaction of the hydrogen ligand with the silicon atom. An insight into this possibility is gained from the structural investigations ^{93,94,97} of $(\pi-C_5H_5)(CO)_2HMnSi(C_6H_5)_3$, $(\pi-C_5H_5)(CO)_2HMnSiCl_2(C_6H_5)$ and $(CO)_4FeHSi(C_6H_5)_3$, in which the hydrogen ligands were located experimentally. In both manganese compounds the hydrogens were located at 1.55(4) Å and 1.49(6) Å respectively from the manganese atoms and 1.76(4) Å and 1.79(6) Å respectively from the silicon atoms. However, in the iron compound the hydrogen atom was 1.64(10) Å from the iron atom and 2.73(10) Å from the silicon atom. In the two manganese hydrides the hydrogen ligands are constrained to be close to the silicon atoms, due to steric crowding, the hydrogen being only 2.08(4) Å from the carbonyl in $(\pi-C_5H_5)(CO)_2HMnSi(C_6H_5)_3$ and 1.98(6) Å from the carbonyl

in $(\pi\text{-C}_5\text{H}_5)(\text{CO})_2\text{HMnSiCl}_2(\text{C}_6\text{H}_5)$. There is no possibility of increasing the H-Si distance without increasing the hydrogen contact with the carbonyl groups. However in $(\text{CO})_4\text{FeHSi}(\text{C}_6\text{H}_5)_3$ the hydrogen is not constrained to be close to the silicon atom, since it is in a sterically less crowded environment than the manganese hydrides. Thus the long Si-H contact observed is indicative of a terminally bound hydrogen with no attraction to the silicon atom. This is interpreted as meaning that there is no inherent stability of the weakly bridged hydrogen in this series in preference to a simple terminal hydrogen.

Thus in conclusion, in this series of transition metal hydrides, the hydrogen atoms are bound terminally to the transition metals in all the rhenium complexes. The hydrogens only approach the silicon atoms, as in the tungsten and manganese complexes, as a result of steric crowding and not as a result of any unusual attraction to the silicon atoms.

CHAPTER V: DITHIOLENE¹⁰⁰ INTRODUCTION

Interest in the bidentate dithiolene ligands began in the mid 1930's when R. E. D. Clark discovered^{101,102} that toluene-3,4-dithiol and 1-chlorobenzene-3,4-dithiol reacted with zinc, cadmium, mercury and tin halides to form complexes of the type $[M(\text{dithiol})_2]$. This reaction was found to be especially effective in the analytical determination of tin^{103,104} and of molybdenum and tungsten^{105,106,107} and most attention was directed towards this end. By the early 1960's several dithiolene complexes had been characterized^{108,109,110} and were found to be of the form $M(\text{dithiol})_2$ involving a variety of dithiolene ligands combined with nickel, cobalt, palladium, and molybdenum. These bis dithiol complexes were found to possess two unusual properties. Firstly, they exhibited the unusual square planar geometry^{111,112,113,114} with the sulfur atoms in an almost perfect square about the metal. And secondly, they underwent facile reversible oxidation-reduction reactions¹¹⁵ without changes in coordination geometry. The oxidized and reduced species were found to be related simply by one electron transfers and could be detected using polarography and voltammetry.

Attempts to produce the bis complexes of $S_2C_2Ph_2$ with V, Cr, Mo, Re, W, Ru, and Os¹¹⁶ instead yielded

the six coordinate *tris* complexes^{117,118,119} which were similar to the *bis* complexes in that they also underwent the facile oxidation-reduction reactions.^{119,120,121} The discovery¹²² that $\text{Co}[\text{S}_2\text{C}_2(\text{CN})_2]_2^-$ reversibly added one mole of ligand to form the complex $\text{Co}[\text{S}_2\text{C}_2(\text{CN})_2]_3^{3-}$ led to the interesting suggestion that the six coordinate cobalt complex and possibly even the other *tris* complexes could be trigonal prismatic. In addition, doubt about the octahedral coordination of these complexes was raised because of the inability to separate $\text{Co}[\text{S}_2\text{C}_2(\text{CN})_2]_3^{3-}$ and $\text{Mo}[\text{S}_2\text{C}_2(\text{CF}_3)_2]_3$ into their optical enantiomers.¹²³ The possibility of trigonal prismatic coordination was extremely unusual since no six coordinate molecular complexes had been observed with non-octahedral coordination. Trigonal prismatic coordination had been observed¹²⁵ as early as 1923 in the compounds MoS_2 and WS_2 , and later¹²⁶ in NiAs . However these were infinitely extended lattices and molecular packing was believed responsible for their unusual coordination.¹²⁴ It is noteworthy that on the basis of "directed valence" calculations, it had even been predicted by Hultgren¹²⁷ in 1932, that the only stable six coordinate complexes were trigonal prismatic and octahedral, the former being preferred for low lying d orbitals and the latter being preferred

for higher energy d orbitals. In addition octahedral coordination would be favoured by increasing ionic character in the metal-ligand bonds and by the bulkiness of large ligands.

The existence of trigonal prismatic coordination in a molecular complex was not observed until 1965 when the X-ray structure determination^{128,129} of $\text{Re}[\text{S}_2\text{C}_2(\text{C}_6\text{H}_5)_2]_3$ was completed. The subsequent structural determinations of $\text{Mo}(\text{S}_2\text{C}_2\text{H}_2)_3$ ¹³⁰ and $\text{V}[\text{S}_2\text{C}_2(\text{C}_6\text{H}_5)_2]_3$ ^{131,132} also showed trigonal prismatic geometry and verified that the rhenium compound was not an isolated example but only one of a possible series of trigonal prismatic structures. In all three compounds the metals were surrounded by six sulfur atoms at the corners of a trigonal prism, with the dithiolene ligands radiating from the metals in a "paddle-wheel" arrangement. There was also a striking similarity in the prism dimensions of the three compounds (Table 48). The intra- and interligand sulfur-sulfur distances are similar in all cases with the approximate values 3.06 Å and 3.08 Å respectively. The shortness of these "non-bonded" contacts led to the speculation that some sulfur-sulfur bonding was involved¹²⁴ in stabilizing the trigonal prism. Another remarkable feature of the three complexes was

the similarity in the metal-sulfur bond lengths, averaging 2.33 Å, despite the fact that the covalent and ionic radii¹³³ of vanadium differed from those of molybdenum and rhenium by 0.07 Å. This similarity was viewed as an added consequence of the interligand S-S bonding.¹²⁴ In addition the S-C distances, averaging 1.69 Å were found to be consistent with considerable double bond character as seen from a comparison with the S=C double bond in thiourea¹³⁴ [SC(NH₂)₂] and its derivatives,¹³⁵ measuring 1.720 Å.

Slight differences are, however, present in the three compounds which lead to distortions from the idealized D_{3h} symmetry. Re[S₂C₂(C₆H₅)₂]₃ and Mo[S₂C₂(CN)₂]₃ both have approximate C_{3h} symmetry caused by twisting of the phenyl groups out of the ligand planes in the former and by a deviation of the S₂C₂ planes from the MS₂ planes by 18° in the latter. In V[S₂C₂(C₆H₅)₂]₃ the unique ligand on the crystallographic two-fold differs slightly from the other two, however the molecule still closely approximates D_{3h} symmetry.

Comparison of the electron spin resonance and electronic spectra in the solid state and in solution¹³⁶ confirmed that the trigonal prismatic coordination was also present in solution and therefore was a

consequence of intramolecular phenomena rather than intermolecular effects. It was also apparent in all the electronic spectra that the dominant feature was an intense two-band pattern in the visible region,¹³⁷ the first at about $15,000 \text{ cm}^{-1}$ ($\epsilon \sim 25000$) and the second at about $24,000 \text{ cm}^{-1}$ ($\epsilon \sim 15000$). This was believed to be characteristic of all trigonal prismatic d³ complexes.

An attempt to explain the stability of the trigonal prism over the octahedron, two separate orbital treatments were presented. In the first, by Schrauzer and Mayweg¹³⁸ no reason for the stability of the trigonal prism is obvious. Orbital calculations performed on a hypothetical octahedral complex $\text{MS}_6\text{C}_6\text{R}_6$ yielded the same orbital ordering as the trigonal prismatic calculations. Also objections based on electron spin resonance spectra have been raised¹³⁹ concerning the ordering of the highest occupied and lowest unoccupied levels for this scheme. The scheme by Gray et al.,¹³⁷ which seems more consistent with electron spin resonance spectra, electronic spectra and polarographic work is therefore favoured in this work. Both schemes are discussed further in Chapter IX where a detailed explanation of the trigonal prism is given based on

Gray's molecular orbital calculations.

Although the neutral *tris* dithiolenes were found to be trigonal prismatic, subsequent structural determinations on $V[S_2C_2(CN)_2]_3^{2-}$,¹⁴² $Mo[S_2C_2(CN)_2]_3^{2-}$,¹⁴¹ and $Fe[S_2C_2(CN)_2]_3^{2-}$ ¹⁴² showed coordinations which varied from highly distorted octahedrons for the vanadium and molybdenum dianions to an almost regular octahedral coordination for the iron dianion. Interligand sulfur-sulfur distances in the three were greater than for the neutral trigonal prisms and thus were consistent with a breakdown in the sulfur-sulfur bonding which had been proposed¹²⁴ as a stabilizing factor in the prism. In addition the extra electrons in the molybdenum dianion as compared to the neutral molybdenum complex were located in an orbital which was said to be antibonding in the trigonal prism¹⁴¹ thus offering an explanation of the deviation from the trigonal prismatic coordination. The trend therefore emerged that the neutral *tris* 1,2-dithiolenes were trigonal prismatic whereas the dianions were octahedral or distorted octahedral. The reasons for the trigonal prismatic and octahedral coordination in these dithiolenes was not obvious however and little was published correlating the observed structures to the molecular orbital descriptions of either Gray or

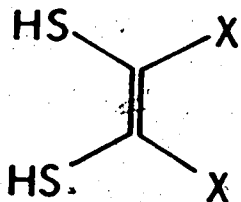
Schrauzer.

The compounds $\text{Mo}(\text{S}_2\text{C}_6\text{H}_4)_3$, $[(\text{C}_6\text{H}_5)_4\text{As}][\text{Nb}(\text{S}_2\text{C}_6\text{H}_4)_3]$, and $[(\text{CH}_3)_4\text{N}]_2[\text{Zr}(\text{S}_2\text{C}_6\text{H}_4)_3]$, which form the subject matter for the remainder of this thesis, therefore constitute an interesting and potentially informative series. Firstly the $\text{M}(\text{S}_2\text{C}_6\text{H}_4)_3^{n-}$ ($n = 0, 1, 2$ for $\text{M} = \text{Mo}, \text{Nb}, \text{Zr}$, respectively), moieties form an isoelectronic series so that the only differences are in the central metal. From a molecular orbital viewpoint, this means only the d orbital energies vary throughout the series. Hence, the effect that varying the central metal, and thus the metal d orbitals, will have on the coordination of the metals can be observed, and hopefully correlated to Gray's molecular orbital description for trigonal prismatic geometry. Also since identical ligands ($\text{S}_2\text{C}_6\text{H}_4^{2-}$) are involved, subtle geometry changes involving angles and bond lengths can be more readily compared, than if differing ligands are used.

From a comparison of their electronic spectra^{137,143.} in Table 18 it is obvious that gross differences exist within the three compounds. For the molybdenum^{137,144} and niobium¹⁴³ complexes the spectra were similar, both having absorptions which were believed characteristic of trigonal prismatic

coordination.¹³⁷ The spectrum¹⁴³ of $Zr(S_2C_6H_4)_3^{2-}$ however, was found to be vastly different and was not indicative of a trigonal prism. Thus on the basis of the electronic spectral results it seems that varying the central metal from Mo to Nb to Zr causes changes in the coordination, presumably destabilizing the trigonal prism and favouring a tendency towards octahedral coordination as was observed in $Mo[S_2C_2(CN)_2]_3^{2-}$ and $V[S_2C_2(CN)_2]_3^{2-}$. It was believed that a complete structural determination of this series of *tris* 1,2-dithiolene complexes would prove useful in understanding further the factors which stabilize trigonal prismatic coordination. It was also of interest to discover whether the electronic spectra were reliable indicators of the coordination geometry in these compounds.

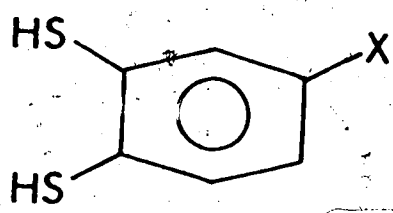
The common 1,2-dithiol ligands and their normal abbreviations, which will be used in this thesis, are shown below.



X = H dithioglyoxal

= CN maleonitriledithiol (mnt)

= C_6H_5 *cis* 1,2-diphenylethene-1,2-dithiol (sdt)



X = H benzene-1,2-dithiol
(bdt)
= CH₃ toluene-3,4-dithiol
(tdt)

TABLE 18: ELECTRONIC SPECTRA FOR MOLYBDENUM,
NIOBIUM, AND ZIRCONIUM BENZENE DITHIOLS^{137,143}

COMPLEX	COLOUR	BAND MAXIMA, cm ⁻¹ (ε in parentheses)
Mo(S ₂ C ₆ H ₄) ₃ ¹⁴⁴	Dark Green	11,500 sh (1000); 14,463 (20,900); 22,990 (17,400)
[(C ₆ H ₅) ₄ As][Nb(S ₂ C ₆ H ₄) ₃]	Dark Purple	17,700 (10,700); 27,200 (13,800); 30,700 sh (9,120).
[(C ₂ H ₅) ₄ N] ₂ [Zr(S ₂ C ₆ H ₄) ₃]	Red	20,000 sh (2,030); 35,800 sh (25,200).

CHAPTER VI: THE CRYSTAL AND MOLECULAR STRUCTURE
OF TRIS (BENZENE-1,2-DITHIOLATO)
MOLYBDENUM, $[\text{Mo}(\text{S}_2\text{C}_6\text{H}_4)_3]$.

EXPERIMENTAL

Dark green crystals of $\text{Mo}(\text{bdt})_3$ suitable for X-ray diffraction study, prepared by the reaction of molybdenum pentachloride with benzene dithiol,¹³⁷ were kindly supplied by Dr. Takats and Mr. Martin.¹⁴³ Preliminary photography revealed *mmm* Laue symmetry, indicating an orthorhombic space group. The systematic absences as determined from Weissenberg ($0k\ell$, $l k\ell$; CuK_α X-radiation) and Precession ($h0\ell$, $h1\ell$, $hk0$, hkl ; MoK_α X-radiation) photographs are $0k\ell: k + \ell = 2n + 1$ and $h0\ell: h = 2n + 1$, consistent with the space groups Pnam and $\text{Pna}2_1$. Precise lattice parameters were obtained at 22°C from a least squares refinement of the setting angles of 12 reflections which were accurately centred on a Picker automatic four-circle diffractometer, using CuK_α X-radiation ($\lambda = 1.54051 \text{ \AA}$). The cell parameters and their standard deviations are: $a = 16.093(3) \text{ \AA}$, $b = 10.177(1) \text{ \AA}$, and $c = 11.906(2) \text{ \AA}$. The observed density, obtained by floatation in aqueous zinc bromide solution, is $1.74(2) \text{ g cm}^{-3}$ and

is in good agreement with the calculated value of 1.75 g cm^{-3} , obtained assuming four molecules of molecular weight 516.60 a.m.u. per unit cell of volume 1952.84 \AA^3 . For space group $\text{Pna}2_1$ there are 4 general equivalent positions and no restrictions are possible. However for Pnam there are 8 general equivalent positions so the molecules are restricted to lie either on the mirror planes or inversion centres. The tris chelate structure cannot have an inversion centre, hence for space group Pnam , the molecule must possess symmetry m .

Intensity data were collected on the Picker automatic four circle diffractometer using CuK_α X-radiation, filtered with 0.0005" thick nickel foil (in preference to a graphite monochromator¹⁴⁵) and using a 2° take-off angle. The crystal was aligned in a general orientation but with its a^* axis approximately coincident with the diffractometer ϕ axis. The crystal faces were identified and the perpendicular distances between parallel faces of the same form were measured as: $\{1,0,0\}$, 0.206 mm; $\{0,1,0\}$, 0.055 mm; $\{0,0,1\}$, 0.077 mm. A coupled $2\theta/\omega$ scan was used, with a 2θ scan speed, of $1^\circ/\text{min}$ to collect all reflections with $2\theta \leq 125^\circ$. The peak scan was approximately two minutes (2°), increasing as the $\alpha_1\alpha_2$ resolution

increased. Stationary background counts of 40 secs. were collected on either side of the peak. Assuming approximate linearity of background, the intensities and standard deviations were calculated as shown previously in Chapter II. The detector was a scintillation counter and was used in conjunction with a pulse height analyzer tuned to accept 95% of the CuK_α peak. Three standard reflections were collected automatically every 100 data reflections. In addition data collection was interrupted periodically to collect a further five standard reflections to investigate possible decomposition. No significant decomposition was observed over the duration of the data collection. Of the 1806 reflections collected, 1050 were significantly above background with $I/\sigma(I) \geq 3.0$. The data were reduced to structure factor amplitudes by correction for Lorentz, polarization, and absorption effects. Terms used in the Zachariasen extinction correction were calculated at this stage. Standard deviations, $\sigma(F)$, in the structure factors were again computed using a "p factor"⁷⁰ of 0.03.

The linear absorption coefficient⁸⁶ using CuK_α radiation is 110.67 cm^{-1} , giving rise to a range of transmission factors between 0.5768 and 0.3099.

STRUCTURE SOLUTION AND REFINEMENT

A sharpened 3-dimensional Patterson map¹⁴⁶ was computed between the limits $0 \leq u \leq 0.5$, $0 \leq v \leq 0.5$, $0 \leq w \leq 0.5$. The Mo-Mo vectors for both $Pna2_1$ and $Pnam$ (with the molybdenum atom on the crystallographic mirror) are shown in Table 19. It is obvious that the two space groups cannot be distinguished in the Patterson on the basis of the Mo-Mo vectors alone. However, the molybdenum position was obtained as follows. The most intense peak was situated at $(0.500, 0.0, 0.0)$ and was attributed to the vector $(1/2, 1/2-2y, 0)$; thus the y coordinate was obtained as ± 0.25 . The accidentally special y coordinate leads to an ambiguity in the assignment of the next most intense peaks, observed at $(0.325, 0.500, 0.500)$ and $(0.182, 0.500, 0.500)$, as vectors of the form $(1/2-2x, 1/2, 1/2)$ and $(2x, 2y, 1/2)$. Because of this failure to identify the true Harker line vector, two possible solutions for molybdenum coordinates had to be tested by subsequent structure factor calculations and least squares refinement. The solutions to be tested were (a) $x = 0.09$, $y = 0.25$, $z = 0.25$, and (b) $x = 0.16$, $y = 0.25$ and $z = 0.25$.

The fourth largest peak on the map, at $(0.0, 0.0,$

TABLE 19: HARKER VECTORS FOR $\text{Mo}(\text{bdt})_3$

$\text{Pna}2_1$		$\text{Pnam} (z=1/4), \text{SPECIAL POSITION "C"}$	
VECTOR FORM	WEIGHT	VECTOR FORM	WEIGHT
$1/2-2x, 1/2, 1/2$	2	$1/2-2x, 1/2, 1/2$	2
$1/2+2x, 1/2, 1/2$	2	$1/2+2x, 1/2, 1/2$	2
$1/2, 1/2-2y, 0$	2	$1/2, 1/2-2y, 0$	2
$1/2, 1/2+2y, 0$	2	$1/2, 1/2+2y, 0$	2
$2x, 2y, 1/2$	1	$2x, 2y, 1/2$	1
$-2x, -2y, 1/2$	1	$-2x, -2y, 1/2$	1
$2x, -2y, 1/2$	1	$2x, -2y, 1/2$	1
$-2x, 2y, 1/2$	1	$-2x, 2y, 1/2$	1

0.255), was located at 3.04 \AA from the origin and was consistent with a build-up of S-S vectors between sulfur atoms related by a mirror perpendicular to z. Since this was the largest S-S vector, the possibility of the mirror bisecting the triangular faces was excluded and the space group was probably Pnam with the mirror relating the two triangular faces of the trigonal prism. If this were the case, then Mo-S vectors should be observed at w coordinates of about $1/2(0.255) = 0.13$. Three vectors at $2.3 - 2.4 \text{ \AA}$ from the origin were located with w coordinates 0.136 and were consistent with the trigonal prismatic geometry. In addition three vectors were located in the $w = 0$ plane at $3.04 - 3.17 \text{ \AA}$ from the origin and these were consistent with vectors between the sulfur atoms within the triangular faces. From the Mo-S and S-S vectors the sulfur positions were calculated as either: S1(0.11, 0.14, 0.38), S2(0.16, 0.42, 0.38) and S3(0.29, 0.21, 0.38) corresponding to Mo position (b) or S1(0.04, 0.14, 0.38), S2(0.09, 0.42, 0.38) and S3(0.22, 0.21, 0.38) corresponding to Mo position (a).

To obtain the proper x coordinates a least squares refinement was performed with the model based on Mo positions (b). This model showed no signs of successful

refinement and converged after two cycles to give $R_1 = 0.424$ and $R_2 = 0.516$. However the model based on Mo coordinates (a) refined to $R_1 = 0.349$ and $R_2 = 0.435$ in two cycles. Temperature factors were fixed in these cycles, so further refinement of the second model, varying the temperature factors yielded $R_1 = 0.209$ and $R_2 = 0.294$ after the three cycles and thus the model was assumed to be correct. An outline of the solution and refinement is shown in Table 20.

TABLE 20: REFINEMENT OUTLINE

Model	R_1	R_2
(1) Mo and S atoms based on Mo coordinates (0.16, 0.25, 0.25)	0.424	0.516
(2) Mo and S atoms based on Mo coordinates (0.09, 0.25, 0.25)	0.349	0.435
(3) Mo and S atoms of model (2) - varying temperature factors	0.209	0.294
(4) Mo, S, and C atoms; isotropic B's	0.079	0.086
(5) Absorption Correction	0.065	0.075
(6) Mo and S atoms anisotropic	0.050	0.062
(7) H positions added	0.046	0.051
(8) Extinction correction ¹⁴⁷	0.042	0.042
(9) Carbon atoms anisotropic	0.035	0.034

Structure factors were calculated using the atomic scattering factors of the neutral atoms for molybdenum,

sulfur and carbon compiled by Cromer and Mann.⁷⁵ The scattering factors for hydrogen were those of Stewart, Davidson and Simpson.¹⁴⁹ In addition anomalous dispersion corrections,⁷⁶ both real and imaginary, were applied to the molybdenum and sulfur scattering factors ($\Delta f'_{\text{Mo}} = -0.54$, $\Delta f''_{\text{Mo}} = 2.89$, $\Delta f'_S = 0.31$, $\Delta f''_S = 0.58$).

The carbon atoms were located from an electron density difference map phased on model (3). Anisotropic temperature factors for the different groups of atoms were introduced, as indicated by features in electron density difference maps, and can be justified, at the 0.005 significance level, by the subsequent application of Hamilton's R factor ratio test.⁷⁹ In the difference map, phased on model (6), the hydrogen atoms were visible so they were included in subsequent refinements, their positions calculated from the known geometry and orientation of the benzene rings, and using a C-H distance of 1.0 Å. The hydrogen atoms were assigned thermal parameters approximately 15% higher than those of the attached carbon atoms.

Although they were included in the structure factor calculations, their parameters were not refined.

Extinction corrections¹⁴⁷ were applied since comparison of $|F_o|$ and $|F_c|$ for low angle reflections suggested the problem may exist. Verification of the

importance of the extinction correction is evident in the results of the refinements before and after this correction. Before the correction, all reflections except one with $\sin \theta/\lambda \leq 0.084$ were rejected from the refinement on the basis that $| \Delta F/\sigma(F) | > 5.0$, and in all cases $| F_o |$ was less than $| F_c |$ for these reflections. After the extinction correction, only one of these reflections previously rejected was still rejected from the refinement. The final refined value of the extinction scale factor, C , is 2.371×10^{-6} .

Anomalous features in the thermal parameters (*vide infra*) suggested that the scattering factors could be inadequate. Several refinements were attempted using various alternative scattering factors [Mo(IV), ¹⁵⁰Mo(VI), ¹⁵⁰S⁻⁷⁵] but no better agreement in R factor and no more reasonable thermal parameters were obtained. Thus the results from the original refinement are reported.

Programmes used in solution, refinement and presentation of data are listed in Appendix 2.

RESULTS

The observed and calculated structure factor amplitudes, $|F_o|$ and $|F_c|$, are shown in Table 21. The final fractional coordinates of all atoms and their isotropic temperature factors are shown in Table 22, their standard deviations being obtained from the inverse matrix of the final least squares analysis. The anisotropic thermal parameters⁸⁰ (U_{ij} 's) of all anisotropic atoms are shown in Table 23. Relevant intramolecular bond lengths are shown in Table 24 and the intramolecular angles in Table 25. Intermolecular contacts which are close to the predicted van der Waals separations¹⁵¹ are listed in Table 26. These bond lengths, intermolecular contacts and bond angles, along with their standard deviations were obtained from ORFFE (See Appendix 2). Several least squares plane calculations are shown in Table 27, along with the deviations of the atoms from the planes. In addition, Table 28 shows the dihedral angles between selected planes.

In the three dimensional drawings of the molecule, 50% probability thermal ellipsoids are shown for molybdenum and sulfur atoms. For the carbon atoms artificially low isotropic thermal parameters were used

for clarity of the diagram. Similarly the hydrogen atoms were excluded from the plot for clarity. The hydrogen atoms are numbered from H1 to H6 and are bonded sequentially to the second and third carbon atoms in the rings. In the packing diagram in Fig. 13, the open bonds represent molecules at $z = 0.25$ whereas the dark bonds represent molecules at $z = 0.75$.

TABLE 21: OBSERVED AND CALCULATED STRUCTURE
FACTOR AMPLITUDES (ELECTRONS X 10)

K	L	F OBS	FCAL	K	L	F OBS	FCAL	K	L	F OBS	FCAL	K	L	F OBS	FCAL	K	L	F OBS	FCAL
0	2	3512	3133	2	5	455	442	0	5	579	582	6	2	338	294	6	1	578	579
0	4	2258	2159	2	6	148	106	0	5	646	663	6	3	331	332	6	2	245	325
0	6	628	664	3	0	850	850	0	7	1625	1525	6	5	408	454	6	3	404	776
0	8	2010	1969	3	1	642	635	0	8	815	803	6	6	350	339	6	5	505	483
0	12	404	428	3	2	126	143	0	9	896	888	6	7	825	809	6	6	285	273
1	1	2346	2421	3	3	370	383	0	13	288	300	6	9	639	630	6	7	617	595
1	3	278	258	3	4	912	911	1	0	1800	1761	6	10	220	201	6	8	472	442
1	5	440	459	3	4	912	911	1	1	604	620	6	11	304	270	6	9	255	268
1	7	2098	2060	3	5	390	395	1	2	961	978	7	0	766	777	6	11	324	323
1	9	1115	1098	3	7	205	157	1	3	372	383	7	1	451	468	7	0	911	914
1	13	245	276	3	8	371	379	1	4	442	440	7	2	720	714	7	1	823	933
2	0	520	515	3	10	257	266	1	5	442	445	7	4	627	619	7	4	852	853
2	2	836	852	3	11	265	286	1	6	1153	1160	7	6	528	490	7	7	532	508
2	4	1147	1168	3	12	374	347	1	7	594	561	7	7	496	472	7	8	565	560
2	6	1371	1333	4	0	577	567	1	8	1205	1190	7	8	395	383	7	9	244	254
2	8	1089	1067	4	1	164	149	1	9	395	379	7	9	312	317	8	0	604	673
2	10	608	604	4	2	472	457	1	10	429	422	7	10	327	338	8	1	343	366
2	12	420	429	4	3	1447	1417	1	12	217	206	8	0	303	323	8	2	294	317
3	1	798	823	4	4	996	966	1	13	161	166	8	3	935	920	8	3	391	414
3	3	1888	1895	4	5	651	671	2	0	435	420	8	5	745	765	8	5	269	281
3	5	1397	1365	4	7	718	708	2	1	2428	2520	8	6	321	322	8	6	266	272
3	7	421	416	4	8	549	541	2	2	775	794	8	8	351	336	8	7	292	299
3	9	474	477	4	9	312	333	2	3	774	800	8	9	174	157	8	8	362	319
3	11	742	740	4	10	190	142	2	4	920	950	9	0	314	323	9	1	209	205
3	13	460	444	4	11	452	413	2	5	494	520	9	1	546	532	9	3	330	339
4	0	666	679	4	12	319	307	2	6	250	226	9	2	565	587	9	5	273	305
4	2	902	900	5	0	230	213	2	7	763	760	9	4	684	681	10	2	224	234
4	4	1148	1168	5	1	281	290	2	9	696	699	9	6	246	233	10	3	171	180
4	6	779	765	5	3	655	652	2	10	421	393	9	7	341	334	10	4	435	428
4	8	640	631	5	4	389	402	2	11	367	350	10	0	640	654	10	6	180	193
4	10	790	793	5	5	400	402	2	12	375	384	10	1	271	279	11	0	263	246
4	12	550	539	5	6	172	131	2	13	247	284	10	2	201	197	11	1	165	132
5	1	974	992	5	7	340	335	3	0	709	698	10	3	397	415	11	3	333	329
5	3	823	835	5	10	238	255	3	1	586	573	10	4	174	190	11	4	162	190
5	5	811	803	5	11	358	331	3	2	1076	1055	10	5	351	378				
5	7	761	766	5	12	164	165	3	3	1576	1579	10	6	168	191				
5	9	617	627	6	0	230	242	3	4	1260	1256	10	7	265	268				
5	11	456	435	6	1	551	557	3	5	1119	1113	11	0	357	383				
6	0	1262	1263	6	2	196	235	3	6	788	765	11	1	458	442				
6	2	1248	1228	6	4	553	535	3	7	374	368	11	2	395	295				
6	4	923	891	6	6	519	484	3	8	470	479	11	4	218	215				
6	6	568	544	6	8	295	310	3	10	492	496								
6	8	331	303	7	0	1080	1110	3	11	634	656								
6	10	188	233	7	2	206	193	3	12	431	457								
7	1	982	882	7	3	239	268	3	13	306	296								
7	3	785	786	7	4	525	501	4	0	665	656								
7	5	611	600	7	5	207	195	4	1	882	874								
7	7	440	430	7	6	347	314	4	2	703	666								
7	9	383	388	7	8	687	665	4	3	1121	1175								
8	2	411	392	8	1	370	360	4	4	1494	1476								
8	4	749	765	8	2	259	304	4	5	922	922								
8	6	565	585	8	3	408	434	4	6	211	188								
8	8	464	457	8	4	172	215	4	7	597	567								
8	10	504	515	8	5	275	279	4	8	378	382								
9	1	583	582	9	6	282	282	4	9	475	443								
9	3	656	648	9	7	533	525	4	10	347	325								
9	5	461	463	9	8	284	290	4	11	411	422								
9	7	280	267	10	0	588	601	4	12	500	566								
10	0	227	256	10	1	320	300	5	0	1245	1225								
10	2	381	380	10	2	368	397	5	1	341	356								
10	4	485	479	10	3	168	173	5	2	840	827								
10	6	388	391	11	0	164	76	5	3	659	657								
11	1	395	407	11	1	175	177	5	4	487	476								
11	3	263	297	11	2	240	241	5	5	483	487								
				11	3	180	193	5	6	741	729								
				11	4	443	457	5	8	613	778								
								5	10	424	422								
								5	11	318	259								
								5	12	216	228								
								6	0	535	541								
								6	1	859	869								

Table 21. (continued)

K	L	FCPS	FCAL	K	L	FCPS	FCAL	K	L	FCPS	FCAL	K	L	FCPS	FCAL	K	L	FCPS	FCAL
2	10	369	350	9	4	237	280	8	8	247	263	6	2	796	783	6	3	459	501
2	11	777	783	9	5	308	327	8	9	207	212	6	3	245	261	6	5	351	395
2	12	329	340	9	6	239	230	9	0	219	242	6	4	201	161	7	0	236	225
2	13	416	424	9	8	228	255	9	2	216	228	6	5	223	196	7	3	193	142
3	1	1205	1190	10	1	379	420	9	2	185	190	6	6	580	573	7	4	398	396
3	2	1503	1472	10	2	229	257	9	5	226	248	6	8	701	666	7	6	190	186
3	3	614	606	10	4	380	365	9	6	197	223	6	10	195	214	8	3	326	322
3	4	2093	2040	10	5	175	193	10	1	412	422	7	0	284	267	8	5	260	293
3	5	390	383	10	6	177	176	10	4	320	315	7	1	805	803	8	8	197	196
3	6	298	291	11	0	569	571	11	0	427	440	7	3	589	585	9	1	286	305
3	7	462	475	11	1	224	258	11	2	242	232	5	5	526	500	9	2	194	234
3	8	391	395	11	2	159	177	0	0	1346	1359	7	7	450	442	9	4	360	331
3	9	356	331	11	3	179	187	0	1	542	554	7	9	324	314	9	7	220	249
3	10	519	486	1	0	1106	1070	0	2	1742	1653	8	0	219	167	10	0	327	337
3	12	673	682	1	1	670	673	0	3	1265	1274	8	1	236	231	10	3	247	237
4	0	1485	1455	1	2	125	132	0	4	1566	1540	8	2	401	409	0	0	1116	1124
4	1	590	594	1	3	176	214	0	5	728	753	8	4	902	910	0	1	1307	1282
4	2	616	605	1	4	624	620	0	6	531	533	8	6	496	483	0	2	297	293
4	3	990	1000	1	5	228	223	0	7	645	659	8	7	293	270	0	3	798	815
4	4	781	783	1	6	206	182	0	8	257	263	9	0	356	348	0	4	324	331
4	5	460	488	1	7	169	208	0	9	479	470	9	1	260	257	0	5	634	621
4	6	306	298	1	8	435	436	0	10	479	470	9	3	636	640	0	6	246	251
4	7	719	734	1	9	210	185	0	11	498	506	9	4	205	180	0	7	603	604
4	8	446	451	1	11	156	223	0	12	541	564	9	5	508	521	0	8	479	475
4	10	234	232	1	12	156	223	1	0	949	914	10	0	308	305	0	9	566	568
4	11	558	568	2	1	581	602	1	1	474	476	10	2	324	339	0	10	418	422
5	0	723	730	2	2	285	293	1	2	2-5	265	10	4	359	358	1	11	450	440
5	1	628	921	2	3	971	970	1	3	1719	1733	11	1	513	523	1	12	688	695
5	2	424	441	2	4	265	291	1	4	1059	1057	1	2	1099	1049	1	13	148	62
5	3	329	353	2	5	381	384	1	5	1222	1316	1	3	252	248	1	14	873	879
5	4	265	236	2	6	273	253	1	6	408	427	1	4	310	282	1	15	808	815
5	5	756	756	2	7	665	951	1	7	261	246	1	5	999	978	1	16	449	451
5	6	742	733	2	8	309	349	1	8	434	431	1	6	212	194	1	17	638	651
5	7	824	807	2	9	433	449	1	10	251	226	1	7	210	230	1	18	278	252
5	8	413	440	2	11	322	353	1	11	707	693	1	8	210	230	1	19	501	494
5	10	409	414	3	0	1563	1561	1	12	352	362	1	9	669	698	1	20	353	363
5	12	175	200	3	1	1085	1074	2	0	683	677	1	10	257	264	2	1	1130	1137
6	0	575	577	3	2	291	307	2	2	1009	1042	2	0	354	339	2	2	773	776
6	1	915	937	3	3	878	874	2	3	218	228	2	1	678	677	2	3	196	203
6	2	465	444	3	4	312	302	2	4	1251	1296	2	2	477	474	2	4	623	634
6	3	386	395	4	0	237	217	2	5	275	252	2	3	280	262	2	5	268	266
6	4	351	321	4	1	1105	1074	2	6	661	647	2	4	520	525	2	6	644	550
6	5	400	411	4	2	315	292	2	7	434	431	2	5	250	240	2	7	224	240
6	6	431	449	4	3	206	170	2	8	434	431	2	6	221	216	2	8	531	523
6	7	665	675	4	4	550	555	2	9	254	258	2	7	274	261	2	9	332	326
6	8	421	402	4	5	200	175	3	0	173	192	3	1	262	293	3	10	1256	1240
6	9	352	360	4	6	317	324	3	1	242	346	3	2	296	310	3	11	430	416
7	0	888	881	4	7	163	166	3	2	1034	1072	3	3	167	140	3	12	986	980
7	1	330	313	4	8	206	173	3	3	1054	1060	3	4	400	415	3	13	267	240
7	2	563	565	5	0	185	185	3	4	229	220	4	0	805	791	3	14	620	604
7	3	386	396	5	1	177	176	3	5	644	654	4	1	295	302	3	15	181	136
7	4	288	295	5	2	244	258	3	6	243	240	4	2	180	191	3	16	376	359
7	5	396	391	5	3	241	288	3	7	634	613	4	3	707	714	3	17	535	534
7	6	483	466	5	4	165	95	3	8	572	589	4	4	323	329	3	18	321	343
7	7	325	300	5	5	526	544	4	0	541	953	4	5	466	464	4	19	283	293
7	8	453	459	6	0	213	190	4	1	227	220	4	6	209	159	4	20	990	973
7	9	277	274	6	1	228	222	4	2	797	795	4	7	357	325	4	21	229	254
7	10	220	223	6	2	213	237	4	3	625	631	4	8	335	345	4	22	505	499
8	1	358	340	6	3	226	274	4	4	605	793	4	9	262	261	4	23	309	286
8	2	254	265	6	4	295	253	4	5	781	773	5	0	295	276	4	24	463	456
8	3	395	435	7	0	605	602	4	6	442	440	5	1	603	585	4	25	217	188
8	4	563	554	7	1	670	664	4	7	227	270	5	2	218	231	4	26	722	695
8	5	484	456	7	2	261	274	5	1	1460	1458	5	3	301	262	4	27	428	443
8	6	311	295	7	3	282	290	5	2	218	175	5	4	605	605	4	28	540	567
8	7	380	375	7	4	247	246	5	3	208	273	5	5	188	153	4	29	296	272
8	8	295	303	7	5	351	341	5	4	217	318	5	6	345	275	4	30	818	815
9	0	710	722	7	6	322	300	5	5	330	260	5	7	242	240	5	1	721	728
9	1	291	295	8	0	200	210	5	6	688	940	5	8	190	205	5	2	602	566
9	2	532	538	8	1	241	257	5	7	601	608	5	9	230	217	5	3	422	411
9	3	466	515	8	2	189	204	5	8	177	87	6	0	385	386				
				8	3	291	288	6	0	1456	1486	6	1	239	232				

Table 21 (continued)

K	L	FOBS	FCAL	K	L	FOBS	FCAL	K	L	FOBS	FCAL	K	L	FOBS	FCAL	K	L	FOBS	FCAL	
5	4	435	445	6	1	201	210	5	9	195	177	1	9	291	303	2	5	495	502	
5	5	214	223	6	2	215	204	6	1	528	532	2	0	507	564	2	7	271	272	
5	6	650	639	6	4	630	640	6	2	390	361	2	1	600	592	3	0	457	464	
5	7	648	632	7	1	390	390	6	3	293	229	2	2	526	539	3	2	562	571	
5	8	653	637	7	3	411	410	6	4	707	716	2	3	197	208	3	3	362	353	
5	9	306	360	7	5	201	152	6	5	249	241	2	4	549	524	3	4	579	575	
5	10	327	351	2	2	311	207	6	6	283	279	2	6	452	467	3	6	311	305	
6	0	667	683	8	4	326	349	6	7	352	368	2	7	459	498	3	7	218	237	
6	1	571	581	8	6	179	142	6	9	237	239	2	8	407	411	4	0	205	149	
6	2	207	187	9	0	214	203	7	0	319	315	2	9	273	272	4	1	356	356	
6	3	523	569	9	3	300	333	7	1	365	347	2	10	346	363	4	3	542	526	
6	4	216	215	9	5	342	339	7	2	369	357	3	0	524	503	4	4	272	227	
6	5	574	536	10	2	235	223	7	3	379	375	3	3	649	663	4	5	474	432	
6	6	201	205	***H = 10****	7	4	347	353	7	4	347	353	3	4	239	176	4	7	236	202
6	7	460	466	0	0	1334	1351	7	5	282	298	3	5	633	651	5	2	346	328	
6	8	382	345	0	1	965	965	7	6	194	219	3	6	298	298	5	4	614	592	
6	9	348	350	0	2	508	547	7	7	254	225	3	7	315	313	5	6	383	349	
7	0	444	477	0	3	299	265	8	0	402	375	3	8	467	445	6	1	220	229	
7	2	519	519	0	5	288	282	8	2	202	226	3	9	325	313	6	3	511	500	
7	3	271	245	0	6	550	552	8	3	532	520	4	2	453	454	6	5	435	427	
7	4	556	534	0	7	589	570	8	5	422	421	4	4	798	798	7	0	7476	469	
7	5	241	259	0	8	801	793	8	6	267	291	4	6	438	409	7	2	321	320	
7	6	418	416	0	9	345	342	9	1	476	459	4	9	175	128	***H = 15****				
7	8	288	327	0	10	189	213	9	2	325	327	5	1	370	385	1	3	225	126	
8	0	628	665	1	0	479	472	9	4	456	460	5	2	288	242	2	1	220	199	
8	1	261	268	1	1	776	795	***H = 11****	5	3	654	644	5	3	654	644	3	0	353	361
8	3	575	575	1	2	391	403	1	0	362	354	5	4	460	470	3	4	247	302	
8	4	697	714	1	4	391	393	1	1	418	462	5	5	524	506	4	1	303	284	
8	5	537	519	1	5	270	251	1	3	460	502	6	0	465	477	4	3	309	279	
8	7	253	247	1	6	525	531	1	4	271	210	6	2	494	505	5	0	223	234	
8	8	259	257	1	7	848	846	1	5	290	341	6	3	381	391	5	1	243	237	
9	0	460	471	1	8	465	449	1	7	403	379	6	4	463	449	5	4	216	185	
9	1	251	231	1	9	536	536	1	10	179	166	6	5	239	263	6	0	230	273	
9	2	520	512	1	10	255	238	2	0	669	658	6	6	270	255	***H = 16****				
9	3	567	568	2	0	1338	1329	2	1	358	379	7	1	441	458	0	0	298	253	
9	4	455	452	2	1	486	470	2	3	548	559	7	3	307	297	0	1	327	328	
9	5	316	345	2	2	560	560	2	4	546	558	7	4	221	153	0	2	350	337	
9	6	239	221	2	3	526	516	2	5	357	367	7	5	220	270	0	4	846	814	
10	1	211	170	2	5	472	460	2	7	318	317	8	0	341	357	1	0	487	459	
10	2	177	174	2	6	457	476	2	8	427	418	8	1	210	210	1	3	667	601	
10	3	369	371	2	7	375	332	3	0	497	522	8	2	277	266	1	5	491	498	
10	4	296	324	2	8	695	730	3	3	221	165	8	4	166	205	2	0	411	395	
H = 9*	2	9	265	265	3	4	566	575	***H = 13****	1	1	300	346	2	1	399	404			
1	0	812	809	2	10	182	212	1	1	300	346	2	2	345	263	2	1	345	263	
1	1	572	574	2	11	257	273	1	3	415	467	1	3	329	297	2	4	284	285	
1	3	332	294	3	0	610	609	4	5	239	228	1	5	271	254	3	0	227	174	
1	4	685	673	3	1	859	840	4	7	216	126	2	0	475	461	3	1	425	431	
1	7	187	172	3	2	661	641	5	0	375	348	2	4	357	408	3	2	210	186	
1	8	442	430	3	3	323	316	6	0	272	312	4	0	393	404	3	3	202	220	
1	9	222	243	3	4	525	541	6	3	241	183	4	1	355	306	3	4	205	178	
2	1	338	336	3	5	310	285	7	1	233	218	5	0	231	203	3	5	255	199	
2	3	696	718	3	6	262	297	7	4	230	215	5	1	249	260	4	0	403	400	
2	5	375	374	3	7	545	524	8	3	199	207	5	7	231	216	4	2	305	305	
2	7	535	549	3	9	310	330	8	5	170	167	6	0	221	224	4	3	285	264	
2	9	256	271	3	10	203	209	9	0	213	205	6	1	295	284	4	4	215	206	
2	11	251	282	4	0	485	517	***H = 12****	6	3	253	249	4	5	236	246				
3	0	270	250	4	1	577	575	0	0	1012	1017	7	0	656	665	5	1	245	245	
3	4	251	242	4	2	598	557	0	1	503	526	7	4	342	357	5	3	315	267	
4	0	326	292	4	3	305	270	0	2	750	736	8	1	198	229	***H = 17****				
4	2	361	330	4	4	528	525	0	4	402	412	***H = 14****	2	0	280	272				
4	4	710	705	4	5	276	276	0	6	421	429	0	0	337	610	3	0	216	207	
4	7	227	238	4	6	322	328	0	7	213	225	0	1	301	499	3	3	199	152	
4	8	309	300	4	7	477	449	0	8	323	351	0	3	628	645	4	0	272	214	
4	10	178	143	4	8	202	213	0	10	189	204	0	4	282	298	***H = 18****				
5	0	377	384	4	9	347	354	1	0	576	537	0	5	452	484	0	0	527	544	
5	1	624	647	4	10	200	244	1	1	614	623	0	8	218	222	0	2	357	405	
5	3	507	486	5	0	640	625	1	2	205	194	1	2	419	416	0	3	337	323	
5	4	302	306	5	2	221	247	1	3	556	554	1	4	691	686	1	1	241	249	
5	5	523	542	5	3	729	717	1	5	509	525	1	6	372	419	1	2	201	199	
5	6	224	140	5	5	592	597	1	6	220	233	2	0	225	259	1	3	225	212	
5	8	305	290	5	6	487	463	1	7	420	455	2	1	371	360	2	0	272	271	
6	0	369	359	5	8	555	603	1	8	325	326	2	3	588	574	2	1	221	206	

TABLE 22: ATOM COORDINATES AND
ISOTROPIC TEMPERATURE FACTORS

ATOM	x	y	z	B
Mo	0.08815(5)	0.25886(7)	0.25	2.46*
S1	0.0077(1)	0.1371(1)	0.3802(1)	3.28*
S2	0.0632(1)	0.4286(1)	0.3808(1)	3.48*
S3	0.1939(1)	0.2047(1)	0.3808(1)	3.36*
C1	-0.0757(4)	0.0681(5)	0.3096(5)	3.19*
C2	-0.1390(5)	0.0016(7)	0.3648(7)	4.51*
C3	-0.1989(4)	-0.0638(7)	0.3087(7)	4.94*
C4	0.0787(4)	0.5741(5)	0.3091(5)	3.32*
C5	0.0872(5)	0.6936(6)	0.3659(6)	4.55*
C6	0.0959(5)	0.8080(6)	0.3088(7)	6.00*
C7	0.2557(4)	0.0951(6)	0.3091(5)	3.26*
C8	0.3073(4)	0.0067(7)	0.3677(7)	4.30*
C9	0.3565(4)	-0.0801(7)	0.3096(7)	5.30*
H1	-0.1389	0.0016	0.4488	5.2
H2	-0.2438	-0.1121	0.3518	6.0
H3	0.0873	0.6937	0.4499	5.2
H4	0.1023	0.8921	0.3514	6.0
H5	0.3074	0.0066	0.4516	5.2
H6	0.3925	-0.1429	0.3523	6.0

*These values are equivalent isotropic temperature factors⁸¹ corresponding to the anisotropic thermal parameters shown in Table 23.

TABLE 23: ANISOTROPIC TEMPERATURE FACTORS (\AA^2)

Atom	U ₁₁	U ₂₂	U ₃₃	U ₁₂	U ₁₃	U ₂₃
Mo	0.0389(4)	0.0259(3)	0.0287(3)	-0.0003(4)	0.0	0.0
S1	0.0489(10)	0.0400(8)	0.0356(8)	-0.0053(8)	-0.0006(9)	0.0033(8)
S2	0.0547(11)	0.0364(8)	0.0409(9)	0.0026(8)	0.0030(9)	-0.0070(8)
S3	0.0455(10)	0.0461(9)	0.0358(8)	0.0015(8)	-0.0049(8)	-0.0027(7)
C1	0.039(4)	0.034(3)	0.048(4)	0.002(3)	0.000(3)	-0.001(3)
C2	0.051(5)	0.064(5)	0.056(5)	-0.006(4)	0.014(4)	0.016(4)
C3	0.039(4)	0.074(5)	0.075(6)	-0.019(4)	0.012(4)	0.008(4)
C4	0.034(4)	0.033(3)	0.059(4)	0.004(3)	-0.002(3)	-0.007(3)
C5	0.057(5)	0.040(3)	0.075(5)	0.015(4)	0.004(5)	-0.013(4)
C6	0.079(6)	0.037(4)	0.111(7)	0.011(4)	0.005(5)	-0.010(4)
C7	0.034(4)	0.044(4)	0.046(4)	-0.000(3)	-0.002(3)	-0.004(3)
C8	0.048(5)	0.061(4)	0.054(5)	0.005(4)	-0.001(4)	0.004(4)
C9	0.045(5)	0.068(5)	0.088(7)	0.011(4)	-0.009(4)	0.014(4)

TABLE 24: INTRAMOLECULAR CONTACTS (Å)

ATOMS	DISTANCE (Å)	ATOMS	DISTANCE (Å)
Mo-S1	2.370(2)	Mo-S2	2.360(2)
Mo-S3	2.371(2)	S1-S1'	3.100(3)
S2-S2' ^a	3.115(3)	S3-S3'	3.114(3)
S1-S2	3.099(2)	S1-S3	3.074(2)
S2-S3	3.101(2)	S1-C1	1.731(6)
S2-C4	1.728(6)	S3-C7	1.721(6)
C1-C1'	1.419(11)	C1-C2	1.388(8)
C2-C3	1.349(10)	C3-C3'	1.394(16)
C4-C4'	1.408(12)	C4-C5	1.398(8)
C5-C6	1.355(8)	C6-C6'	1.400(16)
C7-C7'	1.408(12)	C7-C8	1.410(8)
C8-C9	1.373(10)	C9-C9'	1.418(16)

^aPrimed atoms are related by a mirror at $z = 1/4$.

TABLE 25: INTRAMOLECULAR ANGLES (DEGREES)

ATOMS	ANGLES	ATOMS	ANGLES
S1-Mo-S1' ^a	81.70 (8)	S2-Mo-S2'	82.57 (8)
S3-Mo-S3'	82.09 (8)	S1-Mo-S2	81.85 (5)
S1-Mo-S3	80.85 (6)	S2-Mo-S3	81.89 (6)
S1-Mo-S2'	136.17 (7)	S1-Mo-S3'	134.43 (6)
S2-Mo-S3'	136.51 (7)	Mo-S1-C1	108.5 (2)
Mo-S2-C4	106.1 (2)	Mo-S3-C7	103.9 (2)
S1-C1-C1'	119.0 (2)	S2-C4-C4'	119.6 (2)
S3-C7-C7'	119.7 (2)	C2-C1-C1'	118.2 (4)
C1-C2-C3	122.1 (8)	C2-C3-C3'	119.7 (5)
C5-C4-C4'	118.9 (4)	C4-C5-C6	120.9 (7)
C5-C6-C6'	120.1 (4)	C8-C7-C7'	119.7 (4)
C7-C8-C9	120.0 (7)	C8-C9-C9'	120.3 (5)
S3-S1-S2	60.30 (5)	S1-S3-S2	60.24 (5)
S1-S2-S3	59.46 (5)		

^aPrimed atoms are related by a mirror at $z = 1/4$.

TABLE 26: INTERMOLECULAR CONTACTS (Å)

ATOM 1	ATOM 2	SYMMETRY OPERATION ON ATOM 2	DISTANCE
S1	H4	$x, y-1, z$	2.941
S1	H3	$\bar{x}, \bar{y}+1, \bar{z}+1$	3.065
S2	H5	$1/2-x, 1/2+y, \bar{z}+1$	2.992
S3	H1	$\bar{x}, \bar{y}, \bar{z}+1$	3.051
S1	C6	$x, y-1, z$	3.736(7)
S1	C5	$\bar{x}, \bar{y}+1, \bar{z}+1$	3.800(7)
S2	C8	$1/2-x, 1/2+y, \bar{z}+1$	3.734(8)
S2	C9	$1/2+x-1, 1/2-y, z$	3.763(7)
S3	C2	$\bar{x}, \bar{y}, \bar{z}+1$	3.791(7)
S2	S2	$\bar{x}, \bar{y}+1, \bar{z}+1$	3.782(3)
C3	C4	$1/2+x-1, 1/2-y, z$	3.581(9)
C3	C9	$1/2+x-1, 1/2-y-1, z$	3.33(10)
C3	C5	$1/2+x-1, 1/2-y, z$	3.749(10)
C4	C9	$1/2+x-1, 1/2-y, z$	3.577(9)
C4	C3	$1/2+x, 1/2-y, z$	3.581(9)
C4	H6	$1/2+x-1, 1/2-y, z$	3.120
C5	H6	$1/2+x-1, 1/2-y, z$	3.180
C4	H2	$1/2+x, 1/2-y, z$	2.927
C5	H2	$1/2+x, 1/2-y, z$	2.848

TABLE 27: LEAST SQUARES PLANE CALCULATIONS^a

(A) ATOMS DEFINING PLANE: S1, Mo, S1'
 EQUATION OF PLANE: $-0.6913X + 0.7225Y - 0.9227 = 0.0$

(B) ATOMS DEFINING PLANE: S2, Mo, S2'
 EQUATION OF PLANE: $-0.9740X - 0.2266Y + 1.9797 = 0.0$

(C) ATOMS DEFINING PLANE: S3, Mo, S3'
 EQUATION OF PLANE: $-0.3080X - 0.9514Y + 2.9444 = 0.0$

(D) ATOMS DEFINING PLANE: S1, S2, S3
 EQUATION OF PLANE: $-0.0016X - 0.0019Y + 1.0Z - 4.5264 = 0.0$

DISTANCE OF Mo FROM PLANE (Å): -1.556

(E) ATOMS DEFINING PLANE: S1', S2', S3'
 EQUATION OF PLANE: $0.0016X - 0.0019Y + 1.0Z - 1.4298 = 0.0$

DISTANCE OF Mo FROM PLANE (Å): 1.556

(F) ATOMS DEFINING PLANE: S1, S1', C1, C1', C2, C2',
 C3, C3'

EQUATION OF PLANE: $0.5094X - 0.8605Y + 1.1429 = 0.0$

DISTANCES OF ATOMS FROM PLANE (Å):

S1	0.005 (2)	S1'	0.005 (2)
C1	-0.074 (6)	C1'	-0.074 (6)
C2	-0.011 (7)	C2'	-0.011 (7)
C3	0.071 (8)	C3'	0.071 (8)
Mo	-0.4017 (7)		

TABLE 26 (Continued)

(G) ATOMS DEFINING PLANE: S2, S2', C4, C4', C5, C5',
C6, C6'

EQUATION OF PLANE: $-0.9899X + 0.1420Y + 0.3898 = 0.0$

DISTANCES OF ATOMS FROM PLANE (Å):

S2	0.002(2)	S2'	0.002(2)
C4	-0.035(6)	C4'	-0.035(6)
C5	0.001(7)	C5'	0.001(7)
C6	0.028(8)	C6'	0.028(8)
Mo	-0.6412(7)		

(H) ATOMS DEFINING PLANE: S3, S3', C7, C7', C8, C8',
C9, C9'

EQUATION OF PLANE: $0.7424X + 0.6700Y - 3.7136 = 0.0$

DISTANCES OF ATOMS FROM PLANE (Å):

S3	0.000(2)	S3'	0.000(2)
C7	-0.008(6)	C7'	-0.008(6)
C8	0.006(7)	C8'	0.006(7)
C9	0.001(7)	C9'	0.001(7)
Mo	-0.8942(7)		

^aX, Y, and Z are in Å and refer to the orthogonal
coordinates along a, b, and c^a.

TABLE 28: DIHEDRAL ANGLES BETWEEN SELECTED PLANES.

ATOMS IN PLANE 1	ATOMS IN PLANE 2	ANGLE
S1, Mo, S1'	S2, Mo, S2'	120.7°
S1, Mo, S1'	S3, Mo, S3'	118.2°
S2, Mo, S2'	S3, Mo, S3'	121.1°
S1, Mo, S1'	S1, S1', C1, C1', C2, C2', C3, C3'	13.1°
S2, Mo, S2'	S2, S2', C4, C4', C5, C5', C6, C6'	21.1°
S3, Mo, S3'	S3, S3', C7, C7', C8, C8', C9, C9'	30.0°

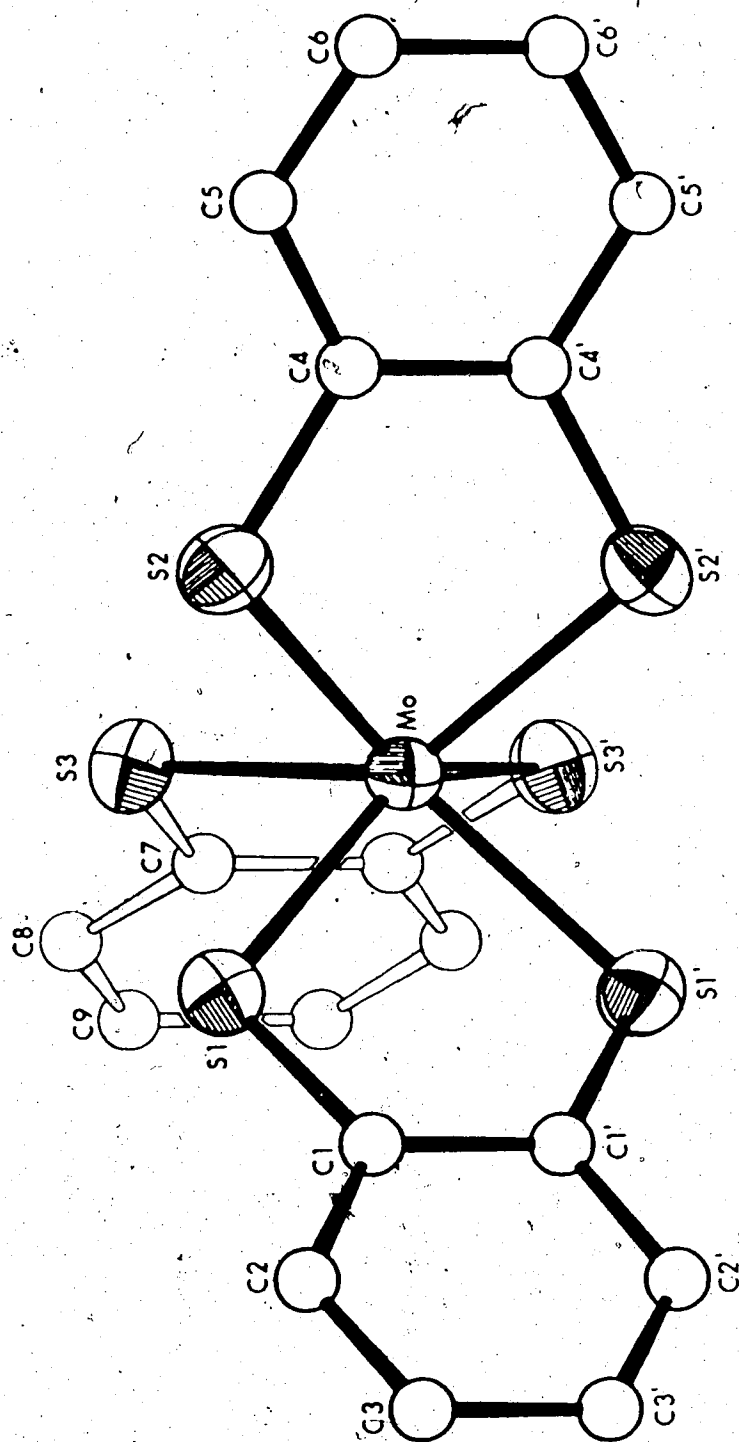


Fig. 9: A PERSPECTIVE VIEW OF $\text{Mo}(\text{S}_2\text{C}_6\text{H}_4)_3$.

DESCRIPTION OF STRUCTURE

A 3-dimensional view of $\text{Mo}(\text{bdt})_3$ is shown in Fig. 9. The sulfur atoms surround the molybdenum in an almost perfect trigonal prismatic coordination with the dithiolene ligands radiating from the molybdenum atom in a "paddle-wheel" arrangement. The molecule deviates from approximate D_{3h} symmetry due to the bending of the $(\text{S}_2\text{C}_6\text{H}_4)$ planes from the MoS_2 planes by an average of 21.4° . In addition C_{3h} symmetry is not achieved due to the three differing $(\text{S}_2\text{C}_6\text{H}_4)/\text{MoS}_2$ dihedral angles (Fig. 12). The molybdenum atom is located on the crystallographic mirror at $z = 1/4$, with the two triangular faces of the prism being related by the mirror.

Again, as was the case for the three previous trigonal prismatic structures, $\text{Re}(\text{S}_2\text{C}_2\text{Ph}_2)_3$,¹²⁹ $\text{Mo}(\text{S}_2\text{C}_2\text{H}_2)_3$ ¹³⁰ and $\text{V}(\text{S}_2\text{C}_2\text{Ph}_2)_3$,¹³² the intra- and interligand sulfur-sulfur distances are approximately equal (3.110 \AA and 3.091 \AA respectively in the present study). These agree favourably with those observed in other prisms and are especially close to those in $\text{Mo}(\text{S}_2\text{C}_2\text{H}_2)_3$ (Table 48). It is interesting that the relative magnitudes of these intra- and interligand S-S distances are reversed to those in the other three

dithiolene trigonal prisms, with the intraligand S-S distances being greater in the present study. This can be attributed to the constraint of the fixed ligand bite holding the intraligand sulfurs apart. That the ligand bite should be greater in the benzene dithiols than in the ethylene dithiols is apparent since the C-C distances in the former are longer, thereby ensuring a larger bite. This was also observed in the trigonal prismatic molecule¹⁵² $\text{Mo}[\text{Se}_2\text{C}_2(\text{CF}_3)_2]_3$, which also has intraligand Se-Se distances which exceed the interligand values [3.317(5) Å and 3.222(3) Å respectively].

The mean Mo-S distance (2.367 Å), although similar to the metal-sulfur distance in other trigonal prisms, is significantly longer than their average of approximately 2.33 Å. In fact they are more closely matched by the metal-sulfur distances in the non-trigonal prismatic species $\text{V}(\text{mnt})_3^{2-}$ ¹⁴⁰ and $\text{Mo}(\text{mnt})_3^{2-}$ ¹⁴¹ (Table 48). This difference is again probably due to the difference in ligands, all previous examples being substituted ethylene dithiol ligands. For this reason a rigid comparison of intramolecular distances and angles will prove more worthwhile within the series of compounds which are the topic of part of this thesis, i.e., $\text{Mo}(\text{bdt})_3$, $[\text{Ph}_4\text{As}][\text{Nb}(\text{bdt})_3]$, and $[(\text{CH}_3)_4\text{N}]_2[\text{Zr}(\text{bdt})_3]$. In addition the molybdenum-

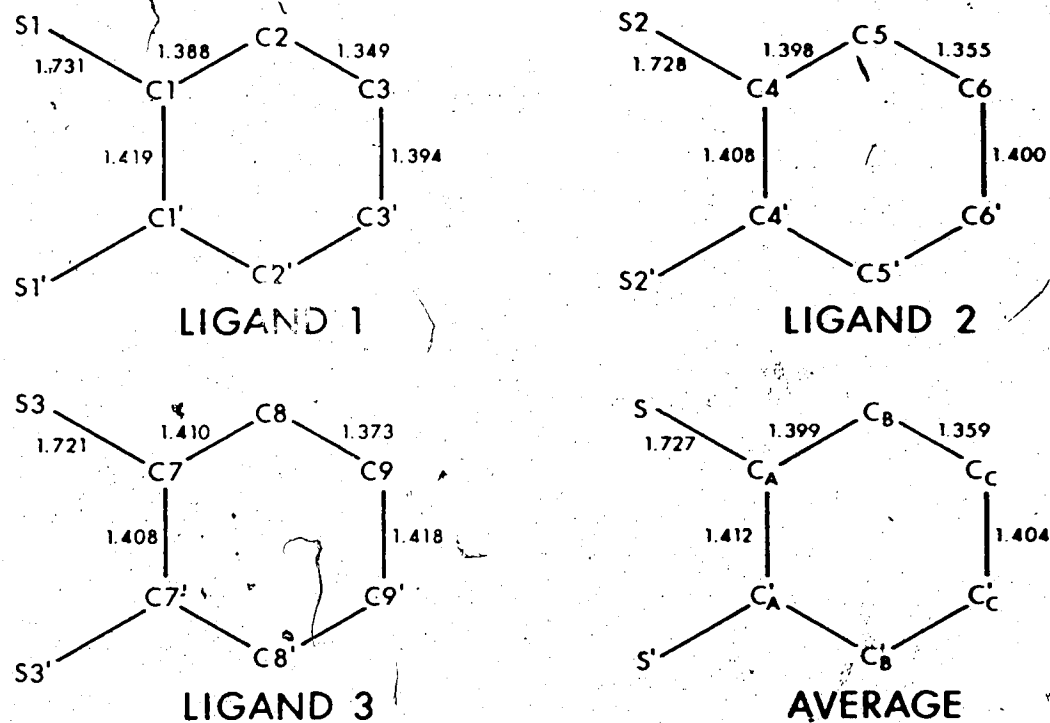


Fig. 10: DIMENSIONS WITHIN THE DITHIOLENE LIGANDS.

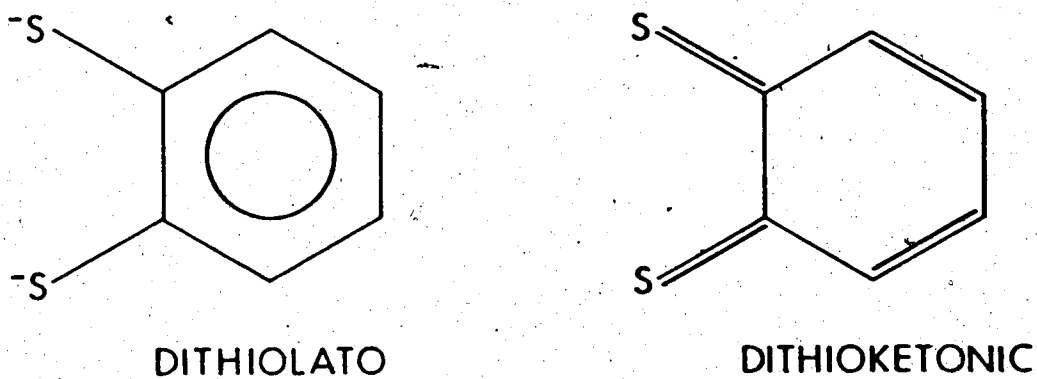


Fig. 11: DITHIOLATO AND DITHIOKETONIC LIMITING FORMULATIONS FOR THE "bdt" LIGAND.

sulfur distances are again shorter than those observed in the 1,1-dithiolato complexes, $\text{Fe}[\text{S}_2\text{CN}(\text{n-C}_4\text{H}_9)_2]_3$,¹⁵³ $\text{Ru}[\text{S}_2\text{CN}(\text{C}_2\text{H}_5)_2]_3$,¹⁵⁴ $\text{Cr}[\text{S}_2\text{P}(\text{CH}_3)_2]_3$,¹⁵⁵ and $\text{V}[\text{S}_2\text{P}(\text{OC}_2\text{H}_5)_2]_3$,¹⁵⁶ although the molybdenum covalent radius is greater than any of these metal radii.^{133'}

Thus a difference in the metal-sulfur bonding between the 1,1-dithiolato and 1,2-dithiolene complexes is obvious with the latter having a greater amount of M-S bonding. This is in agreement with the proposed metal-sulfur multiple bonding in the *tris*(1,2-dithiolenes).¹⁵⁷

The sulfur-carbon distances (mean 1.727 Å) are similar to those in the other trigonal prisms and are once again consistent with a great deal of S=C double bond character, as witnessed by their similarity with the double bonded S=C distance of 1.72 Å in thiourea¹³⁴ $[\text{S}(\text{NH}_2)_2]$ and its derivatives.¹³⁵ The mean carbon-carbon distance (1.393 Å) is similar to that observed in benzene¹⁵⁸ (1.398 Å) and in several di-substituted benzene compounds.¹⁵⁹ However in the benzene dithiol ligands in this structure there is a significant range of C-C distances (Fig. 10). In addition, the C-C distances are consistent with a tendency towards the dithioketonic limit (Fig. 11). However caution must be used since the dithioketonic limit will not be attained due to other resonance

structures, so only a trend towards this limit is noted. Also due to increasing thermal motion of the carbon atoms as the distance from the central atom (Mo) increases, the bonds will appear shorter due to libration of the rings. Thus the shortening of $C_B - C_C$ (Fig. 10) could be partly attributed to thermal motion. However thermal motion of this type cannot cause bond lengthening, so the longer $C_A - C'_A$ bond remains as good evidence of the tendency of the ligand towards its oxidized formulation. At this point it is convenient to note that the thermal parameters in this and similar structures all show an anomalous feature. In molecules of this type it would appear reasonable to expect that the general trend of thermal amplitudes increases steadily as one progresses outward from the centre of gravity of the molecule. This assumes that the thermal motion is dominated by rigid body motion. However the sulfur atoms have larger thermal parameters than their attached carbon atoms. This observation, which appears to be very general for sulfur donor ligands, suggests either the unsuitability of the scattering factors used, or large vibration of the core of the molecule. This feature precludes any attempt at correction of these bond lengths for thermal motion and hence severely restricts the discussion

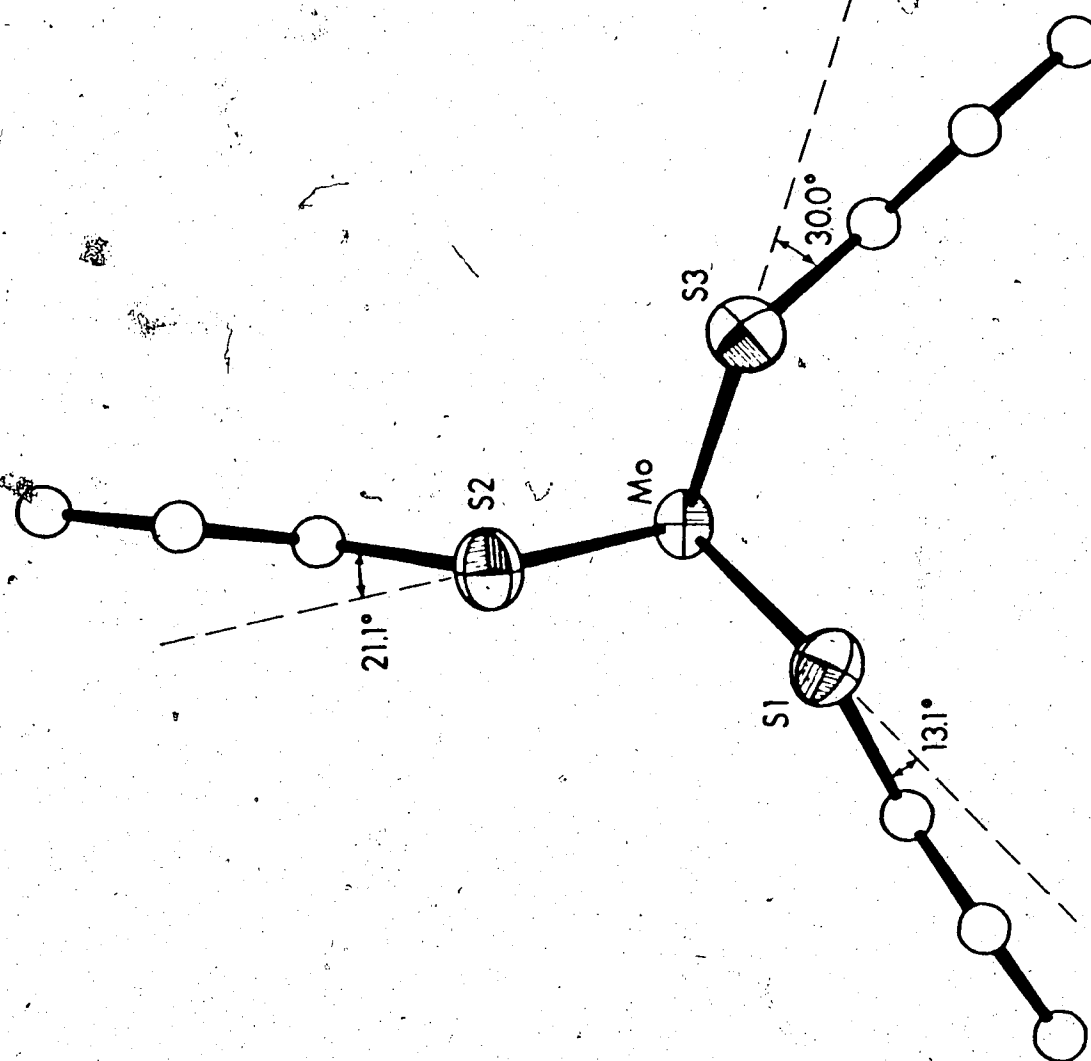


Fig. 12: VIEW OF $\text{Mo}(\text{S}_2\text{C}_6\text{H}_4)_3$ DOWN THE CRYSTALLOGRAPHIC c AXIS.

of the ligand geometry with respect to the pattern of carbon-carbon bond lengths. A more complete view of the ligand in its reduced and oxidized formulation is presented in Chapter IX, based on molecular orbital calculations performed by Birss and Das Gupta.¹⁶⁰

The mean S-M-S angle involving *trans* sulfur atoms is $136 \pm 1^\circ$ in the known trigonal prismatic structures,^{129,130,132} and assuming the constraint of ligand bite, has been calculated¹⁶¹ as approximately 173° in octahedral coordination. The mean value of 135.70° observed in $\text{Mo}(\text{bdt})_3$ is clearly consistent with trigonal prismatic coordination. The intra- and interligand S-Mo-S angles (82.12° and 81.53°) are similar, as expected, and again agree with those found in other trigonal prismatic structures.^{129,130,132}

As mentioned, the molecule deviates from D_{3h} symmetry due to the bend of the ligand planes from the respective S-Mo-S planes, as shown in Fig. 12, in which the molecule is viewed directly down the crystallographic *c* axis and approximate molecular three-fold axis. Similar bending of the ligand planes was observed in $\text{Mo}(\text{S}_2\text{C}_2\text{H}_2)_3$ ¹³⁰ and also in $\text{Mo}(\text{Se}_2\text{C}_2(\text{CF}_3)_2)_3$,¹⁵² where the ligand planes deviate from the MoS_2 and MoSe_2 planes by 18° and 18.6° respectively. Although these deviations are uniform

in these previous two examples, the molecules both having $3/m$ symmetry, they are irregular for $\text{Mo}(\text{bdt})_3$ with the ligand/ MoS_2 dihedral angles being 13.1° , 21.1° , and 30.0° (mean 21.4°). Schrauzer¹³⁰ has attributed this as being due to intramolecular effects, saying that the sulfur may be in a state between sp^2 and sp^3 hybridization, with possible added stabilization from packing forces. However from the structure of $\text{Mo}(\text{bdt})_3$ it is obvious that packing forces contribute significantly, as witnessed by the wide range in dihedral angles observed. Table 26 shows that several intermolecular contacts are comparable to the predicted van der Waals contacts¹⁵¹ (Predicted values: $\text{S}\cdots\text{C}$, 3.70 \AA ; $\text{S}\cdots\text{S}$, 3.70 \AA ; $\text{S}\cdots\text{H}$, 3.05 \AA ; $\text{C}\cdots\text{C}$, 3.70 \AA ; $\text{C}\cdots\text{H}$, 3.05 \AA ; $\text{H}\cdots\text{H}$, 2.40 \AA). Thus packing is very efficient and will probably be important in the bending of the ligand planes. A packing diagram, viewed down the c axis is shown in Fig. 13. The efficient packing is obvious from this diagram with the molecules packing in a gear-wheel arrangement.

As shown in Table 28, a further indication of the regularity of the prism is given by the similarity of the angles between the three MoS_2 planes, all being close to the expected value of 120° . The two tri-

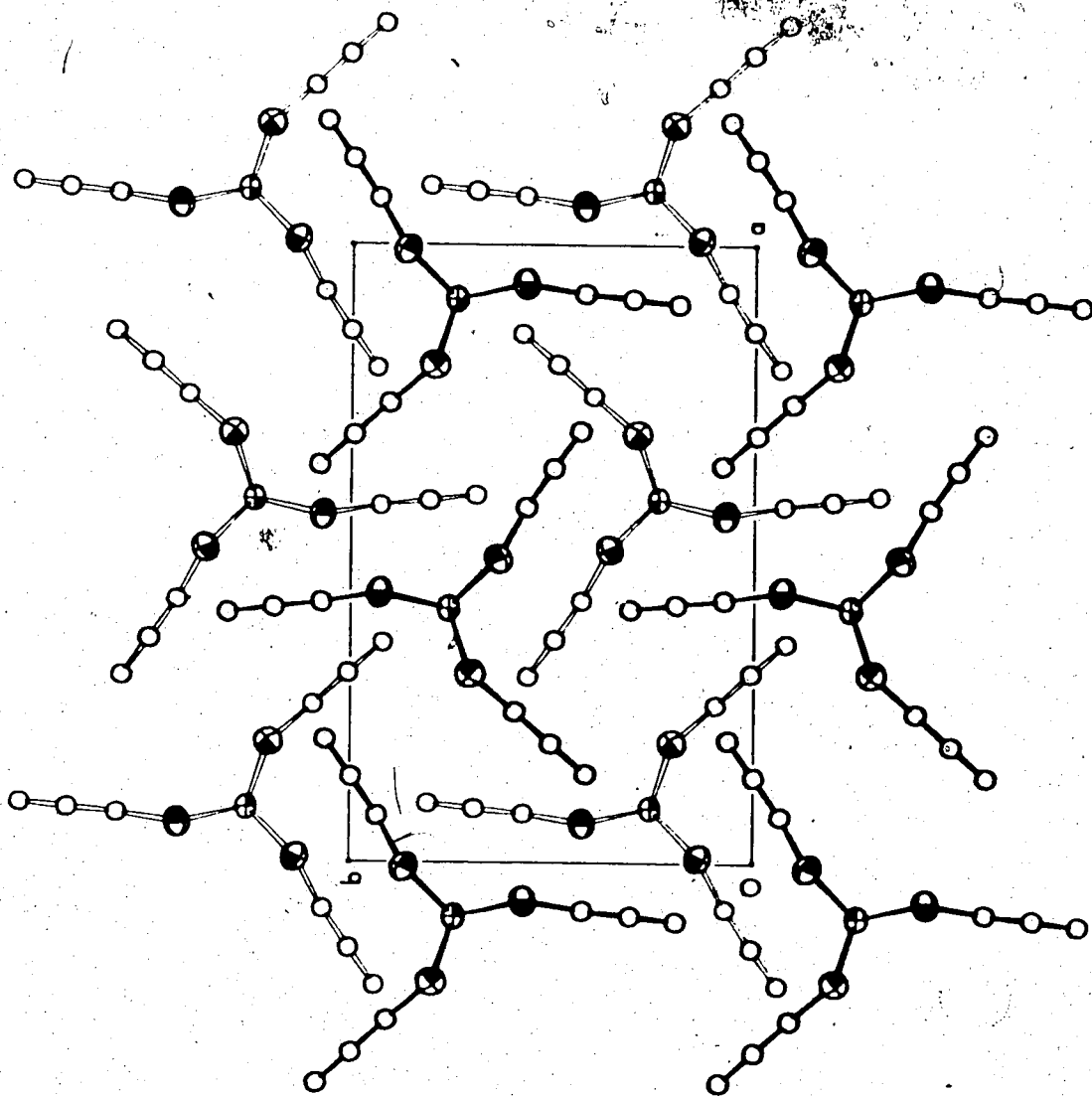


Fig. 13: PACKING DIAGRAM FOR $\text{Mo}(\text{S}_2\text{C}_6\text{H}_4)_3$, PROJECTED
ON THE ab PLANE.

angular faces of the prism are also almost exactly parallel.

The Mo-S-C angles (mean 106.2°) are similar to the values of $109(1)^\circ$ and $109.9(4)^\circ$ observed in $\text{Re}(\text{S}_2\text{C}_2\text{Ph}_2)_3$ and $\text{V}(\text{S}_2\text{C}_3\text{Ph}_2)_3$, however they are significantly smaller, again probably due to differences in the ligands. The S-C-C' angles (mean 119.4°) are in good agreement with the value of 120° . Similarly all C-C-C angles within the benzene rings are close to their expected value of 120° .

CHAPTER VII: THE CRYSTAL AND MOLECULAR STRUCTURE

OF TETRAPHENYLARSONIUM TRIS (BENZENE-
1,2-DITHIOLATO) NIOBIUM, $([(C_6H_5)_4As][Nb(S_2C_6H_4)])$

EXPERIMENTAL

Dark purple crystals suitable for single crystal X-ray diffraction study, prepared by the reaction of sodium cyclopentadienide with benzene dithiol and subsequent reaction with $Nb[N(CH_3)_2]_5$ and crystallization with tetraphenylarsonium chloride,¹⁴³ were kindly supplied by Dr. Takats and Mr. Martin. Preliminary photography indicated $2/m$ Laue symmetry consistent with a monoclinic space group. Systematic absences, as determined by Weissenberg ($h0\ell$, $h\ell\ell$; CuK_{α} X-radiation) and Precession photographs ($0k\ell$, $lk\ell$, $hk0$, hkl ; MoK_{α} X-radiation), are $0k0$: $k = 2n + 1$ and $h0\ell$: $h + \ell = 2n + 1$ indicating the non-standard space group $P2_1/n$, which was retained because of the convenient β angle. The cell parameters obtained at $22^\circ C$ from a least squares analysis of the setting angles of 12 reflections, which were centred accurately on a Picker automatic four circle diffractometer, using CuK_{α_1} X-radiation ($\lambda = 1.54051 \text{ \AA}$), are:
 $a = 22.983(7) \text{ \AA}$, $b = 12.747(4) \text{ \AA}$, $c = 13.150(3) \text{ \AA}$,
 $\beta = 92.09(2)^\circ$. The observed density, obtained by

floatation in aqueous zinc bromide solution, is $1.52(2)$ g cm^{-3} and is in reasonable agreement with the theoretical value of 1.54 g cm^{-3} calculated assuming four molecules with formula weight 896.94 a.m.u. per unit cell of volume 3867.12 \AA^3 .

Intensity data were collected on the Picker automatic diffractometer, using CuK_α X-radiation, filtered using a 0.0005" thick Ni foil, and using a 2° take-off angle. The crystal was aligned in a general orientation but with its b^* axis approximately coincident with the ϕ axis of the instrument. Crystal faces were identified and perpendicular distances between faces of the same form were measured as: $\{1,0,0\}$, 0.206 mm; $\{\bar{2},1,0\}$, 0.206 mm; $\{\bar{2},\bar{1},0\}$, 0.206 mm; $\{\bar{1},0,1\}$, 0.155 mm; $\{1,0,1\}$, 0.175 mm.

In the data collection a coupled $2\theta/\omega$ scan was used with a 2θ scan speed of $1^\circ/\text{min}$ to collect all reflections with $2\theta \leq 115^\circ$. The peak scan was 2° (2 min) for low angle reflections but increased with increasing 2θ due to compensation for $\alpha_1\alpha_2$ separation. Background counts were measured for 20 seconds at the limits of the two theta scan. The scattered X-rays were detected by a scintillation counter used in conjunction with a pulse height analyzer tuned to accept 95% of the CuK_α peak. Three standard reflections

were collected automatically every 100 data reflections. Another five standard reflections were collected manually every 10 hours to detect more precisely decomposition and crystal centering errors. No significant decomposition was observed but small fluctuations ($\pm 1\%$), due to an instability of the goniometer head, were detected. These fluctuations were not regular and corrections were not made.

Of the 5862 unique reflections collected, 3604 were considered as significantly above background using the criterion $I/\sigma(I) \geq 3.0$. The data were reduced to structure factor amplitudes by correction for Lorentz, polarization and absorption effects. For CuK_α X-radiation, the linear absorption coefficient⁸⁶ is 68.42 cm^{-1} which yielded a range of transmission factors of 0.4359 to 0.3128. Standard deviations were estimated using a "p factor" of 0.03 as outlined in Chapter II. Terms used in the Zachariasen¹⁴⁸ extinction correction were calculated at this stage.

TABLE 29: MAJOR PATTERSON PEAKS AND THEIR ASSIGNMENT

OBSERVED VECTOR	RELATIVE INTENSITY	ASSIGNMENT	CALCULATED POSITION ^a
0.500, 0.063, 0.500	250	1/2, 1/2-2Y ₁ , 1/2	0.500, 0.064, 0.500
0.339, 0.500, 0.106	226	1/2-2X ₁ , 1/2, 1/2-2Z ₁	0.340, 0.500, 0.114
0.209, 0.377, 0.532	159	-(X ₁ +X ₂), (Y ₁ +Y ₂), -(Z ₁ +Z ₂)	0.208, 0.374, 0.544
0.287, 0.440, 0.958	148	1/2+(X ₁ +X ₂), 1/2-(Y ₁ -Y ₂), 1/2+(Z ₁ +Z ₂)	0.292, 0.438, 0.956
0.130, 0.126, 0.578	146	1/2-(X ₁ -X ₂), 1/2-(Y ₁ +Y ₂), 1/2-(Z ₁ -Z ₂)	0.132, 0.126, 0.570
0.500, 0.188, 0.500	140	1/2, 1/2-2Y ₂ , 1/2	0.500, 0.188, 0.500
0.165, 0.424, 0.395	113	2X ₁ , 2Y ₁ , 2Z ₁	0.160, 0.436, 0.386
0.078, 0.500, 0.958	103	1/2-2X ₂ , 1/2, 1/2-2Z ₂	0.076, 0.500, 0.974
0.418, 0.314, 0.532	63	2X ₂ , 2Y ₂ , 2Z ₂	0.424, 0.312, 0.526

^aCalculated on the basis of the consistent solution:

$$x_1 = 0.580, y_1 = 0.218, z_1 = 0.193; x_2 = 0.212, y_2 = 0.156, z_2 = 0.263.$$

STRUCTURE SOLUTION AND REFINEMENT

A sharpened¹⁴⁶ Patterson was calculated between the limits $0 \leq u \leq 0.5$, $0 \leq v \leq 0.5$, $0 \leq w \leq 1.0$. The general positions for space groups $P2_1/n$ are: x, y, z ; $\bar{x}, \bar{y}, \bar{z}$; $1/2 + x, 1/2 - y, 1/2 + z$; and $1/2 - x, 1/2 + y, 1/2 - z$. For one niobium [coordinates (x_1, y_1, z_1)] and one arsenic atom [coordinates (x_2, y_2, z_2)] per general position, the major peaks in the map can be assigned as shown in Table 29.

A brief outline of the refinement is shown in Table 30.

TABLE 30: REFINEMENT OUTLINE

MODEL	R_1	R_2
(1) Nb and As positions, B's fixed	0.421	0.507
(2) Nb, As, and S positions, isotropic B's	0.270	0.359
(3) Nb, As, S with isotropic B's, benzene rings as rigid bodies	0.076	0.087
(4) Absorption and Extinction ¹⁴⁷	0.064	0.072
(5) Nb, S, and As anisotropic	0.056	0.065
(6) Nb, S, and As anisotropic, ligand carbons individual isotropic, H atoms and benzene rings on arsenic as rigid bodies	0.049	0.051
(7) Model (6) but with anisotropic dithiolene carbons	0.047	0.048

Structure factors were calculated using the atomic scattering factors for the neutral atoms for niobium, arsenic, sulfur, and carbon as tabulated by Cromer and Mann.⁷⁵ The scattering factors for hydrogen were those of Stewart, Davidson and Simpson.¹⁴⁹ In addition, anomalous dispersion corrections⁷⁶ were applied to the niobium, arsenic and sulfur scattering factors ($\Delta f'_{\text{Nb}} = -0.58$, $\Delta f''_{\text{Nb}} = 2.68$, $\Delta f'_{\text{As}} = -1.17$, $\Delta f''_{\text{As}} = 1.17$, $\Delta f'_{\text{S}} = 0.31$, $\Delta f''_{\text{S}} = 0.58$). Features surrounding the Nb, As and S atoms in the electron density difference map suggested the anisotropic refinement, and the validity was verified by a Hamilton's R Test⁷⁹ at the 0.005 significance level.

Initially the benzene rings were refined as rigid bodies constrained to their well known geometry. In model (6) the carbon atoms of the benzene dithiol ligands were refined individually with isotropic temperature factors, and the phenyl groups on the arsenic atoms were refined as rigid bodies. The hydrogen positions were calculated from the geometry and orientation of the benzene rings and were also added as rigid bodies, using a C-H distance of 1.0 Å. The hydrogen rigid bodies were not refined however. The final model was refined with anisotropic temperature factors on the carbon atoms of the dithiolene

ligands. This was again justified by a Hamilton's R Test⁷⁹ at the 0.005 significance level.

In the final least squares refinement, 284 parameters were varied, and the standard deviation in an observation of unit weight was 1.641. The final value of the refined extinction parameter, C, was 8.74×10^{-7} .

RESULTS

Observed and calculated structure factor amplitudes, $|F_o|$ and $|F_c|$, are shown in Table 31. The final fractional coordinates and isotropic B's of all atoms are shown in Table 32. Standard deviations were obtained from the inverse matrix of the final least squares analysis. Table 33 shows the anisotropic thermal parameters (U_{ij} 's).⁸⁰ Intra-ionic contacts and angles, shown in Tables 34 and 35, were obtained with their standard deviations from ORFFE. Inter-ionic contacts (also obtained from ORFFE) are shown in Table 36. Selected least squares planes are given in Table 37. In Table 38, the dihedral angles between some selected planes are shown.

In Fig. 14 a three-dimensional view of the $\text{Nb}(\text{bdt})_3^-$ anion is shown. Fig. 16 shows the anion and the

$(C_6H_5)_4As^+$ cation together, viewed down the crystallographic b axis. The numbering scheme is shown in both diagrams. For the carbon atoms in the phenyl groups, the first number designates the ring number and the second number is the sequence of the atom in the ring. The carbon atoms are numbered sequentially and for the phenyl groups in the cation the first atom in the numbering scheme is always bonded to the arsenic atom. The hydrogen atoms are not shown but are numbered from H1 to H32 and are bonded, four on each dithiolene ligand and five on each phenyl group, sequentially from C12 to C76.

In the three dimensional representations the niobium, sulfur and arsenic atoms are shown with 50% probability thermal ellipsoids. The carbon atoms are shown, however, with artificially low isotropic thermal parameters, for clarity.

Table 31 (continued)

H	L	FOBS	FCAL	H	L	FOBS	FCAL	H	L	FOBS	FCAL	H	L	FOBS	FCAL	H	L	FOBS	FCAL
-2	4	557	545	17	6	331	378	3	9	387	403	-13	0	1290	1294	-15	2	451	466
-1	4	1372	1341	18	6	426	462	7	9	934	965	-11	0	471	460	-13	2	676	659
0	4	250	224	22	6	825	804	12	9	344	308	-10	0	1501	1478	-12	2	492	503
1	4	1212	1245	22	6	295	303	13	9	719	742	-9	0	533	581	-11	2	1096	1083
2	4	1786	1820	-21	7	578	600	14	9	257	251	-8	0	1617	1622	-10	2	1593	1568
3	4	1503	1570	-19	7	389	384	16	9	465	447	-7	0	502	487	-9	2	337	341
4	4	397	386	-15	7	981	988	17	9	328	353	-6	0	1144	1179	-7	2	925	940
5	4	518	509	-14	7	238	215	-18	10	220	190	-5	0	844	872	-6	2	871	905
6	4	1019	1063	-13	7	493	533	-15	10	318	298	-4	0	1705	1676	-4	2	1961	1797
7	4	190	198	-11	7	556	541	-14	10	567	546	-3	0	1492	1508	-3	2	2767	2514
8	4	986	1011	-10	7	586	575	-11	10	209	233	-2	0	1043	1033	-2	2	1123	1062
9	4	716	719	-9	7	850	836	-8	10	475	463	-1	0	265	282	0	2	444	465
10	4	252	260	-7	7	1510	1485	-6	10	275	287	0	0	2940	2996	1	2	294	341
11	4	204	204	-6	7	106	152	-4	10	712	694	1	0	254	282	2	2	426	466
12	4	625	647	-5	7	545	568	-3	10	385	385	2	0	1026	1033	3	2	1270	1371
13	4	272	264	-4	7	431	449	-2	10	415	397	3	0	1514	1508	4	2	598	665
14	4	310	253	-3	7	232	257	-1	10	469	486	4	0	1676	1676	5	2	863	923
15	4	222	256	-2	7	578	625	0	10	536	537	5	0	878	872	6	2	985	1040
16	4	509	500	-1	7	2165	2142	2	10	1022	1021	6	0	1161	1179	7	2	611	604
17	4	871	863	0	7	228	219	3	10	369	199	7	0	508	487	8	2	2114	2174
18	5	209	226	1	7	257	276	4	10	361	357	8	0	1599	1622	10	2	557	548
19	5	886	877	2	7	599	617	5	10	224	213	9	0	538	581	11	2	258	263
20	5	367	378	3	7	789	791	6	10	593	560	10	0	1487	1478	12	2	454	474
21	5	424	460	4	7	197	171	10	10	982	542	11	0	457	460	12	2	502	513
22	5	795	778	5	7	225	251	13	10	370	379	12	0	947	985	14	2	383	405
23	5	368	262	7	7	951	948	16	10	387	375	13	0	1270	1294	17	2	845	889
24	5	335	306	8	7	226	238	17	10	326	282	14	0	872	699	20	2	574	579
25	5	298	228	9	7	950	931	-14	11	231	227	15	0	595	603	21	2	288	277
26	5	741	723	10	7	222	235	-11	11	769	760	17	0	529	549	-24	3	614	666
27	5	362	361	11	7	562	582	-8	11	530	596	18	0	316	347	-23	3	314	354
28	5	642	600	12	7	408	433	-7	11	493	545	20	0	387	409	-21	3	330	365
29	5	479	470	13	7	325	309	-6	11	539	592	21	0	508	539	-20	3	250	220
30	5	1105	1077	14	7	246	228	-5	11	220	218	24	0	262	291	-19	3	483	502
31	5	1341	1271	15	7	241	189	-4	11	427	487	-24	1	389	442	-18	3	218	336
32	5	157	167	17	7	728	702	-3	11	690	725	-21	1	638	664	-16	3	236	264
33	5	913	882	20	7	251	178	-1	11	361	403	-18	1	326	332	-14	3	857	874
34	5	1209	1222	-18	8	892	925	0	11	274	211	-16	1	556	580	-13	3	676	937
35	5	316	295	-16	8	457	410	1	11	317	294	-15	1	589	576	-12	3	270	249
36	5	1543	1546	-14	8	818	809	4	11	230	219	-14	1	520	510	-11	3	715	690
37	5	310	297	-13	8	421	487	5	11	382	364	-13	1	1330	1355	-10	3	1504	1452
38	5	961	993	-12	8	634	616	6	11	237	263	-12	1	692	652	-9	3	1545	1393
39	5	675	652	-11	8	269	286	7	11	992	967	-11	1	708	697	-7	3	880	872
40	5	1281	1276	-10	8	754	738	9	11	544	551	-10	1	484	515	-8	3	205	224
41	5	2000	2030	-9	8	241	254	10	11	462	362	-9	1	1625	1594	-6	3	2231	2045
42	5	897	939	-8	8	412	351	11	11	229	136	-8	1	381	365	-3	3	1107	1040
43	5	344	312	-6	8	299	272	13	11	614	627	-7	1	726	728	-2	3	1970	1862
44	5	522	569	-5	8	898	722	-14	12	203	233	-5	1	248	241	-1	3	536	528
45	5	316	320	-4	8	1452	1436	-11	12	400	413	-4	1	1704	1625	0	3	877	874
46	5	447	450	-3	8	470	460	-8	12	563	564	-3	1	1340	1260	1	3	863	882
47	5	704	696	-2	8	632	616	-6	12	484	511	-2	1	1706	1633	2	3	339	356
48	5	530	562	-1	8	594	611	-3	12	391	398	-1	1	1188	1114	3	3	745	795
49	5	287	239	2	8	1874	1703	0	12	384	428	0	1	2069	2080	4	3	605	649
50	5	427	422	3	8	410	389	1	12	312	295	1	1	255	284	5	3	227	255
51	5	321	322	4	8	798	800	2	12	373	381	2	1	249	342	6	3	444	458
52	5	211	198	5	8	630	638	4	12	463	451	3	1	3026	3179	7	3	1318	1375
53	5	1144	1132	6	8	377	367	6	12	294	255	4	1	1506	1550	8	3	1466	1491
54	5	343	344	7	8	204	216	10	12	800	802	5	1	711	758	9	3	200	174
55	5	1076	1071	8	8	200	200	11	12	546	509	6	1	1432	1488	10	3	540	520
56	5	305	253	9	8	929	975	12	12	272	272	7	1	690	712	11	3	1429	1478
57	5	847	792	12	8	823	836	-11	13	613	656	8	1	842	885	12	3	1292	1311
58	5	387	357	13	8	429	437	-9	13	253	292	9	1	543	573	13	3	375	371
59	5	843	825	14	8	491	489	-8	13	212	265	10	1	1334	1393	14	3	940	950
60	5	846	776	15	8	411	405	-6	13	498	526	11	1	1477	1476	17	3	543	571
61	5	682	649	16	8	657	611	-3	13	557	560	12	1	271	244	19	3	340	289
62	5	2036	1924	17	8	519	479	-1	13	301	313	13	1	462	498	22	3	249	137
63	5	357	318	18	8	355	298	1	13	315	359	14	1	946	961	23	3	351	342
64	5	703	649	20	8	521	506	3	13	625	624	16	1	729	763	24	3	328	372
65	5	486	464	-19	9	477	521	7	13	275	281	17	1	477	447	-23	4	277	309
66	5	497	544	-18	9	265	234	8	13	354	325	18	1	424	468	-22	4	232	245
67	5	483	499	-17	9	327	339	9	13	456	438	19	1	321	360	-21	4	539	535
68	5	470	476	-15	9	220	291	-6	14	342	374	20	1	395	377	-20	4	524	534
69	5	427	415	-14	9	434	412	-6	14	694	688	21	1	502	581	-18	4	220	202
70	5	410	403	-13	9	318	326	-6	14	694	688	21	1	502	581	-18	4	220	202
71	5	406	411	-12	9	229	160	-24	14	321	291	24	1	217	165	-16	4	410	395
72	5	1072	1095	-11	9	1115	1132	-21	0	553	539	-24	2	327	364	-14	4	601	570
73	5	347	328	-10	9	332	341	-20	0	375	409	-22	2	244	234	-12	4	944	929
74	5	740	767	-7	9	860	888	-18	0	347	347	-21	2	536	528	-12	4	312	269
75	5	286	273	-4	9	739	731	-17	0	545	549	-18	2	557	580	-11	4	983	928
76	5	533	566	-2	9	467	466	-15	0	617	603	-17	2	225	166	-10	4	1498	1460
77	5	874	861	-1	9	1726	1742	-14	0	685	699	-16	2	582	566	-9	4	201	191
78	5	716	740	1	9	921	922												

Table 31 (continued)

M	L	FOBS	FCAL	M	L	FOBS	FCAL	M	L	FOBS	FCAL	M	L	FOBS	FCAL	M	L	FOBS	FCAL
-8	4	359	327	5	6	599	612	-13	9	277	256	7	13	296	255	-13	2	884	956
-7	4	2817	2643	7	6	886	881	-9	9	925	902	8	13	562	552	-12	2	1043	1229
-5	4	1647	1628	8	6	646	639	-7	9	242	197	-5	14	540	544	-11	2	971	951
-4	4	1837	966	9	6	419	445	-4	9	778	777	-2	14	495	541	-10	2	885	849
-3	4	561	521	10	6	989	1033	-3	9	588	617	2	14	559	575	-8	2	644	637
-2	4	737	727	11	6	256	221	-2	9	942	918	-22	0	345	319	-7	2	455	424
-1	4	662	651	12	6	491	522	-1	9	670	677	-20	0	682	696	-6	2	466	428
0	4	508	495	13	6	414	406	1	9	599	611	-19	0	496	485	-5	2	1676	1641
1	4	1606	1607	14	6	298	307	2	9	685	676	-18	0	250	195	-4	2	682	646
2	4	387	395	15	6	665	688	3	9	501	493	-16	0	208	144	-3	2	323	281
3	4	1315	1375	16	6	298	283	4	9	577	584	-15	0	724	727	-2	2	146	168
4	4	1355	1379	17	6	493	468	5	9	782	723	-14	0	559	552	-1	2	854	812
5	4	799	822	18	6	416	381	6	9	765	774	-13	0	455	448	0	2	1741	1718
6	4	854	887	22	6	528	524	7	9	204	203	-11	0	1145	1151	2	2	307	335
7	4	769	817	-21	7	261	250	9	9	526	534	-10	0	1435	1455	3	2	797	846
8	4	830	920	-20	7	301	270	10	9	562	555	-8	0	991	1009	4	2	497	514
9	4	389	427	-17	7	407	388	12	9	585	550	-7	0	1113	1086	5	2	780	852
11	4	328	374	-15	7	492	490	15	9	221	236	-6	0	207	149	6	2	838	907
12	4	604	597	-13	7	367	328	16	9	778	169	-5	0	710	727	7	2	600	615
14	4	1098	1126	-12	7	611	600	18	9	712	678	-4	C	357	329	8	2	307	313
15	4	433	382	-11	7	523	504	-17	10	227	257	-3	C	1633	1657	9	2	910	944
16	4	254	172	-9	7	721	711	-16	10	236	219	-2	0	726	723	10	2	1291	1358
17	4	282	284	-8	7	1070	1054	-12	10	833	838	-1	0	308	345	11	2	347	380
18	4	311	259	-7	7	766	782	-9	10	594	648	-1	0	304	345	12	2	370	438
19	4	565	580	-6	7	438	436	-3	10	387	395	2	0	726	723	13	2	397	425
20	4	290	223	-5	7	959	904	0	10	507	540	3	C	1628	1657	14	2	253	246
21	4	398	395	-4	7	663	660	1	10	560	582	4	0	334	329	15	2	283	322
22	4	232	269	-3	7	578	598	2	10	801	797	5	0	725	727	16	2	404	390
-23	5	539	540	-2	7	519	525	3	10	261	245	7	0	1106	1086	17	2	367	380
-19	5	338	343	-1	7	687	679	5	10	472	457	8	0	989	1009	18	2	580	598
-18	5	217	232	0	7	327	353	7	10	493	540	10	C	1415	1455	19	2	285	297
-17	5	360	277	1	7	664	685	8	10	542	532	11	0	1110	1151	20	2	444	446
-16	5	238	204	3	7	287	332	9	10	277	274	13	0	452	448	21	2	227	209
-15	5	379	417	4	7	378	381	10	10	242	200	14	C	550	552	22	3	324	278
-14	5	400	409	6	7	307	309	12	10	410	427	15	0	713	727	23	3	424	430
-13	5	811	792	7	7	1160	1165	15	10	862	791	19	0	490	485	24	3	569	557
-12	5	294	288	8	7	259	191	16	10	303	261	20	0	689	696	25	3	657	611
-11	5	691	683	9	7	777	771	-13	11	344	395	22	0	318	319	26	3	642	662
-10	5	1553	1472	11	7	256	248	-12	11	410	419	-23	1	255	292	27	3	622	599
-8	5	1858	959	13	7	281	286	-9	11	574	604	-22	1	203	243	28	3	540	559
-7	5	564	469	14	7	583	597	-8	11	453	461	-19	1	318	270	29	3	408	413
-6	5	1875	1878	15	7	383	425	-6	11	824	808	-18	1	628	632	30	3	841	826
-5	5	534	468	16	7	239	252	-5	11	281	212	-17	1	283	262	31	3	739	715
-4	5	861	820	17	7	249	254	-4	11	270	306	-16	1	783	775	32	3	1977	1885
-3	5	441	429	18	7	483	452	-2	11	303	335	-14	1	441	489	33	3	771	732
-2	5	1232	1210	21	7	439	441	-1	11	468	489	-13	1	198	162	34	3	387	384
-1	5	1834	976	-21	8	240	210	0	11	288	275	-12	1	177	159	35	3	747	734
0	5	194	225	-20	8	437	448	2	11	527	525	-11	1	177	159	36	3	761	740
1	5	1637	1620	-18	8	226	253	3	11	331	272	-10	1	1635	1444	37	3	335	353
2	5	365	361	-17	8	345	354	4	11	375	353	-9	1	279	279	38	3	789	772
3	5	1158	1210	-15	8	701	735	5	11	581	574	-8	1	1224	1179	39	3	309	293
4	5	662	699	-14	8	360	365	7	11	240	225	-7	1	958	944	40	3	760	736
5	5	442	435	-13	8	355	361	8	11	457	486	-6	1	908	890	41	3	742	717
6	5	804	818	-12	8	815	811	9	11	325	303	-4	1	402	395	42	3	494	496
7	5	1446	1473	-11	8	947	947	10	11	280	274	-3	1	540	527	43	3	911	901
8	5	1598	1608	-10	8	720	705	11	11	257	230	-2	1	1241	1189	44	3	399	450
9	5	250	226	-8	8	716	690	12	11	257	274	-1	1	379	412	45	3	867	825
10	5	457	454	-7	8	671	660	-13	12	246	257	1	1	1376	1290	46	3	2526	2671
11	5	355	426	-6	8	402	413	-12	12	238	313	2	1	1595	1491	47	3	168	157
12	5	252	257	-4	8	672	612	-9	12	533	542	3	1	208	192	48	3	1140	1133
13	5	349	331	-2	8	386	387	-7	12	420	428	4	1	428	448	49	3	630	701
-20	6	660	679	0	8	959	952	-6	12	231	244	6	1	431	457	50	3	363	346
-16	6	280	291	1	8	990	982	-5	12	649	718	7	1	1045	1063	51	3	885	958
-14	6	631	575	2	8	306	317	-4	12	288	322	8	1	1227	1333	52	3	905	953
-13	6	644	683	3	8	248	291	-2	12	471	479	9	1	1066	1104	53	3	281	273
-12	6	638	622	4	8	828	815	0	12	324	293	10	1	693	712	54	3	360	319
-11	6	319	316	5	8	622	643	2	12	435	473	11	1	772	764	55	3	445	494
-10	6	1877	1832	6	8	507	519	3	12	451	467	12	1	433	448	56	3	358	363
-9	6	1360	1307	7	8	433	420	4	12	240	248	13	1	686	709	57	3	408	413
-8	6	449	428	8	8	497	520	5	12	524	535	14	1	285	261	58	3	549	542
-7	6	656	655	9	8	392	380	6	12	331	322	15	1	740	734	59	3	308	338
-5	6	201	151	10	8	523	523	7	12	202	194	16	1	1316	1303	60	3	310	322
-4	6	182	184	11	8	615	577	-10	13	299	338	17	1	395	398	61	3	513	476
-3	6	376	340	12	8	485	463	-9	13	299	338	18	1	356	347	62	3	301	324
-2	6	1828	1839	13	8	527	553	-8	13	762	715	19	1	310	246	63	3	482	502
-1	6	158	152	14	8	983	1000	-7	13	194	211	20	1	457	431	64	3	355	381
0	6	351	360	15	8	346	324	-2	13	352	390	21	2	555	571	65	3	1173	1144
1	6	1897	1895	16	8	503	463	-1	13	331	370	22	2	540	549	66	3	488	489
2	6	244	251	17	8	273	285	0	13	295	297	23	2	386	400	67	3	893	890
3	6	445	452	-19	9	295	233	1	13	298									

Table 31 (continued)

M	L	FOBS	FCAL	M	L	FOBS	FCAL	M	L	FOBS	FCAL	M	L	FOBS	FCAL	M	L	FOBS	FCAL
			30000	2	6	1069	1047	3	9	261	235	-24	0	324	353	-10	2	507	499
-9	4	929	894	3	6	224	266	4	9	489	495	-23	0	199	145	-9	2	361	360
-8	4	1350	1272	4	6	451	400	5	9	867	858	-22	0	479	500	-8	2	416	413
-7	4	1202	1156	5	6	430	443	6	9	378	353	-21	0	287	340	-7	2	633	803
-6	4	613	575	6	6	604	620	7	9	575	569	-18	0	344	321	-6	2	258	243
-5	4	1940	1883	7	6	567	559	10	9	537	518	-15	0	337	375	-5	2	183	142
-4	4	888	825	8	6	1033	1047	11	9	420	467	-14	0	332	379	-4	2	857	836
-3	4	635	602	9	6	1189	1210	12	9	549	543	-13	0	646	653	-3	2	1866	1741
-2	4	885	870	12	6	689	725	14	9	440	445	-12	0	779	785	-2	2	170	157
-1	4	439	641	13	6	585	570	16	9	419	433	-11	0	800	793	-1	2	655	652
0	4	1815	1818	14	6	242	261	-17	10	304	306	-10	0	218	216	1	2	931	942
1	4	264	237	17	6	442	428	-16	10	368	364	-9	0	344	365	2	2	944	1027
2	4	1043	1087	19	6	253	209	-15	10	424	453	-7	0	970	936	3	2	1400	1480
3	4	1204	1252	20	6	377	348	-14	10	387	420	-5	0	338	344	4	2	547	556
4	4	143	145	21	6	372	349	-13	10	221	272	-4	0	1839	1879	5	2	1365	1415
5	4	804	810	-20	7	356	324	-12	10	326	285	-2	0	1430	1393	6	2	303	315
6	4	419	418	-19	7	376	350	-11	10	618	630	-1	0	255	207	7	2	313	328
7	4	234	243	-18	7	212	225	-10	10	474	510	0	0	556	545	8	2	288	275
8	4	1450	1488	-14	7	678	708	-9	10	226	147	1	0	208	207	10	2	1216	1217
9	4	721	721	-13	7	480	520	-8	10	407	419	2	0	1405	1393	11	2	963	995
10	4	489	453	-12	7	256	254	-7	10	445	441	4	0	1807	1879	12	2	643	664
11	4	267	205	-11	7	215	258	-3	10	420	437	5	0	349	344	13	2	506	506
12	4	301	344	-9	7	869	814	-2	10	547	533	6	0	206	73	14	2	381	384
13	4	347	377	-8	7	408	439	-1	10	671	675	7	0	962	936	15	2	475	491
14	4	330	350	-7	7	698	684	2	10	418	418	9	0	335	365	16	2	312	296
15	4	489	456	-6	7	225	186	3	10	408	395	10	0	181	216	17	2	397	381
16	4	280	315	-5	7	414	417	4	10	606	608	11	0	774	793	18	2	378	404
17	4	280	243	-4	7	675	651	5	10	301	251	12	0	743	785	19	2	334	328
18	4	572	578	-3	7	272	274	7	10	860	821	13	0	627	653	20	2	659	670
19	4	428	410	-2	7	1162	1155	8	10	367	375	14	0	354	379	21	2	234	204
20	4	257	249	-1	7	630	590	9	10	535	514	15	0	362	375	23	2	260	296
21	5	540	531	1	7	157	140	10	10	578	571	18	0	367	321	-23	3	211	207
22	5	396	407	2	7	746	743	13	10	384	401	21	0	334	340	-21	3	356	361
23	5	494	456	3	7	442	474	16	10	247	210	22	0	482	500	-19	3	625	625
24	5	630	622	4	7	354	340	-15	11	254	241	24	0	332	354	-18	3	526	506
25	5	1015	992	5	7	774	792	-14	11	781	832	-24	1	566	570	-17	3	333	330
26	5	451	414	6	7	822	796	-12	11	244	277	-21	1	431	392	-16	3	626	621
27	5	643	667	8	7	199	191	-11	11	387	399	-19	1	737	732	-15	3	653	674
28	5	873	857	9	7	785	775	-10	11	265	247	-17	1	304	329	-13	3	374	371
29	5	393	414	10	7	292	301	-8	11	557	555	-16	1	490	511	-12	3	439	398
30	5	642	640	11	7	807	829	-7	11	233	225	-15	1	382	343	-11	3	858	862
31	5	160	153	12	7	728	725	-6	11	609	661	-14	1	816	798	-10	3	1056	1017
32	5	2150	1972	14	7	256	251	-5	11	263	250	-12	1	446	411	-9	3	977	948
33	5	1728	1598	17	7	348	368	-4	11	370	349	-11	1	246	270	-8	3	561	474
34	5	936	908	19	7	457	413	-3	11	381	390	-10	1	1034	1013	-6	3	1115	1005
35	5	839	858	20	7	360	343	0	11	954	925	-9	1	1278	1285	-5	3	328	307
36	5	626	611	-20	8	262	337	1	11	831	790	-7	1	748	749	-4	3	793	784
37	5	637	634	-18	8	232	158	2	11	329	294	-6	1	1218	1215	-3	3	223	187
38	5	933	996	-17	8	508	561	4	11	482	522	-5	1	395	412	-1	3	2527	2436
39	5	1215	1232	-15	8	225	240	7	11	500	476	-4	1	849	835	0	3	563	559
40	5	2240	2293	-12	8	223	204	10	11	432	436	-3	1	561	523	1	3	517	517
41	5	195	203	-10	8	940	986	-12	12	481	537	-2	1	374	330	2	3	855	873
42	5	241	283	-9	8	236	185	-11	12	622	657	-1	1	913	820	3	3	453	454
43	5	455	483	-5	8	715	757	-9	12	266	278	0	1	645	640	4	3	1880	1908
44	5	514	509	-2	8	570	545	-8	12	225	196	1	1	1061	1109	5	3	813	852
45	5	456	428	-1	8	926	923	-7	12	209	198	2	1	480	479	6	3	878	899
46	5	491	502	2	8	648	653	-5	12	233	233	3	1	292	317	7	3	580	573
47	5	636	691	5	8	615	615	-3	12	684	712	4	1	807	836	8	3	1100	1153
48	5	338	324	6	8	218	275	-2	12	743	779	5	1	581	596	9	3	374	394
49	5	236	154	8	8	1111	1117	0	12	545	559	6	1	1556	1651	11	3	198	170
50	5	419	399	9	8	1049	1064	2	12	355	278	7	1	780	770	12	3	215	181
51	5	309	328	10	8	331	307	3	12	566	589	8	1	722	739	13	3	499	470
52	5	347	364	12	8	296	277	4	12	356	408	9	1	1194	1220	14	3	1125	1137
53	5	886	887	13	8	489	465	6	12	307	297	10	1	622	648	15	3	386	402
54	5	400	397	14	8	330	322	7	12	503	490	12	1	219	207	19	3	491	490
55	5	329	338	15	8	225	280	11	12	497	502	14	1	812	816	22	3	345	327
56	5	503	464	16	8	257	178	-8	12	305	351	15	1	619	626	23	3	219	216
57	5	409	410	17	8	488	435	-6	13	457	493	16	1	927	942	-22	4	285	322
58	5	744	753	-19	9	441	487	-4	13	267	247	18	1	375	327	-21	4	364	396
59	5	248	245	-18	9	304	318	-3	13	468	456	19	1	451	454	-20	4	277	345
60	5	232	214	-15	9	209	220	-2	13	241	282	20	1	361	411	-19	4	364	319
61	5	988	963	-14	9	806	849	-1	13	288	286	21	1	753	766	-18	4	703	695
62	5	613	591	-13	9	621	604	0	13	462	479	22	1	292	251	-17	4	709	702
63	5	1041	978	-12	9	522	516	1	13	348	334	23	1	486	509	-16	4	703	704
64	5	392	414	-9	9	357	312	3	13	520	505	-22	2	275	328	-14	4	873	867
65	5	444	447	-8	9	220	188	5	13	345	366	-18	2	497	517	-13	4	1387	1369
66	5	919	882	-5	9	358	339	6	13	274	243	-15	2	208	206	-12	4	206	215
67	5	390	359	-4	9	746	772	-1	14	182	98	-14	2	645	657	-8	4	346	323
68	5	298	298	-2	9	489	483	0	14	684	684	-13	2	1335	1353	-7	4	1843	1728
69	5	1121	1141	-1	9	260	255	1	14										

Table 31 (continued)

H	L	F085	FCAL	H	L	F085	FCAL	H	L	F085	FCAL	H	L	F085	FCAL
-4	4	1769	1702	17	6	372	382	-4	10	526	546	16	0	523	540
-3	4	998	927	18	6	348	279	-3	10	410	405	17	0	275	241
-2	4	961	964	-21	7	540	561	0	10	439	417	18	0	235	275
-1	4	662	621	-20	7	251	291	1	10	297	315	19	0	243	206
0	4	240	250	-18	7	307	370	2	10	277	202	20	0	677	721
1	4	1478	1490	-17	7	212	175	3	10	629	591	-23	1	346	361
2	4	1908	1855	-14	7	426	480	4	10	541	555	-17	1	256	272
3	4	876	915	-13	7	259	176	5	10	484	489	-16	1	678	660
4	4	500	535	-12	7	515	506	6	10	269	252	-15	1	328	315
5	4	1507	1535	-11	7	766	738	7	10	280	347	-14	1	732	729
6	4	1442	1463	-10	7	442	451	8	10	210	176	-13	1	475	486
7	4	215	212	-9	7	253	232	9	10	259	232	-12	1	284	311
8	4	251	240	-7	7	269	319	10	10	456	455	-11	1	404	386
9	4	619	640	-6	7	609	618	11	10	364	391	-10	1	779	770
10	4	1053	1092	-5	7	741	734	-15	11	364	391	-8	1	1083	1079
11	4	432	454	-4	7	409	365	-14	11	213	170	-7	1	1140	1153
12	4	388	371	-3	7	534	540	-13	11	419	453	-6	1	636	642
13	4	565	566	2	7	661	694	-12	11	638	669	-5	1	937	940
14	4	586	981	4	7	852	879	-8	11	270	303	-4	1	947	919
15	4	442	436	5	7	834	830	-7	11	323	339	-3	1	1923	1841
16	4	464	417	6	7	276	266	-6	11	536	540	-2	1	331	357
17	4	244	207	7	7	584	556	-5	11	232	240	0	1	157	91
18	4	216	204	8	7	444	420	-4	11	300	328	2	1	1077	1153
19	4	323	371	9	7	605	639	-3	11	292	292	3	1	924	1024
-20	5	538	527	12	7	340	289	-1	11	609	602	4	1	718	743
-19	5	358	281	13	7	556	575	2	11	219	156	5	1	931	950
-18	5	215	182	17	7	290	329	3	11	944	946	6	1	538	573
-17	5	565	565	19	7	411	378	4	11	279	310	7	1	800	834
-16	5	1119	1075	-18	8	275	286	5	11	364	332	8	1	704	721
-15	5	1362	1310	-17	8	536	554	6	11	581	548	9	1	693	782
-14	5	262	262	-15	8	428	493	7	11	611	595	10	1	839	825
-13	5	207	161	-14	8	422	459	8	11	243	213	14	1	280	326
-12	5	868	842	-12	8	383	392	9	11	240	190	15	1	331	330
-11	5	340	389	-8	8	888	875	-10	12	530	550	16	1	398	396
-10	5	868	838	-7	8	275	294	-9	12	252	280	17	1	705	751
-9	5	940	904	-5	8	198	213	-5	12	332	389	20	1	286	278
-8	5	2274	2176	-4	8	858	832	-4	12	541	565	22	1	365	307
-7	5	347	357	-3	8	421	387	-3	12	316	347	23	1	570	557
-6	5	1440	1451	-1	8	219	202	0	12	509	506	-23	2	311	280
-5	5	592	614	1	8	426	460	1	12	106	106	-20	2	452	493
-4	5	1402	1426	2	8	1225	1229	2	12	362	397	-17	2	323	320
-3	5	1713	1735	6	8	640	626	3	12	737	739	-15	2	487	508
-2	5	852	842	7	8	1179	1202	4	12	737	739	-13	2	843	835
-1	5	349	346	9	8	268	218	5	12	879	867	-12	2	203	175
0	5	258	271	10	8	462	496	-8	12	260	209	-11	2	459	458
1	5	709	735	11	8	286	336	-7	13	314	361	-10	2	224	223
2	5	585	583	12	8	324	366	-2	13	417	440	-9	2	226	225
3	5	464	465	13	8	250	237	-1	13	562	608	-7	2	171	164
4	5	241	133	14	8	312	331	2	13	593	546	-6	2	1334	1303
5	5	421	437	15	8	522	492	3	13	456	460	-5	2	1485	1420
6	5	247	269	16	8	240	231	4	13	289	288	-4	2	986	996
7	5	639	635	17	8	275	218	5	13	257	275	-3	2	522	512
8	5	211	202	-14	9	262	269	-23	0	237	274	-1	2	756	708
9	5	339	374	-13	9	231	304	-20	0	719	721	0	2	911	902
-10	6	278	281	-12	9	849	852	-19	0	248	206	1	2	469	475
-11	6	472	458	-11	9	593	587	-18	0	272	275	2	2	504	506
-12	6	261	197	-10	9	397	360	-17	0	265	241	3	2	1084	1193
-13	6	471	469	-9	9	307	290	-16	0	529	540	4	2	245	242
-14	6	1072	1040	-8	9	207	88	-15	0	265	264	5	2	856	919
-15	6	620	613	-7	9	229	232	-13	0	796	783	6	2	889	910
-16	6	826	796	-6	9	388	406	-11	0	350	340	7	2	1355	1403
-17	6	842	804	-2	9	277	296	-10	0	531	517	8	2	984	912
-18	6	421	405	-1	9	278	306	-9	0	360	319	9	2	675	491
-19	6	660	653	1	9	297	195	-8	0	392	364	10	2	838	905
-20	6	254	206	2	9	836	815	-7	0	360	402	11	2	216	224
-21	6	344	367	3	9	527	522	-6	0	1813	1829	12	2	379	392
-22	6	714	687	4	9	890	508	-5	0	2028	2114	13	2	497	487
-23	6	875	852	5	9	692	682	-3	0	520	517	14	2	584	620
-24	6	1074	1070	6	9	433	441	-1	0	667	649	15	2	678	671
-25	6	992	987	7	9	521	235	1	0	607	649	16	2	758	782
-26	6	485	505	8	9	880	875	2	0	516	517	17	2	307	285
-27	6	226	260	9	9	412	447	3	0	2028	2114	18	2	275	279
-28	6	693	665	10	9	435	456	4	0	1809	1829	19	2	217	173
-29	6	812	871	11	9	595	621	5	0	358	402	20	2	272	303
-30	6	552	560	12	9	288	268	6	0	370	364	21	2	510	467
-31	6	357	368	-17	10	231	239	7	0	328	319	22	2	412	474
-32	6	270	213	-15	10	307	328	8	0	526	517	23	2	1035	1026
-33	6	231	252	-12	10	238	253	9	0	352	340	24	2	478	455
-34	6	222	225	-11	10	233	276	10	0	796	783	25	2	236	223
-35	6	337	270	-10	10	467	435	11	0	228	284	26	2	422	447
-36	6	640	647	-9	10	705	703	12	0			27	2		

Table 31 (continued)

M	L	FOBS	FCAL	M	L	FOBS	FCAL	M	L	FOBS	FCAL	M	L	FOBS	FCAL	M	L	FOBS	FCAL
7	5	342	336	4	8	1039	1006	-5	13	247	213	-10	2	718	695	5	4	686	713
9	5	610	633	5	8	832	823	-2	13	422	375	-9	2	373	315	6	4	248	262
11	5	779	792	7	8	539	515	-1	13	373	408	-7	2	716	702	7	4	318	369
12	5	663	638	8	8	820	800	0	13	356	351	-6	2	277	239	8	4	332	362
14	5	663	686	9	8	306	277	2	13	334	322	-4	2	641	609	9	4	345	364
16	5	559	518	11	8	475	450	5	13	354	348	-3	2	1332	1319	10	4	790	790
17	5	395	402	13	8	650	638					-2	2	813	770	11	4	398	424
18	5	380	351	14	8	318	330	-22	C	379	381	-1	2	665	646	13	4	826	847
20	5	656	662	18	8	449	397	-21	0	369	391	1	2	374	360	14	4	536	526
21	5	212	183	-16	9	362	393	-20	0	255	235	2	2	888	896	16	4	582	546
-21	6	282	322	-15	9	369	384	-18	0	349	374	3	2	704	730	17	4	1006	971
-19	6	258	227	-12	9	434	433	-15	0	369	354	4	2	934	948	19	4	565	526
-16	6	294	336	-10	9	664	647	-14	0	727	736	5	2	976	1036	-21	5	261	285
-15	6	570	583	-8	9	639	603	-13	0	925	888	6	2	200	175	-19	5	275	255
-14	6	463	481	-7	9	261	298	-12	0	584	598	8	2	222	207	-16	5	741	742
-13	6	434	435	-5	9	580	577	-11	0	925	871	9	2	440	482	-15	5	428	410
-10	6	392	394	-4	9	645	637	-9	C	1142	1140	11	2	433	392	-14	5	760	802
-9	6	570	522	-3	9	481	413	-8	0	204	160	12	2	1009	1066	-11	5	1213	1145
-8	6	470	447	0	9	261	122	-7	0	1072	1103	13	2	992	1021	-10	5	355	345
-7	6	628	618	2	9	625	640	-6	0	370	369	14	2	260	217	-9	5	352	365
-6	6	683	677	3	9	672	675	-5	0	612	634	15	2	593	606	-8	5	644	632
-3	6	675	649	4	9	554	595	-4	0	693	651	16	2	514	538	-6	5	222	223
-2	6	221	241	5	9	404	417	-3	C	847	858	17	2	676	698	-5	5	391	396
-1	6	557	564	6	9	325	341	-1	0	704	684	18	2	297	300	-4	5	958	927
0	6	1253	1258	8	9	480	508	0	0	669	650	20	2	262	286	-3	5	674	662
1	6	446	422	9	9	499	487	1	0	671	684	22	2	283	273	-2	5	662	631
3	6	416	397	10	9	456	428	3	0	814	858	-22	3	332	335	-1	5	923	928
4	6	446	428	11	9	681	701	4	0	685	651	-18	3	420	410	2	5	285	289
5	6	505	479	12	9	328	338	5	0	616	634	-16	3	818	823	3	5	703	686
6	6	476	444	16	9	337	312	6	0	360	369	-15	3	248	291	4	5	770	809
8	6	915	908	-16	10	241	293	7	0	1066	1103	-14	3	613	611	5	5	292	296
9	6	364	371	-13	10	434	480	8	0	217	160	-13	3	425	442	6	5	472	494
10	6	236	228	-12	10	426	433	9	0	1124	1140	-11	3	464	471	7	5	386	363
11	6	312	292	-11	10	431	432	11	0	878	871	-10	3	481	496	8	5	498	492
14	6	243	229	-10	10	337	351	12	0	605	598	-9	3	890	883	10	5	241	216
15	6	494	510	-8	10	344	392	13	0	888	888	-8	3	259	230	11	5	396	341
16	6	278	235	-7	10	377	390	14	C	722	736	-7	3	460	458	12	5	290	240
17	6	487	483	-5	10	580	584	15	0	396	354	-4	3	185	152	13	5	562	612
18	6	457	420	-2	10	899	882	16	0	351	374	-4	3	1258	1170	14	5	747	752
-20	7	270	260	-1	10	499	529	20	0	230	235	-3	3	176	158	15	5	222	134
-18	7	254	263	0	10	519	525	21	0	394	391	-2	3	246	260	16	5	1040	1035
-17	7	347	343	1	10	726	685	22	0	369	381	-1	3	1630	1539	17	5	344	279
-16	7	247	273	2	10	224	204	-22	1	349	345	0	3	978	942	20	5	212	204
-15	7	544	570	7	10	953	950	-19	1	225	213	1	3	391	352	20	5	254	224
-12	7	559	524	8	10	504	508	-18	1	413	407	2	3	1507	1481	-19	6	290	305
-10	7	481	414	12	10	241	253	-14	1	959	963	3	3	218	222	-17	6	277	297
-8	7	286	279	13	10	481	485	-13	1	393	378	4	3	439	448	-13	6	535	546
-6	7	330	281	14	10	322	307	-12	1	814	809	5	3	502	530	-11	6	423	426
-5	7	675	692	-14	11	415	442	-11	1	896	879	6	3	470	515	-9	6	475	455
-4	7	1282	1278	-13	11	235	194	-9	1	520	524	7	3	362	350	-8	6	594	587
-3	7	501	477	-9	11	332	317	-8	1	189	135	9	3	339	353	-6	6	651	648
-1	7	230	233	-8	11	324	313	-7	1	679	671	11	3	283	284	-5	6	208	122
1	7	278	288	-7	11	256	245	-6	1	1150	1142	12	3	567	613	-4	6	1225	1213
2	7	832	853	-5	11	460	474	-5	1	281	271	13	3	838	840	-4	6	393	406
3	7	304	307	-4	11	523	518	-4	1	994	977	14	3	853	849	-1	6	528	524
5	7	400	395	-2	11	470	452	-3	1	294	234	16	3	622	640	1	6	409	412
6	7	688	698	-1	11	361	326	-1	1	682	655	18	3	242	267	2	6	534	479
7	7	387	340	1	11	701	713	0	1	698	702	20	3	426	425	3	6	663	676
8	7	483	481	4	11	721	735	1	1	508	529	-21	4	335	346	4	6	597	587
11	7	537	507	5	11	321	292	2	1	991	1069	-20	4	233	210	5	6	305	354
14	7	717	710	6	11	283	294	3	1	352	384	-19	4	706	729	6	6	513	544
17	7	220	171	9	11	235	182	4	1	1467	1550	-18	4	247	219	7	6	624	609
19	7	227	218	10	11	491	520	5	1	316	329	-17	4	581	539	8	6	641	635
-18	8	295	371	11	11	282	279	6	1	1924	1941	-16	4	277	215	12	6	463	447
-17	8	297	289	12	11	283	306	7	1	368	460	-12	4	405	365	13	6	719	733
-15	8	217	235	-11	12	285	288	8	1	931	945	-11	4	624	602	14	6	340	373
-14	8	531	500	-8	12	259	247	10	1	440	444	-9	4	484	481	15	6	424	391
-13	8	563	560	-5	12	461	499	11	1	731	772	-8	4	483	515	16	6	284	256
-12	8	314	349	-3	12	378	387	13	1	524	556	-6	4	532	550	17	6	446	436
-11	8	267	221	-2	12	683	687	14	1	237	191	-4	4	343	340	18	6	553	562
-10	8	335	317	-1	12	236	255	15	1	706	752	-3	4	882	840	19	6	205	230
-7																			

Table 31 (continued)

M	L	F005	FCAL	M	L	F005	FCAL	M	L	F005	FCAL	M	L	F005	FCAL	M	L	F005	FCAL
-7	7	584	570	-1	11	452	455	-16	2	290	250	-19	5	333	345	-3	8	344	346
-6	7	1180	1176	0	11	466	473	-15	2	270	207	-16	5	483	489	-2	8	379	406
-5	7	256	73	2	11	406	399	-11	2	269	187	-14	5	608	637	-1	8	322	318
-2	7	848	854	3	11	225	218	-10	2	506	511	-12	5	257	277	0	8	431	414
-1	7	612	635	4	11	220	236	-9	2	646	623	-11	5	406	417	1	8	596	588
0	7	417	402	6	11	439	417	-7	2	762	743	-10	5	438	431	5	8	945	952
1	7	340	366	7	11	391	382	-6	2	337	294	-9	5	414	408	6	8	267	283
2	7	272	295	8	11	289	321	-5	2	950	893	-8	5	783	745	7	8	293	175
3	7	496	527	9	11	270	209	-4	2	791	761	-6	5	714	679	9	8	464	424
4	7	418	409	10	11	315	323	-3	2	1707	1622	-5	5	824	834	10	8	511	459
5	7	401	422	11	11	219	224	-2	2	401	382	-4	5	480	459	11	8	501	514
6	7	783	803	-9	12	241	229	-1	2	811	802	-1	5	374	320	13	8	439	422
7	7	344	357	-7	12	390	380	1	2	584	627	0	5	794	798	-10	8	577	551
8	7	234	198	-4	12	320	341	2	2	476	566	1	5	249	197	-9	9	347	353
10	7	422	393	-3	12	611	640	4	2	364	365	2	5	374	387	-8	9	783	801
12	7	492	501	-2	12	252	200	5	2	425	475	3	5	277	278	-7	9	274	197
14	7	270	276	-1	12	520	584	6	2	183	166	4	5	223	190	-4	9	647	624
15	7	401	389	1	12	236	239	7	2	527	520	5	5	326	307	-3	9	287	263
16	7	354	554	4	12	502	471	8	2	1174	1176	7	5	383	355	-2	9	764	748
-17	8	315	287	5	12	303	279	9	2	209	207	8	5	258	251	1	9	430	381
-13	8	249	268	7	12	234	234	10	2	264	227	10	5	679	667	4	9	644	635
-11	8	600	771	11	12	234	234	10	2	726	750	14	5	530	567	8	9	472	450
-10	8	520	516	-21	0	482	534	11	2	337	347	15	5	327	310	10	9	414	366
-9	8	623	600	-17	0	585	592	12	2	302	280	16	5	376	398	11	9	359	350
-8	8	419	410	-15	0	632	683	13	2	508	521	18	5	794	779	12	9	580	577
-7	8	465	432	-14	0	284	303	14	2	373	398	19	5	203	145	13	9	272	273
-6	8	747	719	-13	0	671	648	15	2	1025	1050	-19	6	339	315	14	9	288	262
-5	8	853	811	-12	0	324	220	16	2	304	265	-17	6	414	402	-13	10	372	446
-3	8	827	815	-8	0	678	698	17	2	206	132	-16	6	354	353	-10	10	308	335
-2	8	211	62	-7	0	1481	1515	18	2	434	379	-15	6	583	560	-9	10	308	312
-1	8	347	339	-6	0	256	250	-19	3	476	523	-13	6	481	462	-7	10	348	353
0	8	277	277	-5	0	933	930	-16	3	246	312	-10	6	228	228	-6	10	214	171
2	8	732	718	-4	0	447	452	-15	3	404	457	-9	6	628	578	-5	10	662	642
3	8	541	538	-3	0	378	399	-14	3	248	234	-8	6	213	138	-3	10	280	244
4	8	434	442	-2	0	509	477	-11	3	714	745	-7	6	822	820	-2	10	431	436
7	8	457	445	-1	0	1532	1482	-8	3	510	495	-5	6	285	272	1	10	594	603
9	8	688	692	1	0	1455	1488	-7	3	484	500	-4	6	505	512	5	10	335	286
10	8	340	327	2	0	595	477	-6	3	603	567	-3	6	1013	982	7	10	333	351
11	8	835	834	3	0	403	399	-5	3	1281	1235	-2	6	554	548	8	10	251	258
15	8	452	448	4	0	422	452	-4	3	300	223	0	6	302	275	9	10	300	325
16	8	412	382	5	0	940	930	-3	3	962	939	2	6	204	198	11	10	285	285
-14	9	464	448	6	0	271	250	-2	3	354	297	3	6	878	857	-8	11	201	210
-12	9	222	242	7	0	446	1515	0	3	374	338	5	6	860	882	-2	11	602	630
-10	9	333	289	8	0	288	698	1	3	864	846	6	6	235	241	4	11	397	401
-9	9	342	354	12	0	288	280	2	3	198	182	7	6	328	347	8	11	318	315
-8	9	714	720	13	0	639	648	4	3	305	288	11	6	674	694	9	11	207	233
-6	9	1279	1303	14	0	291	303	6	3	850	876	12	6	250	250	-5	12	622	677
-5	9	527	497	15	0	653	683	7	3	191	137	13	6	255	266	-4	12	400	420
-4	9	570	562	17	0	597	592	9	3	461	455	15	6	643	638	1	12	481	510
-2	9	440	431	21	0	486	534	10	3	293	346	17	6	443	458	3	12	204	152
0	9	327	364	-20	1	561	590	12	3	813	836	-16	7	719	704	12	12	204	152
3	9	233	231	-19	1	332	257	13	3	443	458	-14	7	483	482	-15	0	1050	1043
4	9	287	350	-16	1	514	506	16	3	246	212	-13	7	378	373	-14	0	260	217
5	9	459	504	-14	1	577	543	18	3	367	386	-12	7	329	353	-13	0	362	354
6	9	750	732	-13	1	463	474	19	3	526	544	-10	7	834	835	-8	0	990	987
8	9	458	449	-12	1	508	486	-19	3	237	197	-9	7	240	182	-7	0	203	179
12	9	484	485	-10	1	508	898	-17	4	305	317	-8	7	704	677	-6	0	265	164
13	9	401	391	-8	1	672	606	-15	4	620	621	-7	7	675	701	-5	0	888	905
14	9	465	481	-7	1	546	593	-13	4	628	617	-6	7	747	757	-4	0	483	498
-15	10	272	267	-6	1	725	776	-11	4	409	445	-4	7	783	751	-3	0	994	1019
-11	10	252	281	-5	1	524	536	-9	4	256	237	-3	7	316	316	-2	0	551	556
-9	10	392	372	-4	1	1354	1339	-8	4	716	663	-2	7	618	549	-1	0	851	796
-8	10	592	591	-2	1	948	942	-6	4	253	260	-1	7	227	206	1	0	775	796
-7	10	737	720	-1	1	470	451	-3	4	248	264	0	7	653	624	2	0	558	556
-4	10	317	314	0	1	387	391	-2	4	1011	980	1	7	226	281	3	0	984	1019
-3	10	698	689	2	1	241	225	-1	4	690	645	2	7	393	385	4	0	488	498
0	10	290	334	3	1	214	190	0	4	275	287	3	7	324	274	5	0	913	905
1	10	222	83	4	1	1947	2023	1	4	466	473	4	7	247	251	7	0	213	179
2	10	291	270	5	1	882	952	2	4	324	339	8	7	971	978	9	0	954	987
3	10	656	681	7	1	366	402	3	4	318	322	10	7	216	165	13	0	370	354
4	10	283	295	8	1	416	466	4	4	584	585	12	7	309	281	14	0	274	217
5	10	500	542	9	1	696	744	5	4	285	321	13	7	420	390	15	0	1034	1043
6	10	374	374	10	1	940	949	6	4	319	303	14	7	516	497	-18	1	478	510
9	10	453	460	12	1	1036	1076	7	4	232	223	16	7	282	282	-16	1	227	248
11	10	522	540	13	1	234	184	8	4	894	900	17	7	324	286	-12	1	1056	1060
12	10	246	260	16	1	624	604	10	4	373	348	-18	8	295	284	-7	1	576	570
13	10	198	197	18	1	284	329	11	4	345	351	-15	8	237	221	-6	1	1419	1382
-12	11	235	242	19	1	252	288	13	4	287	311	-13	8	725	730	-5	1	448	463
-10	11	276	283	20	1	327	303	15	4	533	564	-12	8	285	296	-4	1	725	695
-7	11	323	363	21	1	219	217	16	4	1090	1106	-9	8	335	327	-3	1	238	216
-6	11	347	378	-19	2	260	183	19	4	335	378	-7	8	1002	976	-2	1	644	622
-5	11	218	250	-18	2	312	317	20	4	248	234	-6	8	341	341	-1			

TABLE 32: ATOM COORDINATES
AND ISOTROPIC TEMPERATURE FACTORS

ATOM	x	y	z	B
Nb	0.58136(2)	0.21418(5)	0.19528(4)	2.47*
As	0.20939(3)	0.15780(7)	0.26735(6)	3.31*
S1	0.52186(8)	0.1130(1)	0.0746(1)	3.26*
S2	0.57210(8)	0.3413(2)	0.0567(1)	3.60*
S3	0.51630(8)	0.1329(2)	0.3169(1)	3.75*
S4	0.56193(8)	0.3659(1)	0.3010(1)	3.54*
S5	0.63390(8)	0.0503(1)	0.2242(1)	3.54*
S6	0.68163(7)	0.2798(2)	0.1989(1)	3.51*
C11	0.4876(3)	0.2027(6)	-0.0067(5)	2.82*
C12	0.4412(3)	0.1741(6)	-0.0731(5)	3.43*
C13	0.4164(3)	0.2420(7)	-0.1411(6)	4.21*
C14	0.4364(3)	0.3455(7)	-0.1445(6)	4.09*
C15	0.4824(3)	0.3765(6)	-0.0820(6)	3.69*
C16	0.5091(3)	0.3074(6)	-0.0132(5)	3.06*
C21	0.5210(3)	0.2120(7)	0.4254(5)	3.81*
C22	0.4989(4)	0.1770(7)	0.5182(7)	4.93*
C23	0.4971(4)	0.2458(9)	0.6005(7)	6.19*
C24	0.5165(4)	0.3452(9)	0.5921(7)	6.09*
C25	0.5395(3)	0.3818(7)	0.5039(7)	4.70*
C26	0.5405(3)	0.3143(6)	0.4180(6)	3.41*
C36	0.7256(3)	0.1716(6)	0.1733(5)	3.19*

Table 32 (continued)

ATOM	x	y	z	B
C35	0.7837(3)	0.1875(6)	0.1505(6)	3.86*
C34	0.8198(3)	0.1032(8)	0.1328(6)	4.97*
C33	0.7983(4)	0.0024(7)	0.1415(6)	5.04*
C32	0.7418(4)	0.0137(6)	0.1648(6)	4.66*
C31	0.7040(3)	0.0717(6)	0.1835(5)	3.17*

RIGID BODIES

(a) Phenyl Carbon Atoms

C41	0.1589(2)	0.0435(3)	0.2397(4)	3.4(2)
C42	0.1656(3)	-0.0184(4)	0.1533(3)	4.1(2)
C43	0.1319(3)	-0.1087(4)	0.1387(4)	4.5(2)
C44	0.0915(2)	-0.1371(3)	0.2105(4)	4.7(2)
C45	0.0847(3)	-0.0752(4)	0.2968(3)	4.9(2)
C46	0.1184(3)	0.0151(4)	0.3114(4)	4.3(2)
D	3.710(3) ^a			
E	0.982(4)			
F	4.924(4)			
C51	0.1688(2)	0.2697(3)	0.3259(4)	3.4(2)
C52	0.1118(2)	0.2914(4)	0.2916(4)	4.4(2)
C53	0.0845(1)	0.3833(4)	0.3226(3)	4.9(2)
C54	0.1140(2)	0.4533(3)	0.3877(4)	4.9(2)
C55	0.1710(2)	0.4315(4)	0.4220(4)	4.7(2)
C56	0.1984(1)	0.3397(4)	0.3910(3)	4.0(2)

Table 32 (continued)

ATOM	x	y	z	B
D	5.779 (3)			
E	2.731 (4)			
F	4.418 (3)			
C61	0.2679 (4)	0.1098 (4)	0.3600 (10)	3.6 (2)
C62	0.3211 (5)	0.0725 (4)	0.3265 (5)	5.1 (2)
C63	0.3613 (3)	0.0279 (4)	0.3961 (7)	5.7 (2)
C64	0.3482 (4)	0.0207 (4)	0.4990 (10)	5.1 (2)
C65	0.2950 (5)	0.0580 (4)	0.5318 (5)	4.9 (2)
C66	0.2548 (3)	0.1026 (4)	0.4622 (7)	4.3 (2)
D	2.023 (3)			
E	1.217 (8)			
F	5.084 (8)			
C71	0.2370 (5)	0.2098 (4)	0.1429 (8)	3.3 (1)
C72	0.1963 (5)	0.2212 (4)	0.0622 (4)	4.4 (2)
C73	0.2126 (7)	0.2680 (5)	-0.0285 (7)	5.5 (2)
C74	0.2696 (5)	0.3034 (4)	-0.034 (8)	5.4 (2)
C75	0.3103 (5)	0.2920 (4)	0.0423 (4)	6.3 (2)
C76	0.2940 (7)	0.2452 (4)	0.1330 (7)	5.2 (2)
D	1.109 (4)			
E	2.521 (8)			
F	4.425 (8)			

Table 32 (continued)

ATOM	x	y	z	B
(b) Phenyl Hydrogen Atoms				
H1	0.7990	0.2619	0.1446	4.5
H2	0.8613	0.1152	0.1151	5.0
H3	0.8243	-0.0598	0.1281	5.0
H4	0.7250	-0.0880	0.1705	4.5
D	3.159			
E	0.277			
F	5.085			
H5	0.4840	0.1029	0.5229	5.4
H6	0.4809	0.2184	0.6663	6.0
H7	0.5158	0.3948	0.6530	6.0
H8	0.5537	0.4557	0.4962	5.4
D	3.448			
E	1.285			
F	1.748			
H9	0.4267	0.0982	-0.0685	4.1
H10	0.3826	0.2199	-0.1869	4.7
H11	0.4182	0.3963	-0.1949	4.7
H12	0.4978	0.4509	-0.0846	4.1
D	0.281			
E	2.406			
F	4.529			
H13	0.1945	0.0016	0.1020	4.6

Table 32 (continued)

ATOM	x	y	z	B
H14	0.1369	-0.1535	0.0773	5.1
H15	0.0674	-0.2020	0.2004	5.0
H16	0.0556	-0.0953	0.3482	5.5
H17	0.1132	0.0597	0.3730	5.1
D	3.707			
E	0.981			
F	5.973			
H18	0.0905	0.2414	0.2452	5.0
H19	0.0436	0.3989	0.2983	5.9
H20	0.0944	0.5191	0.4100	5.5
H21	0.1922	0.4816	0.4685	5.1
H22	0.2391	0.3241	0.4154	4.7
D	5.779			
E	2.732			
F	5.465			
H23	0.3305	0.0773	0.2529	5.1
H24	0.3994	0.0013	0.3725	6.1
H25	0.3770	-0.0107	0.5486	5.8
H26	0.2856	0.0531	0.6052	5.3
H27	0.2166	0.1290	0.4856	4.7
D	2.020			
E	1.219			
F	6.134			

Table 32 (continued)

ATOM	x	y	z	B
H28	0.1555	0.1957	0.0691	5.1
H29	0.1836	0.2756	-0.0864	5.6
H30	0.2814	0.3364	-0.1034	6.2
H31	0.3511	0.3173	0.0352	6.8
H32	0.3230	0.2374	0.1909	5.6
D	1.111			
E	2.515			
F	5.467			

*These values are equivalent isotropic temperature factors⁸¹ corresponding to the anisotropic thermal parameters shown in Table 33.

^aD, E, and F are the angles by which the coordinates of the rigid body are rotated with respect to a set of axes X, Y, Z. The origin of these axes is placed at the centre of the ring with the X axis parallel to a^* , the Z axis parallel to c , and the Y axis parallel to the line defined by the intersection of the plane containing a^* and b^* with the plane containing b and c .

TABLE 33: ANISOTROPIC THERMAL PARAMETERS (\AA^2)

ATOM	U_{11}	U_{22}	U_{33}	U_{12}	U_{13}	U_{23}
Nb	0.0324(3)	0.0310(4)	0.0302(3)	-0.0003(3)	0.0007(2)	-0.0025(3)
As	0.0385(5)	0.0502(6)	0.0370(5)	-0.0037(4)	0.0025(4)	-0.0057(5)
S1	0.0510(12)	0.0340(11)	0.0383(11)	-0.0004(9)	-0.0071(9)	-0.0022(9)
S2	0.0515(12)	0.0430(12)	0.0420(11)	-0.0098(11)	-0.0024(9)	0.0051(10)
S3	0.0547(12)	0.0407(13)	0.0475(12)	-0.0054(10)	0.0120(10)	-0.0034(10)
S4	0.0413(11)	0.0397(12)	0.0535(12)	-0.0008(9)	0.0059(9)	-0.0093(10)
S5	0.0457(12)	0.0388(12)	0.0496(13)	0.0048(9)	-0.0042(10)	0.0083(10)
S6	0.0385(10)	0.0394(12)	0.0556(12)	-0.0022(10)	0.0009(9)	-0.0093(11)
C11	0.036(4)	0.036(5)	0.036(4)	-0.005(4)	-0.000(3)	-0.001(4)
C12	0.045(5)	0.048(5)	0.037(4)	-0.007(4)	-0.006(4)	0.000(4)
C13	0.049(5)	0.069(7)	0.041(5)	0.004(5)	-0.004(4)	0.004(5)
C14	0.054(5)	0.062(6)	0.039(5)	0.011(5)	-0.007(4)	0.008(5)
C15	0.053(5)	0.041(5)	0.046(5)	0.006(4)	0.002(4)	0.006(4)
C16	0.036(4)	0.049(5)	0.031(4)	0.006(4)	0.005(3)	-0.005(4)
C21	0.040(4)	0.066(6)	0.039(5)	0.006(5)	0.007(4)	-0.008(5)

Table 33 (continued)

ATOM	U ₁₁	U ₂₂	U ₃₃	U ₁₂	U ₁₃	U ₂₃
C22	0.063(6)	0.067(7)	0.058(6)	0.008(5)	0.011(5)	0.010(5)
C23	0.079(7)	0.111(9)	0.045(6)	0.022(7)	0.011(5)	0.005(6)
C24	0.081(7)	0.109(9)	0.041(6)	0.032(7)	-0.006(5)	-0.021(6)
C25	0.045(5)	0.076(7)	0.057(6)	0.014(5)	-0.011(4)	-0.025(5)
C26	0.040(4)	0.044(5)	0.046(5)	0.006(4)	0.000(4)	-0.007(4)
C31	0.038(4)	0.048(5)	0.034(4)	0.010(4)	-0.002(4)	0.001(4)
C32	0.061(6)	0.053(6)	0.063(6)	0.010(5)	-0.004(5)	0.011(5)
C33	0.061(6)	0.067(7)	0.064(6)	0.029(5)	0.010(5)	0.012(5)
C34	0.043(5)	0.086(7)	0.061(6)	0.020(5)	0.005(4)	0.019(6)
C35	0.040(5)	0.066(6)	0.040(5)	0.003(4)	-0.004(4)	0.007(4)
C36	0.045(5)	0.042(5)	0.034(4)	0.007(4)	-0.002(4)	0.002(4)

TABLE 34: INTRA-IONIC CONTACTS (Å)

ATOMS	DISTANCE	ATOMS	DISTANCE
Nb-S1	2.428 (2)	S2-S6	3.178 (3)
Nb-S2	2.442 (2)	S4-S6	3.294 (3)
Nb-S3	2.458 (2)	S1-C11	1.736 (7)
Nb-S4	2.433 (2)	S2-C16	1.740 (7)
Nb-S5	2.436 (2)	S3-C21	1.747 (7)
Nb-S6	2.451 (2)	S4-C26	1.760 (8)
As-C41	1.891 (4)	S5-C31	1.739 (7)
As-C51	1.883 (4)	S6-C36	1.750 (7)
As-C61	1.880 (4)	C11-C12	1.402 (9)
As-C71	1.896 (4)	C12-C13	1.356 (10)
S1-S2	3.143 (3)	C13-C14	1.398 (10)
S3-S4	3.160 (3)	C14-C15	1.374 (10)
S5-S6	3.147 (3)	C15-C16	1.392 (9)
S1-S3	3.204 (3)	C16-C17	1.424 (9)
S1-S5	3.282 (3)	C21-C22	1.410 (10)
S3-S5	3.184 (3)	C22-C23	1.396 (12)
S2-S4	3.245 (3)	C23-C24	1.349 (13)
C24-C25	1.374 (12)	C33-C34	1.383 (12)
C25-C26	1.422 (10)	C34-C35	1.382 (11)
C26-C21	1.385 (10)	C35-C36	1.395 (9)
C31-C32	1.419 (10)	C36-C31	1.375 (10)
C32-C33	1.363 (11)		

TABLE 35: INTRA-IONIC ANGLES (DEGREES)

ATOMS	ANGLES	ATOMS	ANGLES
S1-Nb-S2	80.40 (7)	Nb-S3-C21	105.5 (3)
S3-Nb-S4	80.47 (7)	Nb-S4-C26	105.4 (3)
S5-Nb-S6	80.18 (7)	Nb-S5-C31	106.1 (3)
S1-Nb-S5	84.87 (7)	Nb-S6-C36	106.0 (3)
S1-Nb-S3	81.94 (7)	S1-C11-C16	120.2 (6)
S3-Nb-S5	81.18 (7)	S2-C16-C61	119.0 (5)
S2-Nb-S4	83.46 (7)	S3-C21-C26	119.7 (6)
S2-Nb-S6	81.03 (7)	S4-C26-C21	121.1 (6)
S4-Nb-S6	84.81 (7)	S5-C31-C36	121.1 (6)
S1-Nb-S4	133.25 (7)	S6-C36-C31	119.9 (6)
S1-Nb-S6	134.51 (7)	C41-As-C51	110.6 (2)
S3-Nb-S2	136.61 (7)	C41-As-C61	107.1 (2)
S3-Nb-S6	136.50 (7)	C41-As-C71	109.0 (2)
S5-Nb-S2	135.63 (7)	C51-As-C61	109.6 (2)
S5-Nb-S4	133.86 (7)	C51-As-C71	105.9 (2)
Nb-S1-C11	106.5 (2)	C61-As-C71	114.6 (2)
Nb-S2-C16	106.1 (3)	C11-C12-C13	122.4 (7)
C12-C13-C14	119.5 (7)	C25-C26-C21	120.0 (8)
C13-C14-C15	120.0 (7)	C26-C21-C22	119.1 (8)
C14-C15-C16	121.2 (7)	C31-C32-C33	121.1 (8)
C15-C16-C11	120.0 (7)	C32-C33-C34	120.3 (8)
C16-C11-C12	117.8 (6)	C33-C34-C35	119.5 (8)

Table 35 (continued)

ATOMS	ANGLES	ATOMS	ANGLES
C21-C22-C23	119.6 (8)	C34-C35-C36	120.4 (8)
C22-C23-C24	120.5 (9)	C35-C36-C31	120.5 (7)
C23-C24-C25	121.8 (10)	C36-C31-C32	118.0 (7)
C24-C25-C26	119.9 (9)	S3-S1-S5	58.80 (6)
S6-S2-S4	61.69 (6)	S5-S3-S1	61.83 (6)
S2-S4-S6	58.16 (6)	S3-S5-S1	59.37 (6)
S2-S6-S4	60.15 (6)		

TABLE 36: INTER-IONIC CONTACTS (Å)

ATOM 1	ATOM 2	SYMMETRY OPERATION ON ATOM 2	DISTANCE
S1	H9	$\bar{x}+1, \bar{y}, \bar{z}$	2.942
S1	H20	$1/2-x, 1/2+y-1, 1/2-z$	2.942
S1	C54	$1/2+x, 1/2-y, 1/2+z-1$	3.409(6)
S1	S1	$\bar{x}+1, \bar{y}, \bar{z}$	3.607(4)
S1	C53	$1/2+x, 1/2-y, 1/2+z-1$	3.661(6)
S2	H17	$1/2+x, 1/2-y, 1/2+z-1$	2.913
S3	H15	$1/2-x, 1/2+y, 1/2-z$	2.855
S4	H3	$1/2-x+1, 1/2+y, 1/2-z$	2.901
S4	C44	$1/2-x, 1/2+y, 1/2-z$	3.523(5)
S4	C45	$1/2-x, 1/2+y, 1/2-z$	3.640(5)
S5	H25	$\bar{x}+1, y, \bar{z}+1$	3.048
S6	H29	$1/2+x, 1/2-y, 1/2+z$	2.908
S6	C33	$1/2-x+1, 1/2+y, 1/2-z$	3.549(9)
S6	C32	$1/2-x+1, 1/2+y, 1/2-z$	3.606(8)
S6	C73	$1/2+x, 1/2-y, 1/2+z$	3.680(5)
C35	C65	$1/2+x, 1/2-y, 1/2+z-1$	3.612(10)
C35	C66	$1/2+x, 1/2-y, 1/2+z-1$	3.688(9)
C34	H14	$\bar{x}+1, \bar{y}, \bar{z}$	3.038
C32	H21	$1/2+x, 1/2-y, 1/2+z-1$	2.811
C32	C55	$1/2+x, 1/2-y, 1/2+z-1$	3.682(9)
C31	H21	$1/2+x, 1/2-y, 1/2+z-1$	2.909
C31	C55	$1/2+x, 1/2-y, 1/2+z-1$	3.495(8)

Table 36 (continued)

ATOM 1	ATOM 2	SYMMETRY OPERATION ON ATOM 2	DISTANCE
C21	C44	$1/2-x, 1/2+y, 1/2-z$	3.638(9)
C23	H18	$1/2+x, 1/2-y, 1/2+z$	2.821
C23	C52	$1/2+x, 1/2-y, 1/2+z$	3.606(11)
C25	H28	$1/2+x, 1/2-y, 1/2+z$	2.942
C25	H8	$\bar{x}+1, \bar{y}+1, \bar{z}+1$	2.980
C25	C25	$\bar{x}+1, \bar{y}+1, \bar{z}+1$	3.517(17)
C26	H15	$1/2-x, 1/2+y, 1/2-z$	2.886
C26	C44	$1/2-x, 1/2+y, 1/2-z$	3.472(8)
C11	C53	$1/2+x, 1/2-y, 1/2+z-1$	3.400(9)
C12	H20	$1/2-x, 1/2+y-1, 1/2-z$	3.049
C12	C53	$1/2+x, 1/2-y, 1/2+z-1$	3.685(9)
C13	H6	$x, y, z-1$	2.996
C13	C75	x, y, z	3.549(10)
C13	H31	x, y, z	2.966
C15	H16	$1/2-x, 1/2+y, 1/2-z$	2.947
C12	C56	$1/2-x, 1/2+y-1, 1/2-z$	3.676(7)
C14	H32	$1/2-x, 1/2+y-1, 1/2-z$	2.811
C14	C76	$1/2-x, 1/2+y-1, 1/2-z$	3.609(7)
C45	H31	$1/2-x, 1/2+y-1, 1/2-z$	2.947
C45	H12	$1/2+x-1, 1/2-y, 1/2+z$	3.023
C45	C75	$1/2-x, 1/2+y-1, 1/2-z$	3.577(8)
C45	C76	$1/2-x, 1/2+y-1, 1/2-z$	3.699(7)
C53	C63	$1/2-x, 1/2+y, 1/2-z$	3.672(7)

Table 36 (continued)

A	ATOM 2	SYMMETRY OPERATION ON ATOM 2	DISTANCE
C54	H23	$1/2-x, 1/2+y, 1/2-z$	2.778
C54	C62	$1/2-x, 1/2+y, 1/2-z$	3.574 (7)
C55	H23	$1/2-x, 1/2+y, 1/2-z$	2.956
C64	C73	$1/2-x, 1/2+y-1, 1/2-z$	3.537 (8)
C65	H1	$1/2+x-1, 1/2-y, 1/2+z$	2.731
C65	C74	$1/2-x, 1/2+y-1, 1/2-z$	3.571 (8)
C66	H1	$1/2+x-1, 1/2-y, 1/2+z$	3.095
H9	H20	$1/2-x, 1/2+y-1, 1/2-z$	2.380

TABLE 37: LEAST SQUARES PLANE CALCULATIONS

(A) ATOMS FORMING PLANE: Nb, S1, S2

$$\begin{aligned} \text{EQUATION OF PLANE: } & -0.8413X + 0.3686Y + 0.3953Z \\ & + 9.1444 = 0.0^a \end{aligned}$$

(B) ATOMS FORMING PLANE: Nb, S3, S4

$$\begin{aligned} \text{EQUATION OF PLANE: } & 0.7683X - 0.2315Y + 0.5967Z \\ & - 11.0967 = 0.0 \end{aligned}$$

(C) ATOMS FORMING PLANE: Nb, S5, S6

$$\begin{aligned} \text{EQUATION OF PLANE: } & -0.0706X + 0.1393Y + 0.9877Z \\ & - 1.9792 = 0.0 \end{aligned}$$

(D) ATOMS FORMING PLANE: S1, S2, C11, C12, C13, C14
C15, C16

$$\begin{aligned} \text{EQUATION OF PLANE: } & -0.6239X + 0.3044Y + 0.7198Z \\ & + 6.3172 = 0.0 \end{aligned}$$

DISTANCES OF ATOMS FROM PLANE (Å):

S1	-0.001 (2)	S2	0.009 (2)
C11	-0.048 (7)	C12	0.041 (7)
C13	0.078 (8)	C14	0.010 (8)
C15	-0.071 (8)	C16	-0.086 (7)
Nb	-0.7144 (6)		

(E) ATOMS FORMING PLANE: S3, S4, C21, C22, C23, C24,
C25, C26

Table 37 (continued)

$$\text{EQUATION OF PLANE: } 0.9191X - 0.3096Y + 0.2438Z \\ - 11.2653 = 0.0$$

DISTANCES OF ATOMS FROM PLANE (Å):

S3	0.004(2)	S4	0.004(2)
C21	-0.090(7)	C22	-0.012(9)
C23	-0.067(9)	C24	0.060(9)
C25	-0.023(8)	C26	-0.067(7)
Nb	-0.7099(6)		

(F) ATOMS FORMING PLANE: S5, S6, C31, C32, C33, C34,
C35, C36.

$$\text{EQUATION OF PLANE: } 0.2788X + 0.0011Y + 0.9603Z \\ - 6.8577 = 0.0$$

DISTANCES OF ATOMS FROM PLANE (Å):

S5	-0.006(2)	S6	0.001(2)
C31	0.036(7)	C32	-0.042(8)
C33	-0.052(9)	C34	-0.004(9)
C35	0.057(8)	C36	0.055(7)
Nb	0.6869(6)		

(G) ATOMS FORMING PLANE: S1, S3, S5

$$\text{EQUATION OF PLANE: } -0.3396X - 0.9393Y + 0.0484Z \\ + 5.3688 = 0.0$$

DISTANCES OF ATOMS FROM PLANE (Å):

Nb	1.5787(6)
----	-----------

(H) ATOMS FORMING PLANE: S2, S4, S6

Table 37 (continued)

$$\begin{aligned} \text{EQUATION OF PLANE: } & -0.3423X - 0.9380Y + 0.0545Z \\ & + 8.5348 = 0.0 \end{aligned}$$

DISTANCES OF ATOMS FROM PLANE (Å):

Nb \rightarrow -1.5699(6)

^aX, Y and Z are in Å and refer to the orthogonal coordinates along a, b, c^{*}.

TABLE 38: DIHEDRAL ANGLES BETWEEN SELECTED PLANES

ATOMS IN PLANE 1	ATOMS IN PLANE 2	ANGLE
Nb, S1, S2	Nb, S3, S4	119.7°
Nb, S1, S2	Nb, S5, S6	120.1°
Nb, S3, S4	Nb, S5, S6	120.2°
Nb, S1, S2	S1, S2, C11, C12, C13, C14, C15, C16	22.8°
Nb, S3, S4	S3, S4, C21, C22, C23, C24, C25, C26	22.6°
Nb, S5, S6	S5, S6, C31, C32, C33, C34, C35, C36	21.8°
S1, S3, S5	S2, S4, S6	0.6°

DESCRIPTION OF STRUCTURE

The portion of the molecule of major interest, i.e. the $\text{Nb}(\text{bd}t)_3^-$ anion, is shown in the three dimensional representation in Fig. 14. The metal is surrounded approximately equidistantly by six sulfur atoms in the form of a trigonal prism, thus it has approximate C_{3h} symmetry. The dithiolene ligands radiate from the metal in a "paddle-wheel" arrangement as was the case for $\text{Mo}(\text{bd}t)_3$ and the other trigonal prismatic dithiolenes.^{129,130,132} The prism is not however as regular as that in $\text{Mo}(\text{bd}t)_3$, with a significant range in niobium-sulfur distances from 2.428(2) Å to 2.458(2) Å. The mean Nb-S distance (2.441 Å) is also significantly longer than the Mo-S distance (2.367 Å) in $\text{Mo}(\text{bd}t)_3$ and thus is the longest metal-sulfur distance observed in any of the trigonal prismatic molecules (Table 48).

It is interesting that in the previous trigonal prismatic structures the metal-sulfur bond lengths had been amazingly constant, considering that the covalent and ionic radii¹³³ of vanadium differed, by approximately 0.07 Å, from those of molybdenum and rhenium. $\text{Nb}(\text{bd}t)_3^-$ is therefore the first example of a prism in which this is no longer true; the Nb-S distance being approximately 0.11 Å longer than

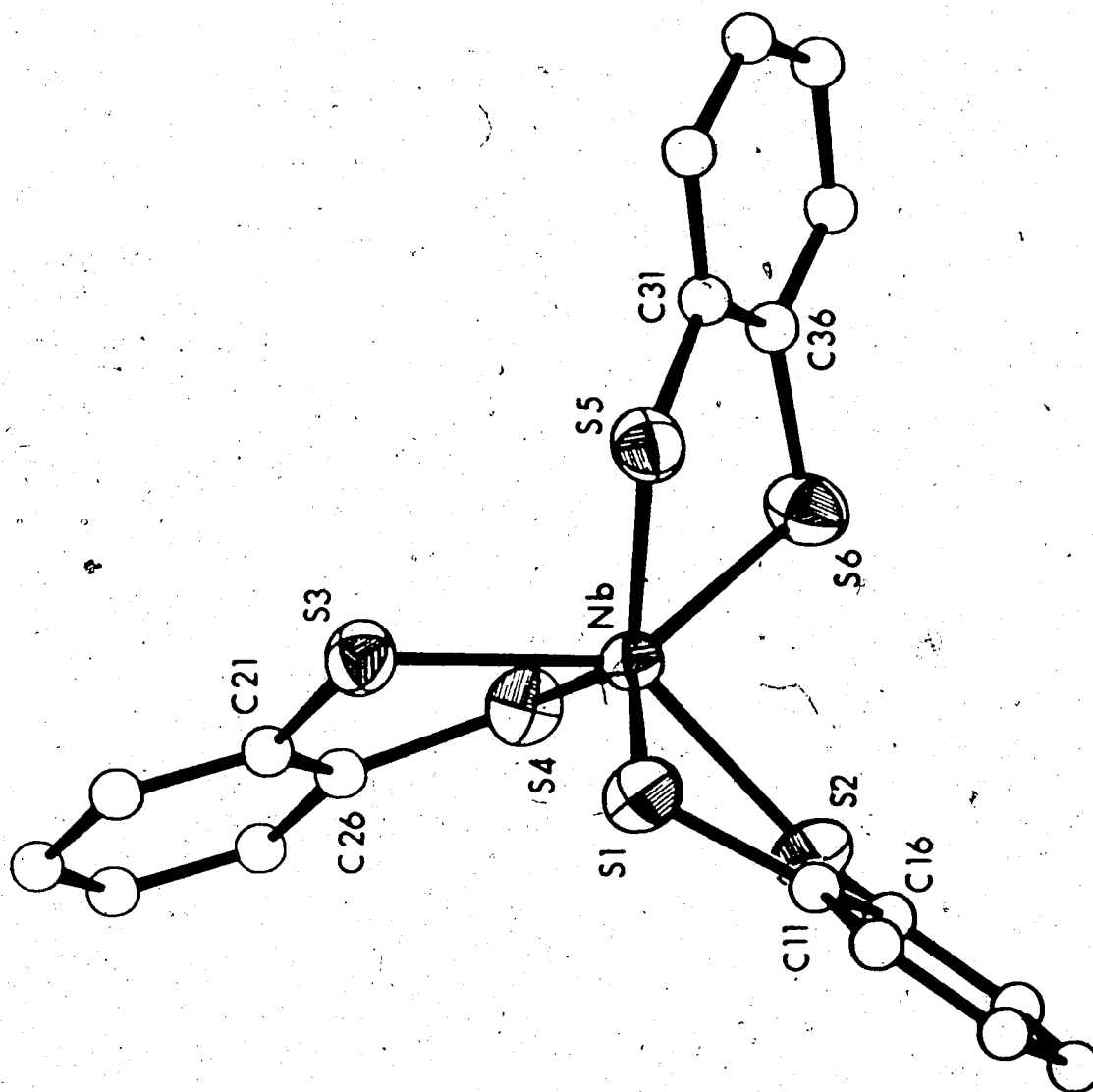


Fig. 14: A PERSPECTIVE VIEW OF THE $\text{Nb}(\text{S}_2\text{C}_6\text{H}_4)_3^-$ ANION.

the metal-sulfur distances in the three other prisms and also 0.074 \AA longer than in $\text{Mo}(\text{bd}t)_3$ (to which this comparison is most useful). The increase in metal-sulfur distances progressing from the molybdenum to the niobium complex is approximately consistent with the corresponding increase in the metal covalent radii.¹³³ Although the values for the metal covalent radii are ambiguous (especially for $\text{Nb}(\text{bd}t)_3^-$ since the extra electron will expand the niobium orbitals increasing its radius from that of the neutral species), a very rough comparison is obtained using Pauling's values. This yields a predicted increase in metal-sulfur bonds of about 0.05 \AA when calculated using the neutral atom radii.

The constancies of the metal-sulfur distances in the previous trigonal prisms, in spite of differing metal radii, had been attributed as a consequence of proposed interligand S-S bonding.¹²⁴ Thus the difference in Nb-S distances compared with Mo-S distances tends to indicate a possible breakdown in S-S bonding and an expected increase in S-S distances. Because of the relatively fixed ligand bite this should manifest itself in longer interligand S-S distances compared to intraligand S-S distances. This is in fact what is observed with the

mean interligand S-S distance (3.231 Å) being significantly longer than the intraligand S-S distance (3.150 Å). Here again slight distortions are obvious with a range in interligand S-S distances from 3.178(3) Å to 3.294(3) Å.

The sulfur-carbon distances (1.745 Å), although similar to the other *tris* dithiolenes, are longer than any observed previously and more significantly are longer than those in Mo(bdt)₃ (1.727 Å) where the same ligand is involved. Thus the sulfur-carbon bonds have less double bond character in the niobium complex and the ligands are therefore more dithiolate and less dithioketonic in character than for Mo(bdt)₃. The mean carbon-carbon distance within the ligands is again consistent with those observed in benzene¹⁵⁸ and in several disubstituted benzene derivatives,¹⁵⁹ as mentioned in Chapter VI. Again, as was the case for Mo(bdt)₃, there is a wide range in C-C distances (Fig. 15). From the diagram showing the average C-C bond lengths one sees that the C2-C3, C3-C4, and C4-C5 distances are significantly shorter than the other three. This may be interpreted as indicating some contribution from the dithioketonic formulation but this simple interpretation should not be made in the absence of a full analysis of the thermal

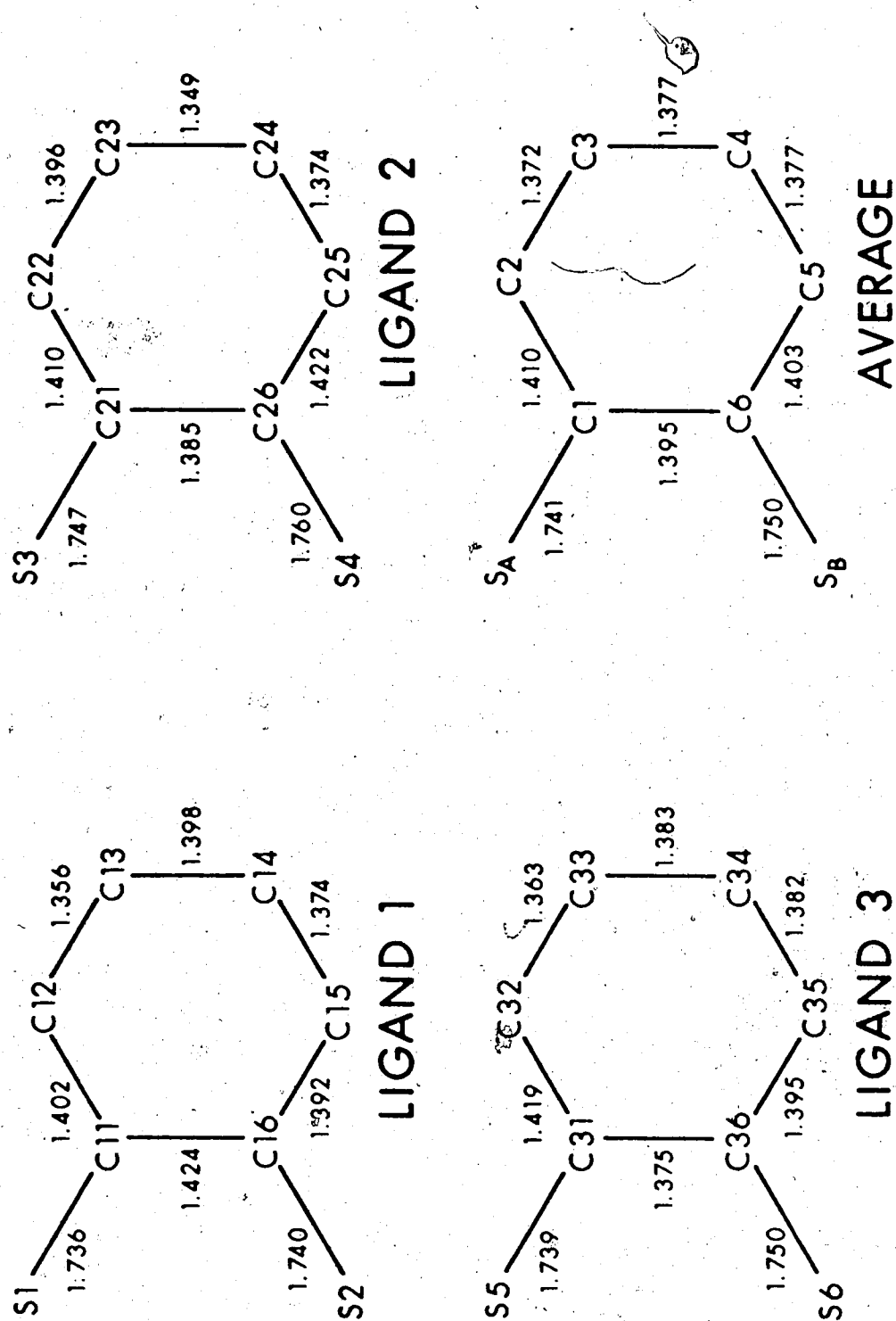


Fig. 15: DIMENSIONS WITHIN THE DITHIOLENE LIGANDS.

parameters and an assessment of their effect on the observed uncorrected bond distances.

The intra- and interligand S-Nb-S angles average 80.35° and 82.88° respectively and are therefore an indication of the slight distortion from trigonal prismatic coordination. Possibly a more significant indication of the distortion, however, is the *range* in the interligand S-Nb-S angles, from $84.87(7)^\circ$ to $81.03(7)^\circ$. The S-Nb-S angles, involving sulfur atoms approximately *trans* to each other, average 135.06° and is again similar to the value of $136(1)^\circ$ found in the other prisms.

The two triangular faces of the prism deviate slightly from being parallel, the angle between their normals being 0.6° . In addition the angles between the NbS₂ planes, as shown in Table 38, are all close to the expected 120° . The Nb-S-C angles average 105.9° and are all in close agreement with each other.

The S-C-C angles ($S_A-C_1-C_6$ and $S_B-C_6-C_1$ in Fig. 15) average 120.1° and are close to the expected value of 120° . This good internal agreement of the Nb-S-C and S-C-C angles adds further proof that the deviations in the interligand S-Nb-S angles are indeed significant.

As was observed in Mo(bdt)₃, Mo(S₂C₂H₂)₃,¹³⁰

and $\text{Mo}[\text{Se}_2\text{C}_2(\text{CF}_3)_2]_3$,¹⁵² the ligand planes again deviate considerably from the corresponding MS_2 planes. These deviations are more regular in $\text{Nb}(\text{bdt})_3^-$ than in $\text{Mo}(\text{bdt})_3$ (see Table 49). Their mean values, 22.4° and 21.4° , respectively are however in good agreement and both are larger than the values of 18° and 18.6° observed in $\text{Mo}(\text{S}_2\text{C}_2\text{H}_2)_3$ and $\text{Mo}[\text{Se}_2\text{C}_2(\text{CF}_3)_2]_3$ respectively. That these dihedral angles are irregular in $\text{Mo}(\text{bdt})_3$ yet regular in $\text{Nb}(\text{bdt})_3^-$ is probably a consequence of packing forces. The flexibility, afforded by the rotational freedom of the phenyl groups of the tetraphenylarsonium cation, allows effective packing without major deformation of the ligand planes. It is probable then that the structure, observed in the crystal, closely approximates the structure in solution. It is interesting that this bend of the ligand plane from the MS_2 plane has been observed in the trigonal prismatic molybdenum dithiolenes and also in the molybdenum diselenato complex, and now has been observed in $\text{Nb}(\text{bdt})_3^-$, which is isoelectronic with the molybdenum analogue. In contrast, the ligand planes were found to be coplanar with the MS_2 planes in both $\text{Re}(\text{S}_2\text{C}_2\text{Ph}_2)_3$ ¹²⁹ and $\text{V}(\text{S}_2\text{C}_2\text{Ph}_2)_3$.¹³²

A three dimensional representation of the

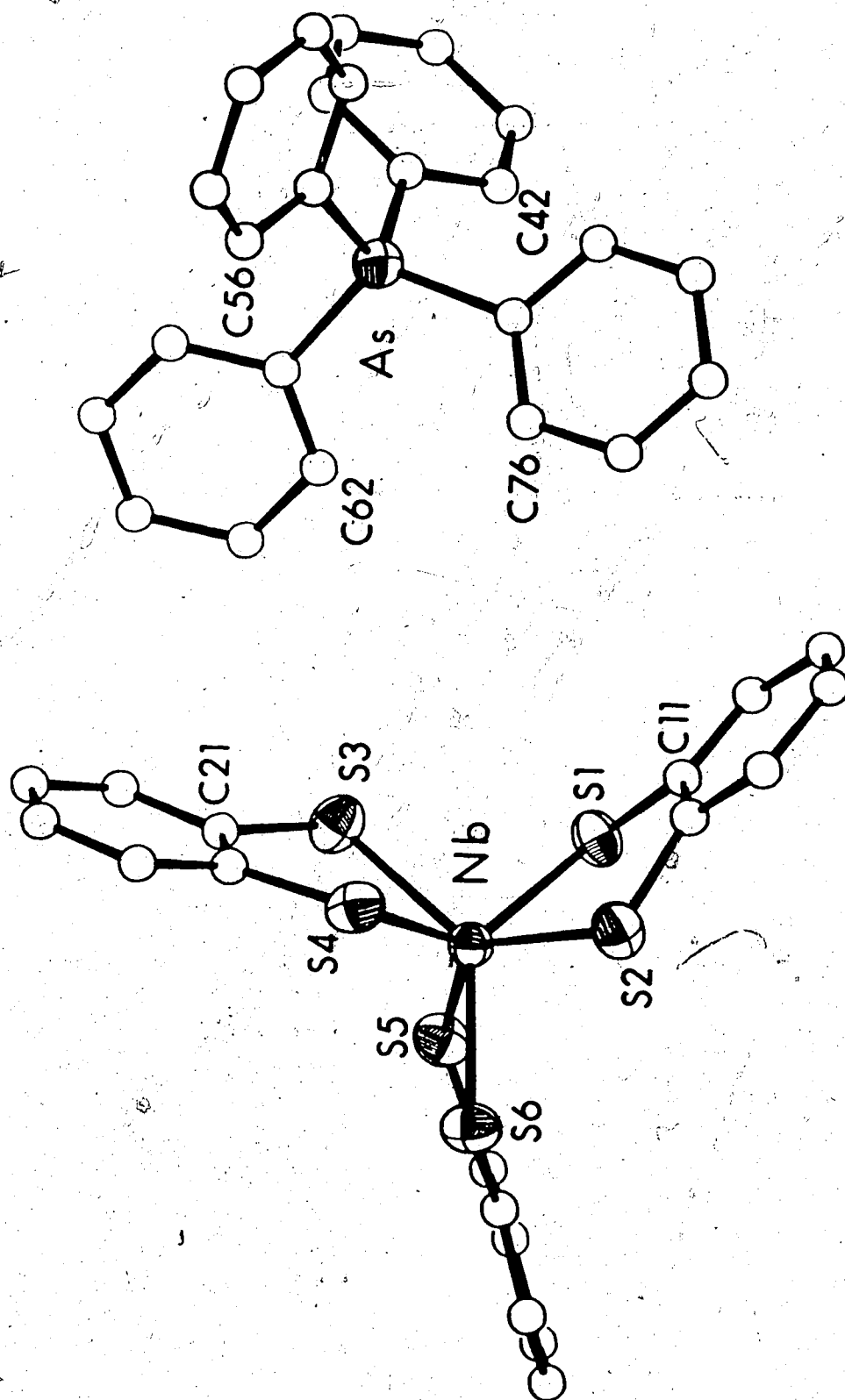


Fig. 16: A PERSPECTIVE VIEW OF $[\text{As}(\text{C}_6\text{H}_5)_4][\text{Nb}(\text{S}_2\text{C}_6\text{H}_4)_3]$,
VIEWED DOWN THE CRYSTALLOGRAPHIC b AXIS.

$\text{Nb}(\text{bdt})_3^-$ anion and the tetraphenylarsonium cation, viewed down the crystallographic b axis, is shown in Fig. 16. The geometry of the cation is quite normal with no unusual features. The arsenic atom is surrounded in almost perfect tetrahedral coordination with the C-As-C angles being close to the predicted 109.5° , and all deviations from this value are easily explained by intermolecular interactions. The arsenic-carbon bonds are similar and the mean (1.888 \AA) approximates the value predicted from the sums of the covalent radii^{133,162} (1.94 \AA), assuming an arsenic-carbon single bond involving sp^2 hybridized carbon atoms. These observed bond lengths agree favourably with other determinations^{163,164} where the tetraphenylarsonium cation was involved.

CHAPTER VIII: THE CRYSTAL AND MOLECULAR STRUCTURE
OF *BIS* (TETRAMETHYLAMMONIUM) *TRIS*
(BENZENE-1,2-DITHIOLATO) ZIRCONIUM,
 $[(\text{CH}_3)_4\text{N}]_2[\text{Zr}(\text{S}_2\text{C}_6\text{H}_4)_3]$.

EXPERIMENTAL

Bright red crystals of $[(\text{CH}_3)_4\text{N}]_2[\text{Zr}(\text{bdt})_3]$, suitable for single crystal X-ray diffraction studies, were kindly supplied by Dr. Takats and Mr. Martin. These crystals were prepared¹⁴³ by the reaction of sodium cyclopentadienide and benzene dithiol and the subsequent reaction with $\text{Zr}[\text{N}(\text{C}_2\text{H}_5)_2]_4$, and crystallization with tetramethylammonium chloride. Preliminary photography showed *mmm* Laue symmetry indicating an orthorhombic space group. Systematic absences determined by Weissenberg ($0k\ell$, $1k\ell$; CuK_α X-radiation) and Precession photography ($h0\ell$, $h1\ell$, $hk0$, hkl ; MoK_α X-radiation) are $h00$: $h = 2n + 1$, and $0k0$: $k = 2n + 1$ consistent with the space group $P2_12_12$. Precise lattice parameters were obtained at 22° from a least squares analysis performed on the setting angles of 12 high angle reflections, accurately centred on a Picker automatic four circle diffractometer, using CuK_α X-radiation. The resulting

cell parameters and estimated standard deviations are: $a = 9.931(2) \text{ \AA}$, $b = 14.368(2) \text{ \AA}$, $c = 11.098(2) \text{ \AA}$. The observed density [$1.38(2) \text{ g cm}^{-3}$], obtained by floatation in a mixture of chloro- and bromo-benzene is consistent with the theoretical value of 1.381 g cm^{-3} , calculated assuming two molecules with formula weight 660.19 a.m.u. occupy the unit cell of volume 1587.9 \AA^3 . Since the space group $P2_12_12$ has four general equivalent positions, the $\text{Zr}(\text{bdt})_3^{2-}$ dianion is therefore restricted to having 2-fold symmetry and must sit on the crystallographic 2-fold axis. The two tetramethylammonium cations can either be related by the two-fold or sit on the two-fold axis.

Intensity data were collected on the Picker automatic diffractometer using CuK_α X-radiation filtered with a 0.0005" thick nickel foil and using a 2° take-off angle. The crystal was mounted in a general orientation but with the a^* axis approximately coincident with the ϕ axis of the diffractometer. A coupled $2\theta/\omega$ scan technique, with a scan speed of 1° min^{-1} , was employed for data collection with all unique reflections with $2\theta \leq 125^\circ$ being collected. The two theta scan range for each reflection was $2^\circ + \Delta 2\theta$ where $\Delta 2\theta$ corresponded to $[2\theta(K_{\alpha_1}) - 2\theta(K_{\alpha_2})]$.

Forty second stationary background counts on each side of the peak were recorded and assuming linearity of background, intensities and standard deviations in the intensities were calculated as shown in Chapter II using a "p factor" of 0.03. A scintillation counter was used in conjunction with a pulse height analyzer, tuned to accept 95% of the CuK_α peak. Three standard reflections were collected automatically every 100 data reflections. In addition several additional reflections were collected manually to assess decomposition. No significant decomposition was observed so no correction was necessary.

Of the 1403 unique reflections collected, 1054 were significantly above background using the criterion $I/\sigma(I) \geq 3.0$. The significant data were then reduced to structure factor amplitudes by correction for Lorentz, polarization and absorption effects. Standard deviations in the structure factors were again calculated as in Chapter II.

The crystal faces were identified and their perpendicular distances to an arbitrarily chosen origin measured as: $(0,1,0)$, 3.268×10^{-3} cm; $(0,\bar{1},0)$, 10.836×10^{-3} cm; $(\bar{1},0,0)$, 20.640×10^{-3} cm; $(0,0,1)$, 3.09×10^{-3} cm; $(1,1,0)$, 0.0 cm; $(1,\bar{1},0)$, 0.0 cm; and $(1,0,\bar{1}2)$, 0.0 cm. The face $(1,0,\bar{1}2)$ is acknow-

ledged as a very unusual choice, but its position is most consistent with the indices chosen, since it is opposite to the (0,0,1) face but inclined to it by about 5°. The absorption coefficient⁸⁶ for CuK_α X-radiation is 66.63 cm^{-1} , leading to a range in transmission factors from 0.756 to 0.423.

In the original data collection several irregularities were observed. These appeared as "pulses" in the counter and their exact cause was unknown, but was probably due to some electronic device connected to the diffractometer power line. The reflections where this was actually observed were rejected. However it was believed (on the basis that several $|F_o|$ values were extremely high) that these pulses had occurred throughout the data collection. For this reason the $hk\ell$ data were recollected along with the $h\bar{k}\ell$ data so all three data sets could be compared and faulty reflections could be excluded. The second $hk\ell$ data set was merged with the $h\bar{k}\ell$ data to obtain improved standard deviations. In this merged data set the number of statistically reliable reflections increased to 1126. The same data collection techniques were used for the second $hk\ell$ data and the $h\bar{k}\ell$ data as was used for the original $hk\ell$ data. Terms used in the Zachariasen extinction correction were calculated at this stage.

STRUCTURE SOLUTION AND REFINEMENT

A sharpened Patterson map¹⁴⁶ was computed between the limits $0 \leq u \leq 0.5$, $0 \leq v \leq 0.5$, $0 \leq w \leq 0.5$. Since the zirconium atom is restricted to lie on the two-fold axis, the Harker vectors are located at $1/2, 1/2, 2z$; and $1/2, 1/2, -2z$, so the solution is trivial yielding the coordinates for the zirconium as $(0.0, 0.0, 0.189)$ from the largest vector at $(0.5, 0.5, 0.378)$. The next six most intense vectors could be interpreted as Zr-S vectors about either the origin or the Zr-Zr Harker vector. From initial inspection of the placement of these vectors, it was evident that the zirconium coordination was close to octahedral and was definitely not trigonal prismatic. Due to the extra symmetry of the Patterson, care had to be taken in choosing the vectors to represent the three independent sulfur atoms, in order for the model to phase correctly. Several arbitrary choices can be made initially. The S1 position was calculated from the vector at $(0.05, 0.168, 0.0)$ yielding the coordinates $(0.05, 0.168, 0.189)$. From the vector at $(0.16, 0.0, 0.18)$ the S2 position was calculated as $(0.16, 0.0, 0.009)$. The position of S3, however, must be chosen in such a way to be consistent with the choice of S1 and S2. There are two

possible choices for the S3 position yielding the positions (0.185, -0.048, 0.315) or (0.185, 0.048, 0.315). A choice between the two was made on the basis of sulfur-sulfur vectors which showed the first position was correct.

In the first refinements, involving only the zirconium and sulfur positions, the y coordinate of S2 was not refined, since it was possible that it could refine in the wrong direction and hamper the phasing. A brief resumé of the refinement is shown in Table 39.

TABLE 39: REFINEMENT OUTLINE

MODEL	R_1	R_2
(1) Zr and S atoms	0.297	0.384
(2) Complete anion (isotropic B's)	0.152	0.243
(3) Anion and Cation (isotropic B's)	0.088	0.106
(4) Anisotropic Zr and S	0.074	0.097
(5) Anisotropic Zr, S, N and C atoms of tetramethyl ammonium	0.069	0.088
(6) Absorption Correction	0.050	0.063
(7) Change of Hand	0.057	0.073
(8) Carbon atoms of dithiolene ligands anisotropic	0.042	0.061
(9) Hydrogen atoms of dithiolene ligands	0.039	0.059
(10) Extinction correction ¹⁴⁷	0.039	0.059
(11) Merged Data	0.034	0.053
(12) Methyl Hydrogens included as rotors	0.029	0.035

Structure factors were calculated using the atomic scattering factors for the neutral atoms for zirconium, sulfur, carbon and nitrogen by Cromer and Mann.⁷⁵ The scattering factors for hydrogen were those of Stewart, Davidson and Simpson.¹⁴⁹ Anomalous dispersion corrections by Cromer⁷⁶ were applied to the zirconium and sulfur scattering factors ($\Delta f'_{\text{Zr}} = -0.62$, $\Delta f''_{\text{Zr}} = 2.42$, $\Delta f'_S = 0.31$, $\Delta f''_S = 0.58$).

A refinement was performed with a change of hand for model (6) and the original model was judged significantly better on the basis of a Hamilton's R test⁷⁹ (at the 0.005 significance level). Hydrogen positions on the dithiolene ligands were calculated from the known geometry and orientation of the benzene rings, using a C-H distance of 1.0 Å. The hydrogen parameters were not refined. The hydrogen atoms were given thermal parameters approximately 10 - 15% greater than their attached carbon atom. An electron density difference map, phased on model (11), failed to locate any of the methyl hydrogen atoms, instead only smears of electron density were observed in the predicted regions. In addition the tetramethylammonium carbon atoms had anomalous thermal parameters, so the difference map was inspected for obvious signs of

disorder involving these carbon atoms. No signs of disorder, however, were obvious. Although the methyl hydrogens were not located, they were added to the structure factor calculations in the form of free rotating rigid bodies.¹⁶⁵ The ideal tetrahedral coordination of the carbon atoms was assumed and the centres of gravity and angles defining the orientation of "hydrogen triangles" were calculated using the assumed geometry, and the direction cosines of the nitrogen-carbon bonds.

Model (11), which is the refinement of the merged data, contains all the corrections performed on the previous models.

RESULTS

Observed and calculated structure factor amplitudes, $|F_o|$ and $|F_c|$, are shown in Table 40. The final fractional coordinates and isotropic temperature factors of all atoms are shown in Table 41. Standard deviations were obtained from the inverse matrix of the final least squares analysis. Table 42 shows the anisotropic thermal parameters (U_{ij} 's)⁸⁰ of all anisotropic atoms. Relevant bond lengths and angles are shown in Tables 43 and 44, and were obtained with

their standard deviations from ORFFE. Several inter-ionic contacts which are comparable to the predicted van der Waals contacts¹⁵¹ are shown in Table 45. Selected least squares planes are shown in Table 46. In addition Table 47 lists the dihedral angles between selected planes.

The numbering scheme for all non-hydrogen atoms is shown in Figures 17 and 18. The hydrogen atoms H1 through H6 are attached sequentially to the carbon atoms (C2 through C9) which are not bonded to sulfur atoms. The hydrogen atoms H7 through H18 are bonded sequentially in groups of three to carbon atoms C10 through C13. Since the hydrogen atoms of the methyl groups were included as hindered rotors, no individual temperature factors are given, rather the temperature factors for the groups are shown in Table 41.

TABLE 40: OBSERVED AND CALCULATED STRUCTURE

AMPLITUDES (ELECTRONS X 10)

K	L	F005	FCAL	K	L	F005	FCAL	K	L	F005	FCAL	K	L	F005	FCAL	K	L	F005	FCAL
C	1	567	575	7	1	148	148	L	1	538	514	7	6	262	256	1	6	414	421
C	2	797	721	7	2	495	493	1	2	962	955	7	7	151	150	1	7	150	145
0	3	114	111	7	3	312	307	1	3	533	537	7	8	159	140	1	9	399	393
0	4	217	214	7	4	427	429	1	5	635	628	7	10	183	195	1	10	259	255
0	5	784	806	7	5	177	167	1	6	566	562	7	11	165	165	1	11	186	175
0	6	967	1008	7	6	569	570	1	7	343	358	8	1	174	174	1	12	113	110
0	7	402	407	7	7	216	216	1	8	264	254	8	2	100	100	2	0	93	31
0	8	106	167	7	8	135	144	1	9	205	204	8	3	157	157	2	1	236	228
0	9	554	545	7	9	137	148	1	10	265	262	8	4	381	381	2	2	260	256
0	10	190	169	7	10	167	185	1	11	164	168	8	5	148	148	2	3	1075	1047
0	11	117	106	8	0	388	381	2	1	314	265	8	6	146	146	2	4	393	390
1	1	1146	1184	8	1	632	642	2	2	939	936	8	7	261	261	2	5	374	384
1	2	345	319	8	2	204	204	2	3	399	400	8	8	193	209	2	7	138	147
1	3	400	402	8	3	197	198	2	4	581	595	8	9	206	214	2	8	290	278
1	4	216	225	8	4	419	417	2	5	246	259	8	10	163	166	2	9	271	272
1	5	167	167	8	5	147	132	2	6	265	261	9	0	343	344	2	10	165	172
1	6	718	727	8	6	191	179	2	7	408	417	9	1	207	214	2	11	271	250
1	7	712	709	8	7	202	202	2	8	222	228	9	2	107	114	3	0	146	152
1	9	201	214	9	1	106	107	2	9	192	197	9	3	143	153	3	1	258	263
1	11	178	164	9	2	285	291	2	10	213	203	9	4	248	245	3	2	158	163
1	12	240	239	9	3	256	256	2	11	106	108	9	5	141	154	3	3	601	604
2	0	420	427	9	4	317	304	2	12	234	234	9	6	114	124	3	4	151	150
2	1	726	686	9	5	231	242	3	0	1585	1617	10	1	137	135	3	5	205	190
2	2	296	311	9	6	144	138	3	1	542	532	10	2	224	223	3	6	192	178
2	3	658	671	9	7	144	155	3	2	240	242	10	3	167	160	3	7	94	88
2	4	266	279	10	0	414	397	3	3	278	261	10	4	233	222	3	8	306	307
2	5	680	657	10	1	337	331	3	4	330	325	10	5	243	227	3	9	391	389
2	6	589	582	10	2	347	345	3	5	523	526	10	6	218	215	3	10	165	177
2	8	217	211	10	3	151	128	3	6	145	143	10	7	108	112	3	11	118	60
2	9	188	181	10	4	305	300	3	7	173	150	10	8	149	155	4	0	477	479
2	10	223	209	10	5	214	213	3	8	83	99	11	0	441	444	4	1	515	520
2	11	223	222	11	0	156	143	3	9	248	249	11	1	265	262	4	2	595	614
2	12	158	143	11	1	357	405	3	10	98	88	11	2	205	202	4	3	471	465
3	1	376	377	11	2	166	156	4	0	335	319	11	3	335	335	4	4	168	164
3	2	154	111	11	3	478	469	4	1	271	280	11	4	177	173	4	5	209	212
3	3	221	233	11	4	144	141	4	2	307	292	11	5	409	396	4	6	141	150
3	5	235	253	11	5	261	268	4	3	387	403	11	6	111	100	4	7	379	381
3	6	214	218	11	6	94	112	4	4	210	198	11	7	119	122	4	8	174	162
3	7	662	675	11	7	96	98	4	5	151	149	12	0	143	160	4	9	179	162
3	8	214	210	11	8	147	167	4	6	445	440	12	1	262	279	4	10	183	177
3	9	221	213	12	0	395	390	4	7	521	517	12	2	258	266	4	11	177	181
3	10	174	169	12	1	279	295	4	8	154	141	12	3	189	202	5	0	125	130
3	12	300	309	12	2	163	164	4	9	279	279	12	4	355	353	5	1	554	564
4	0	1678	1630	12	3	287	281	4	10	151	156	12	5	278	275	5	2	635	630
4	1	754	734	12	4	159	160	4	11	130	150	12	6	132	139	5	3	491	487
4	2	213	208	12	5	397	393	4	12	209	218	13	0	328	332	5	4	645	642
4	3	178	188	12	6	85	95	5	0	1368	1371	13	1	169	167	5	5	217	210
4	4	131	126	13	0	106	107	5	1	613	615	13	2	152	149	5	6	295	303
4	5	253	262	13	1	128	124	5	2	580	561	13	3	176	169	5	7	323	312
4	6	734	736	13	2	97	107	5	3	379	370	13	4	171	171	5	8	168	172
4	8	160	157	13	3	183	173	5	4	383	378	13	5	111	128	5	9	391	387
4	9	142	147	13	4	192	206	5	5	692	692	13	6	121	119	5	10	136	137
4	10	186	199	13	5	121	121	5	6	299	310	14	0	97	111	5	11	125	138
4	11	159	170	14	0	180	184	5	7	263	265	14	1	90	73	6	0	764	785
4	12	79	83	14	1	128	122	5	8	320	333	15	0	73	77	6	1	266	269
5	1	566	500	14	2	112	101	5	9	135	150	16	0	73	77	6	2	799	806
5	2	426	432	14	3	90	113	5	10	311	303	16	1	84	82	6	3	551	541
5	3	177	185	14	4	84	103	5	11	162	160	0	2	1160	1162	6	4	175	174
5	4	587	576	15	0	132	118	6	0	293	287	0	3	919	978	6	5	382	378
5	6	381	386	15	1	96	91	6	1	743	725	0	4	1375	1394	6	6	179	179
5	7	487	485	16	0	181	179	6	2	478	467	0	5	783	793	6	7	333	332
5	8	88	67	16	1	93	108	6	3	351	335	0	6	139	147	6	8	307	311
5	9	263	255	0	2	100	101	6	4	738	740	0	7	620	631	6	9	162	157
5	11	216	218	0	3	682	709	6	5	163	160	0	8	101	63	6	10	129	134
6	0	1670	1703	0	4	659	672	6	6	567	581	0	9	287	288	7	1	528	520
6	1	373	380	0	5	514	534	6	7	322	339	0	10	349	336	7	2	180	177
6	2	343	351	0	6	623	610	6	8	192	198	0	11	239	230	7	3	372	370
6	3	286	270	0	7	115	94	6	9	282	288	0	12	105	90	7	4	581	572
6	4	429	430	0	8	808	794	6	10	154	149	0	13	124	127	7	5	220	214
6	5	865	846	0	9	643	625	6	11	182	196	1	0	385	369	7	6	352	344
6	6	298	305	0	10	282	281	7	0	671	677	1	1	676	675	7	7	238	235
6	7	244	241	0	11	397	404	7	1	443	435	1	2	972	967	7	8	264	261
6	9	202	192	0	12	192	190	7	2	432	441	1	3	767	765	7	9	180	173
6	10	269	266	0	13	206	208	7	3	503	503	1	4	1042	1060	8	0	345	340
6	11	168	171	1	0	1585	1547	7	4	171	173	1	5	269	267	8	1	107	110
								7	5	500	490					8	2	229	226

Table 40 (continued)

K	L	F085	FCAL	K	L	F085	FCAL	K	L	F085	FCAL	K	L	F085	FCAL				
20000																			
8	3	261	258	1	9	289	282	8	8	131	115	2	6	288	284	9	9	99	127
8	4	163	173	1	10	202	202	8	9	217	215	2	7	203	199	10	0	303	315
8	5	199	191	2	0	535	533	8	10	131	146	2	8	444	442	10	1	180	199
8	6	225	211	2	1	124	114	9	0	223	228	2	9	186	190	10	2	174	180
8	7	127	138	2	2	594	592	9	1	182	177	2	10	162	157	10	3	382	382
8	8	252	259	2	3	355	326	9	2	377	380	2	11	125	129	10	4	139	134
8	9	112	92	2	4	889	887	9	3	92	77	3	0	410	400	10	5	127	130
8	10	84	90	2	5	247	234	9	4	352	349	3	1	372	368	10	6	183	182
9	1	316	387	2	6	164	155	9	5	213	212	3	2	267	263	10	7	103	98
9	2	92	98	2	7	137	151	9	6	187	191	3	3	446	434	10	8	189	190
9	3	110	121	2	8	367	363	9	7	242	238	3	4	358	362	11	0	181	177
9	4	299	297	2	9	344	339	9	8	100	82	3	5	276	282	11	1	217	215
9	5	133	131	2	10	88	96	10	0	153	148	3	6	342	343	11	2	205	204
9	6	259	254	3	1	131	138	10	1	369	371	3	7	189	191	11	3	135	140
9	7	91	109	3	2	548	565	10	2	170	158	3	8	136	123	11	4	226	226
9	8	186	187	3	3	718	711	10	3	153	154	3	9	280	280	11	5	131	140
9	9	117	127	3	4	540	526	10	4	179	182	3	10	211	199	11	6	55	142
10	0	386	381	3	5	240	240	10	5	136	160	3	11	90	87	11	7	109	112
10	1	155	147	3	6	171	169	10	6	213	188	4	0	130	119	12	2	214	216
10	2	375	370	3	7	471	469	10	7	214	211	4	1	306	297	12	3	183	178
10	3	220	223	3	8	244	242	10	8	148	160	4	2	460	473	12	4	172	162
10	4	293	292	3	9	365	359	10	9	192	192	4	3	550	554	12	5	109	108
10	5	122	112	3	10	88	92	11	0	296	288	4	4	376	386	12	6	162	170
10	6	233	236	3	11	189	188	11	1	128	120	4	5	297	289	12	7	151	154
10	7	140	129	4	0	115	126	11	2	357	354	4	6	286	291	12	8	157	159
10	8	242	235	4	1	587	600	11	3	255	265	4	7	256	251	13	4	161	163
11	1	363	356	4	2	403	402	11	4	117	119	4	8	382	383	13	5	105	116
11	2	215	208	4	3	200	299	11	5	158	166	4	9	150	158	13	6	105	122
11	3	213	223	4	4	641	636	11	6	219	205	4	10	119	123	13	7	163	155
11	4	306	309	4	5	294	287	11	7	231	235	4	11	193	191	14	4	117	101
11	5	106	93	4	6	257	256	12	0	87	89	5	0	89	52	15	0	93	99
11	6	182	180	4	7	142	144	12	1	367	364	5	1	616	610	15	1	127	130
11	7	186	187	4	8	321	317	12	2	175	175	5	2	449	443	20000			
11	8	131	133	4	9	236	236	12	3	175	170	5	3	323	344	0	1	672	675
12	0	335	338	5	0	117	113	12	4	215	212	5	4	549	549	0	2	101	98
12	1	293	294	5	1	210	206	12	5	132	130	5	5	305	300	0	3	107	96
12	2	237	235	5	2	673	668	12	6	132	135	5	6	204	196	0	4	273	288
12	3	160	151	5	3	746	743	12	7	143	155	5	7	223	229	0	5	294	284
12	4	157	139	5	4	164	164	13	0	217	215	5	8	233	246	0	6	475	489
12	5	180	189	5	5	211	217	13	1	228	228	5	9	142	151	0	7	118	114
12	6	206	217	5	6	134	136	13	2	184	186	6	0	404	400	0	8	173	168
12	7	223	221	5	7	332	350	13	3	123	120	6	1	285	288	0	9	82	88
12	8	93	82	5	8	439	450	13	4	132	124	6	2	457	465	0	10	652	664
12	9	126	134	5	9	133	120	14	1	119	120	6	3	546	536	1	1	330	331
12	10	152	154	5	10	159	157	14	2	93	113	6	4	123	127	1	2	331	323
13	0	126	98	5	11	108	105	14	3	94	105	6	5	224	230	1	3	184	189
13	1	148	140	6	0	99	99	15	2	84	94	6	6	167	185	1	4	228	240
13	2	144	148	6	1	461	461	15	3	89	93	6	7	217	217	1	5	396	382
13	3	133	133	6	2	261	267	20000		6	8	342	338	1	6	509	514		
13	4	89	114	6	3	513	518	0	0	435	439	6	9	95	180	1	7	196	203
13	5	90	92	6	4	521	522	0	1	532	524	6	10	112	119	1	8	330	341
13	6	98	77	6	5	143	143	0	2	735	734	7	0	414	420	1	9	157	159
13	7	85	88	6	6	234	326	0	3	124	117	7	1	370	380	1	10	149	153
13	8	85	80	6	7	233	223	0	4	209	196	7	2	391	398	2	0	366	368
13	9	82	92	6	8	247	247	0	5	268	249	7	3	210	213	2	1	720	721
14	0	82	92	6	9	367	371	0	6	271	270	7	4	320	317	2	2	392	390
30000																			
14	1	329	334	6	10	117	117	0	7	417	422	7	5	272	258	2	3	179	172
14	2	893	894	6	11	73	36	0	8	147	134	7	6	284	285	2	4	160	140
14	3	765	725	7	0	282	286	0	9	178	159	7	7	97	121	2	5	285	265
14	4	890	982	7	1	279	281	0	10	93	93	7	8	235	255	2	6	293	281
14	5	332	314	7	2	516	526	1	0	199	203	7	9	85	91	2	7	507	498
14	6	150	140	7	3	611	607	1	1	710	717	8	0	293	293	2	8	140	157
14	7	519	524	7	4	346	341	1	2	490	486	8	1	347	343	2	9	81	65
14	8	248	244	7	5	88	131	1	3	335	312	8	2	262	251	2	10	863	890
14	9	136	132	7	6	166	165	1	4	630	622	8	3	259	254	3	1	335	336
15	0	459	470	7	7	241	234	1	5	233	230	8	4	144	149	3	2	416	418
15	1	317	317	7	8	375	380	1	6	219	216	8	5	192	197	3	3	201	204
15	2	632	631	7	9	103	87	1	7	341	334	8	6	280	288	3	4	121	128
15	3	1339	1354	7	10	88	89	1	8	320	318	8	7	116	130	3	5	336	329
15	4	341	349	8	0	352	347	2	0	67	90	9	0	360	364	3	6	420	415
15	5	483	389	8	1	427	429	2	1	495	489	9	1	180	178	3	7	147	155
15	6	199	197	8	2	245	251	2	2	564	581	9	2	142	130	3	8	268	272
15	7	224	221	8	3	109	101	2	3	270	256	9	3	304	301	3	9	134	133
15	8	495	581	8	4	270	256	2	4	537	526	9	4	178	170	4	0	223	221
				8	5	319	315	2	5	286	275	9	5	151	159	4	1	620	627
				8	6	190	206	2	6	301	295	9	6	136	148				

Table 40 (continued)

K	L	FOBS	FCAL	K	L	FOBS	FCAL	K	L	FOBS	FCAL	K	L	FOBS	FCAL	K	L	FOBS	FCAL	
4	2	347	339	0	3	141	133	9	4	280	279	7	4	149	155	10	0	221	215	
4	3	178	172	0	5	481	490	9	6	149	154	7	5	275	281	10	2	176	186	
4	4	295	301	0	6	480	468	9	7	127	126	7	6	231	228	10	3	126	123	
4	5	261	247	0	10	126	133	10	0	149	154	7	8	141	134	11	1	174	171	
4	6	263	263	1	1	601	605	10	3	328	331	8	1	320	317	**H = 9****				
4	7	333	327	1	2	174	175	10	4	155	148	8	2	164	175	C	2	151	145	
4	8	114	112	1	3	192	175	10	5	282	284	8	3	124	122	0	4	245	238	
4	9	134	143	1	4	156	149	10	6	102	84	8	4	249	241	1	0	86	79	
4	10	110	102	1	5	333	329	11	2	178	168	8	5	98	103	1	2	221	217	
5	0	252	263	1	6	335	341	11	4	145	158	8	6	121	127	1	3	351	347	
5	1	244	255	1	7	370	367	11	5	81	44	8	7	157	168	2	1	314	331	
5	2	155	165	2	0	808	823	12	0	164	151	9	0	281	285	2	2	242	250	
5	3	149	153	2	1	197	197	12	1	132	136	9	1	118	135	2	3	153	145	
5	4	254	238	2	2	160	174	12	4	80	93	9	2	169	177	2	4	308	301	
5	5	464	462	2	3	111	125	13	0	120	118	9	3	149	157	2	5	111	112	
5	6	228	235	2	4	339	343	13	1	101	94	9	4	175	172	2	6	90	110	
5	7	134	130	2	5	461	460	13	2	160	163	9	5	269	273	3	0	252	251	
5	8	250	250	2	6	465	469	**H = 7****				9	6	113	105	3	1	123	112	
5	10	166	171	2	7	147	160	0	2	119	127	10	1	191	191	3	2	378	371	
6	0	86	107	2	8	229	223	0	4	274	274	10	2	175	170	3	3	397	398	
6	1	297	300	2	9	124	128	0	6	181	173	10	3	98	95	3	5	191	185	
6	2	229	228	2	10	168	167	0	7	146	148	10	4	105	120	3	7	204	191	
6	3	102	102	3	1	477	494	0	8	88	92	11	0	228	224	4	0	100	87	
6	4	292	299	3	2	181	182	0	9	129	136	12	0	120	117	4	1	198	203	
6	6	251	257	3	3	192	193	1	0	255	260	12	1	120	137	4	2	147	142	
6	7	290	283	3	4	219	218	1	1	202	209	**H = 6****				4	3	189	190	
6	9	150	143	3	6	275	275	1	2	158	134	0	1	140	127	4	4	291	278	
6	10	86	94	3	7	388	384	1	3	213	208	0	3	522	531	4	6	138	149	
7	0	348	354	3	8	95	98	1	4	262	268	0	5	139	149	5	1	106	89	
7	1	319	337	3	9	162	157	1	5	446	448	0	7	85	91	5	2	222	219	
7	2	107	115	3	10	71	64	1	6	214	213	0	8	104	120	5	3	219	206	
7	3	390	384	4	0	486	496	1	7	86	79	1	2	327	320	5	4	124	117	
7	5	338	342	4	1	462	473	1	8	66	79	1	3	134	138	5	5	106	85	
7	6	254	254	4	2	176	166	2	1	473	471	1	4	375	362	6	0	102	104	
7	8	201	211	4	3	161	150	2	2	391	385	2	2	332	334	6	2	127	120	
7	9	96	115	4	4	193	200	2	3	214	202	2	3	323	328	6	3	93	91	
8	0	209	214	4	5	473	483	2	4	360	364	2	4	131	135	6	4	102	117	
8	1	278	281	4	6	335	338	2	5	174	164	2	5	333	327	6	5	153	134	
8	2	470	465	4	7	106	93	2	6	230	206	2	7	160	170	7	0	84	85	
8	4	304	291	4	8	212	221	2	7	193	197	2	8	187	184	7	2	212	201	
8	6	140	150	4	10	184	187	2	9	121	120	3	1	278	275	7	3	184	186	
8	7	208	202	5	0	326	320	3	0	574	562	3	2	267	267	7	4	93	92	
8	8	85	82	5	1	364	366	3	1	337	337	3	3	236	246	8	0	92	69	
8	9	115	126	5	2	375	384	3	2	278	278	3	4	424	425	8	1	261	262	
9	0	137	143	5	4	182	185	3	3	310	319	3	5	204	201	8	2	91	80	
9	1	185	184	5	5	183	188	3	4	258	249	3	6	84	85	8	3	116	106	
9	2	130	124	5	6	229	214	3	5	471	470	4	C	220	218	8	4	196	201	
9	3	277	271	5	7	224	226	3	6	163	152	4	1	130	106	9	0	195	191	
9	4	195	186	5	8	124	128	3	7	96	107	4	2	242	245	9	2	230	228	
9	5	309	310	5	9	116	134	3	8	154	174	4	3	419	416	**H = 10****				
9	8	130	130	6	0	436	436	3	9	89	79	4	4	220	230	0	2	161	157	
10	0	230	237	6	1	258	256	4	0	282	294	4	5	132	125	0	3	131	149	
10	1	115	108	6	4	220	216	4	1	271	263	4	6	145	140	C	4	150	124	
10	2	243	242	6	5	394	394	4	2	339	336	5	1	165	160	1	1	191	192	
10	4	284	279	6	6	271	268	4	3	168	169	5	2	159	168	1	5	97	111	
10	5	187	175	6	7	103	95	4	4	286	278	5	4	253	240	2	0	262	262	
10	6	181	177	6	8	107	112	4	5	247	253	5	5	164	155	2	2	274	276	
10	7	103	119	6	9	107	112	4	6	218	203	5	7	101	110	2	3	170	157	
11	0	119	108	7	1	233	222	4	7	179	184	6	2	120	120	2	5	120	116	
11	1	241	242	7	2	206	217	5	0	239	239	6	3	129	133	3	1	309	313	
11	3	220	220	7	3	223	223	5	1	255	253	6	4	99	85	3	2	94	107	
11	4	121	105	7	4	205	196	5	2	121	108	6	5	98	124	3	3	163	161	
11	5	261	254	7	5	185	173	5	3	159	160	7	1	192	206	3	4	190	201	
12	1	150	168	7	6	217	211	5	4	326	340	7	2	125	118	4	0	182	173	
12	2	219	229	7	7	218	219	5	5	186	183	7	3	145	147	4	2	226	224	
12	4	190	195	8	0	333	325	6	6	185	173	7	4	145	147	4	3	211	211	
13	0	126	131	8	1	249	251	6	1	215	222	7	5	161	167	4	4	97	95	
13	1	136	127	8	2	123	118	6	2	181	166	8	0	310	307	5	1	116	122	
13	3	193	193	8	3	212	222	6	3	145	135	8	2	273	262	5	2	140	138	
13	4	121	111	8	4	319	320	6	4	153	162	8	3	137	141	6	1	87	65	
14	1	102	93	8	5	391	386	6	5	176	189	8	4	174	178	6	2	104	101	
14	2	128	137	8	6	150	153	6	6	104	111	8	5	98	105	7	1	111	122	
H = 8**				8	8	130	131	6	7	199	208	9	1	314	313	**H = 11****				
0	0	765	769	8	9	1	228	224	7	0	310	320	9	2	105	100	C	1	117	118
C	1	381	389	9	1	371	373	7	1	173	169	9	3	136	129	1	0	233	236	
0	2	103	100	9	2	106	99	7	2	232	238	9	4	196	196	2	1	264	278	

TABLE 41: ATOM COORDINATES AND ISOTROPIC
TEMPERATURE FACTORS

Atom	x	y	z	B
Zr	0.0	0.0	-0.18983(6)	3.01*
S1	-0.1645(2)	-0.0080(2)	-0.0132(1)	4.56*
S2	0.0535(2)	0.1716(1)	-0.2142(2)	4.15*
S3	-0.1851(2)	0.0474(1)	-0.3350(1)	4.33*
C1	-0.0697(7)	-0.0046(7)	0.1207(5)	4.55*
C2	-0.1364(10)	-0.0100(8)	0.2326(6)	7.08*
C3	-0.0686(11)	-0.0036(10)	0.3391(5)	8.76*
C4	-0.0580(7)	0.2186(4)	-0.3220(5)	3.71*
C5	-0.0480(8)	0.3120(5)	-0.3527(6)	5.13*
C6	-0.1351(10)	0.3523(6)	-0.4355(7)	6.07*
C7	-0.2330(10)	0.2999(8)	-0.4869(8)	6.57*
C8	-0.2475(8)	0.2068(6)	-0.4570(6)	5.08*
C9	-0.1597(7)	0.1658(5)	-0.3737(5)	3.93*
N	-0.4980(8)	-0.2008(3)	-0.1384(5)	4.45*
C10	-0.3933(9)	-0.2662(8)	-0.1198(14)	10.92*
C11	-0.5023(15)	-0.1388(7)	-0.0264(8)	10.01*
C12	-0.4761(11)	-0.1372(7)	-0.2393(8)	9.07*
C13	-0.6332(9)	-0.2452(6)	-0.1408(10)	7.08*

RIGID BODIES

H1	-0.2398	-0.0170	0.2308	7.90
H2	-0.1198	-0.0085	0.4177	9.60

Table 41 (continued)

Atom	x	y	z	B
D	4.610 ^a			
E	1.571			
F	1.571			
H3	0.0269	0.3512	-0.3143	6.20
H4	-0.1241	0.4203	-0.4566	7.00
H5	-0.2981	0.3283	-0.5469	7.90
H6	-0.3209	0.1671	-0.4949	6.30
D	3.391			
E	2.447			
F	3.747			
<u>HINDERED ROTORS</u>				
H7	-0.3503	-0.2810	-0.1985	11.00
H8	-0.3250	-0.2381	-0.0636	
H9	-0.4316	-0.3238	-0.0827	
BARRIER	0.02 ^b			
RADIUS	0.946			
D	0.721			
E	1.373			
F	0.0			
H10	-0.5980	-0.1260	-0.0060	11.00
H11	-0.4537	-0.0797	-0.0446	
H12	-0.4571	-0.1722	0.0416	
BARRIER	0.02			

Table 41 (continued)

ATOM	x	y	z	B
RADIUS	0.946			
D	0.625			
E	3.106			
F	0.0			
H13	-0.775	-0.1230	-0.2447	9.5
H14	-0.5275	-0.0785	-0.2238	
H15	-0.5078	-0.1674	-0.3144	
BARRIER	0.02			
RADIUS	0.946			
D	0.676			
E	6.091			
F	0.0			
H16	-0.6652	-0.2550	-0.0568	8.0
H17	-0.6972	-0.2034	-0.1853	
H18	-0.6265	-0.3065	-0.1838	
BARRIER	0.02			
RADIUS	0.946			
D	0.444			
E	4.689			
F	0.0			

*Equivalent isotropic temperature factors corresponding to the anisotropic thermal parameters shown in Table 42.

^aD, E, and F are as described for Table 32.

^bBARRIER (B_d) is the relative barrier to rotation of the hindered rotor group. $B_d = V_0/2kT$, where V_0 = potential barrier to rotation (kcal mol⁻¹).

TABLE 42: ANISOTROPIC THERMAL PARAMETERS (\AA^2)

Atom	U_{11}	U_{22}	U_{33}	U_{12}	U_{13}	U_{23}
Zr	0.0369(4)	0.0467(4)	0.0309(3)	0.0033(5)	0.0	0.0
S1	0.0519(10)	0.0724(12)	0.0491(8)	-0.0014(13)	0.0142(8)	-0.0058(13)
S2	0.0503(10)	0.0535(9)	0.0536(10)	-0.0022(8)	-0.0099(8)	0.0043(8)
S3	0.0479(10)	0.0663(10)	0.0502(10)	0.0035(9)	-0.0149(9)	-0.0029(8)
C1	0.093(5)	0.042(3)	0.038(3)	-0.021(6)	0.013(3)	-0.003(5)
C2	0.134(8)	0.080(6)	0.055(4)	-0.051(6)	0.042(5)	-0.029(5)
C3	0.200(12)	0.096(5)	0.036(3)	-0.065(11)	0.021(4)	-0.015(7)
C4	0.049(4)	0.055(4)	0.038(3)	0.009(3)	0.004(3)	0.005(3)
C5	0.074(6)	0.061(4)	0.060(4)	0.011(4)	0.012(4)	0.009(4)
C6	0.080(6)	0.080(6)	0.071(5)	0.033(5)	0.011(5)	0.024(5)
C7	0.081(7)	0.116(7)	0.052(5)	0.044(6)	-0.004(5)	0.026(6)
C8	0.058(5)	0.088(6)	0.047(4)	0.022(4)	-0.012(4)	0.014(5)
C9	0.049(4)	0.070(4)	0.030(3)	0.018(4)	0.005(3)	0.002(3)
N	0.042(3)	0.054(3)	0.073(3)	-0.005(4)	-0.000(5)	0.017(3)

Table 42 (continued)

Atom	U ₁₁	U ₂₂	U ₃₃	U ₁₂	U ₁₃	U ₂₃
C10	0.048(6)	0.110(8)	0.257(16)	0.028(5)	0.031(8)	0.081(10)
C11	0.153(10)	0.113(7)	0.114(7)	-0.049(9)	-0.003(11)	-0.018(6)
C12	0.083(8)	0.137(8)	0.124(7)	-0.012(6)	0.006(6)	0.075(7)
C13	0.063(6)	0.095(7)	0.111(8)	-0.018(5)	-0.009(6)	0.032(6)

TABLE 43: INTRA-IONIC CONTACTS (Å)

ATOMS	DISTANCE (Å)	ATOMS	DISTANCE (Å)
Zr-S1	2.555 (2)	Zr-S2	2.537 (2)
Zr-S3	2.538 (2)	S2-S3	3.255 (2)
S1-S1'	3.275 (3)	S1-S2'	3.424 (3)
S2-S3'	3.662 (2)	S1-S3	3.665 (2)
S1-C1	1.759 (6)	S2-C4	1.764 (6)
S3-C9	1.772 (7)	C1-C1'	1.391 (14)
	1.410 (8)	C2-C3	1.364 (11)
	1.366 (22)	C4-C5	1.388 (9)
	1.389 (10)	C6-C7	1.355 (13)
	1.386 (11)	C8-C9	1.400 (9)
	1.388 (9)	N-C10	1.416 (10)
N-C11	1.530 (10)	N-C12	1.462 (9)
N-C13	1.487 (10)		

TABLE 44: INTRA-IONIC ANGLES (DEGREES)

ATOMS	ANGLE	ATOMS	ANGLE
S1-Zr-S1'	79.74 (8)	S2-Zr-S3	79.80 (6)
S1-Zr-S3	92.06 (6)	S1-Zr-S2'	84.51 (7)
S3-Zr-S2'	92.40 (6)	S3-Zr-S3'	101.19 (8)
S1-Zr-S2	105.03 (7)	S2-Zr-S2'	167.76 (8)
S1-Zr-S3'	159.80 (7)	Zr-S1-C1	107.7 (2)
Zr-S2-C4	108.2 (2)	Zr-S3-C9	108.0 (2)
S1-C1-C1'	122.4 (2)	S2-C4-C9	121.9 (5)
S3-C9-C4	121.8 (5)	C1'-C1-C2	118.2 (5)
C1-C2-C3	121.8 (9)	C2-C3-C3'	119.9 (6)
C9-C4-C5	118.6 (6)	C4-C5-C6	121.4 (7)
C5-C6-C7	119.6 (8)	C6-C7-C8	120.7 (8)
C7-C8-C9	119.9 (8)	C8-C9-C4	119.8 (6)
C10-N-C11	106.8 (10)	C10-N-C12	114.7 (8)
C10-N-C13	112.4 (6)	C11-N-C12	105.1 (6)
C11-N-C13	103.8 (8)	C12-N-C13	112.9 (7)
S2'-S1-S3	62.10 (5)	S2'-S3-S1	55.71 (5)
S1'-S2-S3'	62.19 (5)		

TABLE 45: INTER-IONIC CONTACTS (Å)

ATOM 1	ATOM 2	SYMMETRY OPERATION ON ATOM 2	DISTANCE (Å)
S2	H5	$1/2+x, 1/2-y, \bar{z}-1$	3.031
S2	C10	\bar{x}, \bar{y}, z	3.786 (9)
S3	H2	$x, y, z-1$	2.930
S3	C12	$\bar{x}-1, \bar{y}, z-1$	3.756 (11)
C1	C10	$1/2-x-1, 1/2+y, \bar{z}$	3.446 (15)
C1	C13	$1/2+x, 1/2-y-1, \bar{z}$	3.657 (13)
C1	C10	$1/2+x, 1/2-y-1, \bar{z}$	3.730 (15)
C2	C13	$1/2+x, 1/2-y-1, \bar{z}$	3.662 (14)
C2	C10	$1/2-x-1, 1/2+y, \bar{z}$	3.733 (17)
C3	C6	$1/2-x-1, 1/2+y-1, \bar{z}$	3.754 (12)
C4	H5	$1/2+x, 1/2-y, \bar{z}-1$	3.036
C4	C13	$\bar{x}-1, \bar{y}, z$	3.687 (12)
C5	H6	$1/2+x, 1/2-y, \bar{z}-1$	2.832
C5	C8	$1/2+x, 1/2-y, \bar{z}-1$	3.666 (10)
C8	C13	$\bar{x}-1, \bar{y}, z$	3.745 (13)
	C12	$\bar{x}-1, \bar{y}, z$	3.792 (13)
C9	C13	$\bar{x}-1, \bar{y}, z$	3.494 (12)

TABLE 46: LEAST SQUARES PLANE CALCULATIONS

(A) ATOMS FORMING PLANE: Zr, S1, S3

$$\text{EQUATION OF PLANE: } 0.5985X - 0.2147Y - 0.7718Z = -1.6254^a$$

(B) ATOMS FORMING PLANE: Zr, S1, S1'

$$\text{EQUATION OF PLANE: } -0.0622X + 0.9978Y = 0.0$$

(C) ATOMS FORMING PLANE: S2, S3, C4, C5, C6, C7, C8, C9.

$$\text{EQUATION OF PLANE: } 0.6201X - 0.2685Y - 0.7372Z = -1.4221$$

DISTANCES OF ATOMS FROM PLANE (\AA):

S2	0.000(3)	C6	0.014(12)
S3	0.002(3)	C7	-0.013(14)
C4	-0.032(10)	C8	-0.016(15)
C5	-0.015(11)	C9	0.044(15)
Zr	-0.1303(8)		

(D) ATOMS FORMING PLANE: S2, S2', C1, C1', C2, C2', C3, C3'

$$\text{EQUATION OF PLANE: } -0.0717X + 0.9974Y = 0.0$$

DISTANCES OF ATOMS FROM PLANE (\AA):

S1	0.003(3)	C2	-0.046(13)
S1'	-0.003(3)	C2'	0.046(13)
C1	-0.016(10)	C3	0.044(15)
C1'	0.016(10)	C3'	-0.044(15)

(E) ATOMS FORMING PLANE: S1, S3', S2'

$$\text{EQUATION OF PLANE: } 0.9176X + 0.3961Y - 0.03372Z = -1.5424$$

Table 46 (continued)

^ax, y, and z are in Å and refer to the orthogonal coordinates along a, b and c*.

TABLE 47: DIHEDRAL ANGLES BETWEEN
SELECTED PLANES

ATOMS IN PLANE 1	ATOMS IN PLANE 2	ANGLE (DEGREES)
(1) Zr, S2, S3	Zr, S2', S3'	101.1
(2) Zr, S2, S3	Zr, S1, S1'	104.7
(3) Zr, S2, S3	S2, S3, C4, C5, C6, C7, C8, C9	3.9
(4) Zr, S1, S1'	S1, S1', C1, C1', C2, C2', C3, C3'	0.5
(5) S2, S3, C4, C5, C6, C7, C8, C9	S2', S3', C4', C5', C6', C7', C8', C9'	95.0
(5) S2, S3, C4, C5, C6, C7, C8, C9	S1, S1', C1, C1', C2, C2', C3, C3'	108.2

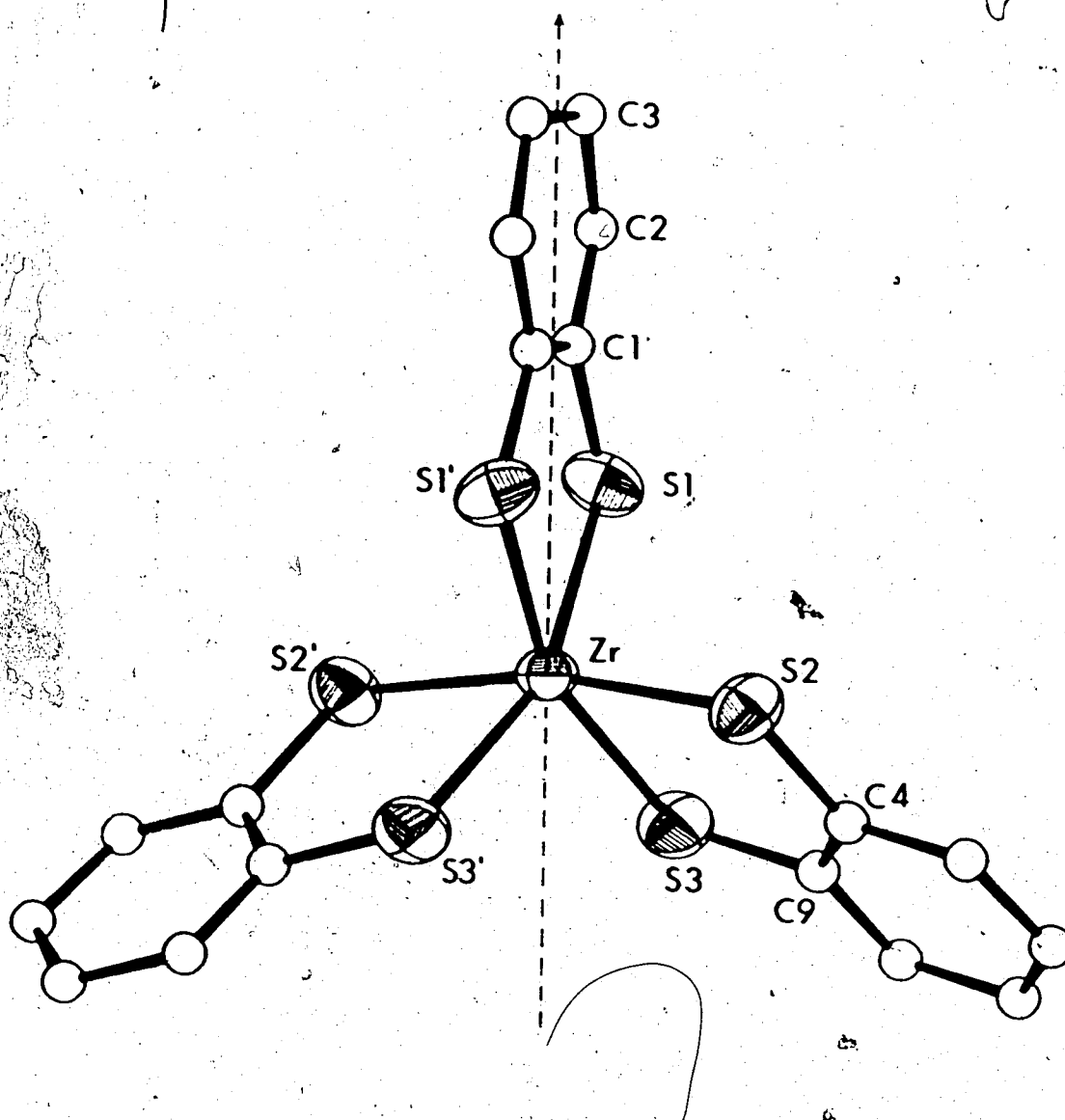


Fig. 17: A Perspective View of the $\text{Zr}(\text{S}_2\text{C}_6\text{H}_4)_3^{2-}$ Dianion, Viewed Down the Approximate Molecular 3-Fold Axis.

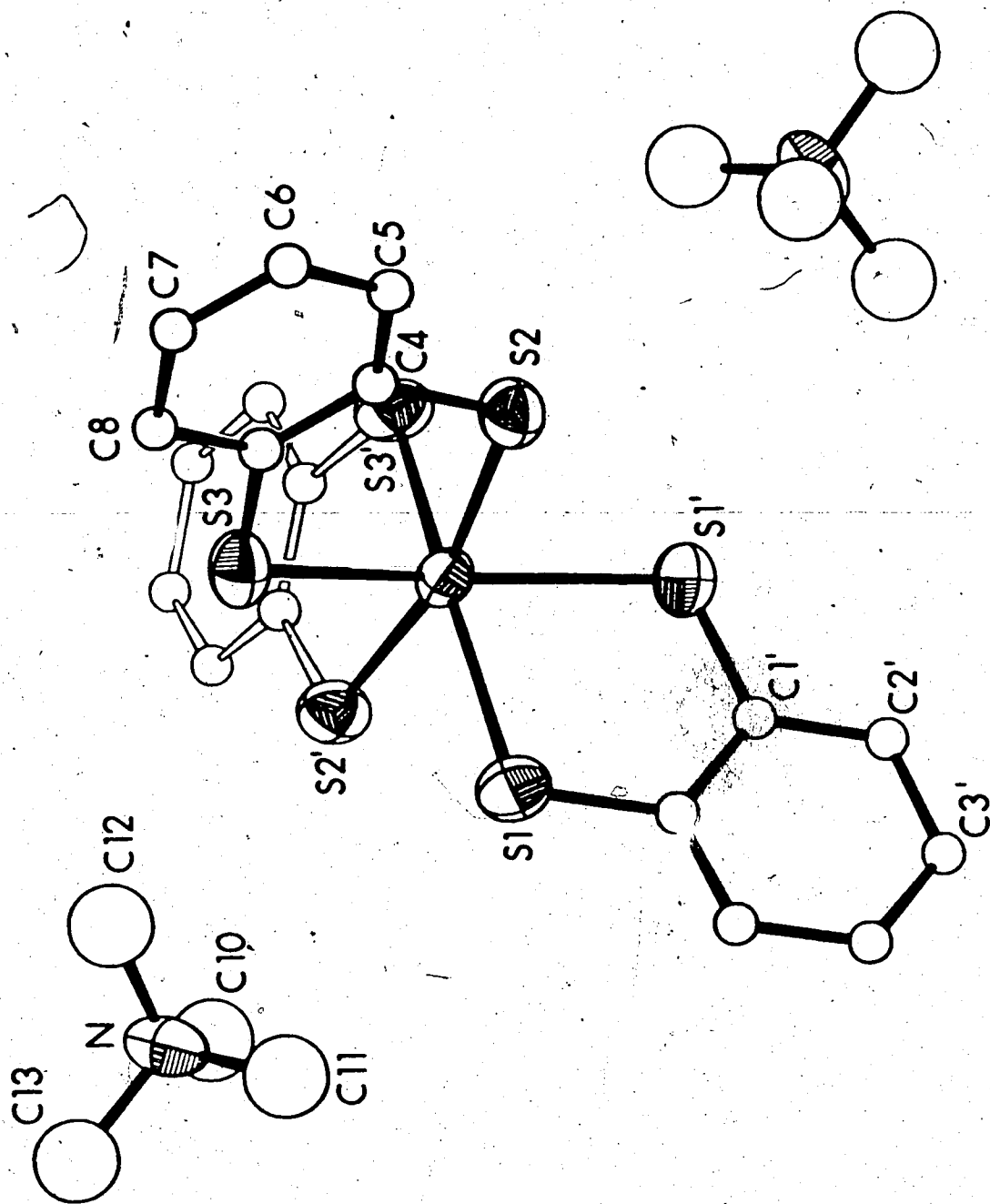


Fig. 18: A Perspective View of $[N(CH_3)_4]_2[Zr(S_2C_6H_4)_3]$

DESCRIPTION OF STRUCTURE

The $Zr(bdt)_3^{2-}$ dianion, viewed down its approximate three-fold axis, is shown in Fig. 17, and the dianion and the two tetramethylammonium cations are shown in Fig. 18. The dianion is located on the crystallographic two-fold axis whereas the tetramethylammonium cations sit in general positions.

In the dianion, the six sulfur atoms are approximately equidistant from the zirconium atom and form a coordination polyhedron which is intermediate between an octahedron and a trigonal prism. Since the $ZrS_2C_6H_4$ fragments are approximately planar, the symmetry of $Zr(bdt)_3^{2-}$ approximates D_3 . The dithiolene ligands radiate from the zirconium atom in a "propeller-like" arrangement as opposed to the "paddle-wheel" arrangement in the trigonal prisms.

In describing the degree of distortion of the metal coordination from either of the trigonal prismatic or octahedral limits, two parameters are especially useful; the S-M-S angles involving sulfur atoms which are almost *trans* to each other, and the projection angle between the two triangular faces of the prism (trigonal twist angle).

In a regular trigonal prism the S-M-S angle between pseudo '*trans*' sulfur atoms is approximately

136°. In an octahedron this angle is 180°. These two extremes are shown in Fig. 19, the S2-M-S4 angle being the angle of interest. However, for an

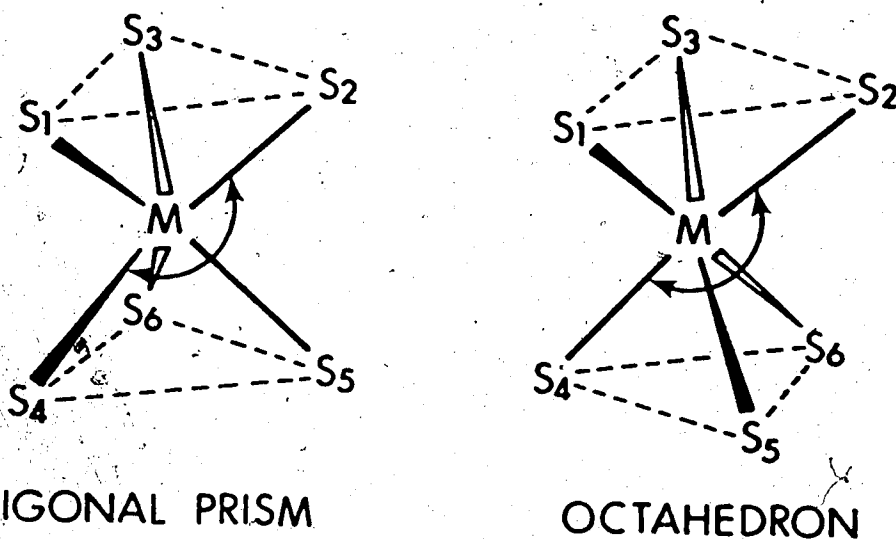


Fig. 19. *Trans* S-M-S Angles in the Trigonal Prism and the Octahedron.

intraligand S-Zr-S angle of $\sim 80^\circ$, considering only the geometric constraints of the ligand, a *trans* S-Zr-S angle of 170° is obtained as the corrected octahedral limit.¹⁶¹ The values observed for the $\text{Zr}(\text{bdt})_3^{2-}$ dianion [$167.76(8)^\circ$ and $159.80(7)^\circ$] are thus closer to the octahedral limit and on this basis the zirconium coordination can be described as distorted octahedral. The non-equivalence of these two independent values indicates that the distortion is not regular and that one ligand (containing S1 and S1') is

rotated more towards the trigonal prismatic structure than the other two ligands.

The other indication of the degree of distortion from the prismatic or octahedral limits is the trigonal twist or projection angle shown in Fig. 20. In the trigonal prism where the two triangular faces are eclipsed, this angle equals 0° , whereas in the ideal octahedron this angle is 60° . Again however, because of the constraint of ligand bite in these bidentate ligands, the octahedral limit is not attained. Rather, this angle will be limited by the ratio of intra-

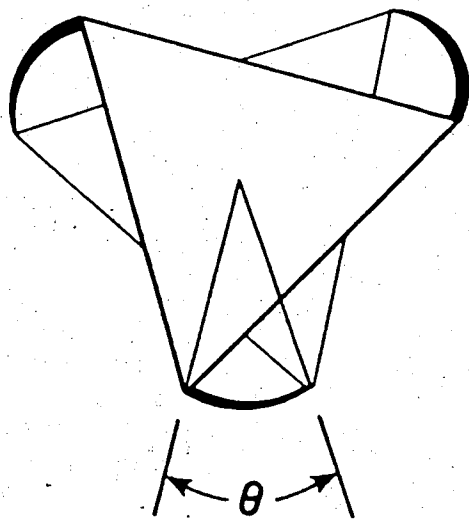


Fig. 20. Trigonal Twist Angle Projected Perpendicular to the Molecular 3-Fold Axis.

ligand S-S distances to the M-S distances. For the $(\text{t})_3^{2-}$ dianion, this ratio (1.284) predicts¹⁶⁶ (on the basis of minimizing interligand repulsions) a twist angle of approximately 48° for the corrected octahedral limit. An average twist angle in this structure is calculated at 37° using equilateral triangles that correspond to a best fit with the observed individual atom coordinates. Thus the twist angle differs from the corrected octahedral limit by only 11° . By comparison, in the structure¹⁶⁷ of $\text{Al}(\text{O}_2\text{C}_7\text{H}_5)_3$, the observed trigonal twist angle (48.1°) is essentially that calculated using the constraints of ligand bite and this appears typical of structures where the only factor favouring the prism is minimization of the interligand repulsions. Thus the deviation of 11° from the corrected octahedral limit is significant and indicates a genuine tendency towards trigonal prismatic coordination in this structure.

The Zr-S distances (av. 2.543 \AA) are longer than those observed in the molybdenum and niobium *tris* (benzene dithiol) complexes (see Table 48) and thus complete a trend through this series with the metal-sulfur distances increasing approximately as predicted by their covalent radii.¹³³ As with the niobium complex, the metal-sulfur distances again

contain irregularities of statistical significance. The Zr-S distance within the ligand bisected by the two-fold axis [2.555(2) Å] is longer than the other two independent Zr-S distances [2.537(2) Å and 2.538(2) Å].

Although this complex is of considerable interest in relation to the other tris dithiolenes, it is also interesting in its own right. The number of structurally characterized six coordinate zirconium complexes is small¹⁶⁸ and indeed $[\text{N}(\text{CH}_3)_4]_2[\text{Zr}(\text{bdt})_3]$ is believed to be the first example of a six coordinate zirconium-sulfur complex. The observed Zr-S distances lie midway between the values 2.49 Å and 2.58 Å, corresponding to the sums of the covalent and ionic (Zr^{4+} and S^{2-}) radii^{133,169} respectively.

The intraligand S-Zr-S angles (av. 79.77°) are slightly less than those observed in $\text{Mo}(\text{bdt})_3$ and $\text{Nb}(\text{bdt})_3$ (82.12° and 80.35° respectively) and complete a trend through the series. This trend is due to the relatively fixed ligand bite which does not increase as rapidly as the metal-sulfur distances.

The S-C distances seem to be an excellent indication of the tendency of the ligand towards either the oxidized or reduced formulations. In $\text{Zr}(\text{bdt})_3^{2-}$ the average S-C distance (1.765 Å) is very close to

that predicted for a single bonded sulfur-carbon distance (1.77 Å).^{84,133} Thus the ligand geometry approximates that corresponding to the dithiolato formulation and the formal oxidation state of (IV) appears to be a reasonable description for the zirconium atom in this structure. This structure is important in demonstrating that the ligand can attain the dithiolato limit. The carbon-carbon distances within the ligands (av. 1.384 Å) are close to those observed in benzene.¹⁵⁸ However, as in the molybdenum and niobium complexes, shortening of the C_C-C_D bond is observed (see Fig. 21), probably due to thermal motion of the rings. In addition, in ligand 1, which is bisected by the crystallographic two-fold axis, the bond lengths vary significantly throughout the ring. One worrying feature of this ring is the presence of anomalously high thermal parameters (U₁₁'s) of the carbon atoms. This seems to indicate either a disorder or a systematic error is present. The disorder could correspond to the non-equivalence of Zr-S1 and Zr-S1' distances for a particular model. However, this problem is unlikely to affect the general conclusions of this study. The C-C bond lengths within the rings are therefore unreliable and no chemical significance should be placed on their

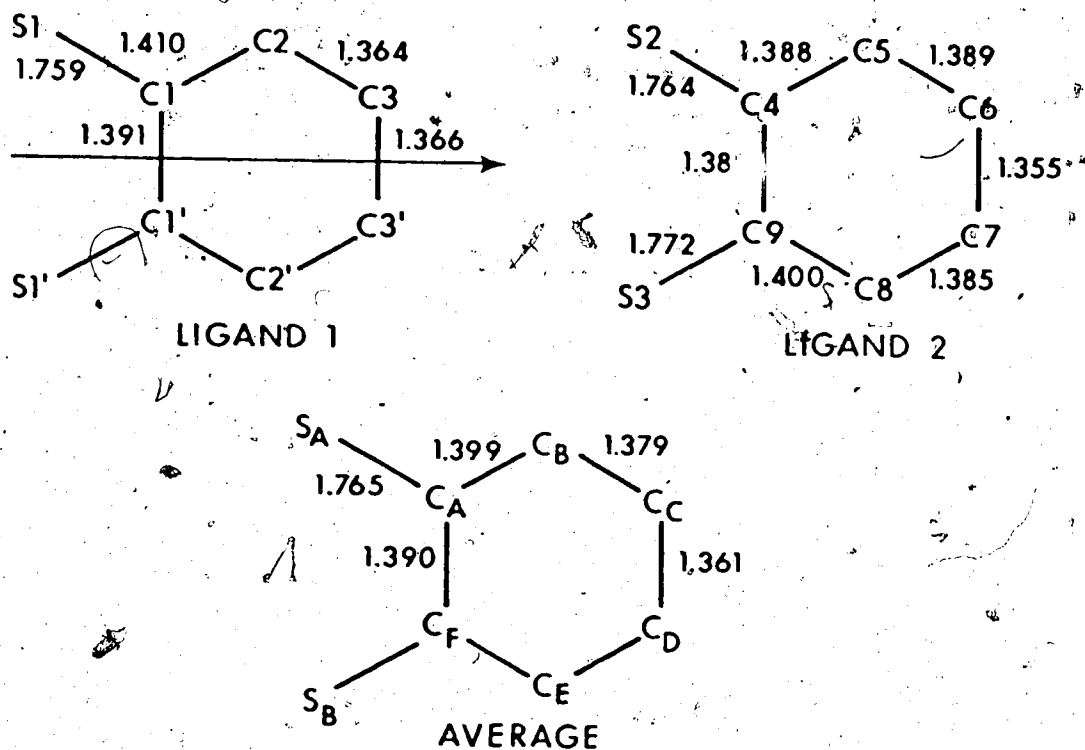


Fig. 21: Dimensions Within the Dithiolene Ligands.

differences.

The interligand S-S distances are, as expected, much longer than the intraligand distances, this due merely to the distortion towards the octahedron which maximizes the interligand separations. In addition the intraligand S-S distances in $Zr(bdt)_3^{2-}$ are longer than those in $Mo(bdt)_3$ and $Nb(bdt)_3$, and are due to increasing S-C distances through the series. The

TABLE 48: SELECTED DISTANCES (Å) FOR
FOR TRIS(1,2-DITHIOLENE) COMPLEXES

COMPOUND	M-S	S-S (INTRA)	S-S (INTER)	S-C	REFERENCE
Re(S ₂ C ₂ Ph ₂) ₃	2.325(4)	3.032(10)	3.050(8)	1.69 ^a	129
Mo(S ₂ C ₂ H ₂) ₃	2.33(1)	3.10	3.11	1.70(3)	130
V(S ₂ C ₂ Ph ₂) ₃	2.338(4)	3.060(6)	3.065	1.69(1)	132
V[S ₂ C ₂ (CN) ₂] ₃ ²⁻	2.36(1)	3.13(2)	3.20	1.72(2)	140
Mo[S ₂ C ₂ (CN) ₂] ₃ ²⁻	2.373(4)	3.113	3.188	1.74(1)	141,170
W[S ₂ C ₂ (CN) ₂] ₃ ²⁻	2.371(5)	3.112	3.193	1.73(2)	170
Fe[S ₂ C ₂ (CN) ₂] ₃ ²⁻	2.261(2)	3.147(2)	3.19	1.731(4)	142
In[S ₂ C ₂ (CN) ₂] ₃ ³⁻	2.604(8)	3.40(1)	3.89(1)	1.72(3)	171
Mo(S ₂ C ₆ H ₄) ₃	2.367(2)	3.110(3)	3.091(2)	1.727(6)	THIS WORK
Nb(S ₂ C ₆ H ₄) ₃ ⁻	2.441(2)	3.150(3)	3.232(3)	1.744(7)	"
Zr(S ₂ C ₆ H ₄) ₃ ²⁻	2.543(2)	3.265(3)	3.584(2)	1.765(6)	"

^aWhere standard deviations are not shown, they were not given in the original paper. In Re(S₂C₂Ph₂)₃ the standard deviations are not shown due to a wide range in S-C distances.

TABLE 49: SELECTED ANGLES FOR TRIS (1,2-DITHIOLENE) COMPLEXES (DEGREES)

COMPOUND ^d	S-M-S (INTRA)	S-M-S (TRANS)	PROJECTION ANGLE	DIHEDRAL MS ₂ /LIGAND ANGLE	COORDINATION
Re(S ₂ C ₂ Ph ₂) ₃	81.4(4)	-136	<1	--	TRIGONAL PRISM
Mo(S ₂ C ₂ H ₂) ₃	82.5	-136	0	18	"
V(S ₂ C ₂ Ph ₂) ₃	81.7(2)	-136	8.5 ^a	--	"
V[S ₂ C ₂ (CN) ₂] ₃ ²⁻	--	158.6	TWISTED ^b	--	DISTORTED OCTAHEDRON
Mo[S ₂ C ₂ (CN) ₂] ₃ ²⁻	82.3(2)	156	28	-2	"
W[S ₂ C ₂ (CN) ₂] ₃ ²⁻	82.1(2)	156	28	-2	"
Fe[S ₂ C ₂ (CN) ₂] ₃ ²⁻	88.0(1)	--	-60	--	OCTAHEDRON
In[S ₂ C ₂ (CN) ₂] ₃ ³⁻	81.5(8)	169.3(3)	--	--	DISTORTED OCTAHEDRON
Mb(S ₂ C ₆ H ₄) ₃	82.18(8)	135.70(7)	0	13.1, 21.1, 30, 0	TRIGONAL PRISM
Nb(S ₂ C ₆ H ₄) ₃	80.35(7)	135.06(7)	0.7	22.4	TRIGONAL PRISM
Zr(S ₂ C ₆ H ₄) ₃ ²⁻	79.77(7)	163.78(8)	37.0	3.9, 0.5	DISTORTED OCTAHEDRON

^a Calculated in ref. 172 from atomic coordinates given in original paper.

^b No coordinates or twist angle given.

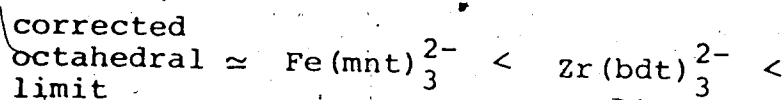
^c Trigonal twist angle projected perpendicular to molecular 3-fold axis.

^d References shown in Table 48.

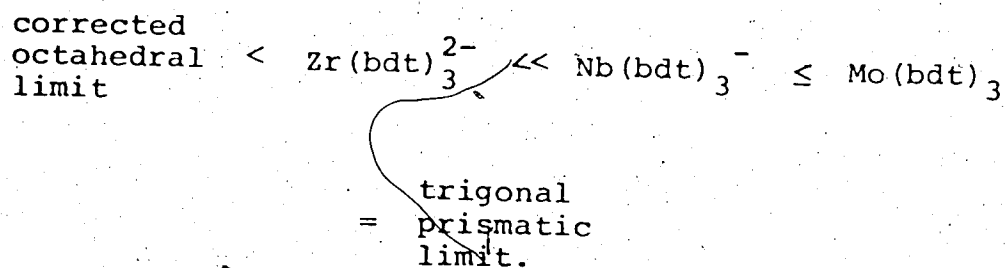
S-C-C and C-C-C angles within the ligands are all close to the expected value of 120° .

An interesting feature observed in $\text{Mo}(\text{bdt})_3$ and isoelectronic $\text{Nb}(\text{bdt})_3^-$ is the large bend of the MS_2 planes from the ligand S_2C_6 planes (21.4° and 22.4° respectively). This had also been observed in $\text{Mo}(\text{S}_2\text{C}_2\text{H}_2)_3^{130}$ and $\text{Mo}[\text{Se}_2\text{C}_2(\text{CF}_3)_2]_3^{152}$ but was not observed in $\text{Re}(\text{S}_2\text{C}_2\text{Ph}_2)_3^{129}$ or $\text{V}(\text{S}_2\text{C}_2\text{Ph}_2)_3^{132}$. In $\text{Zr}(\text{bdt})_3^{2-}$ these planes are approximately coplanar, the dihedral angles between ZrS_2 and S_2C_6 planes being 3.9° and 0.5° . Although Schrauzer had attributed¹³⁸ the bend observed in $\text{Mo}(\text{S}_2\text{C}_2\text{H}_2)_3$ as due to hybridization of the sulfur atoms between sp^2 and sp^3 , it is then difficult to account for the near planarity of the ligands in the zirconium, rhenium and vanadium complexes.

Comparison of the angular parameters in Table 49 allows the complexes to be placed in order of increasing tendency toward the trigonal prismatic structure. Consideration must be given to the general criticism of X-ray crystallographic studies, that one cannot guarantee that the observed geometry corresponds to the ground state. Thus the differences between $\text{V}(\text{mnt})_3^{2-}$ and $\text{Mo}(\text{mnt})_3^{2-}$ [or $\text{W}(\text{mnt})_3^{2-}$] may not be significant. The order for the dianionic species is then:



The corresponding order for the isoelectronic series, as described in this thesis is:



Chapter IX presents a general rationalization for these trends.

A perspective view of the dianion and the tetramethylammonium cations is shown in Fig. 18. As expected the cations are close to tetrahedral, with the small distortions present being due to packing effects. The average N-C distance (1.474 Å) agrees quite well with that predicted (1.47 Å) assuming single bonded covalent radii.¹³³ This value is also in good agreement with previous structural determinations in which the tetramethylammonium cation was involved.^{173,174}

CHAPTER IX: TRIGONAL PRISMATIC vs. OCTAHEDRAL
COORDINATION IN TRIS (1,2-DITHIOLATO) COMPLEXES

The isoelectronic series of tris (1,2-dithiolato) complexes, described in the latter part of this thesis, show dramatic changes in the coordination polyhedron. These changes, from an almost perfect trigonal prism in the neutral molybdenum complex, to a very slightly distorted trigonal prism in the niobium complex anion, to a distorted octahedron in the zirconium complex dianion, are accompanied by smooth increases in metal-sulfur distances, sulfur-carbon distances, and interligand sulfur-sulfur distances (see Table 48). These changes correspond to the increasing importance of the dithiolato formulation for the ligand, that is, $S_2C_6H_4^{2-}$. The increase in interligand sulfur-sulfur distances would lead to a reduction in direct sulfur-sulfur bonding, which has been postulated as a factor in stabilizing the prism.^{137,138,170} In this chapter the structural trends are correlated with molecular orbital energy level diagrams.

Two energy level schemes have been presented to account for the stability of the prism in certain tris (1,2-dithiolato) complexes. One of these schemes, due to Schrauzer and Mayweg¹³⁸ (which will be referred to as scheme 1) is presented for an unspecified first

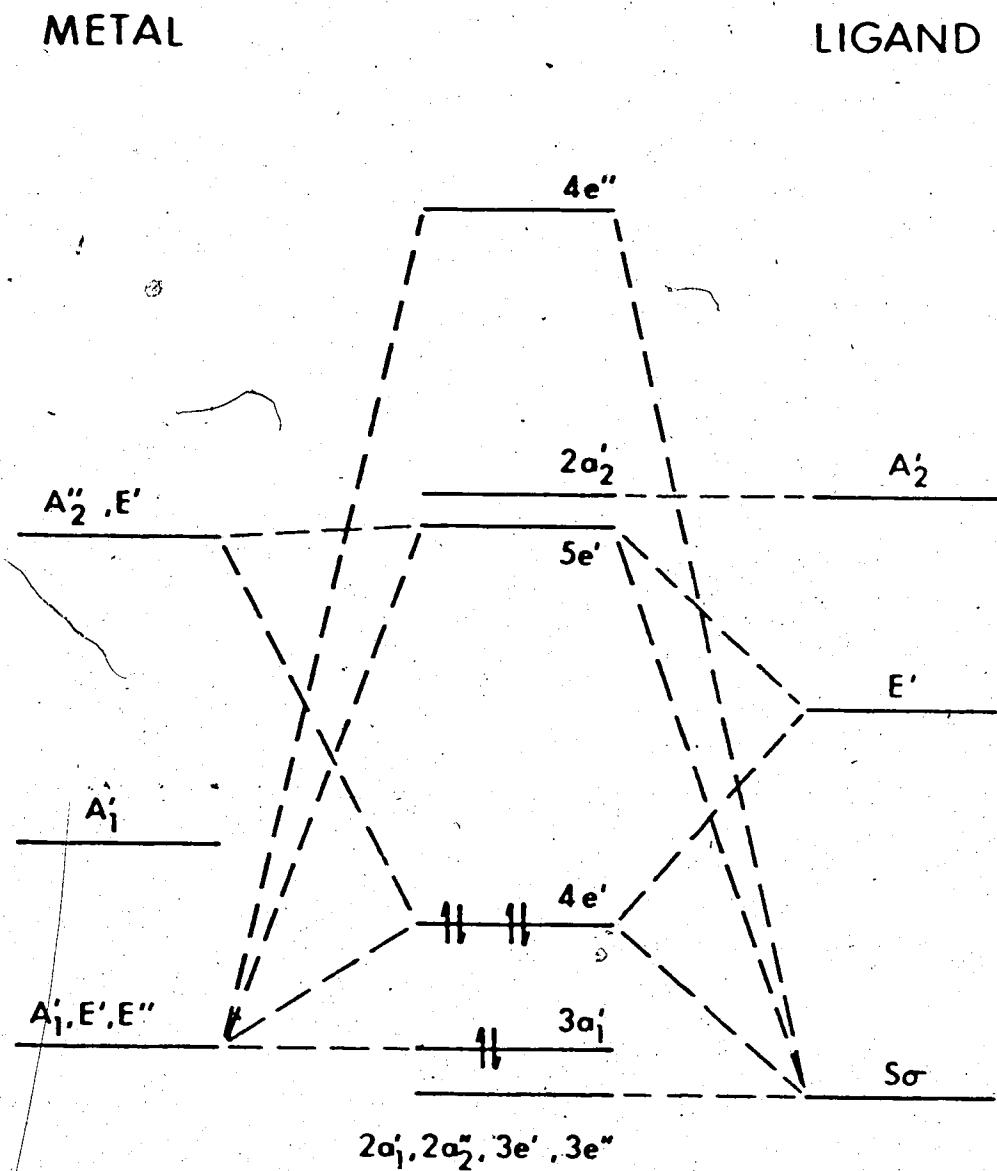


FIG. 22: MOLECULAR ORBITAL ENERGY LEVELS OF INTEREST FOR TRIGONAL PRISMATIC DITHIOLENES, BY G. N. SCHRAUZER AND V. P. MAYWEG

transition series element. The important levels of this scheme are shown in Fig. 22. The alternative scheme, due to Gray *et. al.*¹³⁷ (which will be referred to as scheme 2), is shown in Fig. 23. The differences between the two schemes arise, in part, from the relative positions of the metal and ligand orbitals.¹³² Both schemes agree on the importance of the interaction of the metal $d_{x^2-y^2}$ and d_{xy} orbitals with appropriate combinations of ligand π orbitals (symmetry b_1 for an isolated ligand) to give bonding $4e'$ and anti-bonding $5e'$ levels. Scheme 2, however, proposes an additional significant interaction between the metal d_{z^2} orbital and ligand non-bonding sigma orbitals, giving one bonding ($2a'_1$) and one antibonding ($3a'_1$) level. Scheme 1 has also been challenged on the basis of electron spin resonance studies,^{132,175} and can be shown to be inconsistent with the electronic spectra in this series of compounds. Specifically it predicts an increase in the frequency that would correspond to the transitions $3a'_1 \rightarrow 5e''$ and $3a'_1 \rightarrow 2a'_2$ when comparing the niobium complex with the molybdenum complex, which is the opposite of the experimental results (Table 18). Scheme 2 correctly predicts the experimental observations, as Gray *et. al.*¹³⁷ attribute the transitions as due to $2a''_2(\pi_h)$, $3e'(\pi_h) \rightarrow 3a'_1(d_{z^2})$.

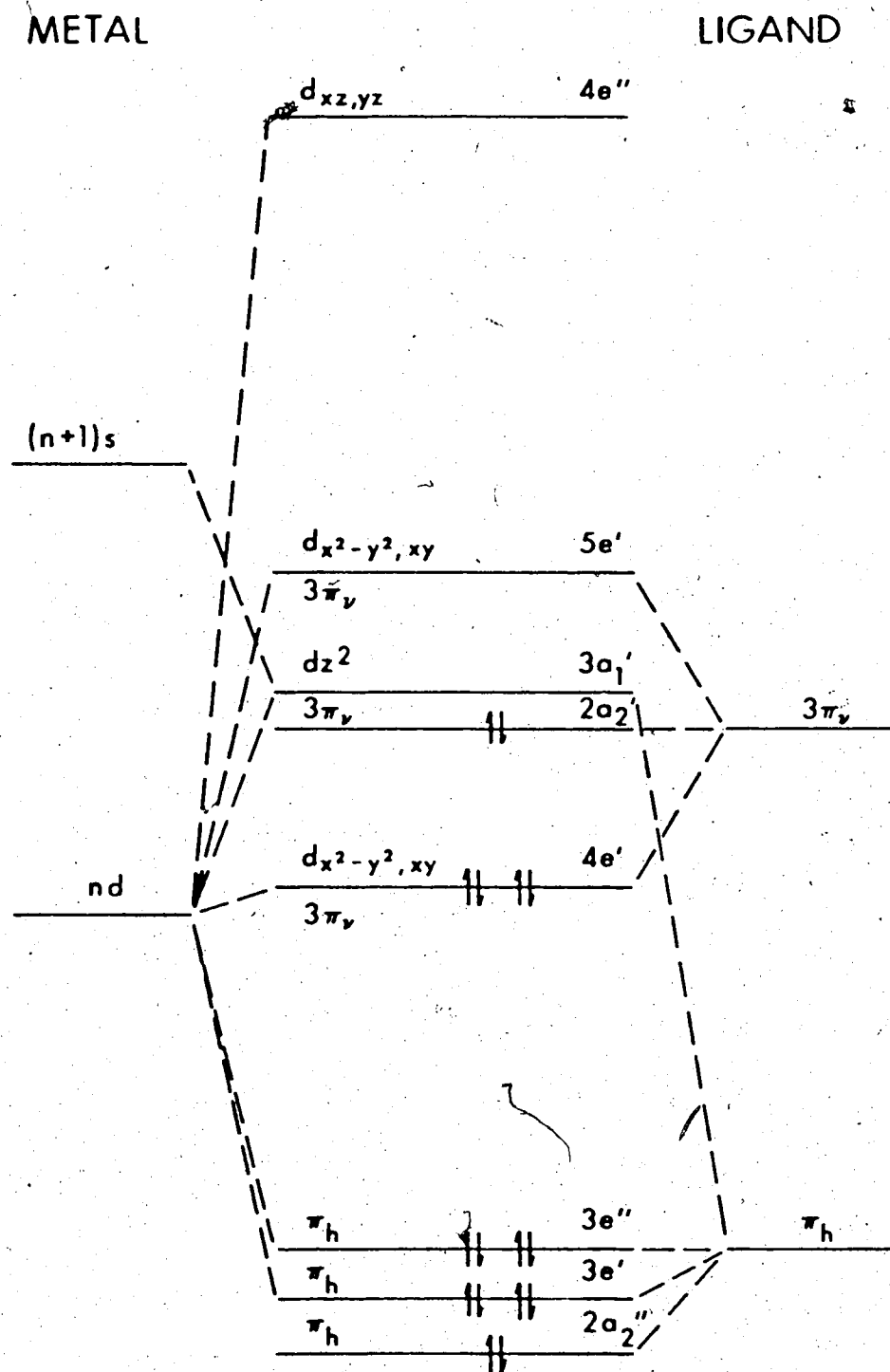


FIG. 23: MOLECULAR ORBITAL ENERGY LEVELS OF INTEREST FOR TRIGONAL PRISMATIC DITHIOLENES, BY H. B. GRAY *et. al.*

Since scheme 2 seems more consistent with the experimental results, it is favoured over scheme 1, and therefore will be used in all subsequent discussions. In this M.O. description (Fig. 23), the levels $2a_2''$, $3e'$ and $3e''$ consist mainly of sulfur sp^2 hybrid orbitals (π_h) at 120° to the σ orbitals pointing at the metal. The $2a_2'$ orbital is non-bonding and the $3a_1'$ is principally metal in character, having symmetry d_{z^2} . The $4e'$ and $5e'$ are both metal ($d_{x^2-y^2}, d_{xy}$) and ligand ($3\pi_v$) in character and both are strongly delocalized over the metal and ligands. Stability of the prism was postulated, by Gray *et. al.* as due to interaction of the sulfur π_h orbitals with the metal d_{z^2} orbital producing the stable bonding orbital $2a_1'$, which is always filled; also the interaction of the metal $d_{x^2-y^2}$ and d_{xy} orbitals with the $3\pi_v$ ligand orbitals produces the stable $4e'$ orbitals which are also filled in these complexes.

In order to use the M.O. scheme by Gray *et. al.* it must be shown that it will apply to the series of interest in this thesis. Considering the ligand and metal orbitals separately, it can first be shown that the energy levels of the molybdenum 4d and rhenium 5d orbitals are similar.¹⁷⁶ Therefore use of the molybdenum atom instead of rhenium in scheme 2 is justified.

The energy levels of the ligands $S_2C_2H_2$ and $S_2C_6H_4$ can be compared using the calculations of Birss and Das Gupta.¹⁶⁰ The π orbitals for these ligands, the calculated orbital energies and geometries are presented in Figs. 24, 25 and 26. Each ligand is shown in the reduced form (corresponding to the dithiolato limit) and in the neutral or oxidized form (2π electrons less). The π orbitals of particular interest are the $2b_1$ for $S_2C_2H_2$ and $3b_1$ for $S_2C_6H_4$. Comparing the oxidized forms of the ligands, the energies of the $2b_1$ ($S_2C_2H_2$) and $3b_1$ ($S_2C_6H_4$) levels are -16.4 e.v. and -15.3 e.v. respectively. A comparison of the reduced forms of the ligands shows the energies are -10.2 e.v. and -10.0 e.v. for the same levels. The probable error in these energy levels is of the order of 0.3 e.v.. Thus it is clear that the molecular orbital scheme proposed for $Re(S_2C_2H_2)_3$ should closely approximate that used for $Mo(S_2C_6H_4)_3$, because of the near equality of both metal and ligand orbital energies.

As postulated by Gray *et. al.*,¹³⁷ the stability of the prism is due, in part, to the interaction of the ligand 3π , and metal $d_{x^2-y^2}$ and d_{xy} orbitals, producing the $4e'$ orbital. The series, $Mo(bdt)_3$, $Nb(bdt)_3^-$ and $Zr(bdt)_3^{2-}$, permits examination of this

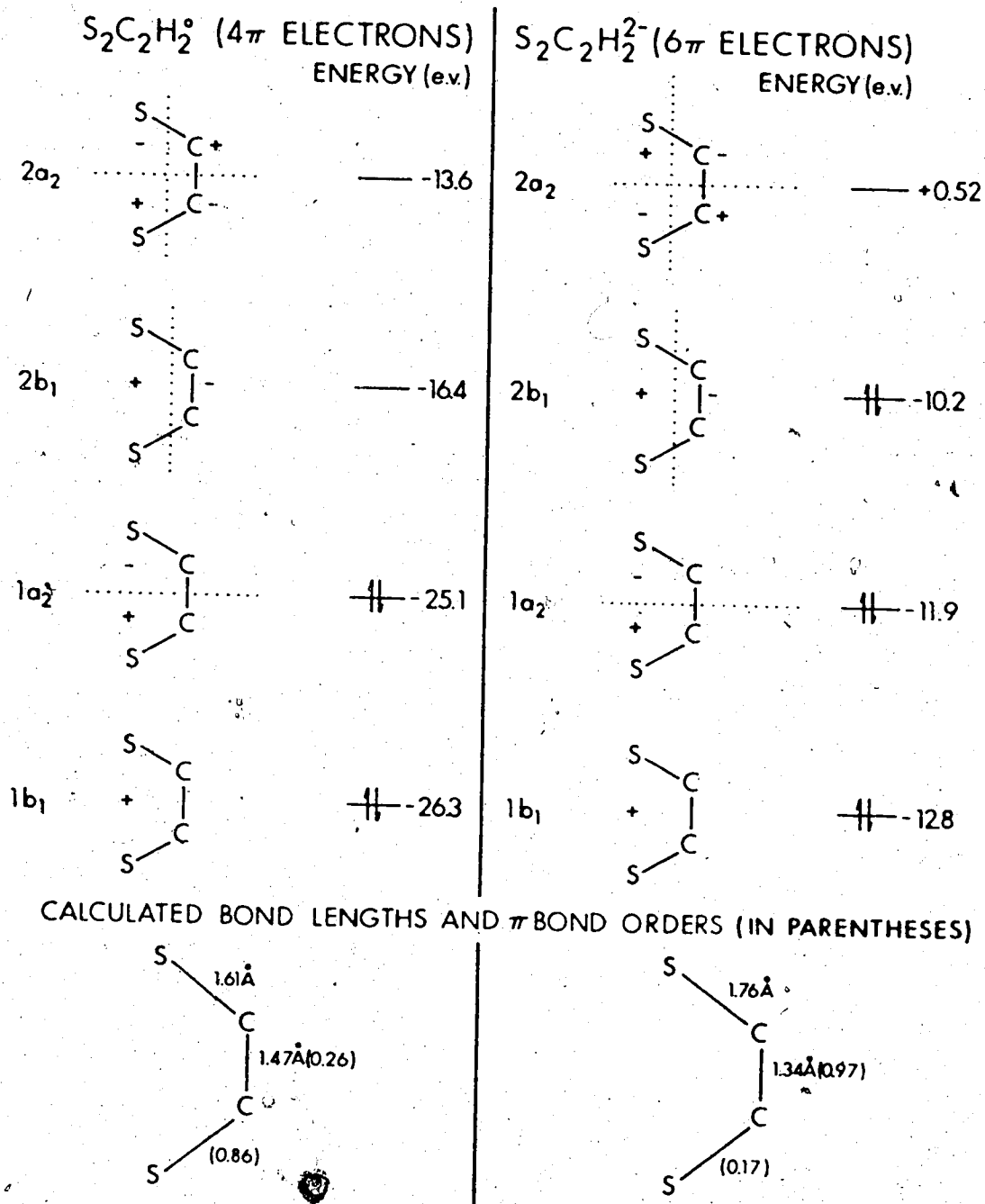


FIG. 24: REPRESENTATIONS OF THE MOLECULAR ORBITALS AND ENERGY LEVELS FOR $S_2C_2H_2$ AND $S_2C_2H_2^{2-}$

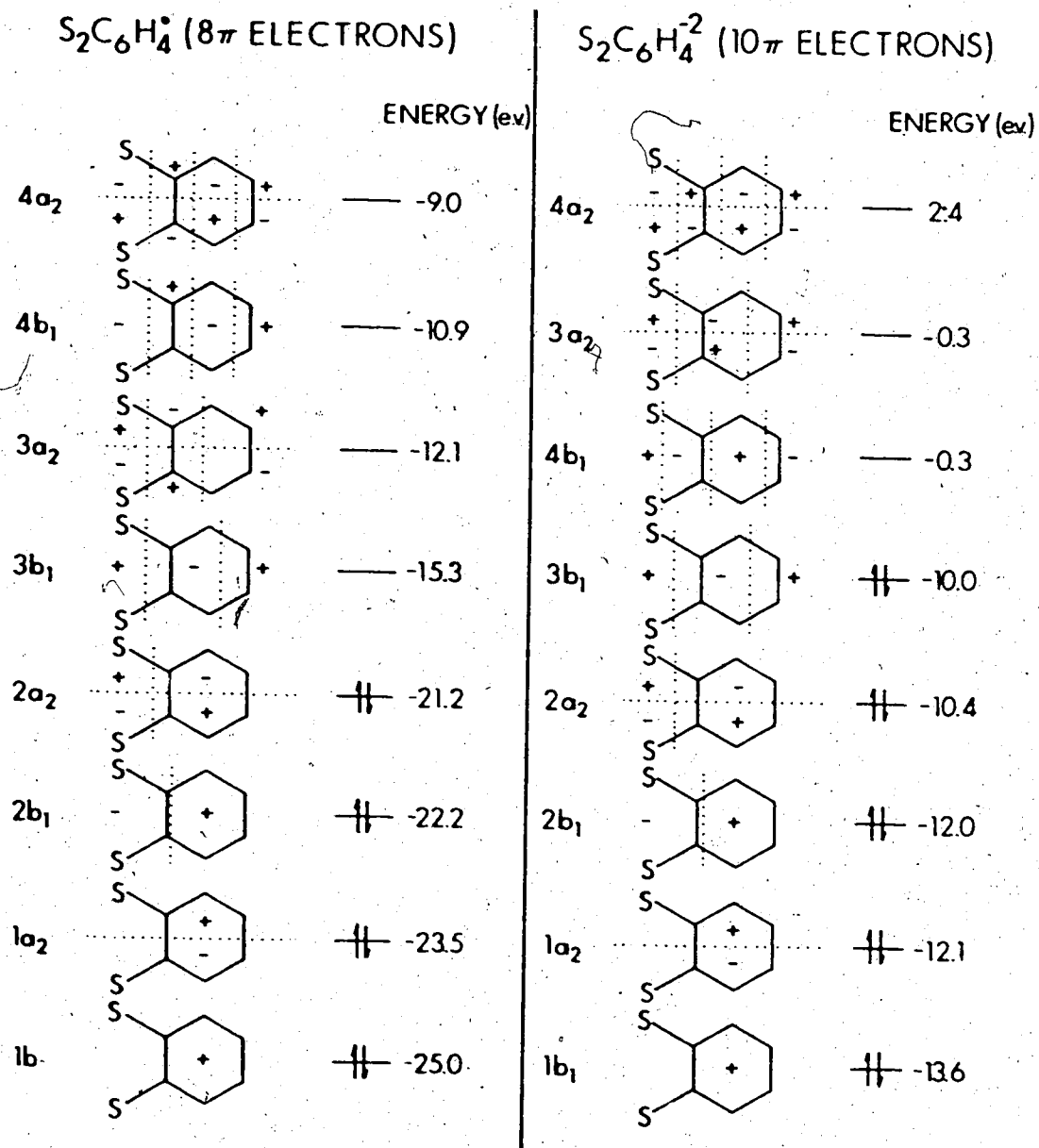
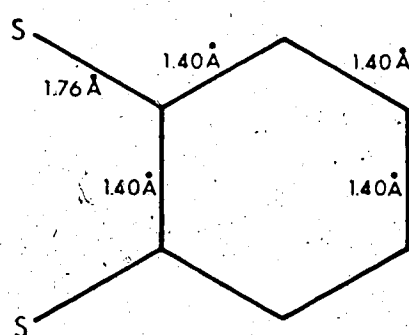
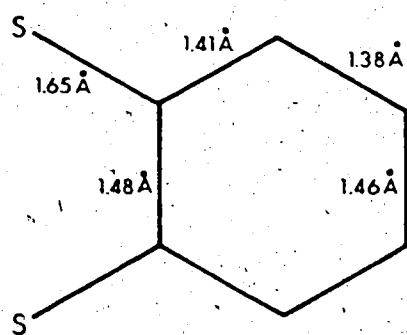
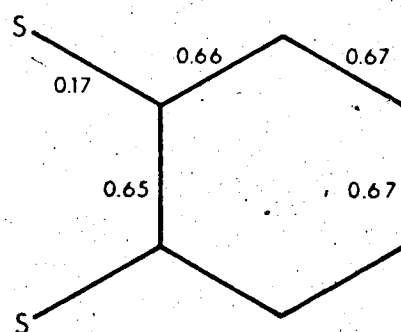
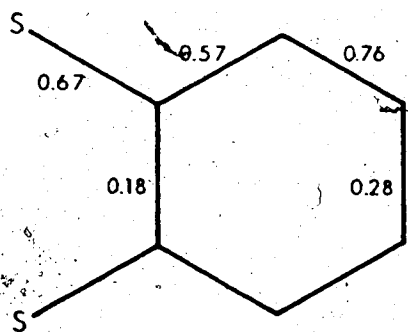


FIG. 25: REPRESENTATIONS OF THE MOLECULAR ORBITALS AND ENERGY LEVELS FOR $S_2C_6H_4$ AND $S_2C_6H_4^{2-}$

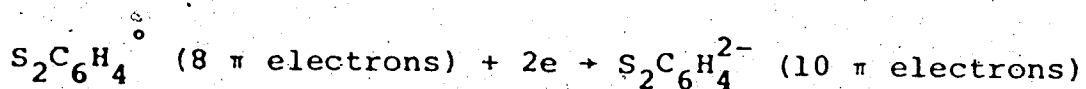
A. CALCULATED BOND LENGTHS

 $S_2C_6H_4^{\circ}$ (8π ELECTRONS) $S_2C_6H_4^{2-}$ (10π ELECTRONS)B. CALCULATED π BOND ORDERSFIG. 26: PREDICTED BOND LENGTHS AND π BONDORDERS FOR $S_2C_6H_4^{\circ}$ AND $S_2C_6H_4^{2-}$

postulate, since in this isoelectronic series no change in the geometry of the coordination polyhedra can be attributed to the occupation of the antibonding orbitals, as has been postulated^{141,170} for the destabilization of the prisms in $\text{Mo}(\text{mnt})_3^{2-}$ and $\text{W}(\text{mnt})_3^{2-}$.

The $4e'$ level should be extremely sensitive to the metal d orbital energies due to the near-equivalence in energy of the d orbitals and the $4e'$ level. The $2a_1'$ level will also be affected but not as much, due to the greater energy separation of it from the metal d orbitals. As the d orbital energies increase, the $4e'$ level should be destabilized and should become more ligand ($3\pi_v$) in character. This increase in the ligand character of the $4e'$ level should be paralleled by a structural change, corresponding to an increase in the contribution of the reduced form structure. The molecular orbital description of the ligands is used in preference to the oversimplified valence bond descriptions, that is, the dithiolato and dithioketonic structures, shown in Fig. 11, since the discussion concerns energy levels and not just geometric changes.

The ligand undergoes extensive geometric changes upon the reduction:



as is shown in Fig. 26. In principle, both sulfur-carbon and carbon-carbon distances could be used in assessing the relative importance of the reduced and oxidized structures in a particular case. In practice, the high uncertainty in the carbon-carbon bond lengths (due to naturally higher standard deviations and large effects due to thermal motion) makes them unsuitable for a semi-quantitative discussion and the more reliable sulfur-carbon distances provide the only useful guide. Sulfur-carbon bond lengths for the *tris*

(benzene-1,2-dithiolato) complexes, described in this thesis, and the theoretical geometries of the oxidized and reduced formulations can be ordered as follows:

$S_2C_6H_4^{\circ}$, (1.648 Å) < Mo(bdt)₃, (1.727 Å) < Nb(bdt)₃⁻, (1.744 Å) < Zr(bdt)₃²⁻, (1.765 Å) = $S_2C_6H_4^{2-}$, (1.763 Å). This series indicates that the ligand tends toward the reduced geometry as the energy of the d orbital increases.

In assessing the ligand and metal orbital character of the 4e' level, it should be noted that appropriate extremes do not correspond to $[S_6C_{18}H_{12}]^{\circ}$ and $[S_6C_{18}H_{12}]^{6-}$ (equivalent to three ligands in the oxidized and reduced forms), since the ligand 3π_v orbitals give rise to the 2a'₂ level as well as the 4e' level (see Fig. 23). This 2a'₂ level is non-bonding,

entirely located on the ligand and is always occupied by two electrons. Hence the discussion of the $4e'$ levels must utilize limiting geometries defined by $[S_6C_{18}H_{12}]^{2-}$ and $[S_6C_{18}H_{12}]^{6-}$, that is, allowing for the $2a_2'$ occupancy.

Fig. 27 shows the plots of S-C bond length vs. S-C π bond order for the ethylene and benzene dithiol ligands, as calculated by Birss and Das Gupta.¹⁶⁰ The limiting extremes, $S_2C_2H_2$ and $S_2C_2H_2^{2-}$, also $S_2C_6H_4$ and $S_2C_6H_4^{2-}$, are shown on the respective plots. For the ligand system $S_6C_{18}H_{12}^{2-}$, the π bond order and bond length can be calculated assuming one contribution of $S_2C_6H_4^{2-}$ for two contributions of $S_2C_6H_4$. This yields a S-C π bond order of 0.50 and a corresponding S-C bond length of 1.69 Å. If the $4e'$ levels are completely ligand in character, the ligand $3\pi_y$ orbitals would contain 6 electrons and would be described as $S_6C_{18}H_{12}^{6-}$. The S-C π bond order and S-C bond length for this extreme are 0.17 and 1.76 Å respectively. These two limits, $S_6C_{18}H_{12}^{2-}$ and $S_6C_{18}H_{12}^{6-}$, then correspond to the extremes that the $4e'$ orbital is completely metal and completely ligand in character, respectively.

In $Mo(bdt)_3$ the average S-C bond length (1.727 Å) corresponds to a π bond order of 0.32 and thus lies

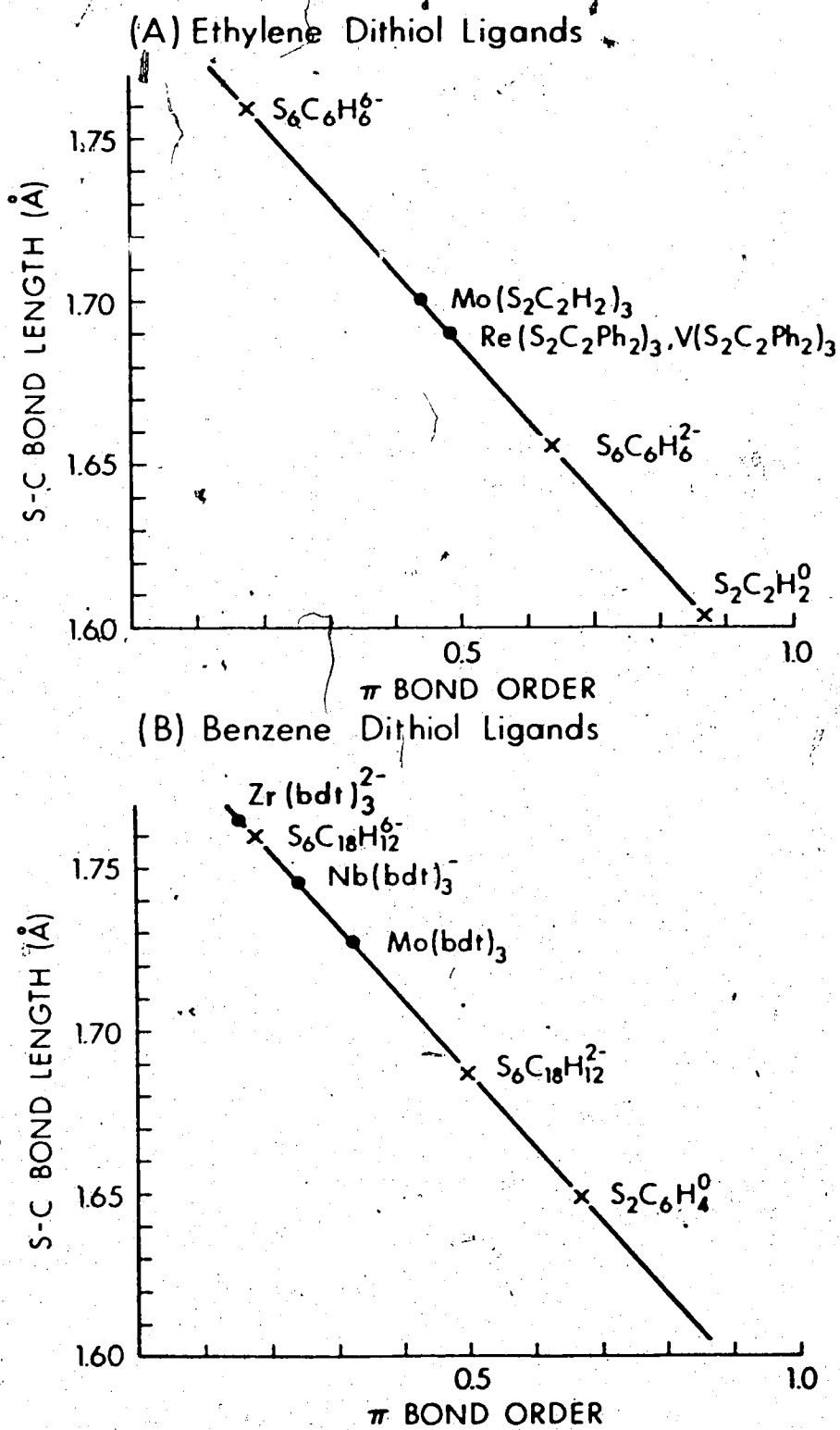


FIG. 27: S-C BOND LENGTH *vs.* π BOND ORDER FOR ETHYLENE AND BENZENE DITHIOL LIGANDS

approximately midway between the $S_6C_{18}H_{12}^{6-}$ and $S_6C_{18}H_{12}^{2-}$ extremes. The $4e'$ level therefore has approximately equal contributions from the metal and ligand orbitals. In $Nb(bdt)_3^-$ the S-C bond length of 1.744 \AA and π bond order of 0.24 corresponds to three quarters of the electron density of $4e'$ being on the ligand and only one quarter of the electron density being on the metal. The S-C bond length of 1.765 \AA in $Zr(bdt)_3^{2-}$ indicates that the ligand has reached the limiting reduced formulation. It is to be noted, however, that there is a tendency in the zirconium coordination toward the trigonal prism, indicating possibly that the $4e'$ level still has a small amount of metal contribution. It is also possible that the tendency toward the prism is favoured by the overlap of the ligand π_h and metal d_{z^2} orbitals, which may still be operative.

In Chapter V it was mentioned that any comparison in bond lengths between ethylene and benzene dithiol ligands should be made with extreme care. This can now be demonstrated with the aid of the calculations by Birss and Das Gupta,¹⁶⁰ shown in Fig. 27. In the ethylene dithiol ligands, employing similar arguments as used for the benzene dithiol ligands, the S-C bond lengths and π bond orders can be calculated for

the $S_6C_6H_6^{2-}$ and $S_6C_6H_6^{6-}$ extremes. These bond lengths and π bond orders are 1.66 Å and 0.64 for $S_6C_6H_6^{2-}$ and 1.76 Å and 0.17 for $S_6C_6H_6^{6-}$. Thus although $Mo(S_2C_2H_2)_3$ has S-C distances (av. 1.70 Å) which are shorter than in $Mo(bdt)_3$, a comparison on Fig. 27 shows that in the two complexes the 4e' level has a similar make-up. It is therefore apparent that for different ligands, even in similar bonding situations, differences in bond lengths are to be expected.

The series of complexes, $Mo(bdt)_3$, $Nb(bdt)_3^-$ and $Zr(bdt)_3^{2-}$ therefore shows the importance of the interaction of the metal $d_{x^2-y^2}$ and d_{xy} with the ligand π_v orbitals in stabilizing the trigonal prism. In addition, the prism stability in this series is maximized in $Mo(bdt)_3$, where the 4e' orbital contains approximately equal contributions from metal and ligand and thus the electrons are completely delocalized over the metal-ligand framework. In the 1,1-dithiolato complexes¹⁷⁷⁻¹⁸⁴ the ligands do not have orbitals of the proper symmetry and energy to overlap with the $d_{x^2-y^2}$ and d_{xy} orbitals of the metal.¹⁵⁷ Therefore this delocalization is not possible and all 1,1-dithiolato complexes have distorted octahedral coordinations.

Interligand sulfur-sulfur bonding has also been

presented as a reason for prism stability,^{137,138,170} and the trends observed in the benzene dithiol series can also be explained by assuming that a breakdown in S-S bonding occurs, progressing from the molybdenum complex through to the zirconium complex. As the d energies increase, so also do the metal radii. Therefore, as the metal radii increase from Mo to Nb to Zr, the interligand S-S distances increase and the slight distortion observed in $\text{Nb}(\text{bd}t)_3^-$ can be explained as a partial breakdown in this S-S bonding. At $\text{Zr}(\text{bd}t)_3^-$ presumably the sulfur atoms have been forced far enough apart to result in a distorted octahedral coordination, due to an almost complete breakdown in S-S bonding. A significant argument, however, against sulfur-sulfur bonding as a major stabilizing force in the prism can be seen in a comparison of $\text{Mo}(\text{mnt})_3^{2-}$ and $\text{W}(\text{mnt})_3^{2-}$ with $\text{Nb}(\text{bd}t)_3^-$. In the niobium complex the interligand sulfur-sulfur distances are greater than those in the molybdenum or the tungsten dianions (see Table 48), yet the niobium complex is trigonal prismatic, whereas the dianions are distorted octahedrons.

The major argument for sulfur-sulfur bonding has been the short sulfur-sulfur contacts observed in the prisms, as compared with the predicted van der Waals

contacts¹⁵¹ (3.70 Å). However these contacts probably arise as a consequence of other factors which stabilize the prism, and are probably not themselves the reason for this geometry. It is believed that the forces between the sulfur atoms are repulsive in nature rather than attractive, as proposed.^{137,138,170} This can offer a possible explanation for the geometry observed¹³² in $V(S_2C_2Ph_2)_3$, which is distorted slightly from the prism by a trigonal twist of 8.5°. If, as suspected, the prism dimensions in the rhenium and molybdenum complexes^{129,130} have reached their minimum, due to increasing S-S repulsions, then in the vanadium complex the smaller size of the metal could result in poor overlap of the metal and ligand orbitals (possibly ligand π_h with metal d_{z^2}). It is then possible that in order to attain the maximum stability, the prism distorts slightly by the observed trigonal twist. In this respect a complete structural determination of $Cr(S_2C_2Ph_2)_3$ is desirable, since X-ray power photographs indicated^{128,129} it is isomorphous with $V(S_2C_2Ph_2)_3$. However, since the chromium radius is smaller than that of vanadium,¹³³ if the above arguments apply, the coordination of the chromium complex should be more distorted from the prism than the vanadium complex.

Any proposed sulfur-sulfur bonding can occur by two mechanisms: overlap of the sulfur p orbitals perpendicular to the ligand plane (π_v orbitals), or overlap of the non-bonding sulfur lone pair (π_h orbitals). It is not believed, however, that either mechanism has a significant effect in stabilizing the prism, since both types of overlap are possible in the 1,1-dithiolato systems, yet these systems invariably have geometries which are close to the "corrected" octahedral limit.

In conclusion, the importance of the $4e'$ molecular orbital in stabilizing the trigonal prism is evidenced in the series: $\text{Mo}(\text{bdt})_3$, $\text{Nb}(\text{bdt})_3^-$ and $\text{Zr}(\text{bdt})_3^{2-}$. The increasing energies of the metal d orbitals, progressing from the molybdenum to the zirconium complex, destabilizes the $4e'$ level, which in turn results in destabilization of the prism. Interligand sulfur-sulfur bonding is not believed to be a significant factor in stabilizing the prism.

REFERENCES

1. G. H. Stout and L. H. Jensen, "X-Ray Structure Determination," 3rd ed., The Macmillan Company, Toronto, Canada, 1970.
2. M. J. Buerger, "Crystal Structure Analysis," John Wiley and Sons, Inc., New York, 1960.
3. M. J. Buerger, "Vector Space," John Wiley and Sons, Inc., New York, 1959.
4. "International Tables for X-Ray Crystallography," 3rd ed., The Kynoch Press, Birmingham, England, 1969, Vols. I, II, and III.
5. W. Hieber and H. Vetter, Z. Anorg. Chem., 212, 145 (1933).
6. G. W. Coleman and A. Blanchard, J. Amer. Chem. Soc., 58, 2160 (1936).
7. R. V. G. Ewens and M. W. Lister, Trans. Faraday Soc., 35, 681 (1939).
8. W. Hieber, Die Chemie, 55, 24 (1942).
9. W. F. Edgell and R. Summitt, J. Amer. Chem. Soc., 83, 1772 (1961).
10. F. A. Cotton and G. Wilkinson, Chem. Ind. (London), 1305 (1956).
11. F. A. Cotton, J. Amer. Chem. Soc., 80, 4425 (1958).
12. G. Herzberg, "Spectra of Diatomic Molecules," 2nd ed., Van Nostrand, New York, 1950, p. 522.
13. W. Hieber and G. Wagner, Z. Naturforsch., B, 13, 339 (1958).
14. W. E. Wilson, Z. Naturforsch., B, 13, 349 (1958).
15. F. A. Cotton, J. L. Down, and G. Wilkinson, J. Chem. Soc., 833 (1959).
16. W. F. Edgell and R. Summitt, J. Amer. Chem. Soc., 83, 1772 (1961).

17. R. M. Stevens, C. W. Kern, and W. N. Lipscomb, J. Chem. Phys., 37, 279 (1962).
18. L. L. Lohr, Jr. and W. N. Lipscomb, Inorg. Chem., 3, 22 (1964).
19. G. M. Sheldrick, Chem. Commun., 751 (1967).
20. T. C. Farrar, S. W. Ryan, A. Davison, and J. W. Faller, J. Amer. Chem. Soc., 88, 184 (1966).
21. T. C. Farrar, F. E. Brinckman, T. D. Coyle, A. Davison and J. W. Faller, Inorg. Chem., 6, 161 (1967).
22. W. C. Hamilton and J. A. Ibers, "Hydrogen Bonding in Solids," W. A. Benjamin, Inc., New York, 1968, Chapter 2.
23. P. G. Owston, J.M. Partridge, and J. M. Rowe, Acta Crystallogr. 13, 246 (1960).
24. P. L. Orioli and L. Vaska, Proc. Chem. Soc., 333 (1962).
25. S. J. La Placa, W. C. Hamilton, and J. A. Ibers, Inorg. Chem., 3, 1491 (1964).
26. S. J. La Placa and J. A. Ibers, J. Amer. Chem. Soc., 85, 3501 (1963).
27. L. Pauling, "Nature of the Chemical Bond," 3rd ed., Cornell University Press, Ithaca, New York, 1960, Chapter 7.
28. E. Huber-Buser, Z. Kristallogr., 133, 150 (1971).
29. S. C. Abrahams, A. P. Ginsberg, and K. Knox, Inorg. Chem., 3, 558 (1964).
30. S. J. La Placa, W. C. Hamilton, J. A. Ibers, and A. Davison, Inorg. Chem., 8, 1928 (1969).
31. R. W. Baker and P. Pauling, Chem. Commun., 1495 (1969).
32. B. R. Davis, N. C. Payne, and J. A. Ibers, Inorg. Chem., 8, 2719 (1969).

33. S. J. La Placa and J. A. Ibers, Acta Crystallogr., 18, 511 (1965).
34. J. J. Daly, J. Chem. Soc., 3799 (1964).
35. B. A. Frenz and J. A. Ibers, "The Hydrogen Series," Vol. 1, Ed., E. L. Muetterties, Marcel Dekker, Inc., New York, 1971, p. 33.
36. Calculated from the van der Waals radius of 1.2 Å; L. Pauling, "The Chemical Bond," Cornell University Press, Ithaca, New York, 1967, p. 152.
37. A. P. Ginsberg, Transition Metal Chemistry, 1, 112 (1965).
38. H. D. Kaesz and R. B. Saillant, Chem. Rev. 72, 231 (1972).
39. L. B. Handy, J. K. Ruff, and L. F. Dahl, J. Amer. Chem. Soc., 92, 7312 (1970).
40. L. B. Handy, P. M. Treichel, L. F. Dahl, and R. G. Hayter, J. Amer. Chem. Soc., 88, 366 (1966).
41. A. S. Foust, W. A. G. Graham, and R. P. Stewart, Jr., J. Organometall. Chem., 54, C-22 (1973).
42. S. W. Kirtley, Dissertation, U.C.L.A., 1971; S. W. Kirtley and C. Knobler, in preparation.
43. M. R. Churchill, P. H. Byrd, H. D. Kaesz, R. Bau, and B. Fontal, J. Amer. Chem. Soc., 90, 7135 (1968).
44. S. W. Kirtley, J. P. Olson, and R. Bau, private communication.
45. L. F. Dahl and R. E. Rundle, Acta Crystallogr., 16, 419 (1963).
46. M. R. Churchill and R. Bau, Inorg. Chem., 6, 2086 (1967).
47. H. D. Kaesz, R. Bau, and M. R. Churchill, J. Amer. Chem. Soc., 89, 2775 (1967).
48. R. P. White, Jr., T. E. Block, and L. F. Dahl, to be published.

49. R. J. Doedens and L. F. Dahl, J. Amer. Chem. Soc., 87, 2576 (1965).
50. R. J. Doedens, W. T. Robinson, and J. A. Ibers, J. Amer. Chem. Soc., 89, 4323 (1967).
51. M. R. Churchill, J. Wormald, J. Knight, and M. J. Mays, Chem. Commun., 458 (1970).
52. E. O. Fischer, O. S. Mills, E. F. Paulus, and H. Wawersik, Chem. Commun., 643 (1967).
53. O. S. Mills and E. F. Paulus, J. Organometal. Chem., 11, 587 (1968).
54. H. D. Kaesz, W. Fellman, G. R. Wilkes, and L. F. Dahl, J. Amer. Chem. Soc., 87, 2753 (1965).
55. S. J. Lippard and K. M. Melmed, Inorg. Chem., 8, 2755 (1969).
56. F. Klanberg and L. J. Guggenberger, Chem. Commun., 1293 (1967).
57. L. J. Guggenberger, Inorg. Chem., 9, 367 (1970).
58. F. Klanberg, E. L. Muettterties, and L. J. Guggenberger, Inorg. Chem., 7, 2272 (1968).
59. S. J. Lippard and K. M. Melmed, Inorg. Chem., 6, 2223 (1967).
60. S. J. Lippard and K. M. Melmed, J. Amer. Chem. Soc., 89, 3929 (1967).
61. P. H. Bird and M. R. Churchill, Chem. Commun., 403 (1967).
62. J. K. Hoyano, M. Elder, and W. A. G. Graham, J. Amer. Chem. Soc., 91, 4568 (1969).
63. M. J. Bennett, W. L. Brooks, M. Cowie, W. A. G. Graham, T. E. Haas, J. K. Hoyano, and K. A. Simpson, Joint Conference of the American Chemical Society and the Chemical Institute of Canada, Toronto, Canada, May 24-29, 1970. Abstracts INOR 50; J. K. Hoyano and W. A. G. Graham, J. Amer. Chem. Soc., submitted for publication.
64. M. J. Bennett and T. E. Haas, private communication.

65. M. Elder, Inorg. Chem., 9, 762 (1970).
66. M. J. Bennett and K. A. Simpson, J. Amer. Chem. Soc., 93, 7156 (1971).
67. D. K. Huggins, W. Fellman, J. M. Smith, and H. D. Kaesz, J. Amer. Chem. Soc., 86, 4841 (1964).
68. J. M. Smith, W. Fellman, and L. H. Jones, Inorg. Chem., 4, 1361 (1965).
69. "International Tables for X-Ray Crystallography," 3rd ed., The Kynoch Press, Birmingham, England, 1969, Vol. I, p. 530.
70. P. W. R. Corfield, Robert J. Doedens and J. A. Ibers, Inorg. Chem., 6, 197 (1967).
71. Calculated from $|F| = [D/(ALp) \cdot I_{rel}]^{1/2}$; see G. H. Stout and L. H. Jensen, "X-Ray Structure Determination," The Macmillan Co., Toronto, Canada, 1968, p. 456.
72. The absorption correction factor, A , is actually the transmission factor as applied to intensities.
73. A. L. Patterson, Phys. Rev., 46, 372 (1934).
74. A. L. Patterson, Z. Kristallogr., A90, 517 (1935).
75. D. T. Cromer and J. B. Mann, Acta Crystallogr., A24, 321 (1968).
76. D. T. Cromer, Acta Crystallogr., 18, 17 (1965).
77. $f_o^{anom} = f_o + \Delta f' + i \Delta f''$ where f_o is the normal scattering factor, $\Delta f'$ is the real correction term and $\Delta f''$ is the imaginary component.
78. G. H. Stout and L. H. Jensen, "X-Ray Structure Determination," 3rd ed., The MacMillan Company, Toronto, Ontario, 1970, p. 234.
79. W. C. Hamilton, Acta Crystallogr., 18, 502 (1965).
80. Anisotropic U's are the thermal parameters expressed in terms of mean square amplitudes of vibration in angstroms.

$$U_{ij} = \frac{\beta_{ij}}{2\pi^2 x_i x_j} \text{ where } x_1 = a^*, x_2 = b^* \text{ and } x_3 = c^*.$$

81. The equivalent isotropic B's are calculated from the expression $B = \frac{4}{3} \sum_{i,j=1}^3 \beta_{ij} a_i \cdot a_j$ where the a_i and a_j are the translation vectors of the direct lattice.
82. L. F. Dahl and R. E. Rundle, J. Chem. Phys., 26, 1750 (1957).
83. N. I. Gapotchenko, N. V. Alekseev, N. E. Kolobova, K. N. Anisomov, I. A. Ronova, and A. A. Johansson, J. Organometal. Chem., 35, 319 (1972).
84. F. A. Cotton and G. Wilkinson, "Advanced Inorganic Chemistry, A Comprehensive Text," 2nd ed., Interscience Publishers, N.Y., 1966, p.105.
85. This seemingly irregular choice of background times and scanning times was due to a modification of the diffractometer in which a manual override of the tens of seconds in the preset time was added to give background and scanning times without continuously changing the preset time controls.
86. "International Tables for X-Ray Crystallography," 3rd ed., The Kynoch Press, Birmingham, England, 1969, Vol. III. p. 166.
87. M. C. Fredette and C. J. L. Lock, Can. J. Chem., 51, 1116 (1973).
88. E. W. Abel, W. Harrison, R. A. N. McLean, W. C. Marsh and J. Trotter, J. Chem. Soc., D, 22, 1531 (1970).
89. M. J. Bennett, W. A. G. Graham, J. K. Hoyano, and W. L. Hutcheon, J. Amer. Chem. Soc., 94, 6232 (1972).
90. K. W. Muir, J. Chem. Soc. (A), 2663 (1971).
91. W. T. Robinson and J. A. Ibers, Inorg. Chem., 6, 1208 (1967).
92. K. W. Muir and J. A. Ibers, Inorg. Chem., 9, 440 (1970).
93. W. L. Hutcheon, Ph.D. Thesis, University of Alberta, 1971, p. 79.

94. K. A. Simpson, Ph.D. Thesis, University of Alberta, 1973, p. 100.
95. A. G. Robiette, G. M. Sheldrick, R. N. F. Simpson, B. J. Aylett, and J. A. Campbell, J. Organometal. Chem. (Amsterdam), 14, 279 (1968).
96. K. Emerson, P. R. Ireland, and W. T. Robinson, Inorg. Chem., 9, 436 (1970).
97. K. A. Simpson, Ph.D. Thesis, University of Alberta, 1973, p. 66.
98. The W-H distance of 1.70 Å was chosen based on the Re-H distance²⁹ and the difference in covalent radii²⁷ of Re and W.
99. R. A. Smith, personal communication; M. J. Bennett and R. A. Smith, manuscript in preparation.
100. "Dithiolene" is the name suggested by McCleverty¹³⁹ for ethylene- and benzene-1,2-dithiolates, to avoid implying the dinegative oxidation state.
101. W. H. Mills and R. E. D. Clark, J. Chem. Soc., 175 (1936).
102. R. E. D. Clark, Analyst, 60, 242 (1936); Analyst, 62, 661 (1937); Tech. Publ. Intern. Tin Res. Dev. Council, A, 41 (1936).
103. R. De Giacomi, Analyst, 65, 216 (1940).
104. C. C. Miller and A. J. Lowe, J. Chem. Soc., 1258 (1940).
105. J. Hamence, Analyst, 65, 152 (1940).
106. J. E. Wells and R. Pemberton, Analyst, 72, 185 (1947).
107. H. G. Short, Analyst, 76, 710 (1951).
108. B. Bähr and H. Schleitzer, Chem. Ber., 90, 438 (1957).
109. D. B. Stevancevic and V. C. Držić, Bull. Inst. Nucl. Sci. "Boris Kidrich", 9, 69 (1959).
110. G. N. Schrauzer and V. P. Mayweg, J. Amer. Chem. Soc., 84, 3221 (1962).

111. R. Eisenberg and J. A. Ibers, Inorg. Chem., 4, 605 (1965); R. Eisenberg, J. A. Ibers, R. J. H. Clark, and H. B. Gray, J. Amer. Chem. Soc., 86, 113 (1964).
112. J. D. Forrester, A. Zalkin, and D. H. Templeton, Inorg. Chem., 3, 1500 (1964).
113. J. D. Forrester, A. Zalkin, and D. H. Templeton, Inorg. Chem., 3, 1507 (1964).
114. C. J. Friche, Jr., Abstract K-10, American Crystallographic Association Meeting, Bozeman, Mont., July 25-31, 1964; Acta. Crystallogr., 20, 107 (1966).
115. A. Davison, N. Edelstein, R. H. Holm, and A. H. Maki, J. Amer. Chem. Soc., 85, 2029 (1963).
116. G. N. Schrauzer, V. P. Mayweg, H. W. Finck, U. Müller-Westerhoff, W. Heinrich, Angew. Chem., 76, 345 (1964).
117. A. Davison, N. Edelstein, R. H. Holm, A. H. Maki, Inorg. Chem., 4, 55 (1965).
118. G. N. Schrauzer, H. W. Finck, and V. P. Mayweg, Angew. Chem., 76, 715 (1964).
119. J. H. Waters, R. Williams, H. B. Gray, G. N. Schrauzer, and H. W. Finck, J. Amer. Chem. Soc., 86, 4198 (1964).
120. A. Davison, N. Edelstein, R. H. Holm, and A. H. Maki, J. Amer. Chem. Soc., 86, 2799 (1964).
121. G. N. Schrauzer, H. W. Finck and V. P. Mayweg, Z. Naturforsch., 196, 1080 (1964).
122. C. H. Langford, E. Billig, S. I. Shupack, and H. B. Gray, J. Amer. Chem. Soc., 86, 2958 (1964).
123. Private communications from R. Archer and C. H. Langford to H. B. Gray, reported in ref. 124.
124. H. B. Gray, R. Eisenberg, and E. I. Stiefel, Advanc. Chem., 62, 641 (1967).
125. R. Dickerson and L. Pauling, J. Amer. Chem. Soc., 45, 1466 (1923).

126. W. G. Wyckoff, "Crystal Structures," Vol. I, Chapter III, p. 28.
127. R. Hultgren, Phys. Rev. 40, 891 (1932).
128. R. Eisenberg and J. A. Ibers, J. Amer. Chem. Soc., 87, 3776 (1965).
129. R. Eisenberg and J. A. Ibers, Inorg. Chem., 5, 411 (1966).
130. A. E. Smith, G. N. Schrauzer, V. P. Mayweg, and W. Heinrich, J. Amer. Chem. Soc., 87, 5798 (1965).
131. R. Eisenberg, E. I. Stiefel, R. C. Rosenberg, and H. B. Gray, J. Amer. Chem. Soc., 88, 2874 (1966).
132. R. Eisenberg, H. B. Gray, Inorg. Chem., 6, 1844 (1967).
133. L. Pauling "The Nature of the Chemical Bond," 3rd ed., Cornell University Press, Ithaca, N.Y., 1960, Chapters 7 and 13.
134. M. R. Truter, Acta Crystallogr., 22, 556 (1967).
135. A. Lopez-Castra and M. R. Truter, J. Chem. Soc., 1309 (1963); W. T. Robinson, S. L. Hart, Jr., and G. B. Carpenter, Inorg. Chem., 6, 605 (1967); M. S. Weininger, J. E. O'Connor, and E. L. Amma, Inorg. Chem., 8, 424 (1969).
136. E. I. Stiefel and H. B. Gray, J. Amer. Chem. Soc., 87, 4012 (1965).
137. E. I. Stiefel, R. Eisenberg, R. C. Rosenberg, and H. B. Gray, J. Amer. Chem. Soc., 88, 2956 (1966).
138. G. N. Schrauzer and V. P. Mayweg, J. Amer. Chem. Soc., 88, 3235 (1966).
139. J. A. McCleverty, "Progress in Inorg. Chem.," Vol. 10, F. A. Cotton, Ed., Wiley, New York, 1968, p. 49.
140. E. I. Stiefel, Zvi Dori, and H. B. Gray, J. Amer. Chem. Soc., 89, 3353 (1967).

141. G. F. Brown, E. I. Stiefel, Chem. Commun., 728 (1970).
142. A. Sequira and I. Bernal, Abstr., Amer. Crystallogr. Ass. Meet., Minneapolis, Minn., Summer 1967, p. 75.
143. Joel L. Martin and Josef Takats, private communication.
144. The spectrum obtained from ref. 137 is for the toluene dithiol complex since the benzene dithiol is not reported. However the two spectra will be almost identical as is observed in $W(\text{tdt})_3$: [12,400 sh (200); 15,670 (23,400); 23,000 sh (900); 25,890 (15,700)] and $W(\text{bdt})_3$: [12,900 sh (1300); 16,060 (20,000); 23,200 sh (2,000); 26,140 (16,500)].¹³⁷
145. H. Hope, Acta Crystallogr., A27, 392 (1971). It was pointed out by Hope that commercially available monochromators could behave quite differently from "ideally imperfect" crystals and allowance should be made for departure from ideal behavior. Due to the potential difficulties involved, it was believed preferable to collect data with filtered radiation.
146. The Patterson map was sharpened by the method of Jacobson, Wunderlich and Lipscomb: R. A. Jacobson, J. A. Wunderlich, and W. N. Lipscomb, Acta Crystallogr., 14, 598 (1961).
147. Extinction corrections were applied to $|F_c|$ by the formula of Zachariasen:¹⁴⁸
- $$|F_c|_{\text{corr}} = |F_c| / [1 + \beta(2\theta)CI],$$
- where C is a parameter varied in the least squares refinement, $\beta(2\theta)$ takes account of the angular variation of the extinction correction.
148. W. H. Zachariasen, Acta Crystallogr., 16, 1139 (1963).
149. R. F. Stewart, E. R. Davidson, and W. T. Simpson, J. Chem. Phys. 42, 3175 (1965).
150. Mo(VI) form factors were obtained directly from the tables but Mo(IV) were estimated from those given for Mo(II) and Mo(VI): D. T. Cromer and J. T. Waber, Acta Crystallogr., 18, 104 (1965).

151. L. Pauling "The Chemical Bond," Cornell University Press, Ithaca, N.Y., 1967, p. 152.
152. C. G. Pierpont and R. Eisenberg, J. Chem. Soc. (A), 2285 (1971).
153. B. F. Hoskins and B. P. Kelley, Chem. Commun., 1517 (1968).
154. A. Domenicano, A. Vaciago, L. Zambonelli, P. L. Loader, and L. M. Venanzi, Chem. Commun., 476 (1966).
155. R. H. Sumner, Ph.D. Thesis, University of Alberta, 1971, p.41.
156. C. Furlani, A. A. G. Tomison, P. Porta, and A. Sgamellotti, J. Chem. Soc. (A), 2929 (1970).
157. R. Eisenberg, Progress in Inorg. Chem., 12, 295 (1970).
158. R. W. G. Wyckoff, "Crystal Structures", Vol. 6, part 1, second ed., p. 1.
159. R. W. G. Wyckoff, "Crystal Structures," Vol. 6, part 1, second ed., p 272-278.
160. F. W. Birss and N. K. Das Gupta, private communication. The method used in calculating the molecular orbital functions and energies takes into account only the electrons of the system. Although it has much in common with a variety of earlier methods, the specific details of the calculation are due to Dewar and Harget [Proc. Roy. Soc., A315, 443 (1970)]. Dewar and Trinajstić [J. Amer. Chem. Soc., 92, 1453 (1970)] have proposed a parameterization for inclusion of sulfur electrons but this has been replaced by one due to Das Gupta and Birss (private communication).
161. The complement of the chelate (bite) angle must equal the supplement of the *trans* angle.
162. F. A. Cotton and G. Wilkinson, "Advanced Inorganic Chemistry, A Comprehensive Text," 2nd ed., Interscience Publishers, N.Y., 1966, p. 115.

163. B. Kamenar and C. K. Prout, J. Chem. Soc., (A), 2379 (1970).
164. F. A. Cotton and C. B. Harris, Inorg. Chem., 7, 2140 (1968).
165. Refinement of a rigid body, which is librating about an axis perpendicular to the plane of the rigid body, was written into SFLS5, the least squares programme, by M. J. Bennett and W. L. Hutcheon. See W. L. Hutcheon, Ph.D. Thesis, University of Alberta, 1970, p. 32.
166. D. L. Kepert, Inorg. Chem., 11, 1561 (1972).
167. E. L. Muetterties and L. J. Guggenberger, J. Amer. Chem. Soc., 94, 8046 (1972).
168. T. A. MacDermott, Coord. Chem. Rev., 11, 1 (1973).
169. F. A. Cotton and G. Wilkinson, "Advanced Inorganic Chemistry, A Comprehensive Text," 3rd ed., Interscience Publishers, N.Y., 1972, p. 927.
170. G. F. Brown and E. I. Stiefel, Inorg. Chem., 12, 2140 (1973).
171. F. W. B. Einstein and R. D. G. Jones, J. Chem. Soc. (A), 2762 (1971).
172. R. A. D. Wentworth, Coord. Chem. Rev., 9, 171 (1972).
173. Von E. Hädicke and W. Hoppe, Acta Crystallogr., B70, 760 (1971).
174. D. S. Kendall and W. N. Lipscomb, Inorg. Chem., 12, 546 (1973).
175. Whei-Lu Kwik and E. I. Stiefel, Inorg. Chem. 12, 2337 (1973).
176. S. Fraga, private communication.
177. T. A. Hanor and D. J. Watkin, Chem. Commun., 440 (1969).
178. S. Merlino, Acta Crystallogr., Sect. B, 24, 1441 (1968)

179. A. Avdeef, J. P. Fackler, Jr., and R. G. Fischer, Jr., J. Amer. Chem. Soc., 92, 6972 (1970).
180. D. L. Johnston, W. L. Rohrbaugh and W. D. Horrocks, Jr., Inorg. Chem., 10, 1474 (1971).
181. P. C. Healy and A. H. White, Chem. Commun., 1446 (1971).
182. S. Merlino, Acta Crystallogr., Sect. B, 25, 2270 (1969).
183. S. Merlino and F. Sartori, Acta Crystallogr., 28, 972 (1972).
184. B. F. Hoskins and B. P. Kelly, Chem. Commun., 45, (1970).
185. G. L. Simon and L. F. Dahl, J. Amer. Chem. Soc., 95, 783 (1973).

APPENDIX 1: MOLECULAR DISORDER IN TETRACARBONYL
RHENIUM BIS (*p*-DIPHENYLSILICON)

RHENIUM TETRACARBONYL, $[\text{Re}_2(\text{CO})_8[\text{Si}(\text{C}_6\text{H}_5)_2]_2]$.

The crystal and molecular structure of $\text{Re}_2(\text{CO})_8[\text{Si}(\text{C}_6\text{H}_5)_2]_2$ was solved by X-ray diffraction techniques by Bennett and Haas.⁶⁴ The compound crystallizes in the monoclinic space group $C2/m$ with two discrete molecules per unit cell, thus imposing site symmetry $2/m$ on the molecule. The unit cell dimensions are: $a = 13.976(3) \text{ \AA}$, $b = 10.549(1) \text{ \AA}$, $c = 12.025(3) \text{ \AA}$, $\beta = 117.57(6)^\circ$, giving an observed density $1.98(2) \text{ g cm}^{-3}$, which agrees well with the calculated value of 2.03 g cm^{-3} . A three dimensional representation of the molecule is shown in Fig. 28. The molecule bears a strong resemblance to the related hydrides $\text{Re}_2(\text{CO})_6\text{H}_4[\text{Si}(\text{C}_2\text{H}_5)_2]_2$ and $\text{Re}_2(\text{CO})_7\text{H}_2[\text{Si}(\text{C}_2\text{H}_5)_2]_2$, having an almost identical Re_2Si_2 framework. As in the hydrides, two mutually *trans* carbonyl groups on each rhenium atom are perpendicular to the Re_2Si_2 plane. The other carbonyl groups are approximately *trans* to the Re-Si bonds.

The crystals contain discrete and disordered molecules, the disorder involving the phenyl groups attached to each silicon atom. One phenyl ring is located approximately in the crystallographic mirror and the other lies approximately perpendicular

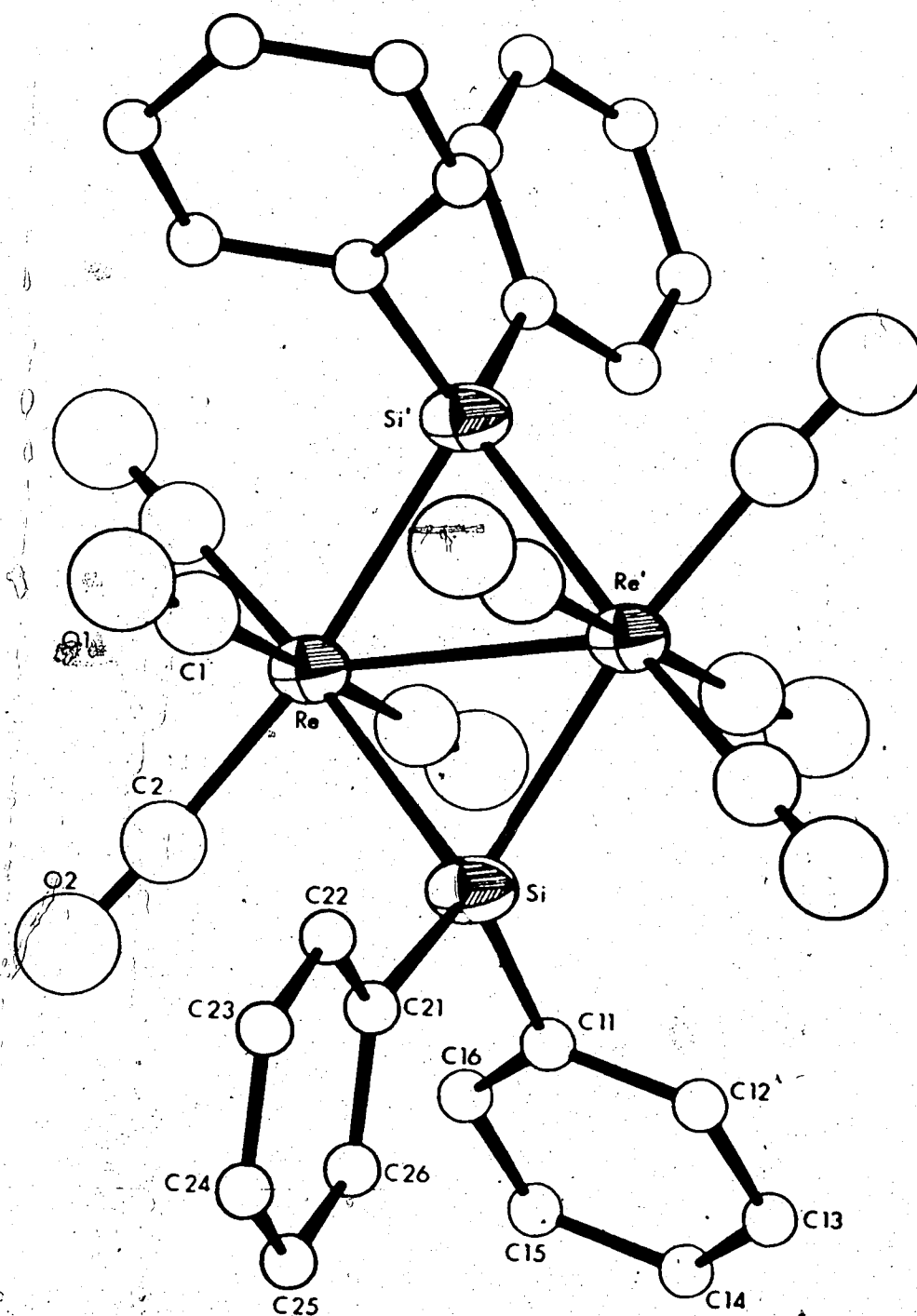


FIG. 28: A PERSPECTIVE VIEW OF $\text{Re}_2(\text{CO})_8[\text{Si}(\text{C}_6\text{H}_5)_2]_2$

to it. Final refinement of this disordered model yielded $R_1 = 0.036$ and $R_2 = 0.057$ for 1153 independent reflections refining 52 parameters in the least squares refinement.

The final anisotropic thermal parameters (U_{ij} 's) for Re and Si are shown in Table 50, and the final positional parameters and the isotropic B's are shown in Table 51. Bond lengths and angles along with their standard deviations are shown in Table 52. In the representation of the molecule (Fig. 28) only one pair of disordered phenyl groups are shown for clarity. In addition the ring carbon atoms are given artificially low thermal parameters, also for clarity of the drawing.

The anomalously large values of U_{22} for both Re and Si were initially interpreted as due to residual absorption effects or other possible systematic errors in the data. However the structural determination¹⁸⁵ of the isomorphous $Mn_2(CO)_8[Si(C_6H_5)_2]_2$ shed new light on this problem. The manganese compound crystallizes in the space group $A2/m$ with cell dimensions, $a = 11.788(2) \text{ \AA}$, $b = 10.480(2) \text{ \AA}$, $c = 13.744(2) \text{ \AA}$ and $\beta = 117.367(6)^\circ$. (This is identical to $C2/m$ with the a and c axes interchanged). Here again the phenyl rings are disordered in the same

TABLE 50: ANISOTROPIC THERMAL PARAMETERS
FOR ORDERED MODEL

Atom	U_{11}	U_{22}	U_{33}	U_{12}	U_{13}	U_{23}
Re	0.0291 (3)	0.0534 (3)	0.0357 (3)	0	0.0167 (2)	0
Si	0.0314 (13)	0.0660 (17)	0.0364 (13)	0	0.0157 (11)	0

TABLE 51: POSITIONAL PARAMETERS AND ISOTROPIC B'S
FOR ORDERED MODEL

Atom	x	y	z	B
Re	0	0.14224 (3)	0	3.06*
Si	0.1388 (2)	0	0.1678 (2)	3.53*
C1	0.0724 (8)	0.1448 (6)	-0.1054 (9)	4.04 (15)
C2	0.1041 (5)	0.2649 (7)	0.1069 (6)	3.99 (12)
O1	0.1162 (7)	0.1518 (5)	-0.1686 (8)	6.09 (16)
O2	0.1682 (7)	0.3414 (6)	0.1658 (7)	6.03 (15)
C11	0.1424 (8)	0.0146 (13)	0.3289 (6)	3.1 (2)
C12	0.1265 (10)	0.1262 (10)	0.3807 (10)	3.9 (3)
C13	0.1301 (10)	0.1237 (10)	0.4987 (10)	4.9 (4)
C14	0.1496 (8)	0.0097 (13)	0.5649 (6)	5.2 (3)
C15	0.1655 (10)	-0.1018 (10)	0.5130 (10)	5.1 (3)
C16	0.1620 (10)	-0.0994 (10)	0.3950 (10)	4.5 (3)
C21	0.2854 (15)	0.0165 (13)	0.2008 (34)	3.5 (2)
C22	0.3172 (22)	-0.0106 (15)	0.1090 (19)	3.9 (2)
C23	0.4261 (29)	-0.0043 (14)	0.1382 (21)	4.7 (2)
C24	0.5033 (15)	0.0292 (13)	0.2591 (34)	4.5 (3)

Table 51 (con't)

Atom	x	y	z	B
C25	0.4715(22)	0.0563(15)	0.3509(19)	6.9(4)
C26	0.3626(29)	0.0500(14)	0.3218(21)	4.6(3)

*Equivalent isotropic temperature factor corresponding to the anisotropic thermal parameters shown in Table 50.

TABLE 52: SELECTED BOND LENGTHS AND ANGLES

(A) BOND LENGTHS (Å)

Re-Re	3.001(1)	Re-Si	2.542(3)
Re-Cl	1.95(1)	Re-C2	1.93(1)
Si-Cl1	1.92(1)	Si-C21	1.91(1)
Cl-O1	1.18(1)	C2-O2	1.17(1)

(B) ANGLES (DEGREES)

Re-Si-Re' ^a	72.3(1)	Si-Re-Si'	107.7(1)
Cl-Re-Cl'	178.4(4)	C2-Re-C2'	95.6(4)
Cl-Re-C2	88.0(3)	Cl-Re-Si	95.1(2)
C2-Re-Si	78.7(2)	Cl1-Si-C21	105.0(4)
Cl1-Si-Re	114.1(3)	Cl1-Si-Re	117.6(4)
Re-Cl-O1	177.2(6)	Re-C2-O2	176.0(7)

^aPrimed atoms are related by either the mirror plane or the two-fold axis, whichever is applicable.

way as the rhenium analogue. In addition the anisotropic thermal parameters for the metals and the silicon atoms are similar in the two compounds. It therefore seems unlikely that the anomalous thermal parameters in both compounds are due to systematic errors in the data.

It was believed possible that the disorder, observed in the phenyl groups, where the data permit resolution of the disorder, could reflect a disorder of the whole molecule. A proper assessment of this possible disorder becomes important then, in order to obtain unambiguous bond lengths and angles.

The high anisotropy in the heavy atom vibrational ellipsoids observed in both the rhenium and manganese compounds provided the clue to the mode of disorder. Since the major axes of the thermal ellipsoids in both compounds were much larger than the other axes, it was believed that the disorder involved slight displacements of the molecule along the crystallographic *b* axis, as shown in Fig. 29. The vibrational ellipsoids are certainly large enough to contain two distinct rhenium and silicon populations, separated from their disorder averaged positions by approximately 0.15 Å.

Thus the completely disordered model was refined

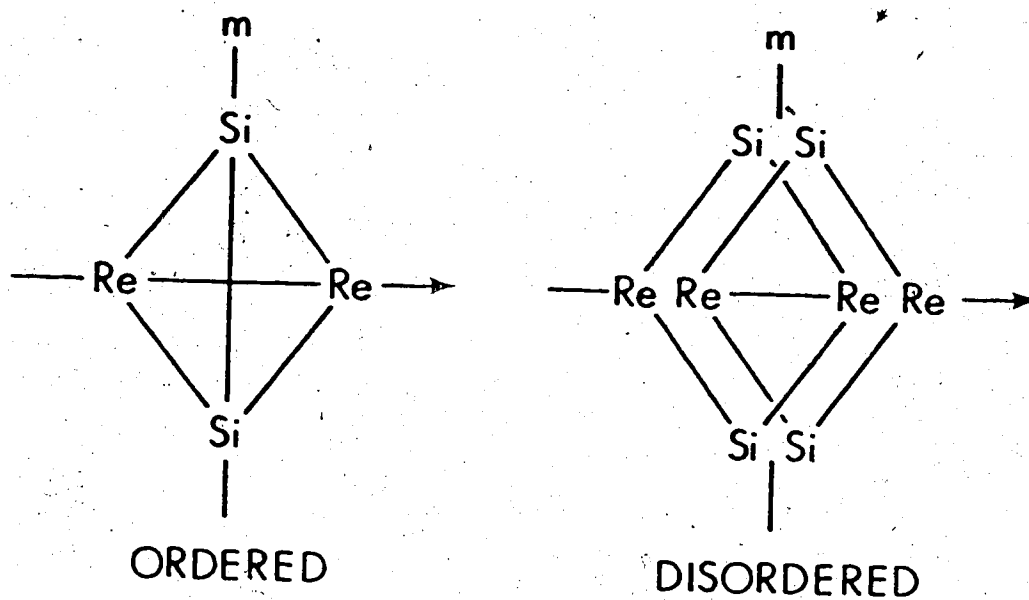


Fig. 29: Mode of Disorder in $\text{Re}_2(\text{CO})_8[\text{Si}(\text{C}_6\text{H}_5)_2]_2$.

to test whether it gave any better fit to the experimental data than the model involving an ordered Re_2Si_2 cluster. In the least squares refinement the parameters for the rhenium and silicon atoms were refined without restriction, other than that imposed by symmetry. However all the parameters for the carbon and oxygen atoms in the carbonyl groups were not refined due to correlations between the x and z coordinates of the two disordered molecules. Thus for one of the disordered forms all coordinates were refined while for the other molecule only the y coordinate was refined. After a cycle of refinement

the x and z coordinates of the second molecule were set equal to those of its disorder-related mate and a further cycle was repeated with the same restrictions on the parameters. This was repeated until further iteration produced no significant shifts.

The final model had all atoms located at approximately 0.3 \AA from their disorder-related partners. Thus the data were of good enough quality to differentiate the two disordered molecules although only 0.3 \AA apart. The validity of the completely disordered model was verified by a Hamilton's R Test⁷⁹ at the 0.005 significance level, showing that the disordered model was significantly better than the ordered model. In the final least squares cycle $R_1 = 0.035$ and $R_2 = 0.056$ for 68 refined parameters. The anisotropic thermal parameters are shown in Table 53. The final positional parameters for all atoms in the completely disordered model are shown in Table 54 along with the isotropic B's of all atoms.

Electron density difference maps were also calculated for each model and were again found to be better for the completely disordered model with less residual electron density in its map. The highest peaks on each map were $1.39e \text{ \AA}^{-3}$ and $1.11e \text{ \AA}^{-3}$ for the ordered and disordered models respectively, this

TABLE 53: ANISOTROPIC THERMAL PARAMETERS FOR DISORDERED MODEL

Atom ^a	U ₁₁	U ₂₂	U ₃₃	U ₁₂	U ₁₃	U ₂₃
Re	0.0274(6)	0.0215(17)	0.0353(6)	0	0.0157(4)	0
Re'	0.0304(6)	0.0211(18)	0.0361(6)	0	0.0175(4)	0
Si	0.0318(12)	0.021(7)	0.0370(12)	0.0000(12)	0.0158(11)	0.0000(13)

^a Primed atoms are the disorder-related atoms.

TABLE 54: POSITIONAL PARAMETERS AND
ISOTROPIC B'S FOR DISORDERED MODEL

Atom	x ^a	y	z	B
Re	0.0	0.1578(4)	0.0	2.18*
Re'	0.0	0.1266(3)	0.0	2.24*
Si	0.1387(2)	0.0178(11)	0.1678(3)	2.37*
Cl	0.0743(11)	0.1594(19)	-0.1030(13)	3.3(4)
Cl'	0.0743	0.1303(20)	-0.1030	3.5(5)
C2	0.1037(10)	0.2773(20)	0.1056(11)	2.9(5)
C2'	0.1037	0.2486(20)	0.1056	3.8(5)
O1	0.1169(10)	0.1697(16)	-0.1672(11)	5.0(4)
O1'	0.1169	0.1349(16)	-0.1672	5.1(4)
O2	0.1674(13)	0.3450(17)	-0.1639(13)	4.0(4)
O2'	0.1674	0.3308(25)	0.1639	8.7(6)
Cl1	0.1423(8)	0.0146(13)	0.3295(6)	3.1(2)
Cl2	0.1268(10)	0.1254(10)	0.3817(10)	4.1(3)
Cl3	0.1301(10)	0.1224(10)	0.4990(10)	4.9(4)
Cl4	0.1488(8)	0.0086(13)	0.5641(6)	5.2(2)
Cl5	0.1643(10)	-0.1022(10)	0.5119(10)	5.3(3)
Cl6	0.1610(10)	-0.0992(10)	0.3946(10)	4.7(3)
C21	0.2861(26)	0.0167(12)	0.2009(33)	3.5(2)
C22	0.3175(22)	-0.0094(15)	0.1092(19)	3.9(2)
C23	0.4259(29)	-0.0036(14)	0.1382(21)	4.6(2)
C24	0.5029(16)	0.0283(12)	0.2589(33)	4.6(3)

Table 54 (con't)

Atom	x	y	z	B
C25	0.4715 (22)	0.0544 (15)	0.3505 (19)	6.5 (4)
C26	0.3631 (29)	0.0486 (14)	0.3215 (21)	4.4 (3)

* Equivalent isotropic temperature factors corresponding to the anisotropic thermal parameters shown in Table 53.

^a Where standard deviations are not given, the parameters were not refined.

density being located in the vicinity of the rhenium atoms in each map.

Thus although it seems that the data are best fitted using the disordered model, the initial ordered model (involving only disordered phenyl groups) is believed to provide a good description of the average geometry, and therefore bond lengths and angles obtained from this model are suitable. This is due to the mode of disorder which involves only a small translation of the whole molecule collinear with the Re-Re bond. The thermal parameters in this model cannot, however, be given any chemical significance since they (especially the U_{22} 's) reflect the disorder present. That the ordered model provides a good description of the average geometry of the molecule is also seen from the bond lengths and angles, which are all reasonable and in good agreement with the related molecules, $\text{Re}_2(\text{CO})_8\text{H}_2\text{Si}(\text{C}_6\text{H}_5)_2$,⁶⁵
 $\text{Re}_2(\text{CO})_6\text{H}_4[\text{Si}(\text{C}_2\text{H}_5)_2]_2$ and $\text{Re}_2(\text{CO})_7\text{H}_2[\text{Si}(\text{C}_2\text{H}_5)_2]_2$.

APPENDIX 2: PROGRAMMES USED IN CRYSTAL
STRUCTURE SOLUTION, REFINEMENT AND ANALYSIS

AUTHOR	PROGRAMME	DESCRIPTION
D. P. Shoemaker	MIXG2	Calculates Picker diffractometer settings from unit cell dimensions and cell type.
M. J. Bennett	PMMO	Transforms raw data to intensities, applying L_p corrections.
M. Elder and K. A. Simpson	D-REFINE	Refines cell parameters for all space groups.
A. Zalkin	FORDAP	Fourier summation for Patterson or Fourier maps.
W. C. Hamilton	GON09 ^a	Absorption corrections for Picker data.
P. Coppens	DATAP ^b	Absorption and Extinction corrections.
C. T. Frewitt	SFLS5	Structure factor calculation and least squares refinement of parameters. Modified by B. M. Foxman and M. J. Bennett for rigid body routine, and by W. L. Hutcheon and M. J. Bennett for the hindered rotor.
J. S. Woods	MGEOM ^a	Calculates bond lengths, angles and best planes.
M. E. Pippy and F. R. Ahmed	NRC-22 ^b	Calculates least squares planes.
W. Busing and H. A. Levy	ORFFE	Calculates bond lengths, angles, and associated standard deviations; modified by B. Penfold for I.B.M. 360 and W. L. Brooks and M. Elder for hindered rotors and rigid bodies.

AUTHOR	PROGRAMME	DESCRIPTION
C. Johnson	ORTEP	Writes Plot Command for Calcomp plotter, for plotting three dimensional molecular representations. Calculates bond lengths and principal axes of anisotropic thermal motion.
M. J. Bennett and B. M. Foxman	MMMR	Calculates starting parameters for rigid bodies and hindered rotors.
M. Cowie	PUBE	Sorts data according to any desired sequence of h, k, or l.
R. C. Elder	PUBTAB	Prints Structure Factor Amplitude Tables; modified by M. Cowie to work in conjunction with PUBE.
G. J. B. Williams	FRAME ^c	Converts continuous paper tape output from automatic diffractometer, in ASCII code to "framed" output on cards in EBCDIC coding, suitable for PMMO input.

^aThis programme was used for the two rhenium hydrides.

^bThis programme was used for the three tris dithiolene complexes.

^cThis programme was used only for $[\text{Ph}_4\text{As}][\text{Nb}(\text{bdt})_3]$. In the other two structures collected by automatic diffractometer, magnetic tape output was used. This was translated from ASCII by a subroutine added to PMMO by myself.